2014

A Dosimetric Comparison of Copper and Cerrobend Electron Inserts

Ben Rusk
Louisiana State University and Agricultural and Mechanical College, brusk1@lsu.edu

A DOSIMETRIC COMPARISON OF COPPER AND CERROBEND ELECTRON INSERTS

A Thesis

Submitted to the Graduate Faculty of the
Louisiana State University and
Agricultural and Mechanical College
in partial fulfillment of the
requirements for the degree of
Master of Science

in

The Department of Physics and Astronomy

by
Benjamin D. Rusk
B.S., Truman State University, 2010
August 2014

Dedicated to my father, David Wm. Rusk.

Acknowledgements

I would like to acknowledge the many people who had a hand in helping with my thesis. I thank Dr. Robert Carver (my supervisory professor) for being helpful and always available for guidance, my committee members (Drs. Kenneth Hogstrom, John Gibbons, Kip Matthews, and Jim Matthews) for their valuable input, and the medical physics staff and students-especially the residents for their much needed assistance and John Chapman for his help in Matlab coding. I would also like to thank my mother for her constant support and encouragement.

This research was supported in part by .decimal, Inc. (Sanford, FL), who provided gifts in-kind, specifically copper inserts and aluminum templates for the Cerrobend inserts. I also thank Mary Bird Perkins Cancer Center for providing resources and facilities.

Table of Contents

List of Tables

List of Figures

Abstract

Purpose: To evaluate dosimetric differences of copper inserts compared to lead-alloy inserts for electron beam therapy.

Methods: Copper inserts were manufactured by .decimal, Inc. and matching lead-alloy, Cerrobend®, inserts were constructed in-house for 32 square field sizes (2x2 to 20x20 cm^2) for five applicator sizes (6x6 to 25x25 cm^2). Percent depth-dose and off-axis relative dose profiles were measured using an electron diode in water for the copper and Cerrobend® inserts for a subset of insert sizes (6x6, 10x10, 25x25 cm^2) and energies (6, 12, 20 MeV) at 100 and 110 cm source-to-surface distances (SSD). Dose outputs were measured for all field size-insert combinations and available energies (6-20 MeV) at 100 cm SSD and for a smaller subset at 110 cm SSD. Using these data, 2D planar absolute dose distributions were generated and compared. Criteria for agreement were ±2% of maximum dose or 1 mm distance-to-agreement for 99% of points.

Results: A gamma analysis of the beam dosimetry showed 94 of 96 combinations of insert size, applicator, energy, and SSD were within the 2%/1 mm criteria. Failures were found for combinations of small field sizes in large applicators at 20 MeV and 100-cm SSD. Copper inserts showed less bremsstrahlung production due to copper's lower atomic number compared to Cerrobend® (greatest difference was 2.5% at 20 MeV). This effect was most prominent at the highest energies for combinations of large applicators with small field sizes. Also, more electrons scattered from the collimator edge of copper compared to Cerrobend®, resulting in an increased dose at the field edge for copper at shallow depths (greatest increase was 1% at 20 MeV).

Conclusions: Inserts for field sizes ≥6x6 cm^2 at any energy, or for small fields (≤4x4 cm^2) at energies <20 MeV, showed dosimetric differences less than 2%/1 mm for more than 99% of points. All areas of comparison criteria failures were from lower out-of-field dose from copper inserts due to a reduction in bremsstrahlung production, a dosimetric difference which is clinically beneficial in reducing dose to healthy tissue outside of the planned treatment volume. All field size-applicator size-energy combinations passed 3%/1 mm criteria for 100% of points.

Chapter 1 Introduction

1.1 Background and Significance

1.1.1 Delivery of Clinical Electron Beams

High energy linear accelerators with multiple energy electron beams have been commercially available since the 1970s. Principal treatment sites for electron beam therapy include skin, chest wall, superficial nodes, and head and neck. The characteristically high surface doses and rapid distal dose falloffs associated with electron beams make them useful in treating superficial tumors with high dose uniformity to the target volume and low dose to deeper tissue. These beam characteristics give electrons advantages over superficial x-rays or brachytherapy for shallow tumors.(Hogstrom, 1991; Hogstrom and Almond, 2006) Clinical electron beams typically have energies ranging from 6 MeV to 20 MeV. Beyond this range, distal dose falloff, lateral penumbra, and bremsstrahlung production increase rapidly, reducing the benefits of using electrons.(Loevinger *et al.*, 1961) Figure 1.1 shows the loss of distal dose fall-off with increasing energy. In addition, this figure shows the difference in the dose as a function of depth for electron beams as compared to high-energy x-rays.

Modern linear accelerators use magnetrons or klystrons (Varian Medical Systems, Inc.) to amplify radiofrequency waves for accelerating electrons.(Karzmark and Pering, 1973) These high energy electrons are shaped by the treatment head and other accessories into a clinical electron beam suitable for patient treatment. Figure 1.2 depicts a modern treatment head which is responsible for redirecting, broadening, and collimating the electron beam. The electron beam is redirected by either 90° or 270° toward the patient

through the use of bending magnets. The electron beam passes through a primary (broadening) and secondary (flattening) foil which results in a beam that is large and uniform enough for clinical use. The beam then passes through dual sealed ion chambers which monitor the dose rate, flatness, and symmetry. Before leaving the treatment head, the electron beam is collimated by two pairs of mechanically adjusted collimator jaws. However, due to the clinically significant scattering of electrons in air, further collimation of the beam beyond the treatment head is necessary, typically by using electron applicators.

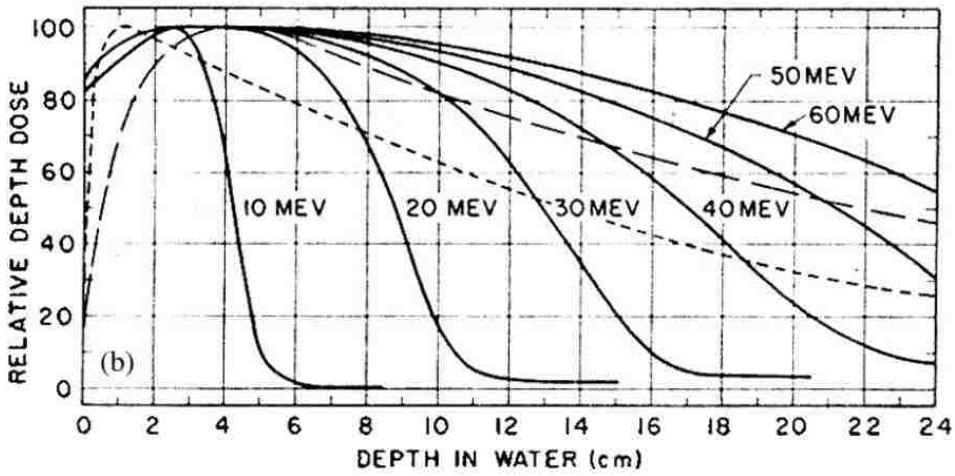

Figure 1.1: Relative percent depth dose curves for electron beam energies (Loevinger, 1961)(Loevinger *et al.*, 1961). Solid lines represent electron depth dose curves of increasing energy for large fields. X-ray depth dose curves for 5 MV (small-dashed line) and 22 MV (long-dashed line) for a 10x10 cm^2 field at 100 cm SSD are shown for comparison.

An electron applicator, as shown in Figure 1.3, attaches below the treatment head and includes three trimmers to further collimate the beam along with a bottom tray for patient-specific collimation. While photon treatments can use multileaf collimators (MLCs) to achieve patient-specific collimation, electron MLC prototypes exist but are not commonly available in commercial treatment machines.(Lee *et al.*, 2000; Hogstrom

et al., 2004) Instead, electron beams use custom inserts for shaping of the lateral field edges to conform to the planning target volume (PTV) while sparing adjacent critical structures and normal tissue.

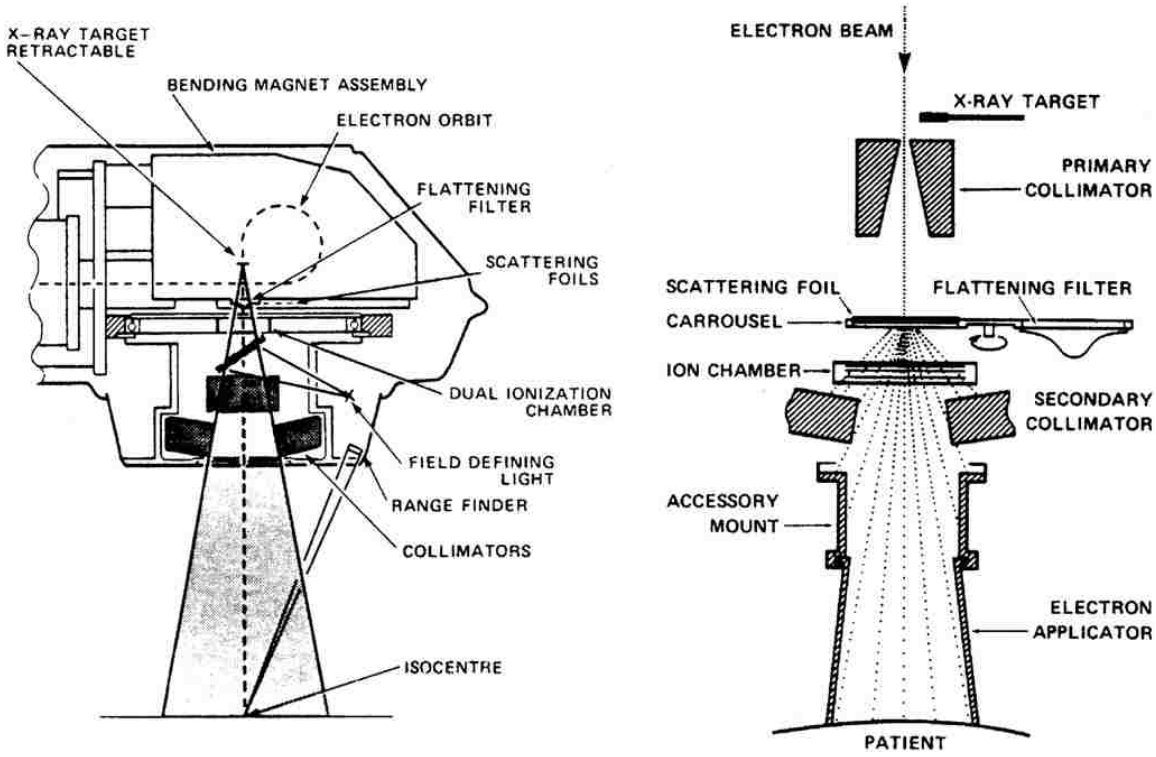

Figure 1.2: Schematic of a Varian linear accelerator treatment head.(Karzmark and Morton, 1989) The image on the left shows the path of the beam into the treatment head, where a bending magnet redirects the beam down through the scattering foils, ionization chambers, and collimators. On the right is a schematic showing the downward path of the electron beam through the parts of the treatment head as well as the electron applicator.

Most clinical applications require the primary beam transmission through the blocked-portion of an insert to be ≤5%, where transmission is defined as the ratio of dose at R_{100} (location of maximum dose) with and without the block in place.(Khan, 2003) The most commonly used electron insert, introduced by Powers et al., utilizes Lipowitz metal, known by the brand name Cerrobend®.(Powers *et al.*, 1973) Cerrobend (MT-A158, MED-TEC, Orange City, IA) by mass contains 50.0% bismuth, 26.7% lead, 13.3% tin

and 10.0% cadmium. The density is 9.4 g/cm^3, which is 17% less than the 11.34 g/cm^3 density of lead, another common radiation shielding material. One significant advantage of Cerrobend is its low melting point of ~70° C compared to 327° C for lead. This low melting point allows for the relatively easy creation of liquid Cerrobend, which can then be poured into a mold. In addition, Cerrobend is harder than lead at room temperature, making the insert more sturdy than one made of lead.

Figure 1.3: Type III Varian electron applicator with labels showing the trimmers and tray for placement of patient-specific inserts.

To create a custom insert, such as those shown in Figure 1.4, the field shape is traced onto and then cut out of a block of Styrofoam, usually with a heated wire. The Styrofoam cutout is placed in a mold which is then filled with molten Cerrobend. The mold has dimensions such that the final insert fits in the insert tray of an electron applicator. Once the Styrofoam is removed, the result is an aperture in the shape of the desired field. This technique for creating custom inserts for external beam therapy has remained relatively

unchanged since the 1970's, however it does hold some disadvantages such as laborious fabrication with challenging reproducibility, as well as environmental and safety precautions.(Powers *et al.*, 1973)

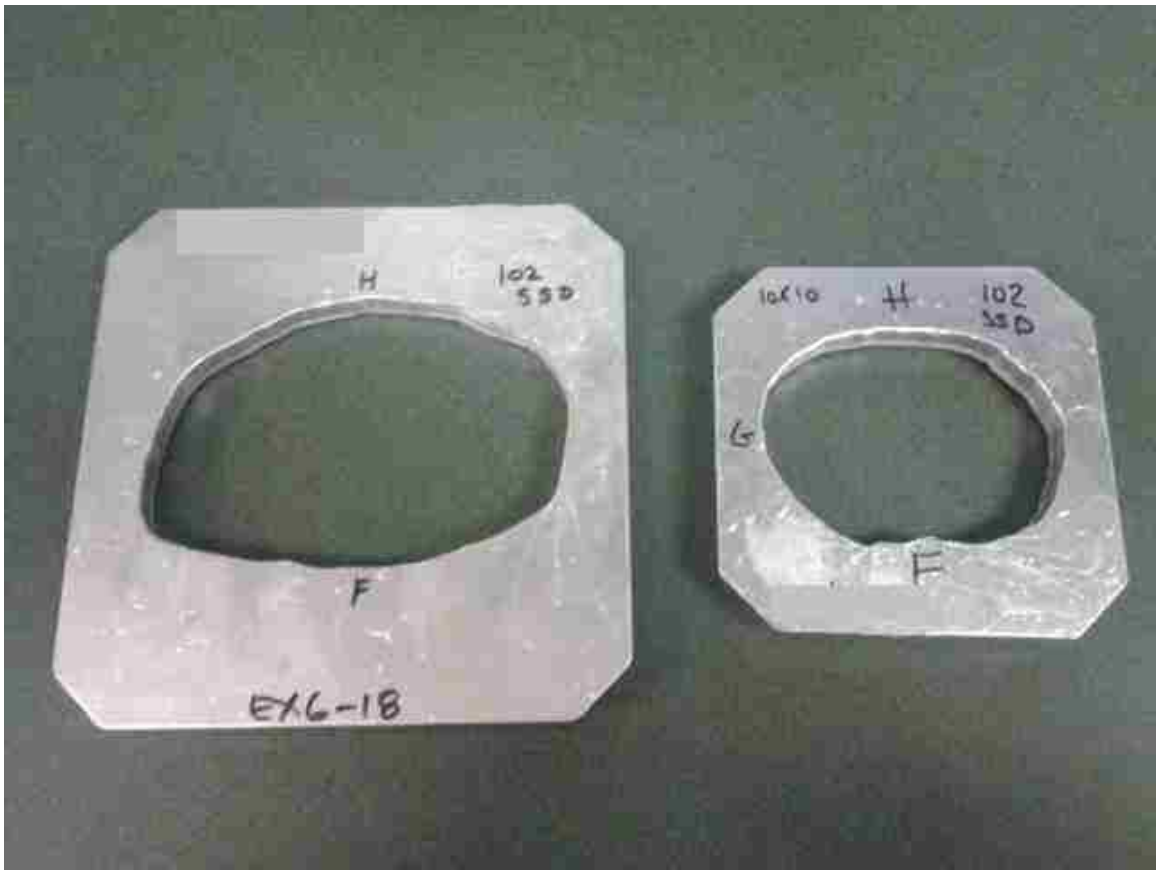

Figure 1.4: Two custom Cerrobend inserts shaped to a patient's PTV. The insert on the left is for a 15x15 cm^2 applicator while the insert on the right is for a 10x10 cm^2 applicator.

1.1.2 Characteristics of Clinical Electron Beams

A percent depth dose (PDD) curve is one of the primary metrics used to quantify the dosimetric properties of an electron beam. A PDD curve shows the central-axis dose as a function of depth. Figure 1.5 shows an example electron central-axis percent depth dose curve measured in water from ICRU Report 35(International Commission on Radiation Units and Measurements., 1972), where relative dose is normalized to 100% at the depth

of maximum dose (R_{100}). For a given energy, the shape of the depth dose curve varies with field size below square fields with sides approximately smaller than $E_{p,o}/2$ in cm, where $E_{p,o}$ is the most probable surface energy in MeV. Beyond this size, increasing the field size has negligible effects on depth dose because the phantom scatter has reached equilibrium. Electrons in water lose their energy predominantly through ionizing events with atomic electrons, resulting in a continuous reduction in beam energy of ~2 MeV/cm. The steep distal falloff is caused by range straggling, which is the scattering and continuous energy loss by the electrons at depths beyond R_{100}.(Jayaraman and Lanzl, 1996) Electron interactions are a stochastic process; an electron experiencing minimal interactions penetrates the maximum distance into a medium, representing the practical range (R_p). The practical range is determined by the intersection of a line tangent to the PDD at a depth of 50% dose (R_{50}) and the extension of the x-ray dose tail to shallower depths. At depths beyond R_p the depth dose curve is not zero due to the dose component from bremsstrahlung photons, D_x. D_x is typically characterized at a depth of $R_p + 1$ cm and is expressed as a percentage of the central-axis maximum dose.

In addition to R_p and D_x, PDD curves are characterized by the dose at the surface, D_s, the depth of the distal 90% relative dose, R_{90}, the depth of 50% dose, R_{50}, and the distance from the 80% to 20% relative dose depths, R_{80-20}. All of these PDD metrics increase with increasing energy over the clinical range of energies (6-20 MeV).

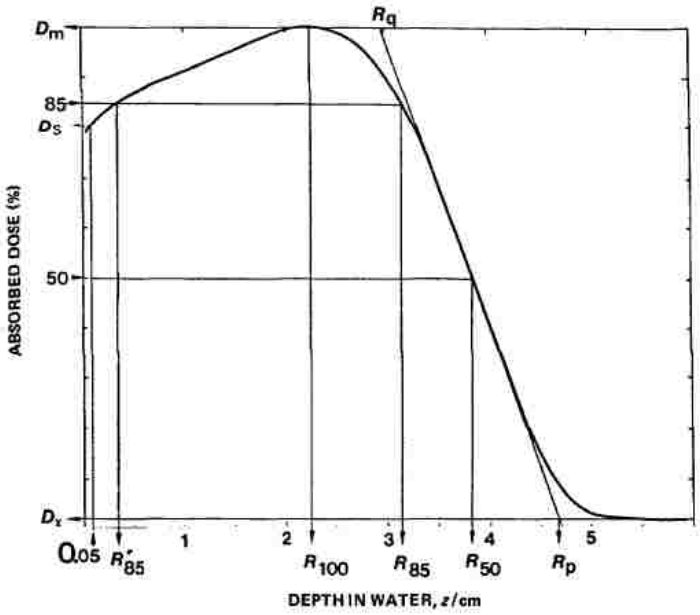

Figure 1.5: Parameters of an electron beam percent depth dose curve from ICRU Report 35(International Commission on Radiation Units and Measurements., 1972).

Along with PDDs, off-axis relative dose profiles are used to quantify the properties of a clinical electron beam. Off-axis relative dose profiles show the dose at a fixed depth as a function of off-axis position, typically normalized to 100% at the central-axis point. The electron energy is assumed to be relatively constant across the lateral dimensions of an electron beam at a given depth and thus the collisional stopping power is also constant. Based on these assumptions, measured off-axis relative ionization profiles are treated as equal to off-axis relative dose profiles at the given depth. Figure 1.6 shows the off-axis relative dose profile for a 12x12 cm^2 field size Cerrobend insert in a 25x25 cm^2 applicator for a beam energy of 12 MeV measured at a depth of 3.0 cm, with the central axis relative ionization normalized to 100%. Off-axis relative dose profiles can be combined with percent depth dose curves to create the 2D relative electron dose distributions.

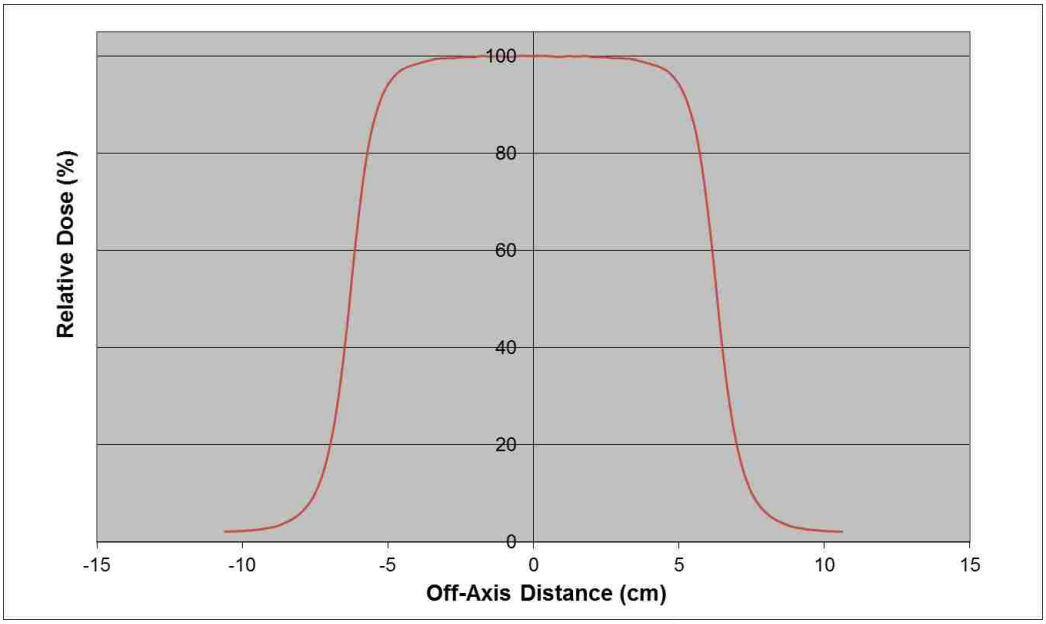

Figure 1.6: Off-axis relative dose profile for a 12x12 cm^2 field size Cerrobend insert in a 25x25 cm^2 applicator for a beam energy of 12 MeV and a depth of 3.0 cm, with the central-axis relative dose normalized to 100%.

The dose delivery rate of a clinical electron beam is characterized by the beam output. Output is determined by measuring the ionization under well-defined reference conditions, e.g. a 10x10 cm^2 open field, 100 cm SSD at R_{100} on the central-axis, compared to the dose rate set during beam commissioning. Ionization measurements under non-reference conditions are benchmarked to a reference ionization measurement to determine relative output. Absolute dose rate at a point is the product of the relative output and the reference output.(Almond *et al.*, 1999)

1.2 Purpose

Custom insert creation requires a separate room for the applicator molds, melting vat, Cerrobend inventory, and safety equipment. These block cutting rooms are primarily used for electron inserts, which typically make up a small percentage (<15%) of total treatments. Many centers only treat with custom electron inserts a few times a year,

making the maintenance of a block cutting room highly inefficient. In-house insert creation also suffers from inconsistencies due to manually cutting Styrofoam and pouring Cerrobend. The effects of those inaccuracies are magnified when there is a need for high precision, such as cases with small field sizes or abutting fields.

Additionally, staff therapists or dosimetrists must be trained in insert creation techniques and proper safety when handling Cerrobend because of the presence of toxic lead and cadmium. The United States Department of Occupational Safety and Health Standards (OSHA) states a time-weighted average permissible exposure limit of 50 µg and 5 µg for lead and cadmium respectively per cubic meter of air for a standard 8 hour workday. These requirements can be met by using fume hoods or ensuring proper ventilation in the block cutting room. Employing an outside vender to mill the patient-specific inserts makes it possible to eliminate block cutting rooms, and use alternative materials, such as copper.

Copper is a durable metal with a physical density (8.96 g/cm^3) similar to Cerrobend (9.4 g/cm^3). Copper is recyclable, environmentally friendly, non-toxic and easily machinable. Additionally copper is more robust than Cerrobend, making it less likely to be damaged from repeated use or accidental drops. Third party vendors such as .decimal Inc. (Sanford, FL) machine custom inserts from patients' treatment planning files, with devices received by the treatment center within 1-3 days of request.(dotdecimal.com)

These vendors can provide precision-milled inserts while the treatment center is spared the cost of maintaining a dedicated block cutting room, staff training, labor costs, and safety precautions normally associated with in-house block creation. In addition, small centers lacking the equipment or training required to create their own inserts can

still treat patients with electron beam therapy using vendor-supplied inserts. Shipment time and cost are two practical disadvantages of using third party vendors.

Of clinical concern when using copper inserts is the validity of commissioning data used for dose calculations in treatment planning systems. Many linear accelerators were commissioned using Cerrobend inserts to determine percent depth dose curves, off-axis relative dose profiles, and output factors. Differences in these dosimetric data between Cerrobend and copper inserts can degrade the accuracy of the treatment planning system's electron dose calculations. Prior to implementing copper inserts for use in patient treatment, it is necessary to investigate dosimetric differences between copper and Cerrobend electron inserts.

The goal of this project was to determine the clinically relevant dosimetric differences caused by the use of copper as compared to Cerrobend inserts used for electron beam therapy. Therefore, standard commissioning beam metrics (PDDs, off-axis relative dose profiles at various depths, and output factors) were measured for a clinically relevant range of applicator sizes (6x6-25x25 cm^2), insert sizes (2x2-20x20 cm^2), energies (6-20 MeV), and SSDs (100 and 110 cm) for the Varian Clinac 21EX at Mary Bird Perkins Cancer Center (Baton Rouge, LA). These beam metrics were combined to generate absolute 2D dose distributions, which were evaluated for clinically significant differences caused by the use of copper inserts compared to Cerrobend inserts.

1.3 Hypothesis and Specific Aims

Hypothesis:

Comparison of 2D dose distributions obtained from matched copper and Cerrobend inserts will show absolute dosimetric differences of less than 2% of the maximum dose or

1 mm distance to agreement for ≥99% of points for all field sizes at SSDs of 100 cm and 110 cm.

Specific Aims:

1. Obtain a matched set of copper and Cerrobend inserts for 9 different field sizes (2x2, 3x3, 4x4, 6x6, 8x8, 10x10, 12x12, 15x15, and 20x20 cm^2) for each available applicator size (6x6, 10x10, 15x15, 20x20, and 25x25 cm^2) for Varian Type III accessories, totaling 32 inserts per material.
2. Measure percent depth dose curves using copper and Cerrobend inserts for all possible field size-applicator combinations for electron energies of 6, 9, 12, 16 and 20 MeV at 100 cm SSD and for a subset of combinations at 110 cm SSD. Measure off-axis relative dose profiles using copper and Cerrobend inserts for a subset of field sizes in the 6x6, 15x15, and 25x25 cm^2 applicators using energies of 6, 12, and 20 MeV at 100 cm and 110 cm SSD. Measure output correction factors (OCF) for all possible field size-applicator combinations for electron energies of 6, 9, 12, 16 and 20 MeV at 100 cm SSD and for a subset of combinations at 110 cm SSD.
3. Quantitatively compare absolute beam dosimetry between copper and Cerrobend inserts using criteria of ±2% of maximum dose or 1 mm distance to agreement.

Chapter 2 Research Design and Methods

2.1 Aim 1: Creation of a Matching Set of Copper and Cerrobend Inserts

Aim 1: Obtain a matched set of copper and Cerrobend inserts for 9 different field sizes (2x2, 3x3, 4x4, 6x6, 8x8, 10x10, 12x12, 15x15, and 20x20 cm^2) for each available applicator size (6x6, 10x10, 15x15, 20x20, and 25x25 cm^2) for Varian Type III accessories, totaling 32 inserts per material.

2.1.1 Creating the Matching Set of Inserts

To compare dosimetric differences between copper and Cerrobend inserts for potential clinical use, dose distributions were measured spanning the clinically relevant range of applicators (6x6 cm^2-25x25 cm^2) and field sizes (2x2 cm^2-20x20 cm^2). Table 2.1 lists all possible field size-applicator combinations. No dose distribution measurements were taken for the open field sizes, such as a 15x15 cm^2 field in the 15x15 cm^2 applicator, because these field size-applicator combinations do not require custom inserts.

The 32 copper inserts were milled by .decimal Inc. along with corresponding aluminum negatives. Both the copper inserts and the aluminum negatives were constructed with crosshairs etched in the material to indicate the center. These negatives were used to create a matching set of Cerrobend inserts in-house at MBPCC. First, the aluminum negatives were centered both laterally and longitudinally inside a mold tray using the etched crosshairs. Next, the molten Cerrobend was poured into the mold tray. Figure 2.1 shows Cerrobend poured into a 15x15 cm^2 applicator mold tray around a centered aluminum negative for a 4x4 cm^2 field, and the resulting Cerrobend insert alongside its matching copper insert. The 32 pairs of matching copper and Cerrobend

inserts are shown in Figure 2.2 and the five Varian Type III electron applicators are shown in Figure 2.3.

Table 2.1: Summary of all insert field size-applicator combinations obtained for dosimetric comparisons A full set was obtained for both copper and Cerrobend.

Field Size (cm)	**Applicator Size (cm)**				
	6x6	**10x10**	**15x15**	**20x20**	**25x25**
2x2	X	X	X	X	X
3x3	X	X	X	X	X
4x4	X	X	X	X	X
6x6		X	X	X	X
8x8		X	X	X	X
10x10			X	X	X
12x12			X	X	X
15x15				X	X
20x20					X

Figure 2.1: (LEFT) Photo of Cerrobend poured into a 15x15 cm^2 applicator mold to generate an insert formed by a 4x4 cm^2 aluminum negative. (RIGHT) The resulting Cerrobend insert alongside its matching copper insert.

Figure 2.2: Full set of 32 matching pairs of copper and Cerrobend inserts. From left to right: 3, 5, 7, 8, and 9 pairs of inserts for the 6x6 cm^2, 10x10 cm^2, 15x15 cm^2, 20x20 cm^2, and 25x25 cm^2 applicators, respectively.

Figure 2.3: All five Varian Type III electron applicators. Pictured from left: 6x6 cm^2, 10x10 cm^2, 15x15 cm^2, 20x20 cm^2, and 25x25 cm^2 applicators.

2.1.2 Quality Assurance of Matching Electron Inserts

Thickness measurements were taken using a digital caliper (SPI, Model No: 1199W-616), which had a manufacturer listed ±0.02 mm precision. The required minimum thickness of lead (t_{Pb}) for shielding an electron beam has been well documented for the

therapeutic energy range of 6-20 MeV (Khan *et al.*, 1991). Shown by Equation 2.1, where $E_{p,o}$ is the most probable energy at the surface (listed in Table 2.2), which was calculated using the beam's practical range (R_p) with an accuracy of 2% in AAPM Task Group (TG) 25.(Khan *et al.*, 1991)

$$t_{Pb}\ (mm) = \frac{E_{p,o}\ (MeV)}{2} \tag{2.1}$$

Density scaling from lead (ρ_{Pb}=11.34 g/cm^3) to Cerrobend ($\rho_{Cerrobend}$=9.38 g/cm^3) and copper (ρ_{Cu}=8.96 g/cm^3) was used to calculate the minimum required thicknesses at each energy and for each material (Equations 2.2 and 2.3), summarized in Table 2.2.

$$t_{Cerrobend}\ (mm) = \frac{\rho_{Pb}}{\rho_{Cerrobend}} t_{Pb}(mm) \tag{2.2}$$

$$t_{Cu}\ (mm) = \frac{\rho_{Pb}}{\rho_{Cu}} t_{Pb}(mm) \tag{2.3}$$

Copper inserts must be ~5.5% thicker than Cerrobend to achieve the same electron shielding due to their relative densities. Inserts were poured to be of sufficient thickness for the highest energy, a standard procedure for clinical practice, which allows the same insert to be used at all energies.

Table 2.2: Minimum thickness necessary to shield electron beams using Cerrobend and copper inserts for the five beam energies available on the MBPCC Varian Clinac 21EX. All inserts were poured to accommodate the highest energy.

Nominal Beam Energy (MeV)	Most Probable Energy $E_{p,o}$ (MeV)	Minimum Thickness-Cerrobend (mm)	Minimum Thickness-Copper (mm)
6	5.95	3.6	3.8
9	8.76	5.3	5.5
12	12.51	7.6	7.9
16	16.36	9.9	10.4
20	19.68	11.9	12.5

In addition, the field size of each insert was measured using a digital caliper with ±0.02 mm precision, except for the largest field size (20x20 cm^2), which was measured using a ruler with 0.5 mm precision. Each square field size in the X and Y direction along the central axis was measured and compared.

2.2 Aim 2: Measurement of Dosimetric Data

Aim 2: Measure percent depth dose curves using copper and Cerrobend inserts for all possible field size-applicator combinations for electron energies of 6, 9, 12, 16 and 20 MeV at 100 cm SSD and for a subset of combinations at 110 cm SSD. Measure off-axis relative dose profiles using copper and Cerrobend inserts for a subset of field sizes in the 6x6, 15x15, and 25x25 cm^2 applicators using energies of 6, 12, and 20 MeV at 100 cm and 110 cm SSD. Measure output correction factors (OCF) for all possible field size-applicator combinations for electron energies of 6, 9, 12, 16 and 20 MeV at 100 cm SSD and for a subset of combinations at 110 cm SSD.

2.2.1 Linear Accelerator

Electron beam dosimetric data was measured at MBPCC on a Varian Clinac 21EX 4/10 linear accelerator (SN: 1412), following the guidelines from TG-106.(Das *et al.*, 2008) Electron energies available were 6, 9, 12, 16, 20 MeV. Applicators used were Varian Type III accessories in sizes of 6x6, 10x10, 15x15, 20x20, and 25x25 cm^2.

2.2.2 Electron Diode Detector

Commissioning data are typically measured in water using an ion chamber or silicon-diode detector. Ion chambers measure the charge liberated by radiation in a known volume of air, and then the absorbed dose in water is determined by applying energy and depth-dependent corrections. Silicon-diode detectors measure ionization in the active

region of the diode, where it is assumed that ionization is proportional to dose, i.e. correction factors are energy independent. Therefore diode detectors can directly measure relative dose. Because diodes are also more sensitive than ion chambers, they have smaller active volumes, which gives greater spatial resolution. Unshielded diodes are known to over respond to lower energy scattered photons, which is why they are not typically used for large photon fields; however this effect is small for electron dosimetry. Thus, dose measurements were made using a p-type electron dosimetry diode detector (IBA EFD^{3G}, #300-605) with an active volume diameter of 2 mm and thickness of 0.06 mm.

The diode was connected to the beam scanning main control unit (MCU), which contained an internal electrometer for PDD and off-axis relative dose profile measurements. For output measurements the diode was connected to an external calibrated electrometer. This arrangement allowed the use of the 2D scanning motors to precisely place the diode at depths for output readings using the MCU software. Since the diode and water phantom setup remained unchanged between scans and output measurements, the setup also ensured consistency in the geometry for all measurements.

2.2.3 Water Phantom and Scanner

All PDDs, off-axis relative dose profiles, and output measurements (100 cm SSD) were taken in a RFA-200 Water Phantom 2D scanning tank using OmniPro scanning software (IBA Dosimetry). The phantom was leveled in all directions to assure scanning would be aligned with the electron beam. The diode was placed near the center of the phantom and the couch adjusted laterally and longitudinally to align the diode with the center of the light field from the linear accelerator. The couch was adjusted vertically to

the desired SSD using mechanical distance indicators. Periodically the SSD was verified by using the optical distance indicator (ODI). The diode was then visually set even to the surface of the water and its position zeroed in the scanning software, which automatically adjusted for the known effective measurement location. Because of the long duration of scanning, care was taken to maintain a constant water level. The water level was checked regularly throughout the day and water added to compensate for any evaporation. Figure 2.4 shows the water phantom setup.

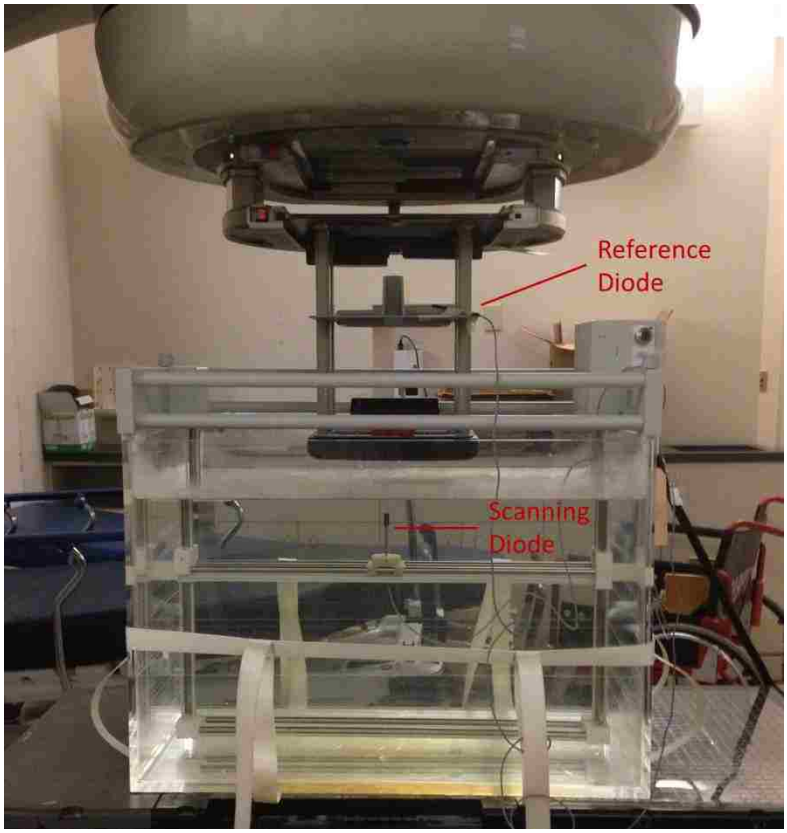

Figure 2.4: Water phantom setup used for 2D beam scanning. The scanning electron diode is shown positioned in the water, and the reference diode upstream from the insert as discussed in section 2.2.4.

2.2.4 Quality Control

A reference diode was placed in the corner of the field, upstream of the insert tray, as shown in Figure 2.4, to serve as a background reading and to properly adjust the

electrometer gain. Care was taken to ensure the reference diode was placed so as to not block the central scanning area of the beam. At the beginning and end of each day of measurements, QA was performed by measuring a 9 MeV PDD using the open field size in whichever applicator was being used for the measurements that day. The beginning-of-day and end-of-day PDDs were then compared to ensure that the R_{50} values were within a tolerance of ±0.1 cm. This ensured that the energy of the 9 MeV beam had not changed throughout the day, that the beam scanner was aligned properly, and that the diode and electrometer were functioning properly. The 9 MeV beam was chosen because of the sharp falloff in the PDD which facilitates R_{50} measurement, while also having greater depth of penetration than the lower energies.

Quality assurance for the mechanical scanning equipment was performed by taking three consecutive PDD scans of the 9 MeV beam at least once per day. Verifying that the R_{50} values of the three scans were within a tolerance of ±0.05 cm ensured that the mechanical components of the 2D scanning phantom were operating properly.

2.2.5 Measurement Subsets

Measurement subsets were chosen to span the range of clinical applications in terms of energy, field size and SSD. Off-axis relative dose profiles, were measured for copper and Cerrobend inserts using three energies (6, 12, and 20 MeV) at 100 cm and 110 cm SSD for the field size-applicator combinations shown in Table 2.3. This subset was also used for measuring PDD curves and outputs at 110 cm SSD. This subset was chosen to sample field sizes using the smallest, middle, and largest sized applicators available on the Varian machine. Most clinical electron beam treatments use an energy, SSD, and field size/applicator size geometry in the range covered by this subset.

Table 2.3: Measurement subset for off-axis relative dose profile measurements using energies 6, 12 and 20 MeV at 100 cm and 110 cm SSD. This measurement subset was also used for PDD and output measurements at 110 cm SSD.

Field Size (cm)	Applicator Size (cm)				
	6x6	10x10	15x15	20x20	25x25
2x2	X		X		X
3x3	X				X
4x4	X		X		X
6x6					X
8x8			X		X
10x10					X
12x12			X		X
15x15					X
20x20					X

A more extensive subset was used for measuring PDD curves and outputs at 100 cm SSD. These measurements were taken at all five available energies (6, 9, 12, 16, and 20 MeV) for all field size-applicator combinations (Table 2.1).

2.2.6 Percent Depth Dose Curves

PDD curves were measured using the OmniPro® scanning software with a 1 mm step size and low scan speed in precision mode. All beam scans followed the guidelines described by TG-25(Khan *et al.*, 1991; Gerbi *et al.*, 2009) and TG-51(Almond *et al.*, 1999). PDD scans were made from deeper to shallower depths, beginning at depths of 8, 12, and 14 cm for energies of 6, 12 and 20 MeV respectively. Each scan's final measurement point was 0.05 cm above the surface of the water to ensure correct placement of the diode. The PDDs were measured immediately prior to the off-axis relative dose profiles for each insert. These PDDs were used to compare beam metrics and to create isodose plots for evaluation and comparison, as described in Section 2.3. PDD curves measured at 9 and 16 MeV were used for comparison of beam metrics only.

2.2.7 Off-Axis Relative Dose Profiles

Off-axis relative dose profiles were measured with the OmniPro® scanning software using a step size of 2 mm and a low scan speed in precision mode. A scan consisted of off-axis profiles measured at a number of depths beginning 0.5 cm below the surface of the water. The number and depths of the off-axis relative dose profiles was selected for each energy to acquire data in the high gradient regions and to cover the entire practical range of the beam. Eleven off-axis profiles were measured for 6 MeV beams (depths of 0.5, 1, 1.5, 2, 2.25, 2.5, 2.75, 3, 3.5, 4, and 5 cm), 15 profiles for 12 MeV beams (depths of 0.5, 1, 1.5, 2, 2.5, 3, 3.5, 4, 4.5, 5, 5.5, 6, 6.5, 7, and 8 cm), and 22 profiles for 20 MeV beams (depths of 0.5, 1, 1.5, 2, 2.5, 3, 3.5, 4, 4.5, 5, 5.5, 6, 6.5, 7, 7.5, 8, 8.5, 9, 9.5, 10, 11, and 12 cm). Accounting for beam divergence at depth, penumbra margins of 4 cm were added to the field edge at the deepest profile and that width was used for all profile measurements. This allowed for construction of a full 2D dose grid which included the out-of-field dosimetry.

2.2.8 Output Correction Factors

Electron beam outputs were measured at 100 cm SSD using a 2D water phantom and at 110 cm SSD using a 1D water phantom (Standard Imaging, DoseView 1D). Dose measurements were taken at R_{100} using an external electrometer (CNMC Model 206 dosimetry electrometer) and the same electron diode used for the PDDs and off-axis relative dose profile measurements. The internal electrometer of the MCU was not designed for measuring output. A cable connecting the diode to the external electrometer outside of the vault allowed for easy transition between the MCU and the external

electrometer. This setup allowed for both beam scanning and outputs to be measured without any changes to the measurement geometry.

Electron inserts placed into the mounting tray of an applicator can potentially shift slightly in all directions. Therefore, initial off-axis profile scans were taken with each new insert to check centering of the insert in the mounting tray, with the insert being adjusted if necessary. Each centering profile was taken in-plane at a depth of 1 cm. Inserts were considered properly centered if the measured off-axis profile centers were <0.05 cm from the beam center, with couch adjustments used to align the diode with the beam center as necessary. Cross-plane centering was done using a ruler to center the insert within the beam crosshairs for Cerrobend inserts, and using the etched crosshairs for the copper inserts.

After ensuring the insert was properly centered, a PDD was measured to determine R_{100}. Using OmniPro®, the diode was repositioned to R_{100}. The diode detector was then disconnected from the MCU and connected to the external electrometer. Three electrometer readings were recorded, each with the machine delivering 200 monitor units (MUs) and then averaged. Cerrobend and copper insert outputs were measured at the R_{100} corresponding to Cerrobend; the average difference in the R_{100} value for matching Cerrobend and copper inserts was less than 0.1 cm, as determined from measured PDDs. This process was repeated for all five beam energies for a single Cerrobend insert, and then repeated for the matching copper insert immediately afterwards. Consecutively measuring the matching Cerrobend and copper inserts resulted in less than 30 minutes passing between measurement sets of the same energy and insert size for the two materials.

The OCFs were computed from both the copper and Cerrobend output readings at 100 cm SSD and 110 cm SSD for the measurement subsets shown Table 2.1 and Table 2.3, respectively. The output correction factor was the ratio of the average copper output reading at the R_{100} for Cerrobend divided by the average Cerrobend output reading at the R_{100} for Cerrobend for a particular applicator-field size combination, where each output reading has been corrected to the output at R_{100} using the measured PDDs, as shown in Equation 2.4. The output correction is necessary because the Cerrobend and copper outputs were measured at R_{100} for Cerrobend. By definition, $\%DD^{Cerrobend}(R_{100}^{Cerrobend})$ is 1.0 but $\%DD^{Copper}\left(R_{100}^{Cerrobend}\right)$ is the percent dose for the copper PDD at the measurement depth of R_{100} for Cerrobend

$$OCF = \frac{O^{Copper}(R_{100}^{Cerrobend})}{O^{Cerrobend}(R_{100}^{Cerrobend})} \times \frac{\%DD^{Cerrobend}(R_{100}^{Cerrobend})}{\%DD^{Copper}(R_{100}^{Cerrobend})} \tag{2.4}$$

The small field electron diode measurements of the OCFs showed unexpected trends. As a secondary check of these measurements, OCFs were measured using a thimble ionization chamber for all available field sizes (2x2 cm^2 – 8x8 cm^2) in the 10x10 cm^2 applicator for all five energies at 100 cm SSD. These OCFs were compared to those obtained with the electron diode.

2.2.9 Validation of Diode Dosimeter

Depth-ionization curves measured with cylindrical ionization chambers must be converted to depth-dose curves by applying a gradient correction accounting for the chambers effective point of measurement and correcting for changes in stopping power ratios at depth. Depth-dose curves measured in water with diode detectors do not require stopping power corrections. However, diode detectors have been shown to have some

variation due to orientation, temperature, radiation damage incurred by the sensitive volume, and have been shown to overestimate the photon background by up to 1% in some cases.(Khan *et al.*, 1991; Rikner, 1985) Silicon diodes can be used to accurately measure relative dose distributions for high energy electron beams (Figure 2.5), but it is recommended that their accuracy be compared to an ionization chamber measurement.(Khan *et al.*, 1991)

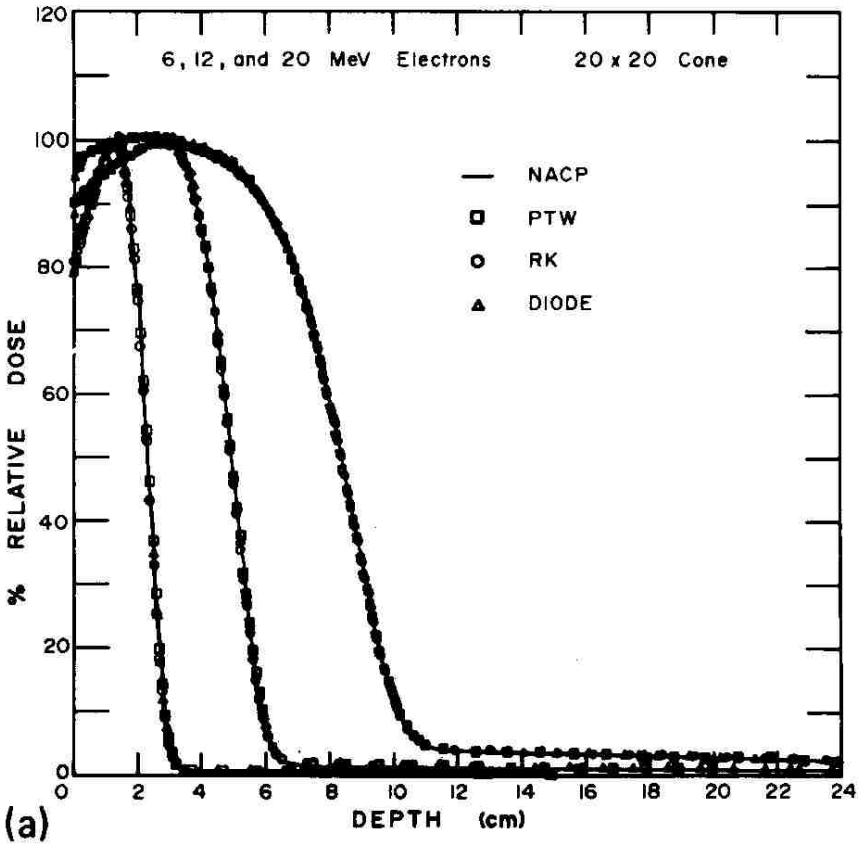

Figure 2.5: Percent depth dose curves obtained by various detectors on a Clinac 1800 at 6, 12, and 20 MeV using a 20x20 cm^2 cone at 100 cm SSD in a water phantom. Measurements were taken with a Nordic Association of Clinical Physicists (NACP) parallel-plate ionization chamber, PTW 0.1 cm^3 thimble ionization chamber, RK 0.1 cm^3 thimble ionization chamber, and an RFA-3 p-type silicon diode detector.(Ten Haken *et al.*, 1987)

PDDs measured with the electron diode described in Section 2.2.2 were compared with those made using a PTW Semiflex Thimble Ionization Chamber (model #31010) with an internal sensitive volume of 0.125 cm^3. A small thimble ionization chamber was used instead of a traditional Farmer chamber to increase the accuracy of the ionization readings for small fields. The center of the ion chamber was positioned at the surface of the water and then shifted, using the Omni pro software, so that the chamber's effective measurement position was at the surface, the scanning system depth was then reset to zero. Percent depth dose curves were measured with both Cerrobend and copper inserts for a field size of 12x12 cm^2 in a 20x20 cm^2 applicator at all five energies (6, 9, 12, 16, and 20 MeV) using both detectors. In addition, electron diode measurements were compared to the accelerator commissioning data. All PDDs were normalized to 100% at D_{max} and shifted to match R_{50} before comparisons.

2.3 Aim 3: Comparison of Beam Dosimetry

Aim 3: 3. Quantitatively compare absolute beam dosimetry between copper and Cerrobend inserts using criteria of ±2% of maximum dose or 1 mm distance to agreement.

2.3.1 Data Processing

Prior to the comparison of absolute beam dosimetry, post processing of the raw data in Omni pro was done in the following order. (1) PDD data were normalized to 100% at the depth of maximum dose; (2) off-axis relative dose profiles were centered; (3) off-axis profiles were symmetrized using the mean value from both sides; (4) profiles were renormalized to the central axis value (from the PDD). No smoothing filters were applied to any scan.

2.3.2 Creation of Relative 2D Dose Distributions

Relative 2D dose distributions are planar dose distributions containing the central axis and the major axis in the transverse direction, normalized such that the central axis dose maximum is 100%. Measured percent depth dose and off-axis relative dose profile data were used to create 2D isodose plots for each combination of applicator, field size, energy, SSD and material. As an example, the 22 off-axis relative dose profiles and central axis PDD acquired for the 15x15 cm^2 field size Cerrobend insert in the 25x25 cm^2 applicator at 20 MeV and 100 cm SSD are shown in Figure 2.6.

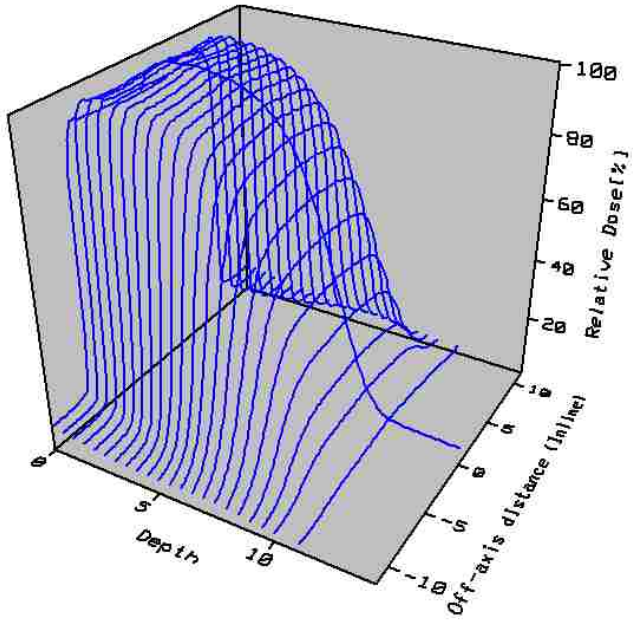

Figure 2.6: Acquired PDD and off-axis relative dose profile data for a 15x15 cm^2 field size in a 25x25 cm^2 Cerrobend applicator for 20 MeV at 100 cm SSD.

The PDD and off-axis relative dose profile data were linearly interpolated into a 2D matrix using Matlab. Relative doses, $D_{Relative}(x,z)$, at each point in the 2D distribution were calculated (Equation 2.5) by linearly interpolating at depth using the PDD and

transversely using the profile off-axis ratios OAR(x), where OAR(x,z) is linearly interpolated at (x,z) locations not directly measured.

$$D_{Relative}(x,z) = PDD(z) \times OAR(x,z) \tag{2.5}$$

Each isodose matrix was calculated with 1 mm resolution in both depth and off-axis dimensions. The maximum depth was that of the deepest off-axis relative dose profile, and the matrix width extended 4 cm past the deepest off-axis profile's beam edge. The depth of each matrix matched the deepest off axis relative dose profile of 5, 8, and 12 cm for beam energies of 6, 12, and 20 MeV respectively.

2.3.3 Creation of Absolute 2D Dose Distributions

The OCFs were used to scale the relative dose matrices for copper inserts to create absolute dose distributions. Absolute 2D dose distributions are the relative dose distributions normalized such that 100% corresponds to the central-axis dose measurement at R_{100} for Cerrobend (Equation 2.6 and 2.7).

$$D_{Absolute}^{Copper}(x,z) = D_{Relative}^{Copper}(x,z) \times OCF \tag{2.6}$$

$$D_{Absolute}^{Cerrobend}(x,z) = D_{Relative}^{Cerrobend}(x,z) \tag{2.7}$$

Absolute 2D dose distributions for matching copper and Cerrobend inserts under the same geometry (i.e. applicator, field size, energy, SSD) were overlaid with isodose lines plotted for visual interpretation of the dose distributions.

2.3.4 Comparison Criteria

To implement copper inserts clinically without re-commissioning, the dosimetric differences between copper and Cerrobend inserts must be negligible. Annual quality assurance procedures from TG-40 (Kutcher *et al.*, 1994) and TG-142 (Klein *et al.*, 2009) recommend measuring a subset of the commissioning data and comparing to the baseline data to determine dosimetric accuracy, as was done in this study. The dosimetric tolerances described by these Task Group reports were used as a comparison criteria.

Cerrobend and copper insert dosimetry data were compared quantitatively by using a Matlab code on dose distributions with the same delivery geometry. Using a 2%/1 mm criteria, the superimposed dose distributions were checked at each point for agreement to within 2% of the central axis maximum dose for Cerrobend, i.e. the 100% point, or a point which agrees within a radius of 1 mm. The percentage of points passing the criteria was recorded. Any comparison containing failing points were re-analyzed using a 3%/1-mm criteria.

The dosimetric criteria of ±2% of maximum dose or ±1 mm distance to agreement (DTA) was based on the TG-40 and TG-142 reports as a metric of clinical impact. Analysis was performed using the percent of maximum dose difference rather than simply the percent difference because of the greater clinical significance of percent of maximum dose. An out-of-field region may show a dose comparison between points of 1% and 0.9% of the maximum dose. Although the absolute percent difference between the points is much larger than 2%, the percent difference in terms of maximum dose (0.1%) shows the dosimetric variance between the two points is clinically insignificant.

Chapter 3 Results and Discussion

3.1 Aim 1: Creation of a Matching Set of Copper and Cerrobend Inserts

Aim 1: Obtain a matched set of copper and Cerrobend inserts for 9 different field sizes (2x2, 3x3, 4x4, 6x6, 8x8, 10x10, 12x12, 15x15, and 20x20 cm^2) for each available applicator size (6x6, 10x10, 15x15, 20x20, and 25x25 cm^2) for Varian Type III accessories, totaling 32 inserts per material.

The Cerrobend and copper inserts were not identical. Unlike the Cerrobend inserts, the copper inserts from .decimal included etched cross hairs centered in the X/Y plane to aid alignment in the tray. Also, due to the nature of manually pouring Cerrobend into molds, the thickness of each Cerrobend insert varied from the planned thickness, whereas the milled copper inserts had more consistent thicknesses.

3.1.1 Thickness Comparison Between Copper and Cerrobend Inserts

Thickness measurements for each insert are shown for copper in Table 3.1 and for Cerrobend in Table 3.2. The milled copper inserts ranged in thickness from 14.63 mm to 14.95 mm. The average measured thickness of all the copper inserts was 14.80 mm with a standard deviation of 0.07 mm. Cerrobend inserts ranged in thickness from 11.03 mm to 14.56 mm. The average measured thickness of all Cerrobend inserts was 12.46 mm with a standard deviation of 0.89 mm. Both the standard deviation and the maximum difference of thicknesses of the Cerrobend inserts were more than ten times greater than those of the milled copper inserts. The method used in this study for manually pouring the molten Cerrobend did not allow the same precision in thickness as the milled copper inserts.

Table 3.1: Measured thicknesses of copper inserts from .decimal, Inc. in mm. The recommended minimum thickness for copper required to stop a 20 MeV beam is 12.5 mm. Precision of the digital caliper was ±0.02 mm for all measurements.

Field Size (cm)	**Applicator Size (cm)**				
	6x6	**10x10**	**15x15**	**20x20**	**25x25**
2x2	14.75	14.82	14.95	14.76	14.89
3x3	14.82	14.71	14.90	14.83	14.85
4x4	14.76	14.81	14.94	14.81	14.81
6x6		14.74	14.81	14.76	14.87
8x8		14.74	14.82	14.80	14.80
10x10			14.72	14.77	14.90
12x12			14.63	14.73	14.85
15x15				14.69	14.77
20x20					14.89

Table 3.2: Measured thicknesses of hand poured Cerrobend inserts in mm. The recommended minimum thickness for Cerrobend required to stop a 20 MeV beam is 11.9 mm, and those of lesser value are bolded. Precision of the digital caliper was ±0.02 mm for all measurements.

Field Size (cm)	**Applicator Size (cm)**				
	6x6	**10x10**	**15x15**	**20x20**	**25x25**
2x2	13.23	**11.34**	12.36	**11.11**	**11.46**
3x3	13.57	12.31	12.22	**11.07**	**11.87**
4x4	13.35	12.71	**11.27**	12.71	**11.03**
6x6		12.44	13.05	12.71	**11.71**
8x8		12.63	12.36	14.56	12.20
10x10			13.11	13.31	**11.07**
12x12			12.59	13.04	12.57
15x15				13.88	13.53
20x20					12.33

Minimum thickness of copper and Cerrobend needed to stop electron beams at the energies measured are shown in Table 2.2. The average thickness of both material inserts was adequate for shielding the highest energy being measured (20 MeV). All 32 copper inserts were above the recommended minimum thickness (12.5 mm) to stop electron beams at 20 MeV, while 23 of 32 Cerrobend inserts were above the recommended minimum thickness (11.9 mm). The thinnest Cerrobend insert was 0.9 mm less than the

recommended thickness for shielding 20 MeV beams. All inserts met the thickness recommendations for 6, 9, 12, and 16 MeV.

Electron transmission measurements for copper and lead (Cerrobend has a density 83% that of lead) are shown in Figure 3.1.(Das *et al.*, 2004) The electron dose transmission at 20 MeV levels off at ~10% at thicknesses over ~14 mm for copper and ~10 mm for lead (equivalent to 12 mm Cerrobend), which is near the 14.63 mm and 11.03 mm minimum thickness for the copper and Cerrobend inserts respectively. The electron transmitted dose ($D\text{-}D_{bremsstrahlung}$) is less than 2% of maximum dose with no shielding in this range, with residual levels being due to bremsstrahlung produced photons, rather than electron transmission. Therefore small variations in shielding thickness in this range have little impact on the total electron transmission, so differences in electron transmission through the copper and Cerrobend inserts is expected to be negligible.

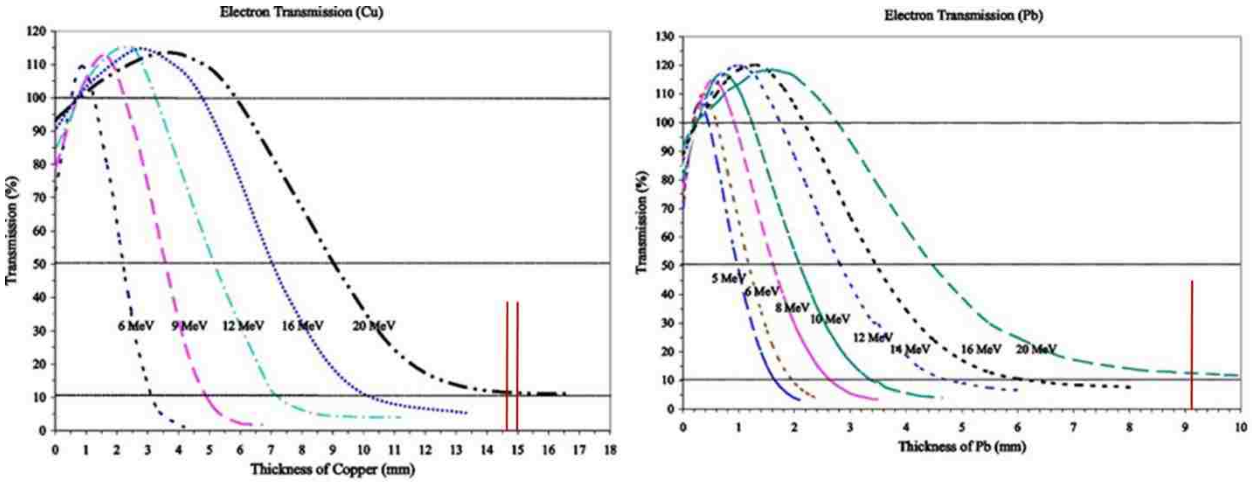

Figure 3.1: Electron transmission through copper and lead shielding from Das et al.(Das *et al.*, 2004) The range of thickness in both the copper (14.63-14.95 mm) and lead equivalent for Cerrobend (9.12-12.04 mm) inserts are shown by red lines on each plot. The highest range of the Cerrobend insert thickness is not pictured because it is beyond the range of the plot.

3.1.2 Field Size Comparison Between Copper and Cerrobend Inserts

The average difference between the X and Y field size for every insert was 0.07 mm with a standard deviation of 0.08 mm for copper and 0.15 mm with a standard deviation of 0.13 mm for Cerrobend. The mean of the X and Y measurements for each insert formed the average field size. Comparing the average field sizes between matching copper and Cerrobend inserts, the average difference (Cerrobend minus copper) in field sizes was 0.15 mm with a standard deviation of 0.10 mm and a maximum difference of 0.33 mm. These differences are negligible (<0.5 mm) and the copper and Cerrobend inserts were treated as having the same field sizes.

3.2 Aim 2: Measurement of Dosimetric Data

Aim 2: Measure percent depth dose curves using copper and Cerrobend inserts for all possible field size-applicator combinations for electron energies of 6, 9, 12, 16 and 20 MeV at 100 cm SSD and for a subset of combinations at 110 cm SSD. Measure off-axis relative dose profiles using copper and Cerrobend inserts for a subset of field sizes in the 6x6, 15x15, and 25x25 cm^2 applicators using energies of 6, 12, and 20 MeV at 100 cm and 110 cm SSD. Measure output correction factors (OCF) for all possible field size-applicator combinations for electron energies of 6, 9, 12, 16 and 20 MeV at 100 cm SSD and for a subset of combinations at 110 cm SSD.

3.2.1 Preparation and Daily Quality Assurance

Scanning system quality assurance from all measurement days passed the criteria of consecutive PDDs having R_{50} values within ±0.05 cm, with the standard deviation in R_{50} of consecutive PDD measurements being 0.005 cm. The average difference in the beginning-of-day minus the end-of-day R_{50} values from each day of measurements were

-0.01 cm ±0.04 cm, less than the ±0.1 cm criteria. Figure 3.2 shows the beginning-of-day QA measurements from October 25, 2013 in the form of three consecutive PDDs, and Figure 3.3 shows an enlarged view of the tail region of the depth dose curves indicating stability of the beam and beam scanner. These plots showed no clinically significant differences between the three scans. This data was representative of the daily QA results, specifically there were no failures of mechanical QA checks.

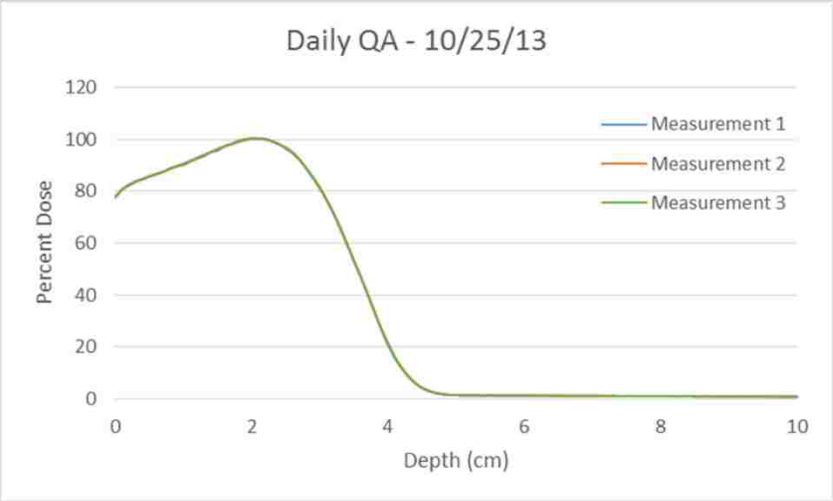

Figure 3.2: Three consecutive percent depth dose curves from a daily quality assurance before measurements on October 25th, 2013 using an open 25x25 cm^2 field at 100 cm SSD.

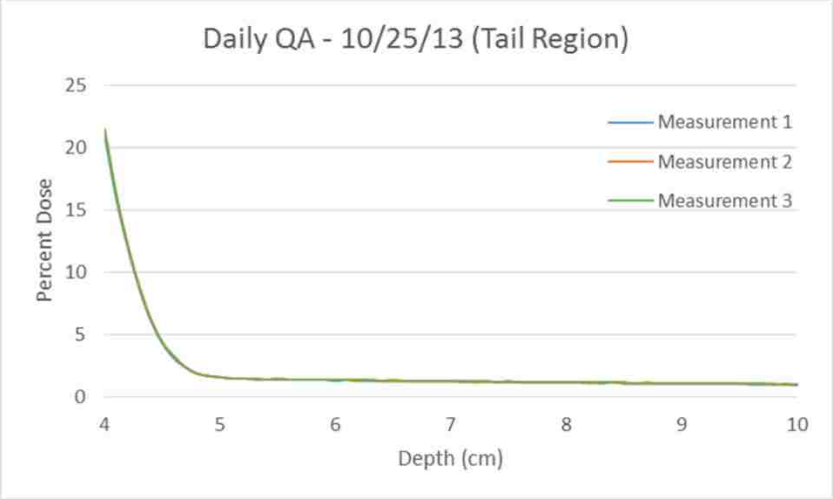

Figure 3.3: Enlarged view of the tail region from the daily QA measurements from October 25th, 2013.

3.2.2 Validation of Diode Dosimeter

PDDs at all 5 energies showed negligible differences between the corrected ion chamber measurements and the diode measurements. Figure 3.4 compares PDDs measured with an ionization chamber and an electron diode for a 12x12 cm^2 field size in a 20x20 cm^2 applicator with a Cerrobend insert at energies of 6, 9, 12, 16, and 20 MeV. The close agreement between the detector comparisons provided verification of the electron diode measurements.

The 6 MeV beam PDDs showed small differences (~0.07 cm) in the fall off region (near R_{90}) possibly due to the machine energy drift. These differences were only seen at the highest gradient fall off of the 6 MeV beam. PDDs for 9 MeV to 20 MeV only showed differences of note in the tail region of the PDDs deeper than R_p. The diode detector measured a larger D_x compared to the ion chamber at all energies. The higher D_x values from the electron diode detector was consistent with the study by Rikner et al.'s comparison of diode and parallel-plate ionization chamber measurements.(Rikner, 1985) Diode readings of D_x were larger compared to the ion chamber readings at all energies, as shown in Table 3.3.

In addition, all PDDs measured with the electron diode agreed with the machine's commissioning percent depth dose data at 100 cm SSD to within ±0.1 cm for R_{50}. Table 3.4 shows a comparison of R_{50} and R_{100} data for the diode measurements and commissioning data.

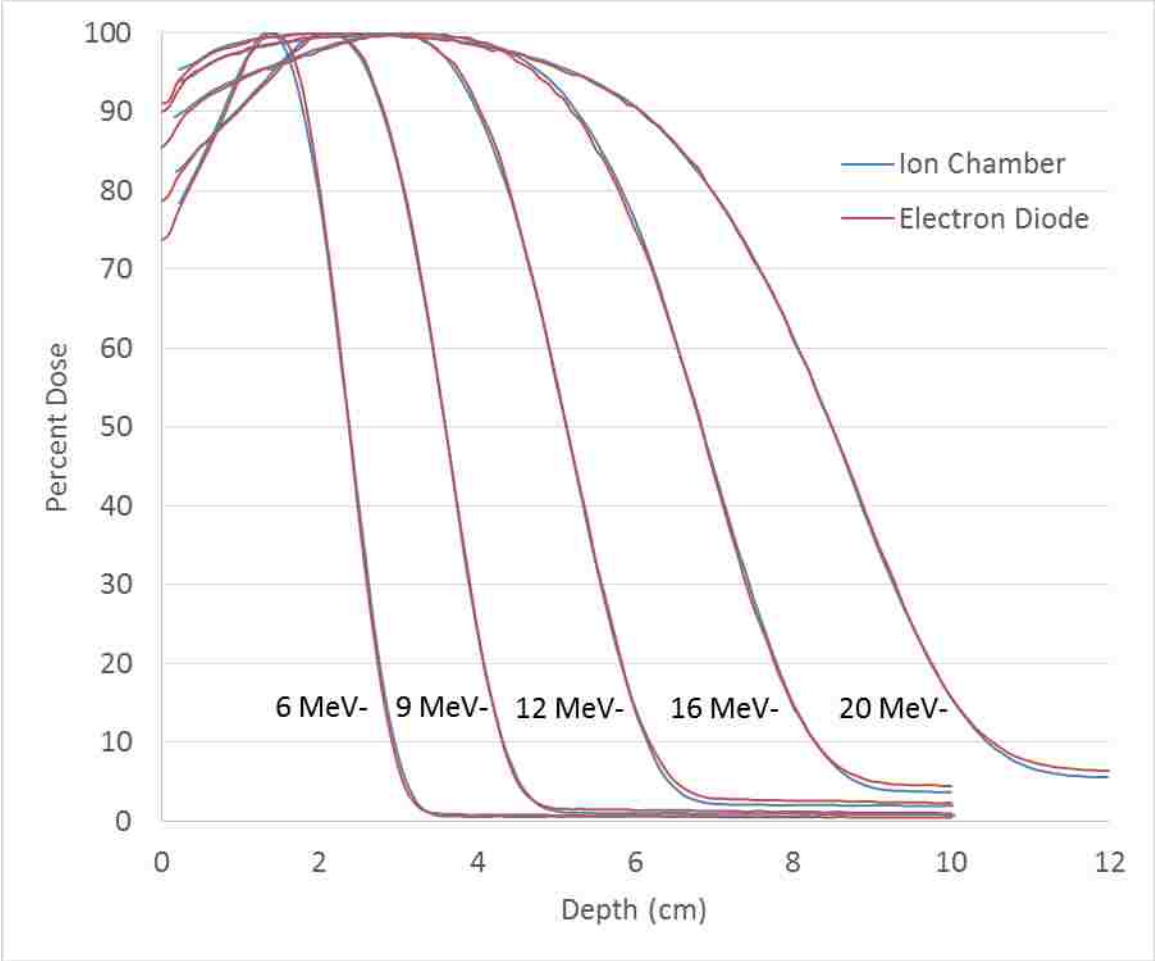

Figure 3.4: Comparison of ionization chamber and electron diode measured PDDs for a 12x12 cm^2 field size in a 20x20 cm^2 applicator with a Cerrobend insert at energies of 6, 9, 12, 16, and 20 MeV.

Table 3.3: D_x measured in a 12x12 cm^2 field size insert in a 25x25 cm^2 applicator at energies of 6, 9, 12, 16, and 20 MeV with the electron diode and ionization chamber.

Energy	Electron Diode (%)	Ion Chamber (%)	Difference (%)
6 MeV	0.60	0.54	0.06
9 MeV	1.00	0.77	0.23
12 MeV	2.30	1.98	0.32
16 MeV	4.47	3.71	0.76
20 MeV	6.40	5.52	0.88

Table 3.4: Percent depth dose data measured using a 12x12 cm^2 field size insert in a 20x20 cm^2 applicator at 100 cm SSD with the electron diode compared to the commissioning data for the Varian Clinac 21EX. Depth of 50% maximum dose (R_{50}) and depth of 100% maximum dose (R_{100}) are shown in cm.

Energy	Diode-R_{50}	Commissioning-R_{50}	Diode-R_{100}	Commissioning-R_{100}
6 MeV	2.38	2.4	1.41	1.4
9 MeV	3.60	3.6	2.13	2.2
12 MeV	5.13	5.2	2.95	3.0
16 MeV	6.84	6.8	3.11	3.3
20 MeV	8.46	8.4	2.25	2.3

Although there were differences as large as 0.9% at depths beyond R_p for 9-20 MeV or as large as 0.07 cm at R_{90} for 6 MeV, they should have no impact on the differences in dose between copper and Cerrobend inserts.

3.2.3 Percent Depth Dose Curves at 100 cm SSD

Percent depth dose curves at 100 cm SSD were measured for all field size (2x2-20x20 cm^2) and applicator (6x6-25x25 cm^2) combinations shown in Table 2.1 for all energies 6-20 MeV using both Cerrobend and copper inserts (Appendix A). PDDs showed negligible (<1%/1 mm) differences between copper and Cerrobend in the surface, peak and fall-off regions. Measured percent depth dose curve comparisons between copper and Cerrobend at 100 cm SSD are shown for all energies and a series of field sizes in the 25x25 cm^2 applicator (Figure 3.5) and the 10x10 cm^2 applicator (Figure 3.6).

Percent depth dose metrics were compared at 100 cm SSD for the 160 pairs of PDDs arising from the 32 field size and applicator size combinations, five energies, and two materials. Metrics included R_{50}, R_{90}, and $R_{80\text{-}20}$. The dose at 1.0 cm depth ($D_{1.0}$) was also compared between the inserts to examine dose differences at shallow depths. The differences in each of these metrics between matching copper and Cerrobend inserts at

the same energy were calculated by taking the Cerrobend value minus the copper value. All data is recorded in Appendix A.

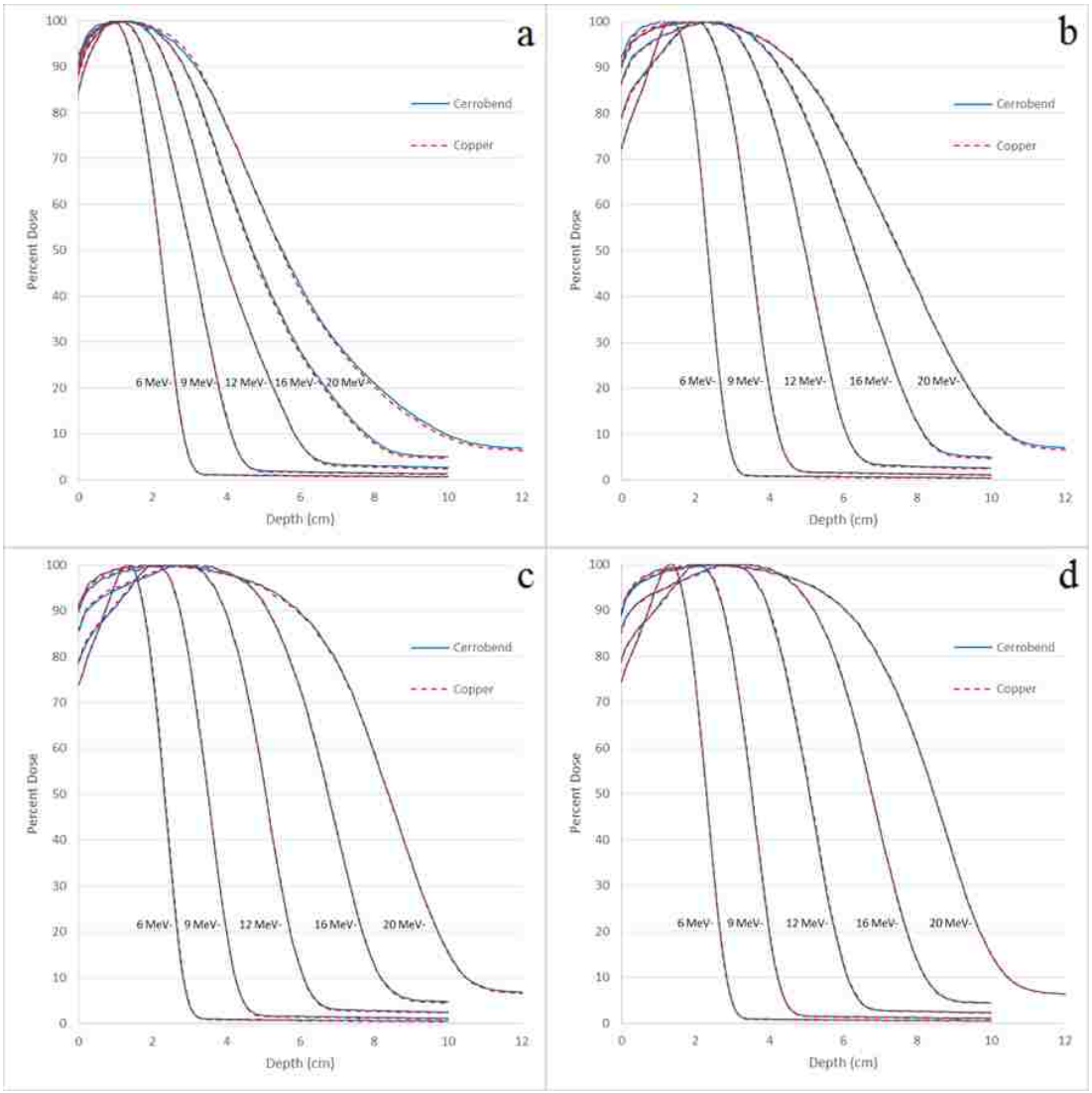

Figure 3.5: Comparison plots of PDDs for different field sizes in the 25x25 cm^2 applicator at 100 cm SSD. Field sizes shown are (a) 2x2 cm^2, (b) 4x4 cm^2, (c) 12x12 cm^2 and (d) 20x20 cm^2.

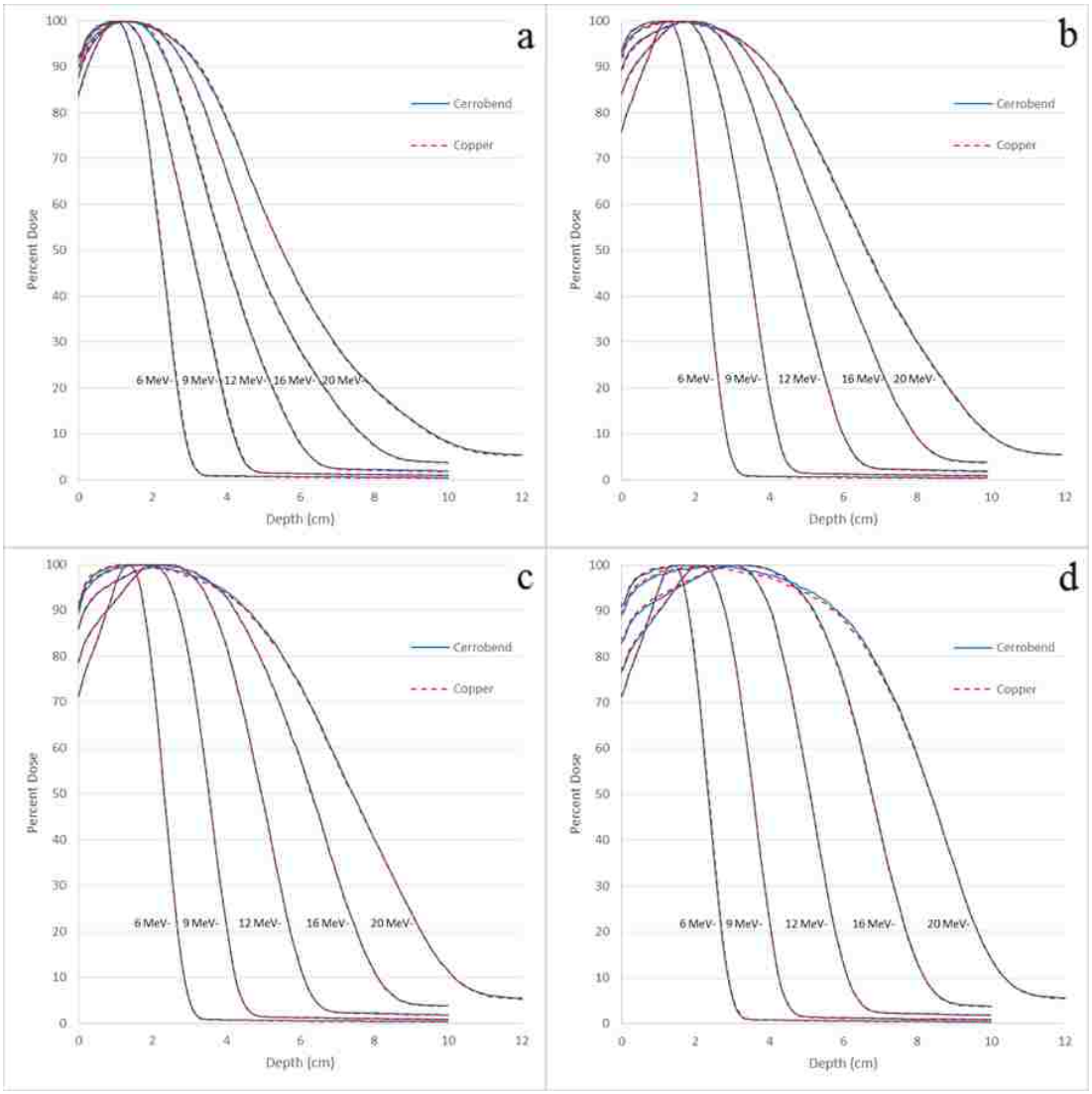

Figure 3.6: Comparison plots of PDDs for different field sizes in the 10x10 cm^2 applicator at 100 cm SSD. Field sizes shown are (a) 2x2 cm^2, (b) 3x3 cm^2, (c) 4x4 cm^2 and (d) 8x8 cm^2.

The average value of the differences with standard deviations between matching Cerrobend and copper insert PDDs by field size (cm^2) and energy (MeV) are shown for R_{50} (Table 3.5), R_{90} (Table 3.6), $R_{80\text{-}20}$ (Table 3.7), and $D_{1.0}$ (Table 3.8). All PDD metric comparisons showed negligible differences (<0.1 cm) between copper and Cerrobend inserts, with a maximum absolute difference of 0.07 cm for R_{50}, 0.13 cm for R_{90}, and 0.08 cm for $R_{80\text{-}20}$. The maximum difference in $D_{1.0}$ between the two materials was -0.90% of

central axis dose maximum. The average differences and individual metric values can be found in Appendix A for all insert combinations at 100 cm SSD.

Table 3.5: Differences (Cerrobend minus copper) in R_{50} (cm) between matching Cerrobend and copper insert PDDs measured at 100 cm SSD, averaged by field size (cm^2) and energy (MeV) across all applicators with standard deviations. Standard deviations were not calculated for the 20x20 cm^2 field size because only one PDD was measured for this field size.

Field Size (cm)	Energy				
	6 MeV	9 MeV	12 MeV	16 MeV	20 MeV
2x2	0.01±0.01	0.01±0.01	0.02±0.02	0.01±0.01	0.02±0.02
3x3	0.00±0.01	0.01±0.01	0.01±0.01	0.01±0.02	0.02±0.02
4x4	0.02±0.03	0.01±0.02	0.02±0.02	0.02±0.02	0.02±0.03
6x6	0.01±0.01	0.02±0.01	0.02±0.01	0.00±0.01	0.01±0.01
8x8	0.01±0.01	0.01±0.01	0.01±0.01	0.01±0.00	0.00±0.01
10x10	0.01±0.01	0.01±0.01	0.01±0.01	0.00±0.01	0.01±0.02
12x12	0.01±0.01	0.01±0.02	0.01±0.01	0.01±0.01	0.01±0.00
15x15	0.01±0.01	0.02±0.01	0.01±0.01	0.02±0.01	0.01±0.01
20x20	0.00	0.01	0.01	0.00	0.00

Table 3.6: Differences (Cerrobend minus copper) in R_{90} (cm) between matching Cerrobend and copper insert PDDs measured at 100 cm SSD, averaged by field size (cm^2) and energy (MeV) across all applicators with standard deviations. Standard deviations were not calculated for the 20x20 cm^2 field size because only one PDD was measured for this field size.

Field Size (cm)	Energy				
	6 MeV	9 MeV	12 MeV	16 MeV	20 MeV
2x2	0.01±0.01	0.01±0.01	0.02±0.02	0.03±0.02	0.04±0.02
3x3	0.01±0.01	0.01±0.01	0.01±0.01	0.02±0.01	0.03±0.03
4x4	0.00±0.01	0.01±0.01	0.01±0.01	0.02±0.01	0.03±0.02
6x6	0.01±0.01	0.02±0.01	0.01±0.01	0.01±0.01	0.06±0.05
8x8	0.01±0.02	0.02±0.01	0.01±0.01	0.02±0.01	0.04±0.03
10x10	0.01±0.01	0.01±0.01	0.01±0.02	0.02±0.02	0.06±0.02
12x12	0.01±0.01	0.00±0.01	0.02±0.01	0.01±0.01	0.05±0.03
15x15	0.01±0.01	0.01±0.00	0.02±0.01	0.02±0.00	0.04±0.01
20x20	0.01	0.01	0.01	0.03	0.01

Table 3.7: Differences (Cerrobend minus copper) in R_{80-20} (cm) between matching Cerrobend and copper insert PDDs measured at 100 cm SSD, averaged by field size (cm^2) and energy (MeV) across all applicators with standard deviations. Standard deviations were not calculated for the 20x20 cm^2 field size because only one PDD was measured for this field size.

Field Size (cm)	Energy				
	6 MeV	9 MeV	12 MeV	16 MeV	20 MeV
2x2	0.00±0.00	0.00±0.01	0.01±0.01	0.03±0.01	0.05±0.02
3x3	0.00±0.00	0.01±0.01	0.01±0.01	0.01±0.01	0.03±0.02
4x4	0.00±0.01	0.00±0.01	0.01±0.01	0.01±0.01	0.02±0.01
6x6	0.00±0.01	0.00±0.00	0.00±0.01	0.00±0.00	0.03±0.02
8x8	0.01±0.00	0.00±0.01	0.01±0.01	0.01±0.01	0.02±0.02
10x10	0.00±0.00	0.01±0.01	0.01±0.01	0.00±0.01	0.01±0.01
12x12	0.01±0.01	0.01±0.01	0.00±0.01	0.01±0.00	0.02±0.01
15x15	0.01±0.00	0.00±0.00	0.01±0.00	0.01±0.01	0.00±0.01
20x20	0.01	0.00	0.01	0.02	0.01

Table 3.8: Differences in $D_{1.0}$ (% of maximum dose, Cerrobend-copper) between matching Cerrobend and copper insert PDDs measured at 100 cm SSD, averaged by field size (cm^2) and energy (MeV) across all applicators with standard deviations. Standard deviations were not calculated for the 20x20 cm^2 field size because only one PDD was measured for this field size.

Field Size (cm)	Energy				
	6 MeV	9 MeV	12 MeV	16 MeV	20 MeV
2x2	-0.02±0.11	-0.12±0.28	0.02±0.36	0.14±0.18	0.00±0.16
3x3	-0.10±0.22	0.08±0.28	-0.06±0.18	0.16±0.11	0.06±0.43
4x4	0.14±0.46	0.10±0.19	-0.06±0.26	-0.10±0.07	0.06±0.43
6x6	-0.15±0.37	-0.23±0.19	-0.10±0.29	-0.17±0.33	0.13±0.30
8x8	-0.07±0.10	-0.15±0.21	-0.52±0.30	-0.25±0.17	-0.07±0.26
10x10	0.00±0.46	-0.10±0.10	-0.17±0.15	-0.27±0.15	-0.27±0.31
12x12	0.37±0.21	-0.40±0.36	-0.60±0.10	-0.53±0.21	-0.27±0.25
15x15	-0.05±0.35	-0.15±0.64	-0.35±0.35	-0.45±0.07	-0.05±0.49
20x20	0.10	0.20	-0.10	-0.20	0.40

3.2.4 Percent Depth Dose Curves at 110 cm SSD

Percent depth dose curves at 110 cm SSD were measured for the subset of field size-applicator combinations listed in Table 2.3 for energies of 6 MeV, 12 MeV, and 20 MeV. The PDDs showed negligible differences between copper and Cerrobend in the surface, peak and fall-off regions. Measured PDD comparisons between copper and Cerrobend at

110 cm SSD are shown in Figure 3.7 for all energies and a series of field sizes in the 25x25 cm^2 applicator.

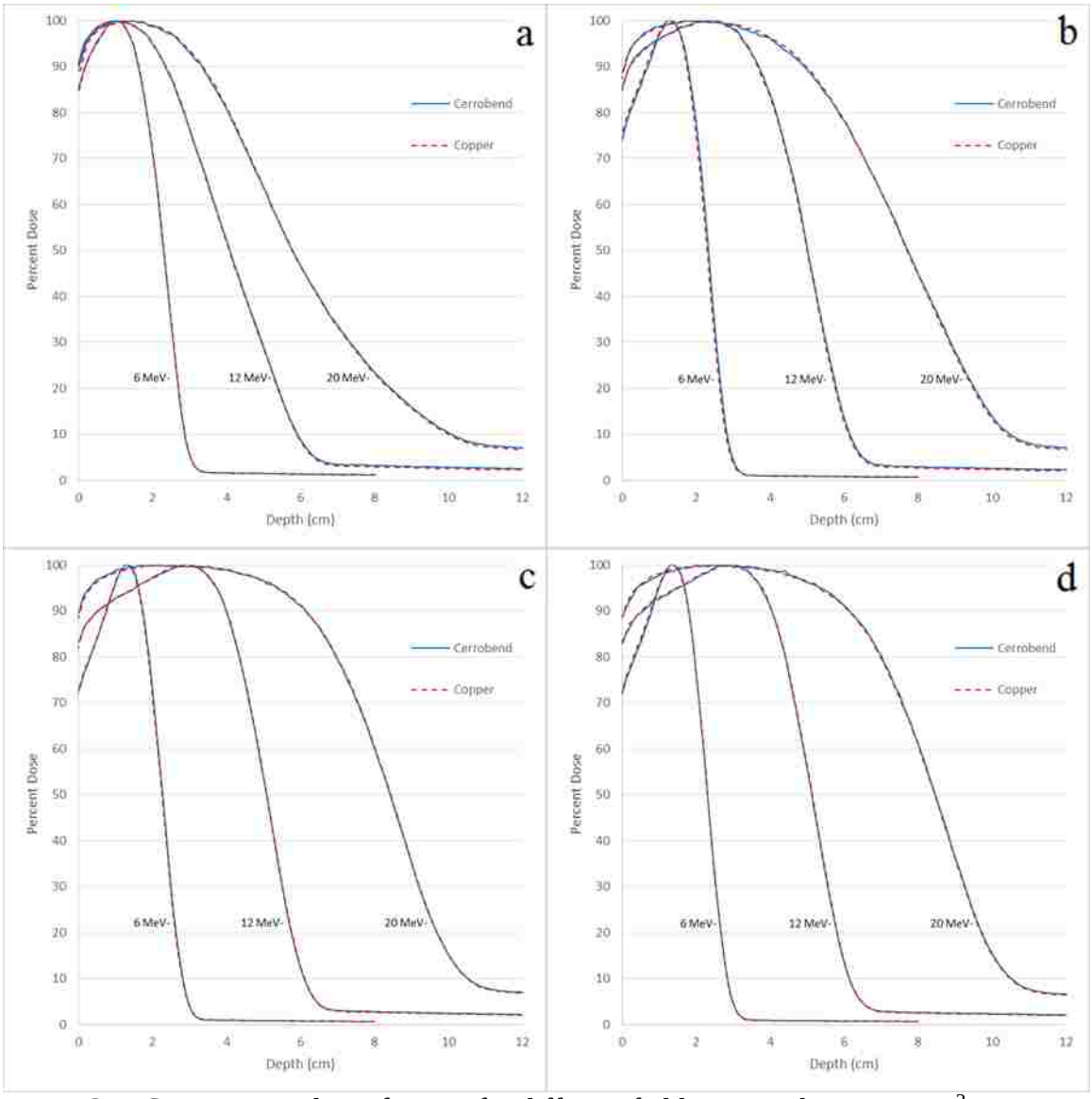

Figure 3.7: Comparison plots of PDDs for different field sizes in the 25x25 cm^2 applicator at 110 cm SSD. Field sizes shown are (a) 2x2 cm^2, (b) 4x4 cm^2, (c) 12x12 cm^2 and (d) 20x20 cm^2.

The same percent depth dose metrics were compared at 110 cm SSD as 100 cm SSD for the 48 pairs of PDDs arising from 16 field size/applicator size combinations, 3 energies, and 2 materials. All differences and individual metric values at 110 cm SSD can

be found in Appendix B. The differences in each of these metrics at the same energy were calculated by taking the Cerrobend values minus the copper values; all data are tabulated in Appendix B.

Tables 3.8-3.11 list the average value of these differences including standard deviation between matching Cerrobend and copper insert PDDs by field size (cm^2) and energy (MeV) for R_{50} (Table 3.9), R_{90} (Table 3.10), R_{80-20} (Table 3.11), and $D_{1.0}$ (Table 3.12). All PDD metric comparisons showed negligible differences between copper and Cerrobend inserts, with a maximum difference of 0.01 cm for R_{50}, -0.09 cm for R_{90}, and 0.09 cm for R_{80-20}. The maximum difference in $D_{1.0}$ between the two materials was 0.80% of central axis dose maximum.

Table 3.9: Differences (Cerrobend minus copper) in R_{50} (cm) between matching Cerrobend and copper insert PDDs measured at 110 cm SSD, averaged by field size (cm^2) and energy (MeV) across all applicators with standard deviations. Standard deviations were not calculated for the 6x6, 10x10, 15x15, and 20x20 cm^2 field sizes because only one PDD was measured for these field sizes.

Field Size (cm)	Energy		
	6 MeV	12 MeV	20 MeV
2x2	0.00±0.01	0.00±0.00	0.00±0.00
3x3	0.00±0.00	0.00±0.00	0.00±0.00
4x4	0.00±0.00	0.00±0.00	0.00±0.00
6x6	0.00	0.00	0.01
8x8	0.00±0.00	0.00±0.00	0.00±0.00
10x10	0.00	0.00	0.00
12x12	0.00±0.00	0.00±0.00	0.00±0.00
15x15	0.00	0.00	0.00
20x20	0.00	0.00	0.00

Table 3.10: Differences (Cerrobend minus copper) in R_{90} (cm) between matching Cerrobend and copper insert PDDs measured at 110 cm SSD, averaged by field size (cm^2) and energy (MeV) across all applicators with standard deviations. Standard deviations were not calculated for the 6x6, 10x10, 15x15, and 20x20 cm^2 field sizes because only one PDD was measured for these field sizes.

Field Size (cm)	Energy		
	6 MeV	12 MeV	20 MeV
2x2	0.00±0.01	0.01±0.01	0.04±0.05
3x3	0.01±0.01	0.00±0.00	0.04±0.05
4x4	0.00±0.01	0.01±0.01	0.00±0.01
6x6	0.00	0.00	0.00
8x8	0.00±0.00	0.01±0.01	0.01±0.01
10x10	0.00	0.00	0.00
12x12	0.01±0.01	0.01±0.01	0.02±0.01
15x15	0.00	0.00	0.00
20x20	0.01	0.01	0.02

Table 3.11: Differences (Cerrobend minus copper) in $R_{80\text{-}20}$ (cm) between matching Cerrobend and copper insert PDDs measured at 110 cm SSD, averaged by field size (cm^2) and energy (MeV) across all applicators with standard deviations. Standard deviations were not calculated for the 6x6, 10x10, 15x15, and 20x20 cm^2 field sizes because only one PDD was measured for these field sizes.

Field Size (cm)	Energy		
	6 MeV	12 MeV	20 MeV
2x2	0.01±0.00	0.02±0.01	0.05±0.05
3x3	0.01±0.01	0.02±0.00	0.03±0.04
4x4	0.00±0.01	0.01±0.01	0.03±0.02
6x6	0.01	0.00	0.03
8x8	0.01±0.01	0.00±0.01	0.03±0.01
10x10	0.00	0.00	0.00
12x12	0.01±0.01	0.01±0.00	0.00±0.00
15x15	0.01	0.01	0.00
20x20	0.01	0.00	0.03

Table 3.12: Differences in $D_{1.0}$ (% of maximum dose, Cerrobend-copper) between matching Cerrobend and copper insert PDDs measured at 110 cm SSD, averaged by field size (cm^2) and energy (MeV) across all applicators with standard deviations. Standard deviations were not calculated for the 6x6, 10x10, 15x15, and 20x20 cm^2 field sizes because only one PDD was measured for these field sizes.

Field Size (cm)	Energy		
	6 MeV	12 MeV	20 MeV
2x2	-0.10±0.46	0.03±0.32	0.33±0.45
3x3	0.15±0.21	0.25±0.07	-0.05±0.35
4x4	-0.23±0.06	0.13±0.06	-0.03±0.31
6x6	-0.10	0.50	0.50
8x8	0.10±0.00	0.20±0.14	0.05±0.35
10x10	0.00	0.30	0.50
12x12	-0.15±0.35	-0.10±0.00	0.25±0.49
15x15	-0.10	-0.50	0.10
20x20	-0.30	-0.40	-0.40

3.2.5 Central Axis Photon Dose

The maximum difference in central axis dose due to x-rays is shown for 100 cm SSD in Table 3.13 and for 110 cm SSD in Table 3.14. Differences and individual D_x values for all insert combinations are listed in Appendix A (100 cm SSD) and Appendix B (110 cm SSD). Percent depth dose curves showed little variation between copper and Cerrobend at depths smaller than the practical range (R_P) for all energies and field size combinations. However, the bremsstrahlung tail region of the PDDs did show consistent differences (≥0.1%) at energies 12 MeV and higher. As energy and applicator size increased, the difference in D_x (Cerrobend minus copper) increased.

The x-ray contamination of electron beams is caused by bremsstrahlung photons being created through electron interactions with the beam line components, such as internal scattering foils, ionization chambers, collimators, and custom electron inserts.(International Commission on Radiation Units and Measurements., 1972)

However, only a portion of the overall X-ray contamination dose is generated by the electron insert.

Table 3.13: Maximum difference in D_x (% of maximum dose, Cerrobend minus copper) between matching Cerrobend and copper insert PDDs measured at 100 cm SSD, by field size (cm^2) and energy (MeV) across all applicators. Included with the maximum difference is the applicator size corresponding to the measurement (1=6x6 cm^2, 2=10x10 cm^2, 3=15x15 cm^2, 4=20x20 cm^2, and 5=25x25 cm^2).

Field Size (cm)	Energy				
	6 MeV	9 MeV	12 MeV	16 MeV	20 MeV
2x2	-0.10 (3)	0.20 (5)	0.30 (5)	0.50 (4,5)	0.50 (4,5)
3x3	0.10 (4)	0.10 (4,5)	0.20 (4,5)	0.30 (4,5)	0.30 (4,5)
4x4	-0.10 (1,2)	0.10 (3,5)	0.20 (5)	0.40 (5)	0.40 (5)
6x6	-0.10 (2)	0.20 (5)	0.20 (5)	0.40 (5)	0.40 (5)
8x8	0.00	0.20 (5)	0.20 (5)	0.40 (5)	0.30 (5)
10x10	0.00	0.00	0.20 (5)	0.20 (4,5)	0.40 (5)
12x12	0.10 (5)	0.00	0.10 (3,4,5)	0.30 (5)	0.30 (5)
15x15	0.00	0.00	0.10 (5)	0.20 (5)	0.20 (4,5)
20x20	0.00	0.00	0.10 (5)	0.00	0.10 (5)

Table 3.14: Maximum difference in D_x (% of maximum dose, Cerrobend minus copper) between matching Cerrobend and copper insert PDDs measured at 110 cm SSD, averaged by field size (cm^2) and energy (MeV) across all applicators. Included with the maximum difference is the applicator size corresponding to the measurement (3=15x15 cm^2, and 5=25x25 cm^2).

Field Size (cm)	Energy		
	6 MeV	12 MeV	20 MeV
2x2	0.00	0.20 (5)	0.30 (5)
3x3	0.00	0.10 (5)	0.20 (5)
4x4	0.10 (5)	0.20 (5)	0.20 (5)
6x6	0.00	0.10 (5)	0.40 (5)
8x8	0.00	0.20 (5)	0.30 (5)
10x10	0.00	0.20 (5)	0.30 (5)
12x12	0.00	0.10 (3,5)	0.20 (5)
15x15	0.00	0.10 (5)	0.20 (5)
20x20	0.10 (5)	0.10 (5)	0.10 (5)

Bremsstrahlung production increased with the surface area of the insert material in the beam. A 2x2 cm^2 field size in a 25x25 cm^2 applicator has 19.4 times more insert material being struck by the electron beam than a 2x2 cm^2 field size in a 6x6 cm^2

applicator (Figure 3.8). Figure 3.9 plots D_x vs. energy and applicator size for a 2x2 cm^2 field size Cerrobend insert. D_x increased with energy as well as applicator size. Field sizes closer to the applicator size (2x2 cm^2 field in 6x6 cm^2 or 10x10 cm^2 applicator) showed little differences in the x-ray dose from copper and Cerrobend inserts. Increasing the applicator size resulted in D_x values from Cerrobend inserts being higher than those from copper inserts, as shown in Figure 3.10. This increased bremsstrahlung production to the center of the field can result in up to a 0.5% of maximum dose increase in central axis dose for Cerrobend inserts compared to copper inserts for the 2x2 cm^2 field size in the 25x25 cm^2 applicator at 20 MeV.

The ratio of relative bremsstrahlung production between copper and Cerrobend inserts should be approximately proportional to the relative radiative stopping powers, which was estimated using the atomic numbers (Z_{Copper}=29, $Z_{Cerrobend}$=76.84) and atomic mass numbers (A_{Copper}=63.55 g/mol, $A_{Cerrobend}$=186.84 g/mol) as shown in Equation 3.1.(International Commission on Radiation Units and Measurements., 1972) This calculation resulted in an estimation that the bremsstrahlung photon production due to the electron insert should be approximately 2.3 times larger from Cerrobend inserts compared to copper inserts. Because the production of bremsstrahlung photons is forward peaked at these energies, the amount of photons reaching the center of the field (D_x) is expected to be lower than the 2.3 times estimation. A further discussion on the differences in bremsstrahlung production between copper and Cerrobend inserts can be found in Section 3.3.1.

$$\frac{D_x^{Cerrobend}}{D_x^{Copper}} \propto \frac{Z_{Cerrobend}(Z_{Cerrobend}+1)}{Z_{Copper}(Z_{Copper}+1)} \times \frac{A_{Copper}}{A_{Cerrobend}} \tag{3.1}$$

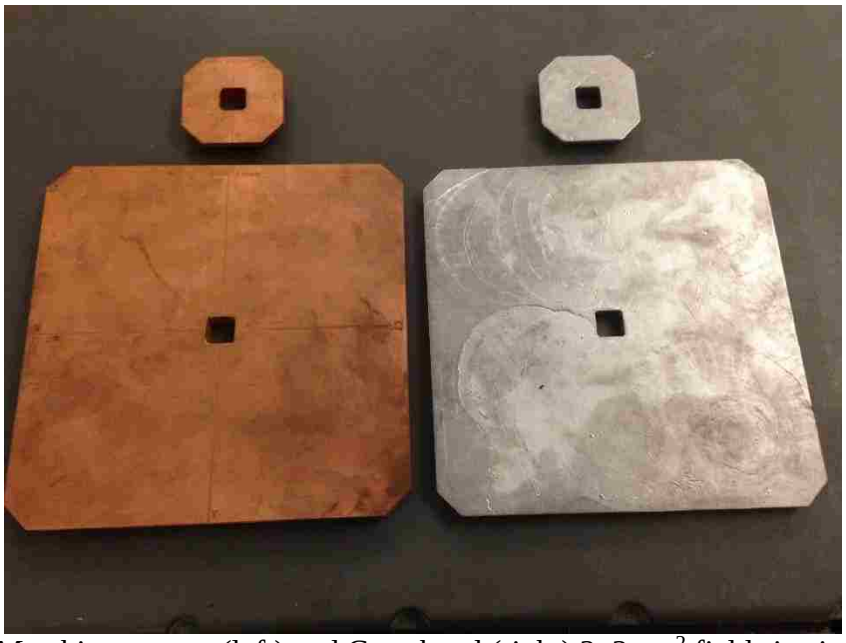

Figure 3.8: Matching copper (left) and Cerrobend (right) 2x2 cm^2 field size inserts for a 6x6 cm^2 applicator (top) and a 25x25 cm^2 applicator (bottom). The larger applicator insert has 621 cm^2 surface area while the smaller applicator insert has 32 cm^2 surface area.

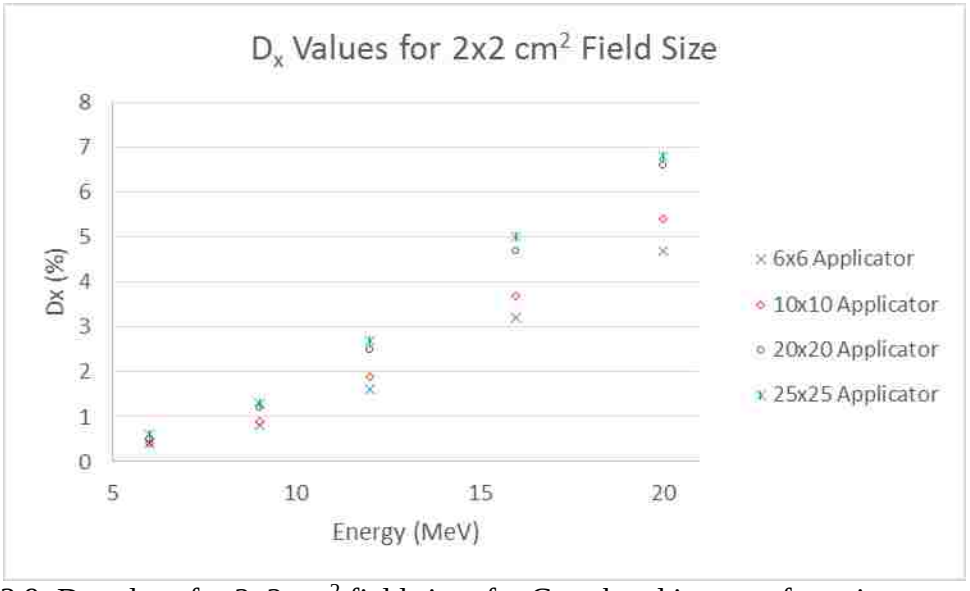

Figure 3.9: D_x values for 2x2 cm^2 field sizes for Cerrobend inserts of varying energies and applicator sizes at 100 cm SSD.

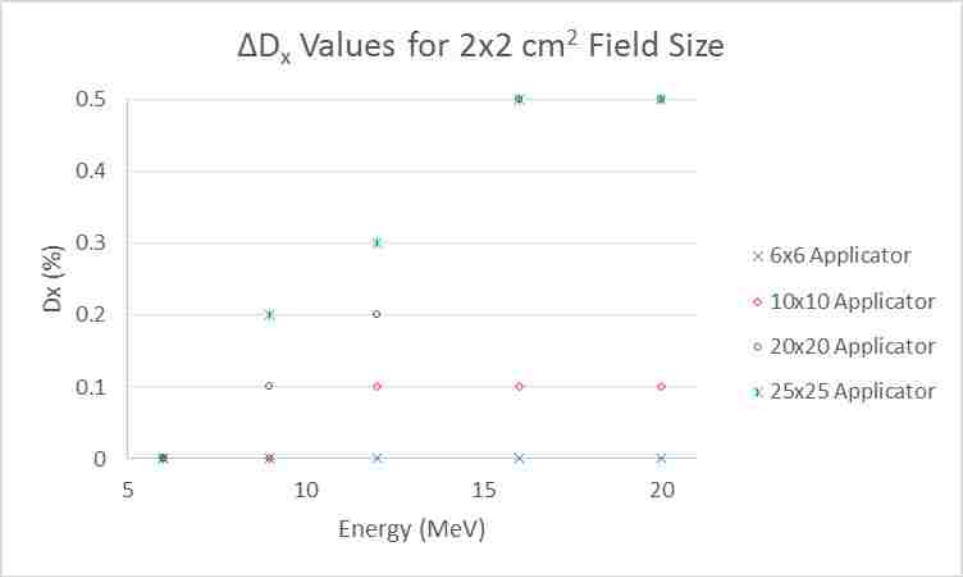

Figure 3.10: ΔD_x values (Cerrobend-Copper) for 2x2 cm^2 field size inserts of varying energies and applicator sizes at 100 cm SSD.

3.2.6 Off-Axis Relative Dose Profiles

Off-axis relative dose profiles for matching copper and Cerrobend inserts were measured consecutively without changes to the water phantom or diode setup. Therefore, the small adjustments in symmetry and centering of the off-axis profiles post-measurement had negligible effects on the dosimetric comparison. The average shift for Cerrobend insert measurements (0.04 cm) and copper insert measurements (0.04 cm) were the same. Figure 3.11 shows the 15 off-axis relative dose profiles measured for the 4x4 cm^2 Cerrobend insert in a 15x15 cm^2 applicator at 100 cm SSD using a 12 MeV beam and each normalized at depth to the central axis dose maximum.

Measured off-axis relative dose profiles from copper and Cerrobend inserts had good overall agreement for all energies, SSDs, and insert/applicator combinations with differences predominantly <2% of maximum dose. The observed dosimetric differences were located near the beam edge and in out-of-field regions, as shown in Figure 3.12.

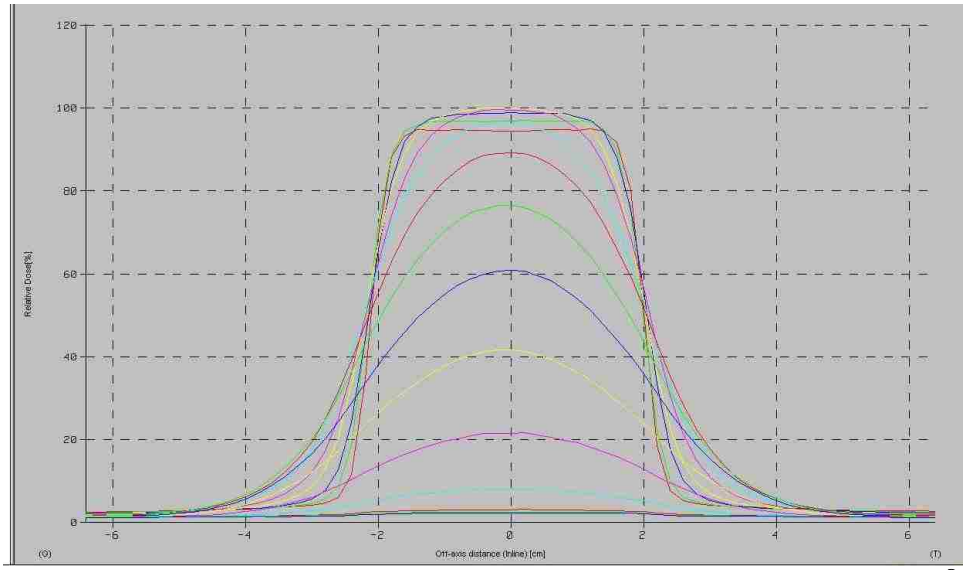

Figure 3.11: Off-axis relative dose profile measurements for a Cerrobend 4x4 cm^2 field size in a 15x15 cm^2 applicator-12 MeV energy at 100 cm SSD. Profiles are normalized to the central axis dose maxima. Profiles were taken at depths of 0.5, 1, 1.5, 2, 2.5, 3, 3.5, 4, 4.5, 5, 5.5, 6, 6.5, 7, 8; the blue profile with a central axis dose of ~60% was measured at 4.5 cm depth.

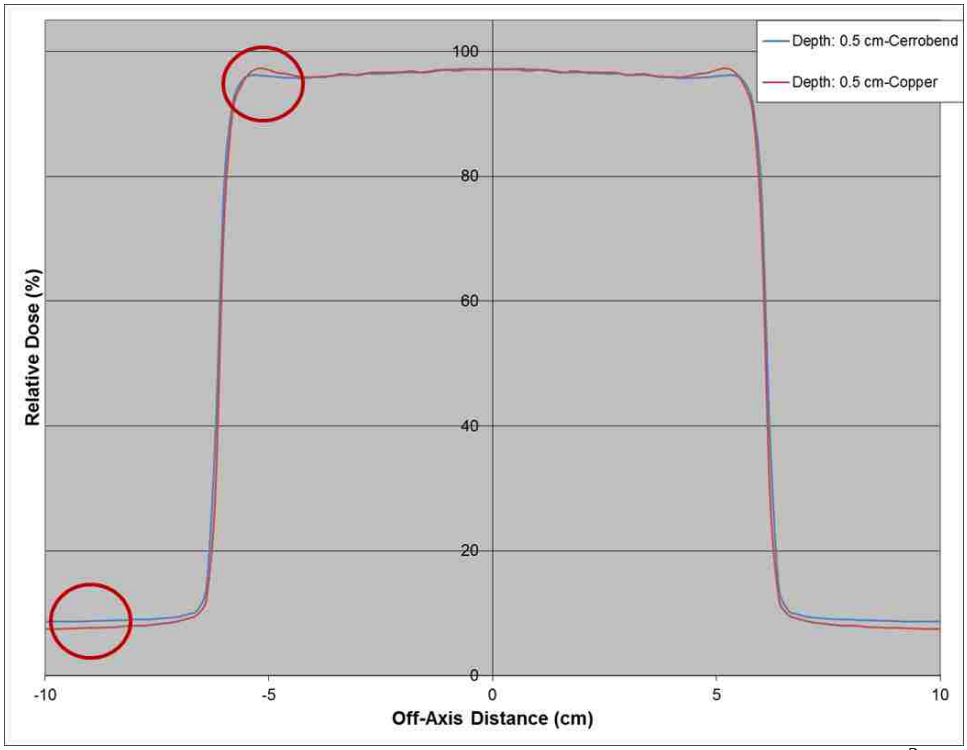

Figure 3.12: Off-axis relative dose profile at a depth of 0.5 cm for a 12x12 cm^2 field size in a 25x25 cm^2 applicator at 20 MeV and 100 cm SSD where 100% equals the central-axis dose maximum. Red circles highlight the two areas of dosimetric differences, the out-of-field dose and the beam edge horns located near the edge of the insert.

Off-axis relative dose profiles showed the greatest differences between copper and Cerrobend at the most shallow depth of 0.5 cm. Figure 3.13 shows profiles at 0.5 cm depth for all three energies with the copper and Cerrobend 2x2 cm^2 and 12x12 cm^2 field size inserts, both in the 25x25 cm^2 applicator at 100 cm SSD.

Off-axis relative dose profiles showed higher doses inside the beam edges for copper inserts than for Cerrobend inserts at depths of less than ~2 cm, being more prominent with higher energy beams and shallower depths. At depths past ~2cm no differences in the dose inside the beam edges between the two materials was observed. These beam-edge horns were caused by electrons scattering from the collimator edge, with an inverse relationship between the absorbed dose from scatter and the density of the collimating material.(Lax and Brahme, 1980; International Commission on Radiation Units and Measurements., 1972) The lower density of copper compared to Cerrobend caused more electron scatter from the insert edge, and thus a higher dose at the field edge. These edge effects never exceeded 2% of central-axis maximum dose.

Dosimetric differences were also seen in the out-of-field region shielded by the insert at off-axis distances greater than ~2 cm beyond the beam edge. While the 6 MeV energy showed no distinct differences in out-of-field dose, off-axis profiles showed higher out-of-field doses for Cerrobend than copper at 12 MeV and 20 MeV, with these differences most noticeable at 20 MeV where they sometimes exceeded the ±2% tolerance. As the depth of the measured profile increased this difference became less pronounced.

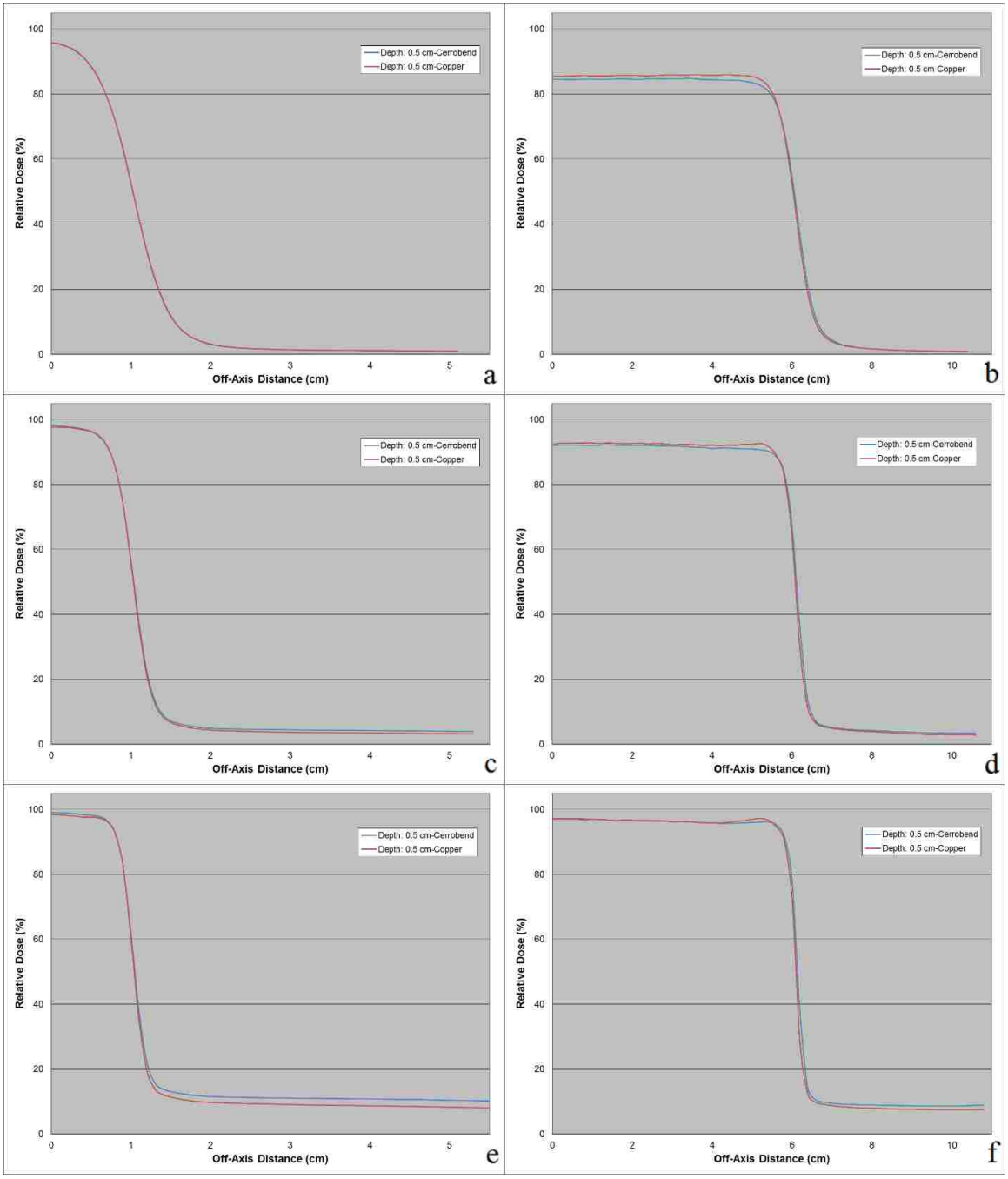

Figure 3.13: Off-axis relative dose profile measurements for copper and Cerrobend inserts of 2x2 cm^2 field size (LEFT) and 12x12 cm^2 field size (RIGHT) for the 25x25 cm^2 applicator at 100 cm SSD for all three energies. Energies of 6 MeV, 12 MeV, and 20 MeV are shown for the 2x2 cm^2 field size (a, c, and e respectively) and the 12x12 cm^2 field size (b, d, f respectively). Profiles are normalized to the central axis dose maxima.

This higher out-of-field dose from Cerrobend inserts as compared to copper inserts was caused by the relative decrease in the amount of bremsstrahlung production in

copper, discussed previously. Because bremsstrahlung production is forward peaked, the x-ray dose differences below the insert material (out-of-field dose) should be larger than the x-ray dose differences along the central-axis (D_x). Out-of-field doses from Cerrobend showed dose increases >2% of maximum dose compared to copper for some inserts. The effects of these differences on the 2D electron dose distributions are discussed in the comparison of isodose distributions in section 3.3.

3.2.7 Output Correction Factors

There was close agreement between R_{100} values for Cerrobend and copper inserts, with an average difference of less than 0.1 cm. The differences in R_{100} locations all resulted in %DD corrections of less than 0.1%. As such, the OCFs were calculated using a value of 1.0 for the %DD correction terms.

All OCFs are shown in Appendix C for 100 cm SSD and Appendix D for 110 cm SSD. OCFs (copper/Cerrobend) at 100 cm SSD ranged from 0.983 (3x3 cm^2 field size/25x25 cm^2 applicator/16 MeV) to 1.009 (6x6 cm^2 field size/10x10 cm^2 applicator/20 MeV). All OCFs at 100 cm SSD were within ±2% of unity. OCFs at 110 cm SSD ranged from 0.990 (2x2 cm^2 field size/25x25 cm^2 applicator/6 MeV, 3x3 cm^2 field size/25x25 cm^2 applicator/20 MeV, and 4x4 cm^2 field size/25x25 cm^2 applicator/20 MeV) to 1.006 (4x4 cm^2 field size/15x15 cm^2 applicator/6 MeV and 8x8 cm^2 field size/15x15 cm^2 applicator/6 MeV). All OCFs at 100 cm SSD were within ±1% of unity.

Average, minimum, and maximum output correction factors at 100 cm SSD for all field sizes and applicator sizes are shown in Table 3.15 at each energy and for all energies combined. The average OCF was 0.999, with Cerrobend having a 0.1% average higher output than copper. Measured average OCFs were 0.999 at 6 MeV, 9 MeV, and 12

MeV, while the average OCF was 0.998 at 16 MeV and 20 MeV. The slightly higher average outputs from Cerrobend inserts compared to copper inserts could be caused by the greater bremsstrahlung production in Cerrobend, especially at higher energies.

Average, minimum, and maximum output correction factors at 110 cm SSD for all field sizes and applicator sizes are shown in Table 3.16 at each energy and for all energies combined. The average OCF over all energies was 0.999, with 6 MeV having the largest average (1.001) and 20 MeV the smallest average (0.997). The slightly higher average outputs from Cerrobend inserts compared to copper inserts at 20 MeV might be caused by the greater bremsstrahlung production in Cerrobend at higher energies.

Table 3.15: Average, minimum, and maximum output correction factors at each energy and for all energies measured at 100 cm SSD.

Energy	Average OCF	Minimum OCF	Maximum OCF
6 MeV	0.999	0.992	1.008
9 MeV	0.999	0.992	1.006
12 MeV	0.999	0.988	1.005
16 MeV	0.998	0.983	1.005
20 MeV	0.998	0.986	1.009
All Energies	0.999	0.983	1.009

Table 3.16: Average, minimum, and maximum output correction factors at each energy and for all energies measured at 110 cm SSD.

Energy	Average OCF	Minimum OCF	Maximum OCF
6 MeV	1.001	0.990	1.006
12 MeV	1.000	0.994	1.005
20 MeV	0.997	0.990	1.003
All Energies	0.999	0.990	1.006

OCFs measured with the thimble ion chamber were compared to those derived from electron diode measurements. The measurement uncertainty of the OCFs was estimated at 0.001 by measuring the 10x10 cm^2 open field OCF three times using the ion chamber.

The total uncertainty of the OCFs could be larger than this, especially for smaller fields, due to the effect of placement variability of the insert within the applicator.

The comparison of OCFs measured by both detectors in the 10x10 cm^2 applicator were within the measurement uncertainty of ±0.001 for the 3x3, 4x4, and 8x8 cm^2 field sizes, and for four of the five energies measured in the 6x6 cm^2 field size (Figure 3.15 - Figure 3.18). For the smallest field size, 2x2 cm^2, the ion chamber OCFs were systematically higher by 0.2 to 0.6% (Figure 3.14). This effect may be attributed to the thimble ionization chamber's larger sensitive volume as compared to that of the electron diode. Because the copper inserts have increased scatter off the edge, the ion chamber may have collected a greater amount of scattered radiation than the diode, causing the ionization chamber OCF (copper/Cerrobend) to be larger compared to the diode OCF.

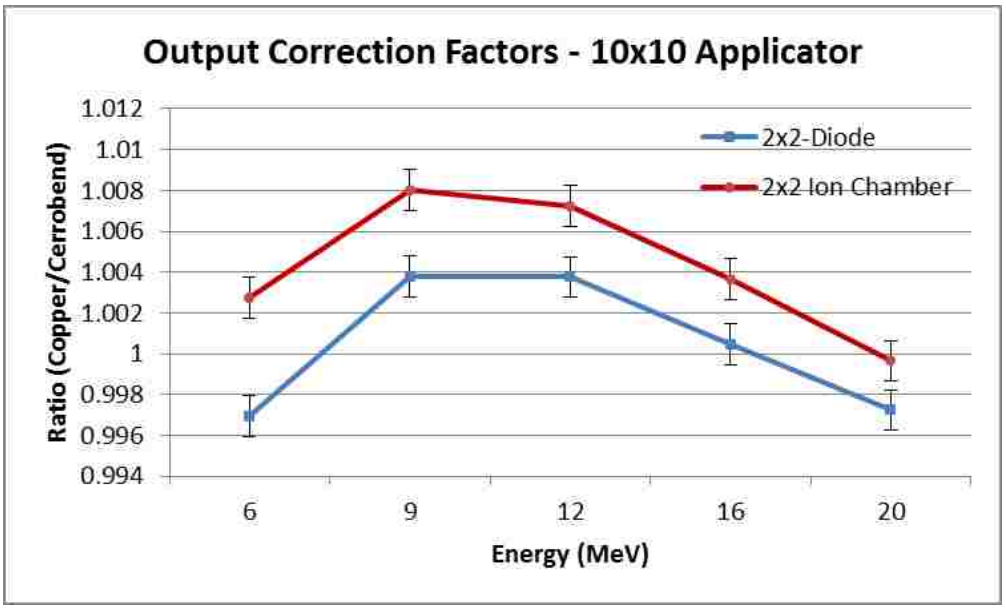

Figure 3.14: Comparison plot of OCFs measured with an electron diode (blue) and ionization chamber (red) for a 2x2 cm^2 insert in a 10x10 cm^2 applicator.

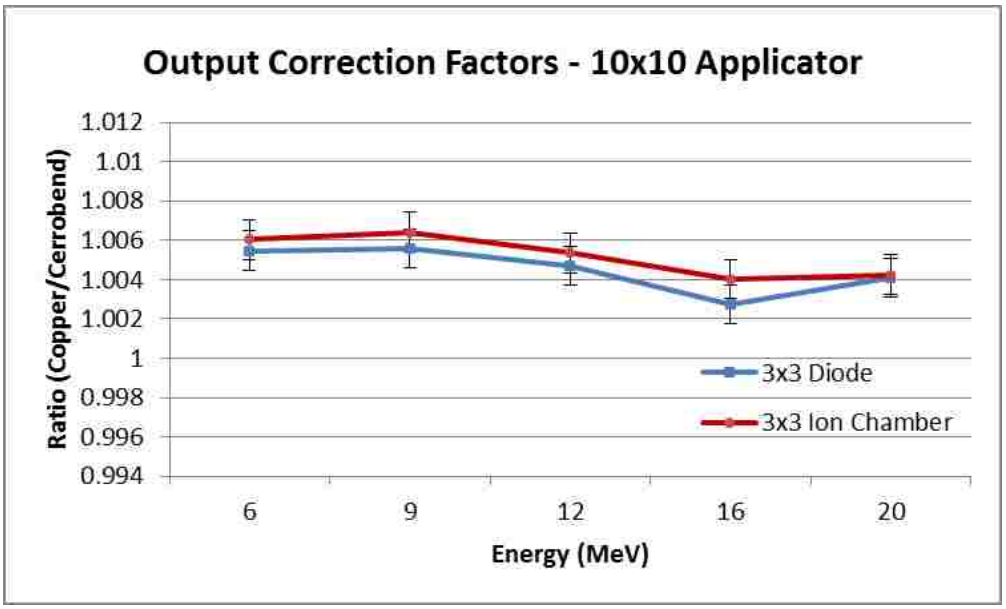

Figure 3.15: Comparison plot of OCFs measured with an electron diode (blue) and ionization chamber (red) for a 3x3 cm^2 insert in a 10x10 cm^2 applicator.

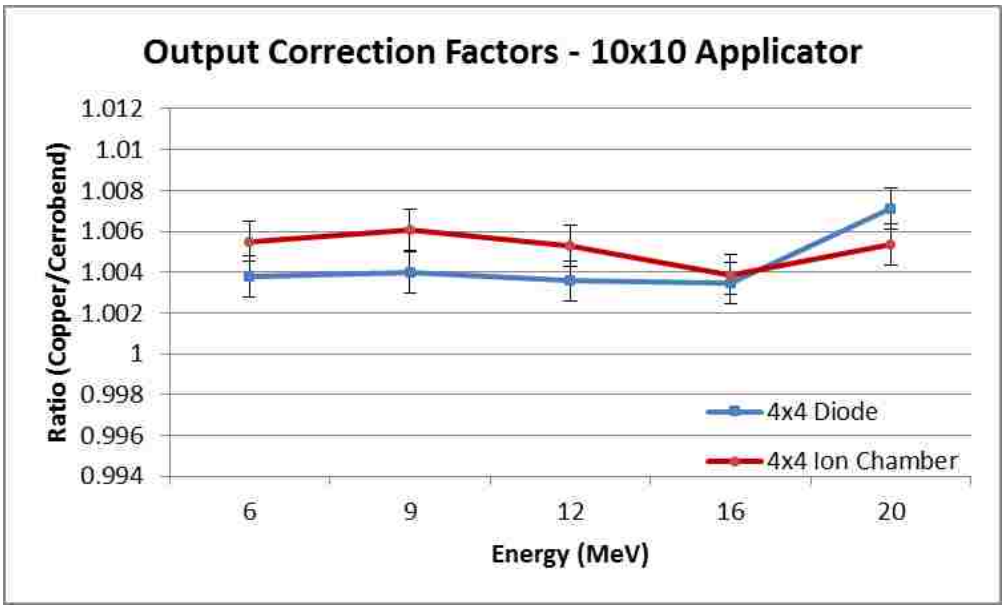

Figure 3.16: Comparison plot of OCFs measured with an electron diode (blue) and ionization chamber (red) for a 4x4 cm^2 insert in a 10x10 cm^2 applicator.

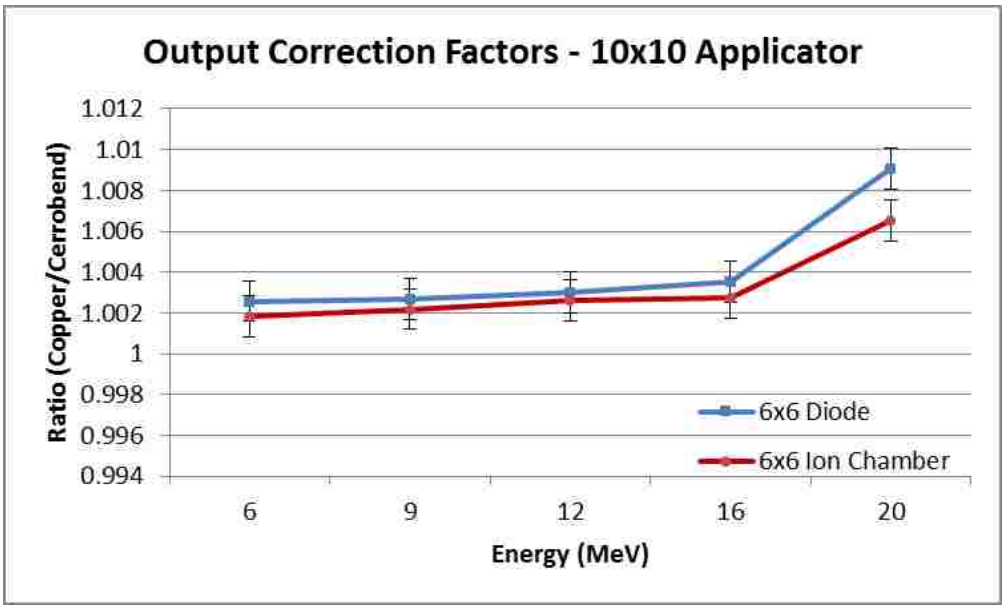

Figure 3.17: Comparison plot of OCFs measure with an electron diode (blue) and ionization chamber (red) for a 6x6 cm^2 insert in a 10x10 cm^2 applicator.

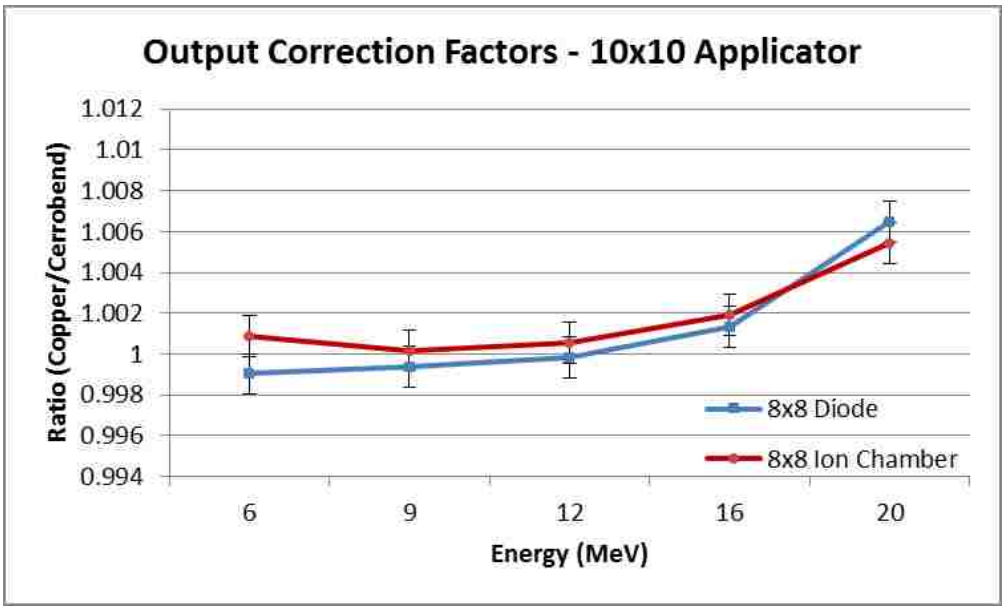

Figure 3.18: Comparison plot of OCFs measured with an electron diode (blue) and ionization chamber (red) for an 8x8 cm^2 insert in a 10x10 cm^2 applicator.

3.3 Aim 3: Comparison of Beam Dosimetry

Aim 3: Quantitatively compare absolute beam dosimetry between copper and Cerrobend inserts using criteria of ±2% of maximum dose or 1 mm distance to agreement.

3.3.1 Analysis of Isodose Plots at 100 cm SSD

Figure 3.19, Figure 3.20, and Figure 3.21 show representative samples of the comparative isodose plots at 6 MeV, 12 MeV, and 20 MeV, respectively. All isodose comparisons are shown in Appendix E (100 cm SSD) and Appendix F (110 cm SSD). The passing percentages for isodose comparisons between the copper and Cerrobend insert measurements using the 2%/1 mm DTA criteria at 100 cm SSD are shown in Table 3.17. Of the 48 total combinations of field size, applicator size, and energy, 43 (90%) passed the 2%/1 mm criteria for 100% of points. For 46 of 48 (96%) combinations, ≥99% of points passed the 2%/1 mm criteria; the two failing combinations were the 2x2 cm^2 field size (98.90% passing) and the 4x4 cm^2 field size (98.35% passing) both in the 25x25 cm^2 applicator at 20 MeV. The other three combinations showing point failures were the next three largest field sizes in the 25x25 cm^2 applicator at 20 MeV: 6x6 cm^2 field size (99.44% passing), 8x8 cm^2 field size (99.92% passing) and the 10x10 cm^2 field size (99.67% passing).

At 20 MeV, the additional out-of-field bremsstrahlung dose produced in the Cerrobend inserts compared to the copper inserts caused the observed failures in the 2%/1 mm criteria. As shown by isodose comparisons for the 2x2 cm^2 field in the 25x25 cm^2 applicator in Figure 3.19-Figure 3.21, this out-of-field effect did not cause criteria failures at 6 MeV and 12 MeV, but caused failures (red pixels) for the 20 MeV beam with

only 98.90% of points passing. Figure 3.23 shows PDDs corresponding to 5 cm off-axis for the Cerrobend and copper inserts at 20 MeV, as indicated by the green line on Figure 3.21. The off-axis dose due to bremsstrahlung photons is higher for the Cerrobend insert than the copper insert by a maximum of 2.2% at 0.5 cm depth in this off-axis region.

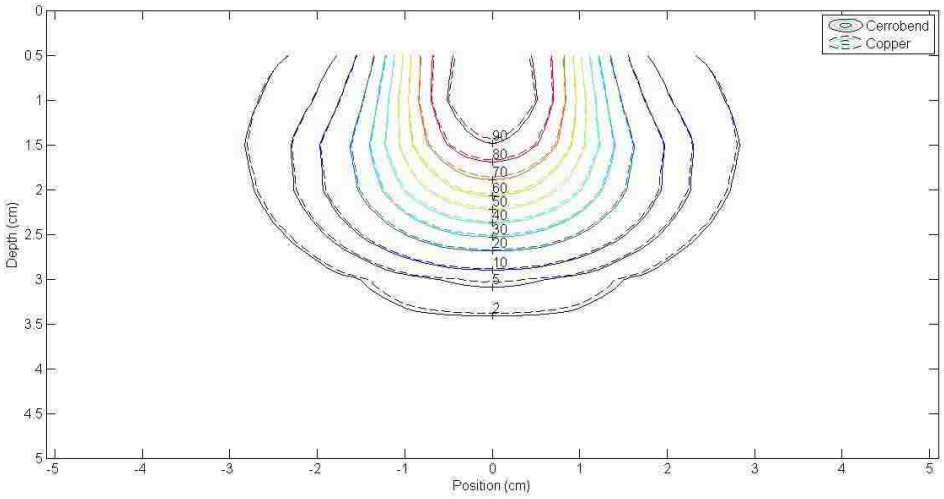

Figure 3.19: Absolute isodose comparison between Cerrobend (solid lines) and copper (dashed lines) for a 2x2 cm^2 insert in a 25x25 cm^2 applicator at 6 MeV and 100 cm SSD. All points passed the 2%/1mm criteria. The OCF was 0.992.

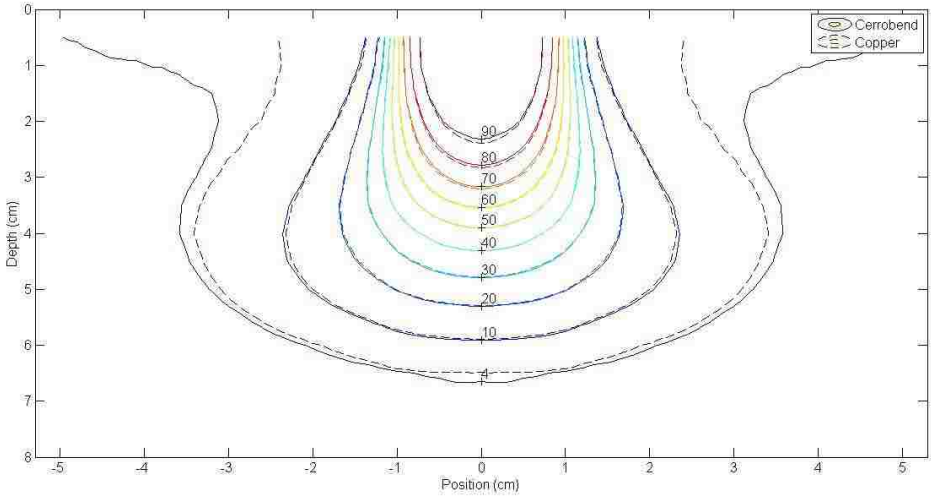

Figure 3.20: Absolute isodose comparison between Cerrobend (solid lines) and copper (dashed lines) for a 2x2 cm^2 insert in a 25x25 cm^2 applicator at 12 MeV and 100 cm SSD. All points passed the 2%/1mm criteria. The OCF was 1.000.

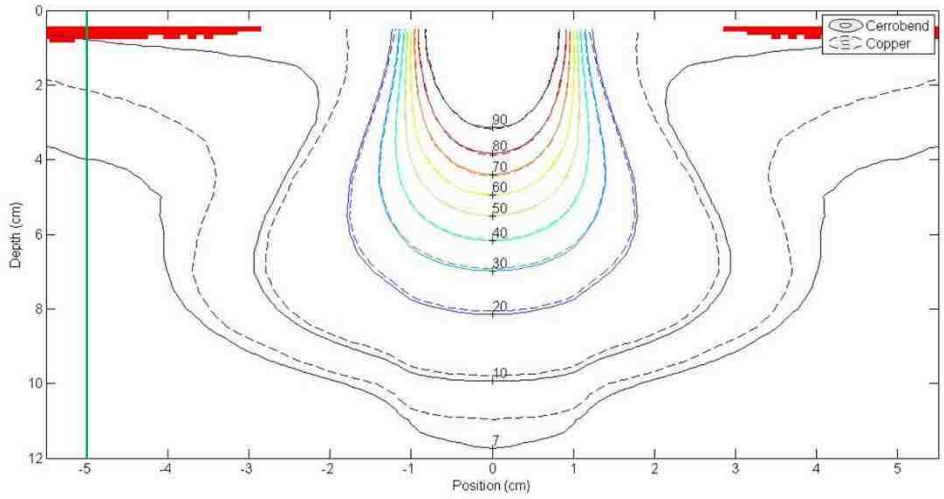

Figure 3.21: Absolute isodose comparison between Cerrobend (solid lines) and copper (dashed lines) for a 2x2 cm^2 insert in a 25x25 cm^2 applicator at 20 MeV and 100 cm SSD. The red pixels on the isodose plot mark points which failed the 2%/1mm criteria (98.90% of points passed criteria). The OCF was 0.991.

All criteria failures occurred out-of-field due the lower bremsstrahlung dose from copper inserts compared to Cerrobend inserts, a difference which reduces dose to healthy tissue and is clinically beneficial. Clinically, an insert is created using the smallest possible applicator for the given field size. The inserts which registered criteria failures in this study were small field size-large applicator combinations which are unlikely to be used for patient treatment.

All Cerrobend inserts showed higher out-of-field surface dose than copper inserts due to increased X-ray production at 12 MeV and 20 MeV; the magnitude of this effect also depended upon the applicator size relative to the insert size. Figure 3.22 compares 12x12 cm^2 inserts in a 25x25 cm^2 applicator at 20 MeV. The magnitude of the elevated surface dose from the 12x12 cm^2 Cerrobend insert was less than that for the 2x2 cm^2 insert for the same applicator size and energy (Figure 3.21). The additional amount of material

around the 2x2 cm^2 field cutout produced more bremsstrahlung photons and resulted in the failure of some points near the surface for the comparison criteria; the larger field size of 12x12 cm^2 had less material and hence less bremsstrahlung production, resulting in 100% of the points passing the 2%/1mm criteria.

Table 3.17: Passing rates for isodose comparisons between copper and Cerrobend inserts using a 2%/1 mm DTA criteria for the measurement subset listed in Table 2.3. 45 of 48 measurements passed the criteria for ≥99% of points, with the three failing measurements all at 20 MeV for the three smallest field sizes in the 25x25 cm^2 applicator. All measurements passed a 3%/1 mm criteria for 100% of points.

Energy	**Field Size**	**Applicator Size (cm)**		
(MeV)	**(cm)**	**6x6**	**15x15**	**25x25**
6	**2x2**	100%	100%	100%
12	**2x2**	100%	100%	100%
20	**2x2**	100%	100%	98.90%
6	**3x3**	100%		100%
12	**3x3**	100%		100%
20	**3x3**	100%		100%
6	**4x4**	100%	100%	100%
12	**4x4**	100%	100%	100%
20	**4x4**	100%	100%	98.35%
6	**6x6**			100%
12	**6x6**			100%
20	**6x6**			99.44%
6	**8x8**		100%	100%
12	**8x8**		100%	100%
20	**8x8**		100%	99.92%
6	**10x10**			100%
12	**10x10**			100%
20	**10x10**			99.67%
6	**12x12**		100%	100%
12	**12x12**		100%	100%
20	**12x12**		100%	100%
6	**15x15**			100%
12	**15x15**			100%
20	**15x15**			100%
6	**20x20**			100%
12	**20x20**			100%
20	**20x20**			100%

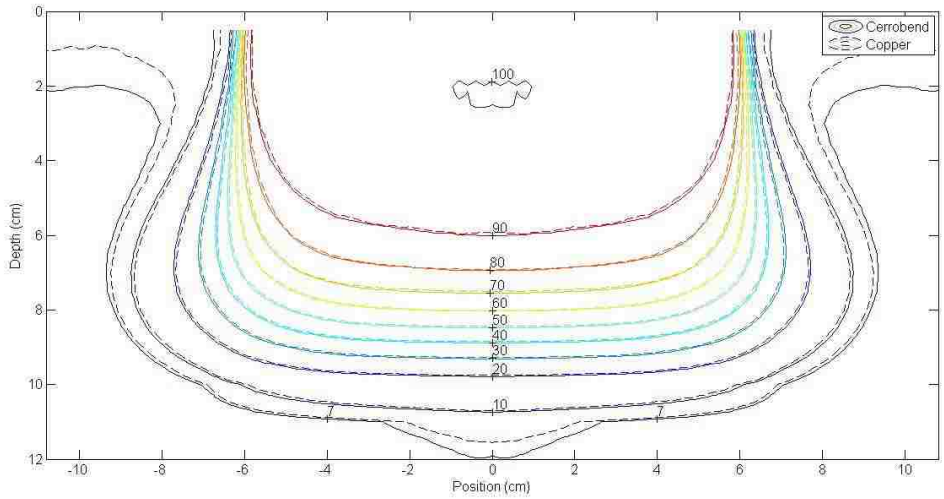

Figure 3.22: Absolute isodose comparison between Cerrobend (solid lines) and copper (dashed lines) for a 12x12 cm^2 insert in a 25x25 cm^2 applicator at 20 MeV and 100 cm SSD. All points passed the 2%/1mm criteria. The OCF was 0.997.

The increased scatter through the edge of copper inserts compared to Cerrobend inserts did not result in criteria failure for any of the isodose comparisons. While this increased scatter was noticeable in some off-axis relative dose profiles at shallow depth, the increased scatter did not impact the isodose comparisons. Maximum differences in the beam edge region for copper inserts was less than the 2%/1 mm criteria when compared to Cerrobend inserts.

An estimation of the bremsstrahlung dose due to the inserts was made using the absolute dose distributions from the 2x2 cm^2 field size and the 12x12 cm^2 field size inserts in the 25x25 cm^2 applicator at 20 MeV (Figure 3.21 and Figure 3.22). The PDD curves 5 cm off-axis were analyzed for the 2x2 cm^2 field, which included D_x contributions from inside the treatment head as well as the insert, and the 12x12 cm^2 field, which included D_x contributions primarily from inside the treatment head. The 12x12 cm^2 field size was chosen because it was large enough to limit any effects from the

insert material at 5 cm off-axis, and the data set contained deeper dose information than the 15x15 cm^2 and 20x20 cm^2 inserts in the same applicator. The PDDs 5 cm off-axis for both field sizes and both materials are plotted in Figure 3.23. D_x values at 12 cm depth for the 2x2 cm^2 field size inserts were 4.17% for Cerrobend and 3.82% for copper. D_x values at 12 cm depth for the 12x12 cm^2 field size inserts were 5.15% for Cerrobend and 4.67% for copper.

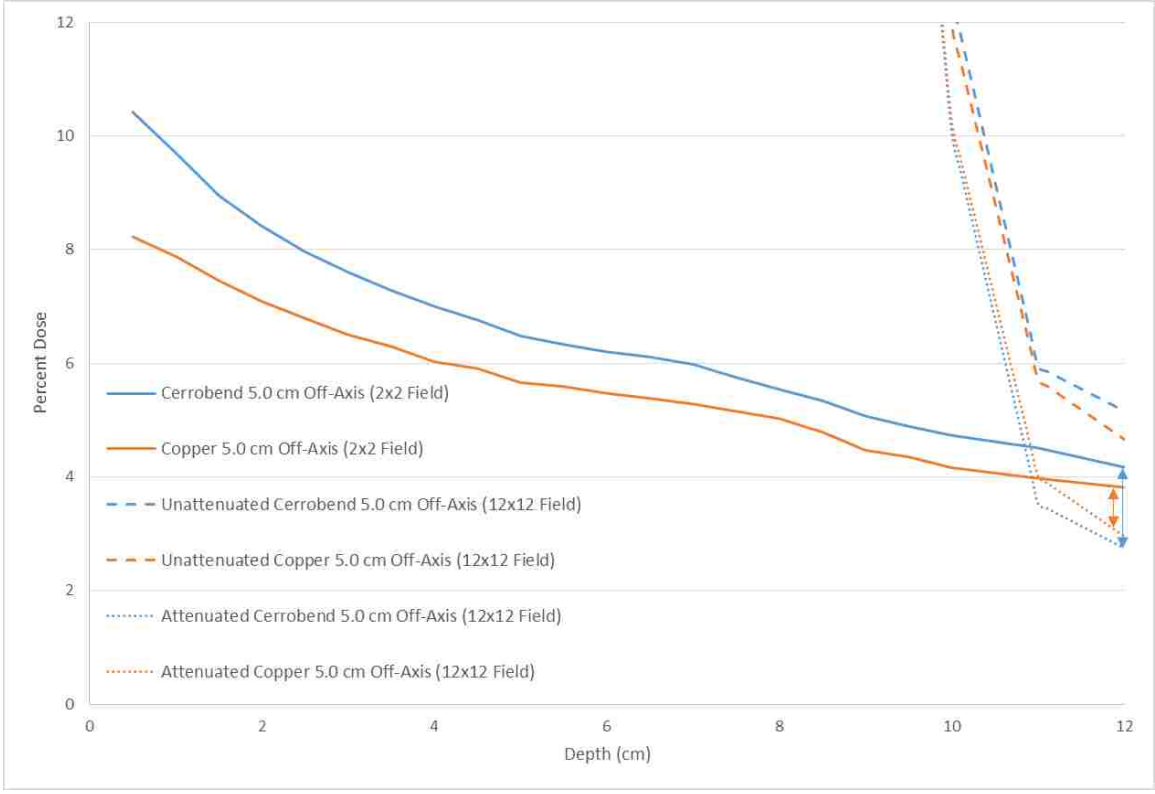

Figure 3.23: Percent depth dose curves corresponding to 5 cm off-axis for the Cerrobend and copper 2x2 cm^2 and 12x12 cm^2 inserts in the 25x25 cm^2 applicator at 20 MeV and 100 cm SSD, and from the 12x12 cm^2 inserts corrected for attenuation as shown in Equation 3.2. Arrows show differences between the 2x2 cm^2 field size D_x and the attenuated 12x12 cm^2 field size D_x, representing the bremsstrahlung dose due to the inserts.

The D_x values at 12 cm depth for the 12x12 cm^2 field size inserts were assumed to be the dose due to photons produced in the treatment head and unattenuated by the insert

($D_{x,head}^{unattenuated}$). To compare with the D_x values from the 2x2 cm^2 field size which were attenuated by the inserts, the D_x for the Cerrobend and copper 12x12 cm^2 inserts was scaled to the equivalent attenuated dose ($D_{x,head}^{attenuated}$) using the linear attenuation coefficients ($\mu_{Cerrobend}$=0.5522 cm^{-1}, μ_{Copper}=0.3054 cm^{-1}) and thicknesses ($t_{Cerrobend}$=1.146 cm, t_{Copper}=1.489 cm) of the 2x2 cm^2 field size copper and Cerrobend inserts as shown in Equation 3.2. The attenuated D_x is plotted in Figure 3.23.

$$D_{x,head}^{attenuated} = D_{x,head}^{unattenuated} \times e^{-\mu t} \tag{3.2}$$

The attenuated photon doses from the treatment head were then subtracted from the attenuated total photon doses ($D_{x,total}^{attenuated}$) from the 2x2 cm^2 field size inserts. The final result was an estimation of the photon dose due primarily to the electron insert ($D_{x,insert}^{attenuated}$), as shown in Equation 3.3.

$$D_{x,insert}^{attenuated} = D_{x,total}^{attenuated} - D_{x,head}^{attenuated} \tag{3.3}$$

The estimated photon dose due to the insert as a percentage of the central-axis dose maximum was 1.43% for the Cerrobend insert and 0.86% for the copper insert, or a 1.7 times increase in bremsstrahlung production from the Cerrobend insert as compared to the copper insert (shown in Figure 3.23). This increase is consistent with the calculation done in Section 3.2.5, which predicted a 2.3 times increase using Equation 3.1.

3.3.2 Analysis of Isodose Plots at 110 cm SSD

Isodose comparisons between the copper and Cerrobend inserts using the 2%/1 mm DTA criteria at 110 cm SSD showed all 48 of 48 comparisons passing the criteria for

100% of points (Table 3.18). Figure 3.24 and Figure 3.25 show the 2x2 cm^2 insert and 12x12 cm^2 insert isodose comparisons, respectively, at 20 MeV in the 25x25 cm^2 applicator at 110 cm SSD. The increased out-of-field dose from the Cerrobend inserts at extended SSD as compared to the copper inserts was still apparent. However, the differences between the out-of-field doses were less than those observed at 100 cm SSD.

Table 3.18: Passing rates for isodose comparisons between copper and Cerrobend inserts using a 2%/1 mm DTA for the 110 cm SSD measurement subset listed in Table 2.3. All measurements passed the criteria for 100% of points.

Energy	**Field Size**	**Applicator Size (cm)**		
(MeV)	**(cm)**	**6x6**	**15x15**	**25x25**
6	**2x2**	100%	100%	100%
12	**2x2**	100%	100%	100%
20	**2x2**	100%	100%	100%
6	**3x3**	100%		100%
12	**3x3**	100%		100%
20	**3x3**	100%		100%
6	**4x4**	100%	100%	100%
12	**4x4**	100%	100%	100%
20	**4x4**	100%	100%	100%
6	**6x6**			100%
12	**6x6**			100%
20	**6x6**			100%
6	**8x8**		100%	100%
12	**8x8**		100%	100%
20	**8x8**		100%	100%
6	**10x10**			100%
12	**10x10**			100%
20	**10x10**			100%
6	**12x12**		100%	100%
12	**12x12**		100%	100%
20	**12x12**		100%	100%
6	**15x15**			100%
12	**15x15**			100%
20	**15x15**			100%
6	**20x20**			100%
12	**20x20**			100%
20	**20x20**			100%

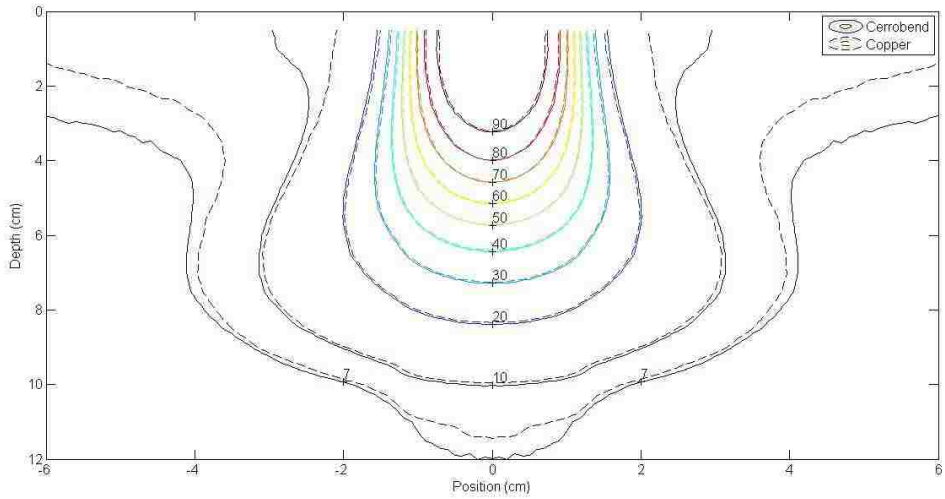

Figure 3.24: Absolute isodose comparison between Cerrobend (solid lines) and copper (dashed lines) for a 2x2 cm^2 insert in a 25x25 cm^2 applicator at 20 MeV and 110 cm SSD. All points passed the 2%/1mm criteria. The OCF was 0.993.

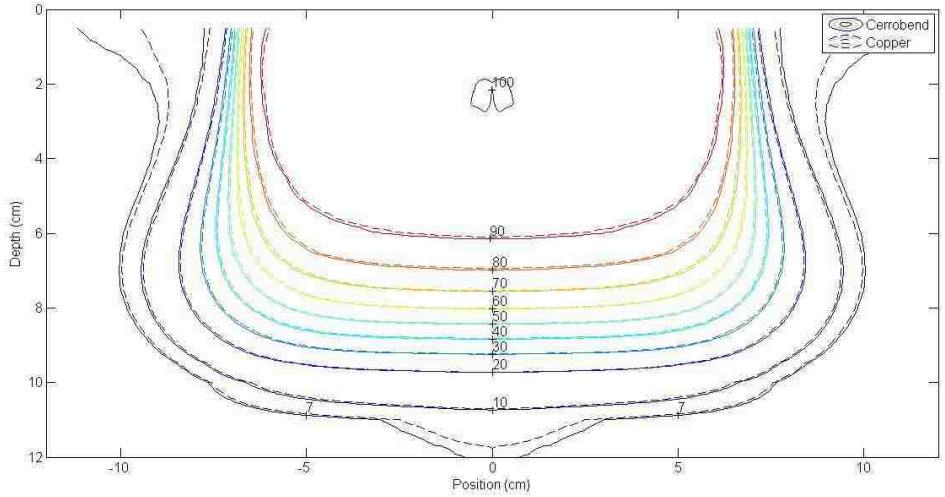

Figure 3.25: Absolute isodose comparison between Cerrobend (solid lines) and copper (dashed lines) for a 12x12 cm^2 insert in a 25x25 cm^2 applicator at 20 MeV and 110 cm SSD. All points passed the 2%/1mm criteria. The OCF was 0.997.

Chapter 4 Conclusions

4.1 Summary of Results

The goal of this research was to evaluate the dosimetric differences of custom milled copper inserts as compared to conventional Cerrobend inserts used for electron beam therapy. Comparisons were made over a range of electron energies (6 MeV to 20 MeV), insert field sizes (2x2 cm^2 to 20x20 cm^2), and applicator sizes (6x6 cm^2 to 25-25 cm^2) for SSDs of 100 and 110 cm. The hypothesis of this work was that the comparison of beam dosimetry between Cerrobend and copper inserts would show absolute dosimetric differences less than 2% of the maximum dose or 1 mm distance to agreement for ≥99% of points for all field sizes at SSDs of 100 and 110 cm.

The dosimetric comparisons resulted in the following observations:

1. At 100 cm SSD, comparisons of the absolute dosimetric difference between copper and Cerrobend inserts showed 100% of the area within 2%/1 mm for all field sizes at energies of 6 and 12 MeV.
2. At 100 cm SSD, comparisons of the absolute dosimetric difference between copper and Cerrobend in small field inserts (2x2 cm^2 and 4x4 cm^2) in the 25x25 cm^2 applicator at 20 MeV resulted in less than 99% of the area passing the 2%/1 mm comparison criteria, with the worst case being a 98.35% passing rate for the 4x4 cm^2 field in the 25x25 cm^2 applicator.
3. At 100 cm SSD, all dosimetric comparisons of copper and Cerrobend inserts passed a 3%/1 mm criteria for 100% of the area.

4. At 110 cm SSD, all dosimetric comparisons of copper and Cerrobend inserts passed a 2%/1 mm criteria for 100% of the area.
5. The use of milled copper inserts resulted in lower out-of-field dose compared to Cerrobend inserts. This difference increased at higher energies and with larger applicators, and decreased at extended SSD (110 cm). This effect caused the 2%/1 mm criteria failures for the small field size-large applicator combinations at the highest measured energy (20 MeV).
6. The use of milled copper inserts resulted in higher edge-of-field dose compared to Cerrobend inserts at shallow depths (<2 cm). However, this effect had no noticeable effect on the absolute dose comparisons (<2%).
7. For all field size-applicator-energy combinations at 100 cm and 110 cm SSD, dosimetric comparisons showed 100% of the area passing the 2%/1 mm criteria inside the area of clinical beam.

4.2 Evaluation of Hypothesis

The results of this study did not support the hypothesis of the work. Using a 2% or 1-mm DTA criteria to compare the absolute dosimetry between copper and Cerrobend inserts, field sizes of 2x2 cm^2 and 4x4 cm^2 did not pass the comparison criteria for ≥99% of the area. All criteria failures occurred out-of-field and were due to the lower bremsstrahlung photon dose from copper as compared to Cerrobend, the worst case being a 98.35% pass rate. Clinically this difference in out-of-field dose from copper inserts is beneficial, as it provides added dose sparing of healthy tissue. In addition, the inserts which registered criteria failures in this study were small field size-large applicator combinations which are unlikely to be used for patient treatment. All copper and

Cerrobend insert dosimetric comparisons passed a 3%/1 mm criteria for 100% of the area.

4.3 Clinical Applications of Current Work

Using custom milled copper inserts for electron beam therapy planned with standard commissioning data measured on Cerrobend inserts should result in minimal absolute dosimetric differences (≥99% of points within ±2% of D_{max} or 1 mm DTA) for standard clinical field sizes (2x2 cm^2 to 20x20 cm^2), applicators (6x6 cm^2 to 25x25 cm^2), and energies (6 MeV to 20 MeV). The primary difference between Cerrobend inserts as compared to copper inserts was lower out-of-field dose found in copper inserts due to a reduction in bremsstrahlung production. Clinically, this dosimetric difference could be beneficial in treatment as the use of copper inserts can reduce the dose received by healthy tissue outside of the planned treatment volume and could also allow for more homogenous dose distributions during field abutment.

4.4 Recommendations for Future Work

Future work relating to this study of custom milled copper inserts should focus on three areas:

1. Small field dosimetry: Because of the greater accuracy associated with machine milled copper inserts compared to in-house poured Cerrobend inserts, copper inserts may be advantageous for treatments requiring high precision with small fields. The capability to deliver small fields with greater accuracy was not addressed in this work, but merits further study.
2. Abutting field dosimetry: Another scenario which could benefit from the precision of milled copper inserts is the abutting of fields. The effects of the

differences in field edge dosimetry between machined copper inserts should be investigated to determine the effects on the dose distributions of abutting fields.

3. Implementation of beveled edges: Machining copper inserts with beveled edges to match the divergence of the beam should result in less scattered electrons at the field edge. This could result in more homogenous dose distributions and improved sparring of normal tissue outside the planned treatment volume.

References

Occupational Safety and Health Standards-Toxic and Hazardous Substances. In: *29 CFR 1910,* ed O S a H Administration

Almond P R, Biggs P J, Coursey B M, Hanson W F, Huq M S, Nath R and Rogers D W 1999 AAPM's TG-51 protocol for clinical reference dosimetry of high-energy photon and electron beams *Med Phys* **26** 1847-70

Das I J, Cheng C-W, Watts R J, Ahnesjö A, Gibbons J, Li X A, Lowenstein J, Mitra R K, Simon W E and Zhu T C 2008 Accelerator beam data commissioning equipment and procedures: Report of the TG-106 of the Therapy Physics Committee of the AAPM *Medical Physics* **35** 4186

Das I J, Cheng C W, Mitra R K, Kassaee A, Tochner Z and Solin L J 2004 Transmission and dose perturbations with high-Z materials in clinical electron beams *Med Phys* **31** 3213-21

Gerbi B J, Antolak J A, Deibel F C, Followill D S, Herman M G, Higgins P D, Huq M S, Mihailidis D N, Yorke E D, Hogstrom K R and Khan F M 2009 Recommendations for clinical electron beam dosimetry: Supplement to the recommendations of Task Group 25 *Medical Physics* **36** 3239

Hogstrom K R 1991 Treatment planning in electron beam therapy *Frontiers of radiation therapy and oncology* **25** 30-52; discussion 61-3

Hogstrom K R and Almond P R 2006 Review of electron beam therapy physics *Physics in medicine and biology* **51** R455-89

Hogstrom K R, Boyd R A, Antolak J A, Svatos M M, Faddegon B A and Rosenman J G 2004 Dosimetry of a prototype retractable eMLC for fixed-beam electron therapy *Med Phys* **31** 443-62

International Commission on Radiation Units and Measurements. 1972 *Radiation dosimetry: electrons with initial energies between 1 and 50 MeV* (Washington,

Jayaraman S and Lanzl L H 1996 *Clinical radiotherapy physics* (Boca Raton: CRC Press)

Karzmark C J and Morton R J 1989 *Primer on Theory and Operation of Linear Accelerators in Radiation Therapy 2nd edn* (Madison, WI: Medical Physics Publishing)

Karzmark C J and Pering N C 1973 Electron linear accelerators for radiation therapy: history, principles and contemporary developments *Physics in medicine and biology* **18** 321-54

Khan F M 2003 *The Physics of Radiation Therapy* (Philadelphia: Lippincott Williams & Wilkins)

Khan F M, Doppke K P, Hogstrom K R, Kutcher G J, Nath R, Prasad S C, Purdy J A, Rozenfeld M and Werner B L 1991 Clinical electron-beam dosimetry: report of AAPM Radiation Therapy Committee Task Group No. 25 *Med Phys* **18** 73-109

Klein E E, Hanley J, Bayouth J, Yin F F, Simon W, Dresser S, Serago C, Aguirre F, Ma L, Arjomandy B, Liu C, Sandin C, Holmes T and Task Group A A o P i M 2009 Task Group 142 report: quality assurance of medical accelerators *Med Phys* **36** 4197-212

Kutcher G J, Coia L, Gillin M, Hanson W F, Leibel S, Morton R J, Palta J R, Purdy J A, Reinstein L E, Svensson G K and et al. 1994 Comprehensive QA for radiation oncology: report of AAPM Radiation Therapy Committee Task Group 40 *Med Phys* **21** 581-618

Lax I and Brahme A 1980 Collimation of high energy electron beams *Acta radiologica. Oncology* **19** 199-207

Lee M C, Jiang S B and Ma C M 2000 Monte Carlo and experimental investigations of multileaf collimated electron beams for modulated electron radiation therapy *Med Phys* **27** 2708-18

Loevinger R, Karzmark C J and Weissbluth M 1961 Radiation therapy with high-energy electrons. I. Physical considerations, 10 to 60 Mev *Radiology* **77** 906-27

Powers W E, Kinzie J J, Demidecki A J, Bradfield J S and Feldman A 1973 A new system of field shaping for external-beam radiation therapy *Radiology* **108** 407-11

Rikner G 1985 Characteristics of a p-Si detector in high energy electron fields *Acta radiologica. Oncology* **24** 71-4

Ten Haken R K, Fraass B A and Jost R J 1987 Practical methods of electron depth-dose measurement compared to use of the NACP design chamber in water *Med Phys* **14** 1060-6

Appendix A Percent Depth Dose Curves at 100 cm SSD

Percent depth dose curves are measured at 100 cm SSD for all possible field size and energy combinations are shown for the 6x6 cm^2 (Figure A.1), 10x10 cm^2 (Figure A.2), 15x15 cm^2 (Figure A.3), 20x20 cm^2 (Figure A.4), and 25x25 cm^2 (Figure A.5) applicators. Table A.1 contains data (differences and Cerrobend values) from the PDDs, metrics include R_{100}, R_{90}, R_{50}, $R_{80\text{-}20}$, $D_{1.0}$ and D_x. All differences were calculated by taking the value from the Cerrobend insert PDD minus the copper insert PDD. The PDDs measured at 20 MeV in the 15x15 cm^2 applicator were measured first and taken to a depth of 10 cm, giving less accurate D_x values than the 20 MeV PDDs measured to a depth of 12 cm. Because of this, the D_x values for these measurements were not included and are marked by an asterisk (*).

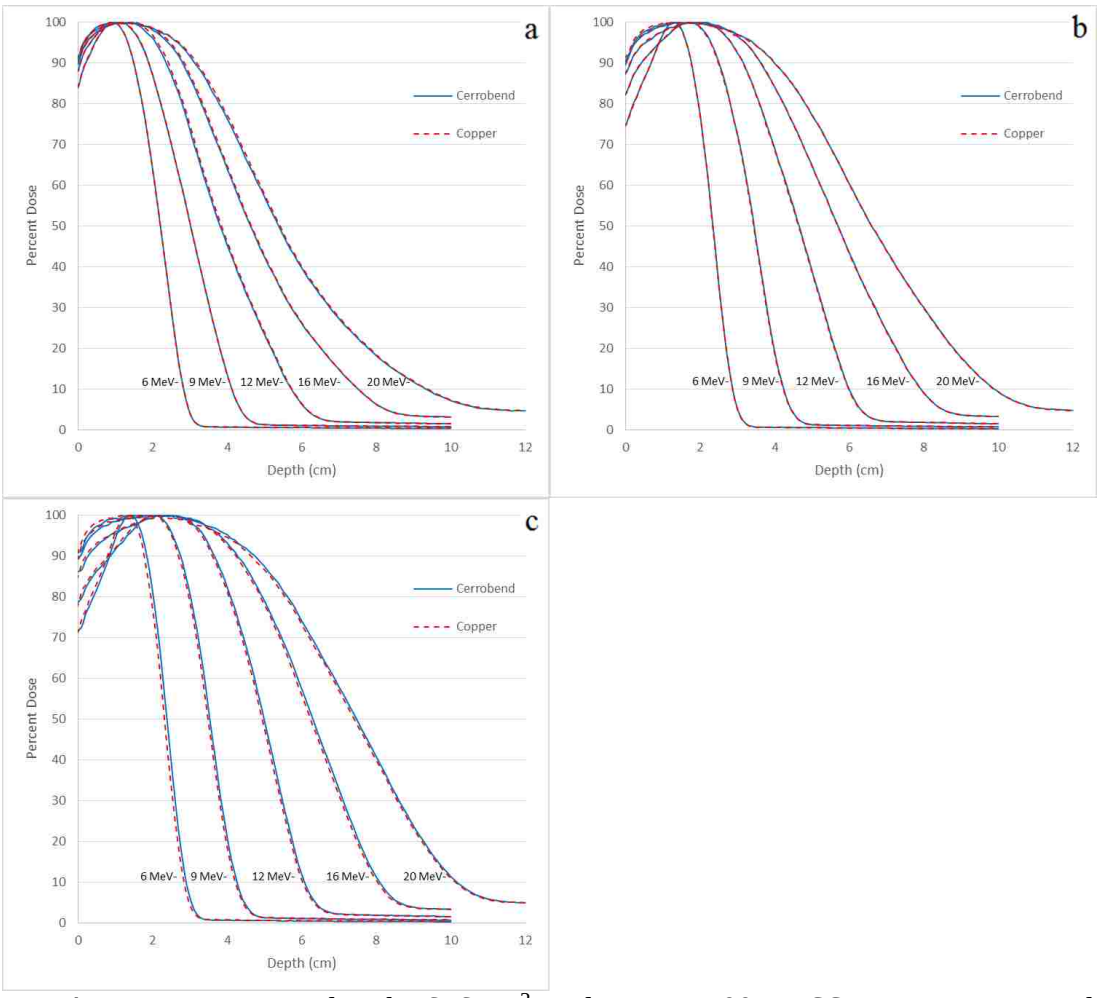

Figure A.1: PDDs measured in the 6x6 cm^2 applicator at 100 cm SSD using copper and Cerrobend inserts of field size: (a) 2x2 cm^2, (b) 3x3 cm^2, and (c) 4x4 cm^2.

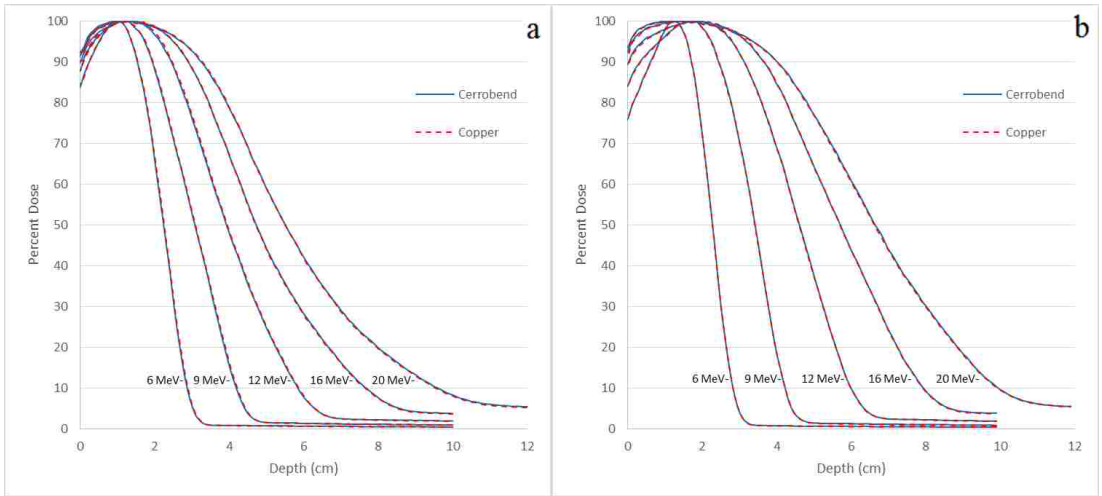

(Figure A.2 continued)

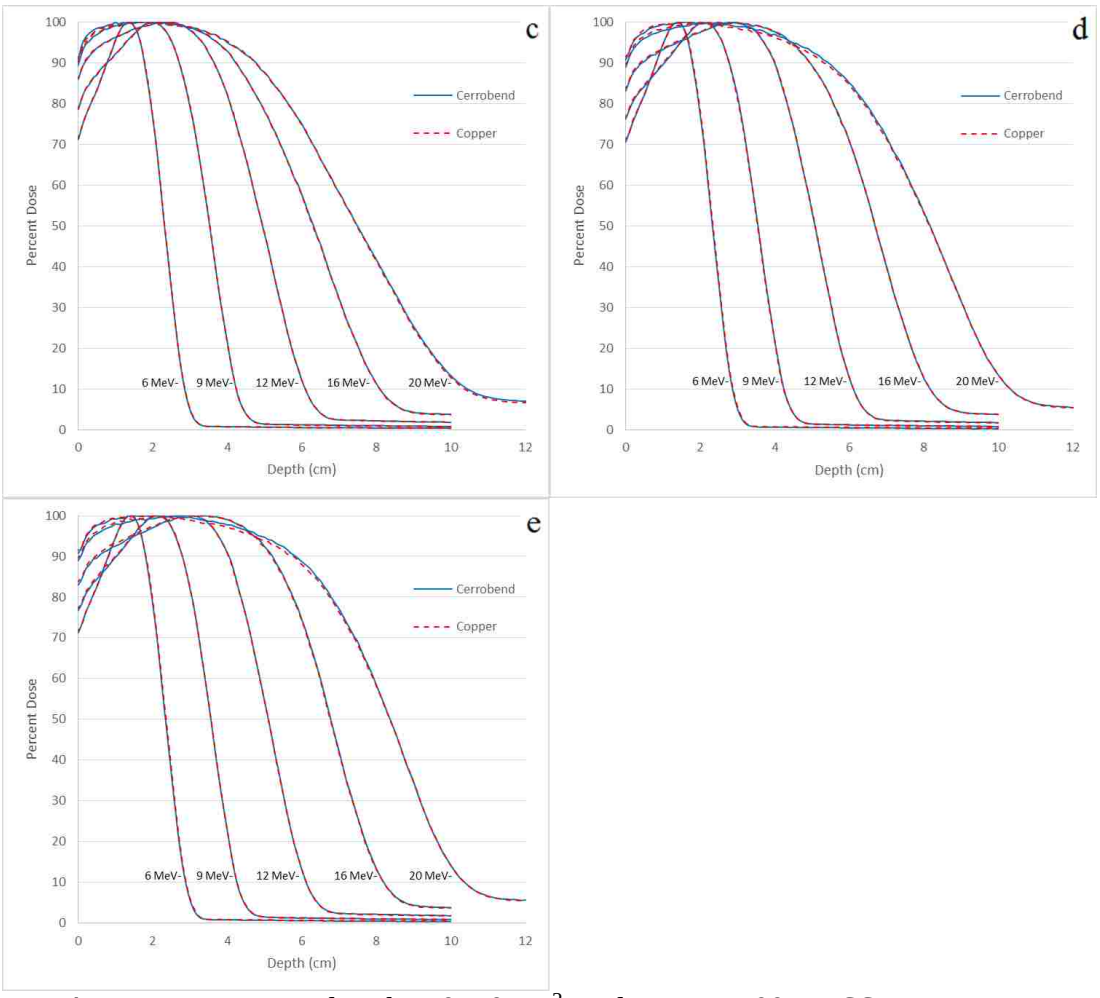

Figure A.2: PDDs measured in the 10x10 cm^2 applicator at 100 cm SSD using copper and Cerrobend inserts of field size: (a) 2x2 cm^2, (b) 3x3 cm^2, (c) 4x4 cm^2, (d) 6x6 cm^2, and (e) 8x8 cm^2.

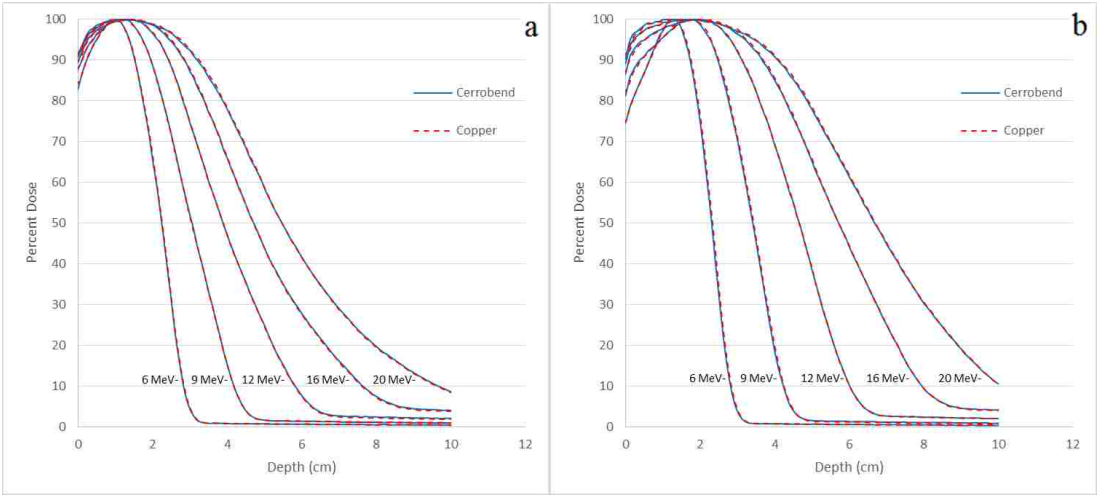

(Figure A.3 continued)

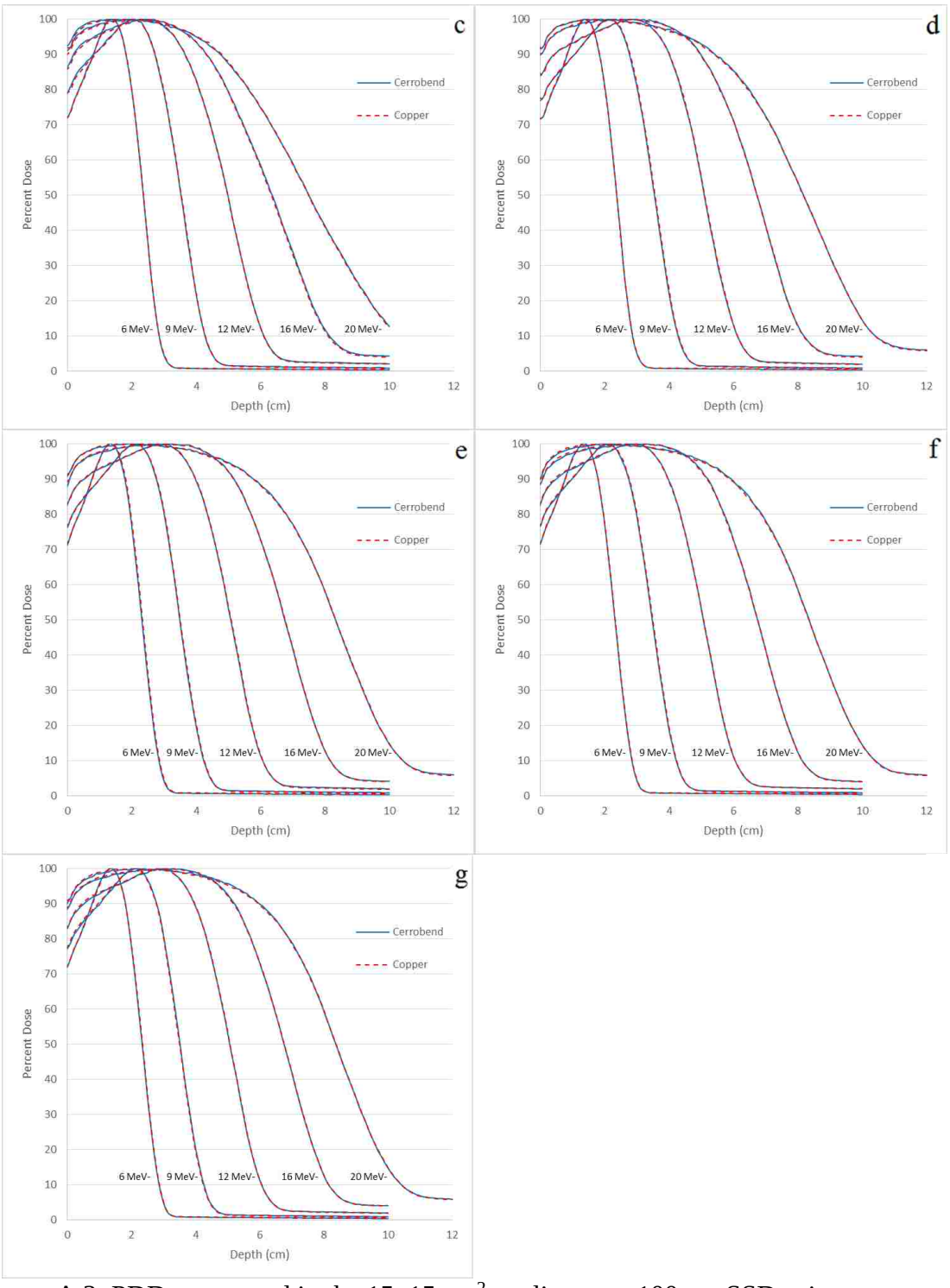

Figure A.3: PDDs measured in the 15x15 cm^2 applicator at 100 cm SSD using copper and Cerrobend inserts of field size: (a) 2x2 cm^2, (b) 3x3 cm^2, (c) 4x4 cm^2, (d) 6x6 cm^2, (e) 8x8 cm^2, (f) 10x10 cm^2, and (g) 12x12 cm^2.

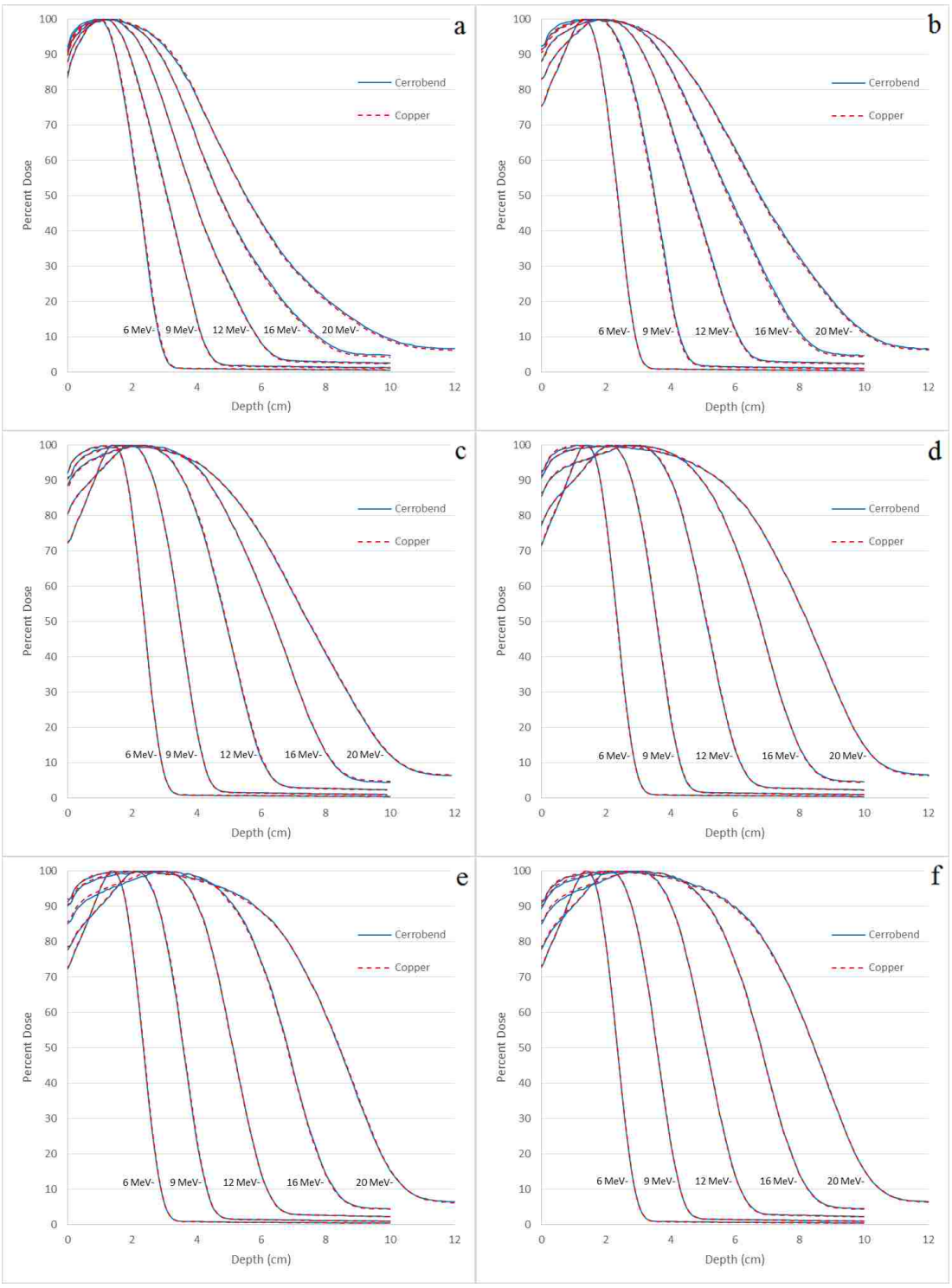
a
b
c
d
e
f
Cerrobend
Copper
Percent Dose
Depth (cm)
6 MeV-
9 MeV-
12 MeV-
16 MeV-
20 MeV-

(Figure A.4 continued)

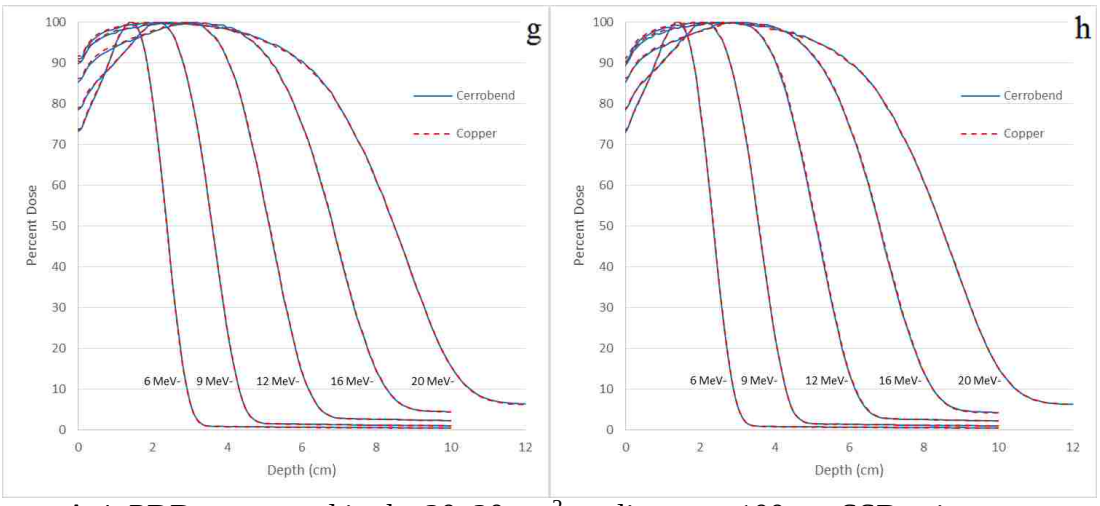

Figure A.4: PDDs measured in the 20x20 cm^2 applicator at 100 cm SSD using copper and Cerrobend inserts of field size: (a) 2x2 cm^2, (b) 3x3 cm^2, (c) 4x4 cm^2, (d) 6x6 cm^2, (e) 8x8 cm^2, (f) 10x10 cm^2, (g) 12x12 cm^2, and (h) 15x15 cm^2.

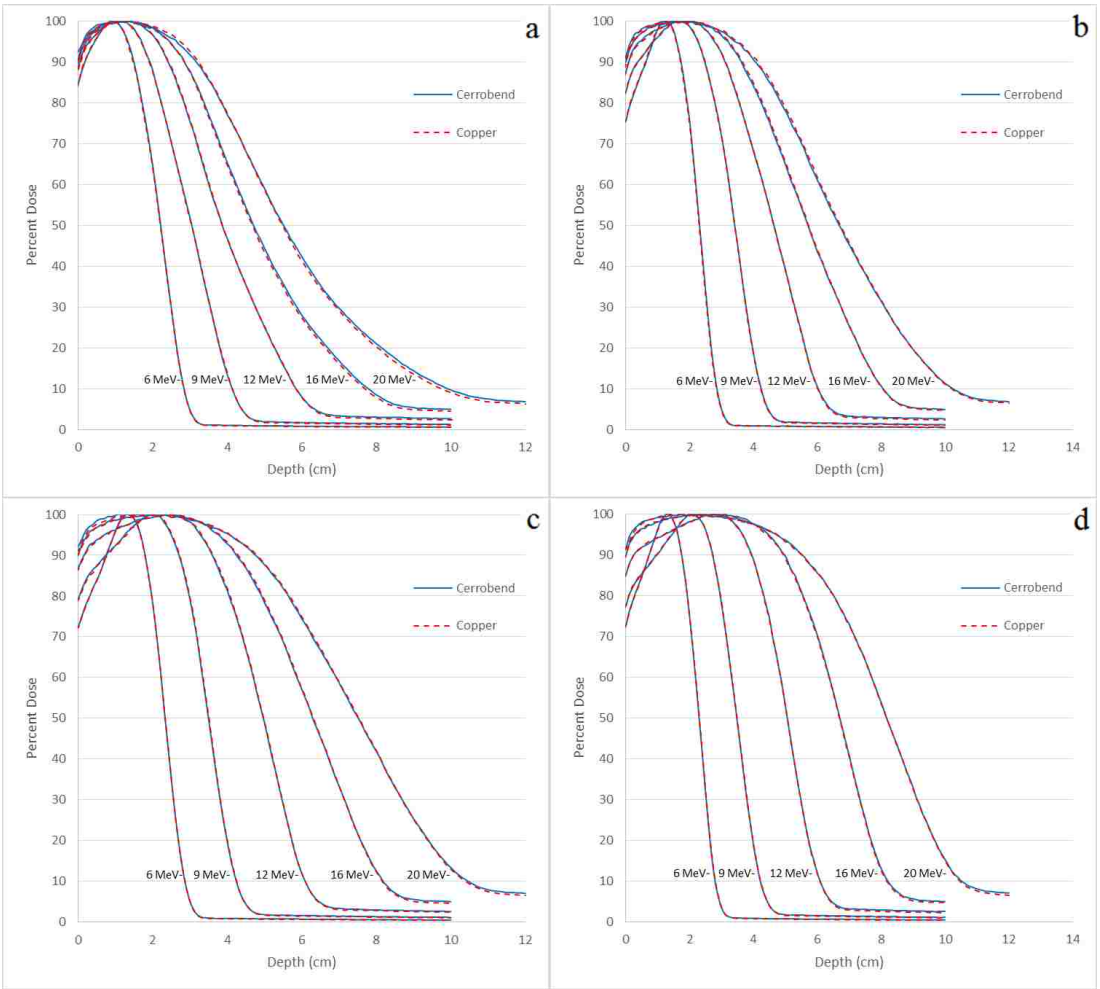

(Figure A.5 continued)

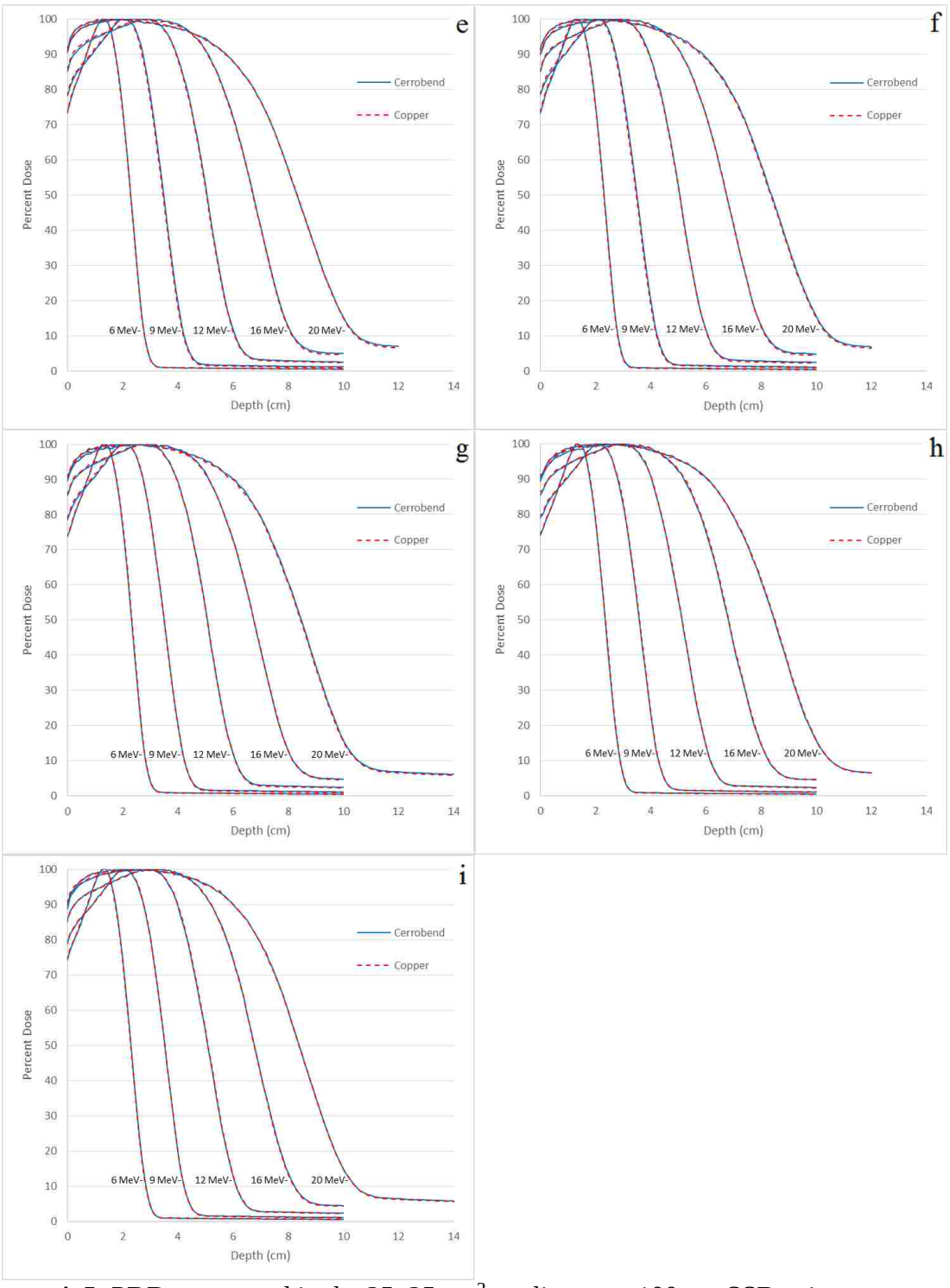

Figure A.5: PDDs measured in the 25x25 cm^2 applicator at 100 cm SSD using copper and Cerrobend inserts of field size: (a) 2x2 cm^2, (b) 3x3 cm^2, (c) 4x4 cm^2, (d) 6x6 cm^2, (e) 8x8 cm^2, (f) 10x10 cm^2, (g) 12x12 cm^2, (h) 15x15 cm^2, and (i) 20x20 cm^2.

Table A.1: Percent depth dose metrics at 100 cm SSD for all possible field size, applicator size, and energy combinations (differences and Cerrobend values).

Applicator Size (cm)	Field Size (cm)	Energy (MeV)	ΔR_{100} (cm)	R_{100} (cm)	ΔR_{90} (cm)	R_{90} (cm)	ΔR_{50} (cm)	R_{50} (cm)	ΔR_{80-20} (cm)	R_{80-20} (cm)	$\Delta D_{1.0}$ (%D_{max})	$D_{1.0}$ (%D_{max})	ΔD_x (%D_{max})	D_x (%D_{max})
6x6	2x2	6	0.00	0.93	0.00	0.93	0.00	2.21	0.00	0.92	0.00	99.80	0.00	0.4
6x6	2x2	9	0.04	1.09	-0.01	1.09	0.00	3.02	0.00	1.59	-0.20	99.70	0.00	0.8
6x6	2x2	12	-0.08	1.29	-0.06	1.29	-0.04	3.81	0.01	2.39	0.20	99.70	0.00	1.6
6x6	2x2	16	0.00	1.29	-0.05	1.29	-0.02	4.63	0.04	3.22	0.20	99.90	0.00	3.2
6x6	2x2	20	-0.04	1.07	-0.03	1.07	-0.04	5.38	0.03	4.01	0.10	100.00	0.00	4.7
6x6	3x3	6	0.00	1.29	0.00	1.29	0.00	2.34	0.00	0.75	-0.20	97.10	0.00	0.3
6x6	3x3	9	0.00	1.69	0.01	1.69	0.01	3.45	0.01	1.17	-0.10	95.70	0.00	0.8
6x6	3x3	12	-0.02	1.91	0.01	1.91	0.01	4.65	0.01	2.02	-0.10	97.70	0.00	1.6
6x6	3x3	16	-0.16	1.63	-0.01	1.63	0.00	5.7	0.01	3.02	0.00	99.00	0.00	3.3
6x6	3x3	20	-0.06	1.43	0.00	1.43	0.00	6.6	0.01	3.99	-0.40	99.30	0.00	4.8
6x6	4x4	6	0.06	1.39	0.01	1.39	0.06	2.38	-0.01	0.71	-0.20	95.80	-0.10	0.3
6x6	4x4	9	0.04	2.03	0.02	2.03	0.04	3.53	0.00	1.00	0.10	92.10	-0.10	0.7
6x6	4x4	12	0.06	2.45	0.00	2.45	0.05	4.99	0.00	1.66	-0.30	95.80	0.00	1.6
6x6	4x4	16	0.00	2.07	-0.02	2.07	0.06	6.3	0.00	2.60	-0.10	98.60	0.00	3.4
6x6	4x4	20	0.02	1.55	0.03	1.55	0.07	7.47	-0.02	3.66	-0.50	99.10	0.00	5
10x10	2x2	6	0.00	0.99	-0.02	0.99	-0.02	2.24	-0.01	0.91	0.00	100.00	0.00	0.4
10x10	2x2	9	-0.04	1.13	-0.02	1.13	-0.01	3.08	-0.01	1.62	-0.20	99.50	0.00	0.9
10x10	2x2	12	-0.12	1.29	-0.02	1.29	-0.02	3.93	0.02	2.39	0.30	99.70	0.10	1.9
10x10	2x2	16	-0.04	1.31	-0.01	1.31	0.01	4.72	0.01	3.21	0.00	99.70	0.10	3.7
10x10	2x2	20	0.02	1.13	-0.03	1.13	0.01	5.51	0.03	4.05	0.00	100.00	0.10	5.4
10x10	3x3	6	0.00	1.35	0.00	1.35	0.00	2.38	0.00	0.76	-0.40	96.00	0.00	0.4
10x10	3x3	9	0.00	1.77	-0.01	1.77	0.01	3.52	0.00	1.20	-0.20	95.30	0.00	0.8
10x10	3x3	12	-0.06	1.91	0.00	1.91	0.01	4.71	0.01	1.99	0.20	97.60	0.10	1.9
10x10	3x3	16	-0.06	1.61	-0.01	1.61	0.00	5.8	0.00	2.98	0.10	99.20	0.20	3.4
10x10	3x3	20	0.08	1.41	0.00	1.41	0.02	6.74	0.00	4.05	-0.40	99.60	0.20	5.5
10x10	4x4	6	0.00	1.35	0.00	1.35	0.00	2.32	0.00	0.74	0.40	95.70	-0.10	0.3
10x10	4x4	9	0.00	1.99	0.00	1.99	-0.01	3.53	0.01	1.05	0.30	92.20	0.00	0.8
10x10	4x4	12	-0.04	2.37	0.00	2.37	-0.01	4.94	0.00	1.66	-0.30	96.10	0.00	1.8
10x10	4x4	16	0.00	1.93	-0.02	1.93	0.01	6.31	0.00	2.63	-0.20	99.00	0.10	3.8
10x10	4x4	20	0.30	1.61	0.03	1.61	0.00	7.42	-0.01	3.75	-0.30	99.50	0.20	5.5
10x10	6x6	6	-0.02	1.37	-0.02	1.37	-0.02	2.33	0.00	0.73	0.10	94.70	-0.10	0.3
10x10	6x6	9	0.00	2.11	0.01	2.11	0.01	3.55	0.00	1.00	-0.50	89.60	0.00	0.8
10x10	6x6	12	-0.02	2.85	0.00	2.85	-0.01	5.08	0.00	1.44	-0.20	93.20	0.00	1.8

(Table A.1 continued)

Applicator Size (cm)	Field Size (cm)	Energy (MeV)	ΔR_{100} (cm)	R_{100} (cm)	ΔR_{90} (cm)	R_{90} (cm)	ΔR_{50} (cm)	R_{50} (cm)	ΔR_{80-20} (cm)	R_{80-20} (cm)	$\Delta D_{1.0}$ (%D_{max})	$D_{1.0}$ (%D_{max})	ΔD_x (%D_{max})	D_x (%D_{max})
10x10	6x6	16	0.56	2.85	0.01	2.85	-0.01	6.69	0.00	2.11	-0.40	97.90	0.00	3.8
10x10	6x6	20	-0.02	1.63	0.13	1.63	0.02	8.17	-0.05	3.13	0.20	99.50	0.00	5.5
10x10	8x8	6	0.00	1.39	-0.01	1.39	-0.02	2.34	0.01	0.74	0.00	94.40	0.00	0.4
10x10	8x8	9	0.04	2.15	0.01	2.15	-0.01	3.56	0.00	1.00	-0.20	89.80	0.10	0.9
10x10	8x8	12	0.02	3.01	0.01	3.01	-0.01	5.1	-0.02	1.41	-0.60	92.50	0.00	1.8
10x10	8x8	16	0.04	3.15	0.03	3.15	0.01	6.78	0.00	1.95	-0.50	97.80	0.00	3.8
10x10	8x8	20	0.24	2.01	0.06	2.01	0.01	8.37	-0.04	2.85	-0.30	99.00	0.20	5.7
15x15	2x2	6	0.00	0.99	-0.01	0.99	-0.01	2.24	0.00	0.91	0.10	100.00	-0.10	0.4
15x15	2x2	9	0.02	1.17	0.00	1.17	0.02	3.06	0.01	1.59	0.20	99.80	0.10	1
15x15	2x2	12	-0.10	1.29	-0.01	1.29	0.00	3.89	0.01	2.42	0.20	99.70	0.10	2.1
15x15	2x2	16	-0.10	1.27	-0.02	1.27	0.00	4.71	0.03	3.27	0.30	99.60	0.20	4.1
15x15	2x2	20	-0.10	1.17	-0.06	1.17	0.00	5.47	0.04	4.09	-0.20	99.50	*	*
15x15	3x3	6	-0.02	1.27	-0.03	1.27	-0.02	2.31	0.01	0.74	-0.10	97.10	0.00	0.4
15x15	3x3	9	-0.02	1.71	-0.02	1.71	-0.02	3.41	-0.01	1.21	0.20	95.60	0.00	0.9
15x15	3x3	12	-0.10	1.93	-0.01	1.93	0.00	4.66	0.00	2.00	-0.30	97.50	0.10	2.1
15x15	3x3	16	-0.02	1.93	-0.03	1.93	0.00	5.72	0.00	3.01	0.20	99.20	0.20	4.2
15x15	3x3	20	-0.12	1.29	-0.04	1.29	-0.02	6.68	0.03	4.05	0.40	99.90	*	*
15x15	4x4	6	-0.02	1.37	0.01	1.37	-0.01	2.35	0.00	0.70	0.80	95.10	0.00	0.4
15x15	4x4	9	0.00	2.03	-0.01	2.03	-0.01	3.53	0.01	1.06	0.20	91.80	0.10	0.9
15x15	4x4	12	-0.04	2.41	-0.01	2.41	0.00	4.98	0.01	1.65	0.30	96.00	0.10	2.1
15x15	4x4	16	-0.04	2.17	-0.01	2.17	0.02	6.36	0.03	2.60	0.00	98.70	0.30	4.3
15x15	4x4	20	-0.46	1.35	-0.05	1.35	0.00	7.5	0.02	3.77	0.30	99.70	*	*
15x15	6x6	6	0.02	1.41	-0.01	1.41	0.00	2.37	0.00	0.70	-0.60	94.00	0.00	0.4
15x15	6x6	9	0.00	2.15	-0.03	2.15	-0.03	3.54	0.00	1.02	-0.10	89.30	0.00	0.9
15x15	6x6	12	0.00	2.87	-0.01	2.87	-0.02	5.09	0.00	1.41	-0.10	93.30	0.10	2
15x15	6x6	16	-0.40	2.39	0.00	2.39	-0.01	6.73	-0.01	2.10	-0.50	97.80	0.10	4.2
15x15	6x6	20	-0.18	1.61	0.05	1.61	0.02	8.18	-0.04	3.17	0.40	99.30	*	*
15x15	8x8	6	-0.02	1.33	-0.04	1.33	-0.02	2.31	0.01	0.73	-0.20	95.40	0.00	0.4
15x15	8x8	9	0.00	2.11	-0.01	2.11	-0.01	3.49	-0.01	0.98	0.10	90.10	0.00	0.9
15x15	8x8	12	-0.02	2.93	-0.03	2.93	-0.02	5.07	0.00	1.38	-0.20	92.90	0.00	2
15x15	8x8	16	-0.26	2.87	0.01	2.87	-0.01	6.75	-0.02	1.98	-0.20	97.50	0.20	4.2
15x15	8x8	20	-0.04	2.03	0.01	2.03	0.00	8.33	0.00	2.87	-0.30	99.00	*	*
15x15	10x10	6	0.00	1.35	0.00	1.35	-0.01	2.32	0.00	0.73	0.50	96.00	0.00	0.4
15x15	10x10	9	0.00	2.09	-0.01	2.09	-0.02	3.48	0.01	0.99	-0.10	90.30	0.00	0.9
15x15	10x10	12	0.04	2.93	0.01	2.93	-0.01	5.06	-0.02	1.37	-0.20	92.90	0.00	2

(Table A.1 continued)

Applicator Size (cm)	Field Size (cm)	Energy (MeV)	ΔR_{100} (cm)	R_{100} (cm)	ΔR_{90} (cm)	R_{90} (cm)	ΔR_{50} (cm)	R_{50} (cm)	ΔR_{80-20} (cm)	R_{80-20} (cm)	$\Delta D_{1.0}$ (%D_{max})	$D_{1.0}$ (%D_{max})	ΔD_x (%D_{max})	D_x (%D_{max})
15x15	10x10	16	-0.04	3.03	0.02	3.03	0.00	6.75	-0.01	1.97	-0.40	97.30	0.10	4.1
15x15	10x10	20	0.44	2.31	0.05	2.31	0.01	8.35	-0.02	2.78	-0.20	98.60	*	*
15x15	12x12	6	0.00	1.37	0.00	1.37	-0.02	2.33	-0.01	0.72	0.60	95.80	0.00	0.4
15x15	12x12	9	0.00	2.11	0.01	2.11	0.03	3.53	0.01	0.99	-0.70	89.70	0.00	0.9
15x15	12x12	12	0.02	2.93	-0.02	2.93	-0.02	5.06	0.00	1.38	-0.60	92.70	0.10	2
15x15	12x12	16	-0.12	3.07	0.02	3.07	-0.01	6.76	-0.01	1.96	-0.60	97.10	0.10	4.1
15x15	12x12	20	0.12	2.23	0.03	2.23	-0.01	8.37	-0.03	2.75	-0.50	98.40	*	*
20x20	2x2	6	-0.02	0.95	-0.01	0.95	-0.02	2.21	0.00	0.95	0.00	100.00	0.00	0.5
20x20	2x2	9	0.00	1.13	0.01	1.13	0.01	3.08	0.00	1.63	0.10	99.70	0.10	1.2
20x20	2x2	12	0.04	1.31	0.00	1.31	0.00	3.9	0.02	2.45	-0.60	99.20	0.20	2.5
20x20	2x2	16	-0.06	1.21	-0.02	1.21	0.02	4.71	0.04	3.28	0.30	99.90	0.50	4.7
20x20	2x2	20	-0.18	1.09	-0.04	1.09	0.02	5.53	0.08	4.20	-0.10	99.80	0.50	6.6
20x20	3x3	6	0.00	1.31	0.01	1.31	0.00	2.36	0.00	0.78	0.00	96.70	0.10	0.5
20x20	3x3	9	0.02	1.75	0.00	1.75	0.02	3.51	-0.02	1.18	0.50	95.60	0.10	1.1
20x20	3x3	12	0.04	1.93	-0.02	1.93	0.03	4.69	0.00	2.04	0.00	97.60	0.20	2.5
20x20	3x3	16	-0.14	1.73	-0.03	1.73	0.04	5.83	0.01	3.06	0.20	98.90	0.30	4.7
20x20	3x3	20	-0.04	1.55	-0.01	1.55	0.04	6.78	0.04	4.10	0.50	99.70	0.30	6.6
20x20	4x4	6	0.00	1.41	0.00	1.41	0.00	2.38	-0.01	0.73	-0.30	94.20	0.00	0.4
20x20	4x4	9	0.00	2.05	0.00	2.05	0.00	3.59	0.00	1.05	-0.20	91.70	0.00	1
20x20	4x4	12	0.06	2.47	-0.02	2.47	-0.02	5	0.01	1.68	0.10	96.30	0.10	2.4
20x20	4x4	16	0.26	2.11	0.00	2.11	0.00	6.4	0.00	2.66	-0.10	98.60	0.30	4.7
20x20	4x4	20	-0.16	1.59	0.00	1.59	0.02	7.58	0.00	3.74	0.40	99.40	0.10	6.5
20x20	6x6	6	0.00	1.39	0.00	1.39	0.00	2.35	0.00	0.73	-0.30	94.70	0.00	0.4
20x20	6x6	9	-0.04	2.09	0.00	2.09	-0.01	3.57	0.00	1.01	-0.10	89.90	0.00	1
20x20	6x6	12	-0.02	2.89	-0.02	2.89	-0.02	5.11	0.01	1.44	-0.40	94.50	0.10	2.3
20x20	6x6	16	-0.10	2.55	0.01	2.55	0.00	6.77	0.00	2.13	0.20	98.80	0.20	4.6
20x20	6x6	20	0.18	1.29	-0.02	1.29	0.00	8.25	0.00	3.14	-0.30	99.70	0.20	6.6
20x20	8x8	6	0.00	1.39	0.00	1.39	-0.01	2.35	0.00	0.73	-0.10	94.70	0.00	0.5
20x20	8x8	9	0.00	2.13	-0.02	2.13	-0.01	3.58	0.00	1.02	-0.10	90.10	0.00	1
20x20	8x8	12	0.02	2.91	-0.01	2.91	0.00	5.13	0.00	1.43	-0.90	93.70	0.10	2.3
20x20	8x8	16	0.08	2.75	0.04	2.75	0.01	6.83	-0.01	2.00	-0.20	98.00	0.10	4.5
20x20	8x8	20	0.36	2.11	0.03	2.11	-0.01	8.42	-0.01	2.89	0.10	99.10	0.20	6.5
20x20	10x10	6	0.00	1.39	-0.01	1.39	-0.01	2.35	0.00	0.74	-0.10	94.80	0.00	0.5
20x20	10x10	9	0.00	2.13	0.00	2.13	-0.01	3.57	-0.01	1.01	0.00	90.40	0.00	1
20x20	10x10	12	0.06	3.01	0.00	3.01	0.01	5.12	-0.01	1.42	-0.30	94.10	0.00	2.3

(Table A.1 continued)

Applicator Size (cm)	Field Size (cm)	Energy (MeV)	ΔR_{100} (cm)	R_{100} (cm)	ΔR_{90} (cm)	R_{90} (cm)	ΔR_{50} (cm)	R_{50} (cm)	ΔR_{80-20} (cm)	R_{80-20} (cm)	$\Delta D_{1.0}$ (%D_{max})	$D_{1.0}$ (%D_{max})	ΔD_x (%D_{max})	D_x (%D_{max})
20x20	10x10	16	0.26	2.99	0.03	2.99	0.00	6.82	0.00	2.00	-0.30	97.50	0.20	4.6
20x20	10x10	20	0.06	2.09	0.05	2.09	0.00	8.46	0.00	2.81	-0.60	98.50	0.20	6.5
20x20	12x12	6	0.00	1.41	0.01	1.41	0.00	2.38	0.01	0.74	0.30	94.60	0.00	0.5
20x20	12x12	9	-0.02	2.13	0.00	2.13	0.00	3.6	-0.01	1.01	0.00	90.40	0.00	1
20x20	12x12	12	-0.06	2.95	-0.02	2.95	-0.01	5.13	0.01	1.43	-0.70	93.80	0.10	2.3
20x20	12x12	16	0.58	3.11	-0.01	3.11	0.00	6.84	-0.01	1.99	-0.70	97.10	0.10	4.5
20x20	12x12	20	0.00	2.25	0.08	2.25	0.01	8.49	-0.02	2.77	-0.30	98.40	0.20	6.4
20x20	15x15	6	0.00	1.39	0.00	1.39	-0.01	2.35	-0.01	0.73	0.20	94.90	0.00	0.5
20x20	15x15	9	0.00	2.11	-0.01	2.11	-0.01	3.57	0.00	1.01	0.30	90.70	0.00	1
20x20	15x15	12	-0.08	2.89	-0.03	2.89	-0.02	5.11	0.01	1.43	-0.60	93.90	0.00	2.2
20x20	15x15	16	0.50	3.11	-0.02	3.11	-0.01	6.81	0.01	1.98	-0.50	97.40	0.00	4.3
20x20	15x15	20	0.56	2.69	-0.03	2.69	0.00	8.46	0.01	2.77	-0.40	98.30	0.20	6.3
25x25	2x2	6	0.00	0.93	0.02	0.93	0.00	2.21	0.00	0.94	-0.20	99.60	0.00	0.6
25x25	2x2	9	0.02	1.13	0.00	1.13	0.02	3.06	0.00	1.58	-0.50	99.40	0.20	1.3
25x25	2x2	12	0.10	1.31	-0.02	1.31	0.04	3.87	0.00	2.43	0.00	99.40	0.30	2.7
25x25	2x2	16	-0.08	1.17	-0.03	1.17	0.02	4.7	0.04	3.33	-0.10	99.60	0.50	5
25x25	2x2	20	-0.08	1.07	-0.02	1.07	0.05	5.53	0.07	4.25	0.20	99.90	0.50	6.8
25x25	3x3	6	0.00	1.25	0.01	1.25	0.00	2.31	0.00	0.75	0.20	98.10	0.00	0.5
25x25	3x3	9	-0.02	1.69	-0.02	1.69	-0.01	3.41	0.01	1.18	0.00	96.00	0.10	1.2
25x25	3x3	12	-0.20	1.77	-0.02	1.77	-0.01	4.64	0.02	2.07	-0.10	97.90	0.20	2.6
25x25	3x3	16	-0.02	1.79	0.00	1.79	-0.01	5.71	0.03	3.08	0.30	99.00	0.30	4.9
25x25	3x3	20	0.12	1.75	-0.08	1.75	-0.04	6.69	0.05	4.10	0.20	99.50	0.30	6.8
25x25	4x4	6	0.00	1.35	0.00	1.35	-0.01	2.33	0.00	0.72	0.00	95.90	0.00	0.5
25x25	4x4	9	-0.02	1.99	-0.01	1.99	-0.01	3.5	0.00	1.02	0.10	92.50	0.10	1.1
25x25	4x4	12	0.08	2.43	-0.01	2.43	-0.01	4.97	0.02	1.69	-0.10	96.10	0.20	2.6
25x25	4x4	16	0.14	2.25	-0.04	2.25	-0.03	6.29	0.02	2.66	-0.10	98.60	0.40	5
25x25	4x4	20	0.12	1.87	-0.03	1.87	-0.01	7.52	0.04	3.77	0.40	99.70	0.40	7
25x25	6x6	6	-0.02	1.31	-0.01	1.31	-0.01	2.3	-0.01	0.71	0.20	96.10	0.00	0.5
25x25	6x6	9	0.00	2.09	-0.02	2.09	-0.01	3.48	0.01	1.02	-0.20	90.20	0.20	1.2
25x25	6x6	12	-0.08	2.75	0.01	2.75	-0.01	5.06	-0.01	1.40	0.30	94.40	0.20	2.6
25x25	6x6	16	0.38	2.93	0.02	2.93	0.00	6.7	0.00	2.13	0.00	98.00	0.40	5
25x25	6x6	20	0.30	2.03	0.02	2.03	-0.01	8.17	0.01	3.17	0.20	99.20	0.50	7.1
25x25	8x8	6	0.00	1.31	0.00	1.31	0.00	2.29	-0.01	0.72	0.00	96.70	0.00	0.5
25x25	8x8	9	0.02	2.07	0.03	2.07	0.02	3.49	-0.01	1.02	-0.40	91.20	0.20	1.2
25x25	8x8	12	0.00	2.85	0.01	2.85	0.00	5.05	-0.01	1.39	-0.40	94.60	0.20	2.5

(Table A.1 continued)

Applicator Size (cm)	Field Size (cm)	Energy (MeV)	ΔR_{100} (cm)	R_{100} (cm)	ΔR_{90} (cm)	R_{90} (cm)	ΔR_{50} (cm)	R_{50} (cm)	ΔR_{80-20} (cm)	R_{80-20} (cm)	$\Delta D_{1.0}$ (%D_{max})	$D_{1.0}$ (%D_{max})	ΔD_x (%D_{max})	D_x (%D_{max})
25x25	8x8	16	0.08	2.33	0.02	2.33	0.01	6.73	0.01	2.02	-0.10	98.60	0.40	5
25x25	8x8	20	-0.04	1.69	0.07	1.69	0.00	8.32	-0.02	2.93	0.20	99.40	0.30	7
25x25	10x10	6	0.02	1.33	0.01	1.33	0.00	2.31	0.00	0.72	-0.40	96.10	0.00	0.5
25x25	10x10	9	0.04	2.09	0.01	2.09	0.01	3.5	0.00	1.03	-0.20	91.00	0.00	1.1
25x25	10x10	12	-0.06	2.77	0.03	2.77	0.00	5.05	-0.01	1.40	0.00	94.40	0.20	2.5
25x25	10x10	16	0.36	2.67	0.00	2.67	-0.01	6.75	0.00	2.00	-0.10	98.20	0.20	4.8
25x25	10x10	20	-0.20	1.69	0.09	1.69	0.03	8.38	0.01	2.88	0.00	99.10	0.40	6.9
25x25	12x12	6	-0.02	1.33	-0.01	1.33	-0.02	2.32	0.00	0.72	0.20	96.10	0.10	0.6
25x25	12x12	9	0.00	2.07	0.00	2.07	0.00	3.51	0.00	1.03	-0.50	90.90	0.00	1.1
25x25	12x12	12	-0.06	2.83	-0.01	2.83	0.00	5.07	0.00	1.38	-0.50	94.40	0.10	2.5
25x25	12x12	16	0.22	2.85	0.00	2.85	-0.01	6.75	-0.01	2.00	-0.30	98.00	0.30	4.8
25x25	12x12	20	-0.34	2.05	0.03	2.05	0.01	8.39	-0.01	2.81	0.00	99.00	0.30	6.8
25x25	15x15	6	0.00	1.37	-0.01	1.37	-0.02	2.35	-0.01	0.74	-0.30	95.00	0.00	0.5
25x25	15x15	9	-0.04	2.11	-0.01	2.11	-0.02	3.58	0.00	1.00	-0.60	90.20	0.00	1.1
25x25	15x15	12	0.00	2.91	-0.02	2.91	0.00	5.14	-0.01	1.45	-0.10	94.30	0.10	2.4
25x25	15x15	16	0.00	2.91	-0.02	2.91	-0.02	6.81	0.00	1.97	-0.40	97.70	0.20	4.7
25x25	15x15	20	0.22	2.41	0.05	2.41	-0.02	8.48	0.00	2.79	0.30	98.70	0.20	6.6
25x25	20x20	6	0.00	1.31	0.01	1.31	0.00	2.3	0.01	0.75	0.10	96.10	0.00	0.5
25x25	20x20	9	-0.04	2.05	-0.01	2.05	-0.01	3.53	0.00	0.99	0.20	90.90	0.00	1
25x25	20x20	12	-0.08	2.91	-0.01	2.91	-0.01	5.08	0.01	1.44	-0.10	94.10	0.10	2.3
25x25	20x20	16	0.44	3.17	-0.03	3.17	0.00	6.77	0.02	1.96	-0.20	97.60	0.00	4.4
25x25	20x20	20	0.24	2.53	-0.01	2.53	0.00	8.45	0.01	2.75	0.40	98.70	0.10	6.4

Appendix B Percent Depth Dose Metrics at 110 cm SSD

Percent depth dose curves are measured at 110 cm SSD for the subset of field size and energy combinations are shown for the 6x6 cm^2 (Figure B.1), 15x15 cm^2 (Figure B.2), and 25x25 cm^2 (Figure B.3) applicators. Table B.1 contains data (differences and Cerrobend values) from the PDDs, metrics include R_{100}, R_{90}, R_{50}, $R_{80\text{-}20}$, $D_{1.0}$ and D_x. All differences were calculated by taking the value from the Cerrobend insert PDD minus the copper insert PDD.

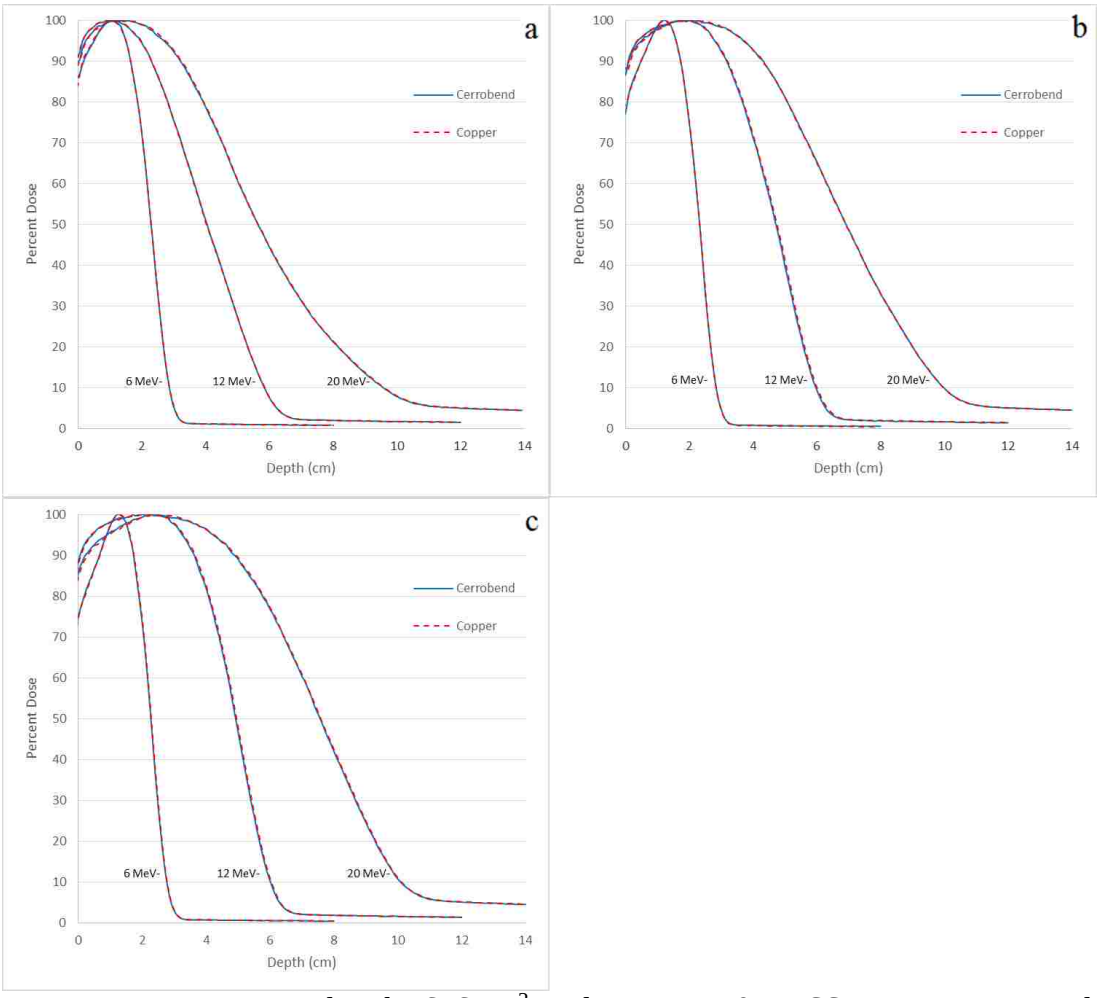

Figure B.1: PDDs measured in the 6x6 cm^2 applicator at 110 cm SSD using copper and Cerrobend inserts of field size: (a) 2x2 cm^2, (b) 3x3 cm^2, and (c) 4x4 cm^2.

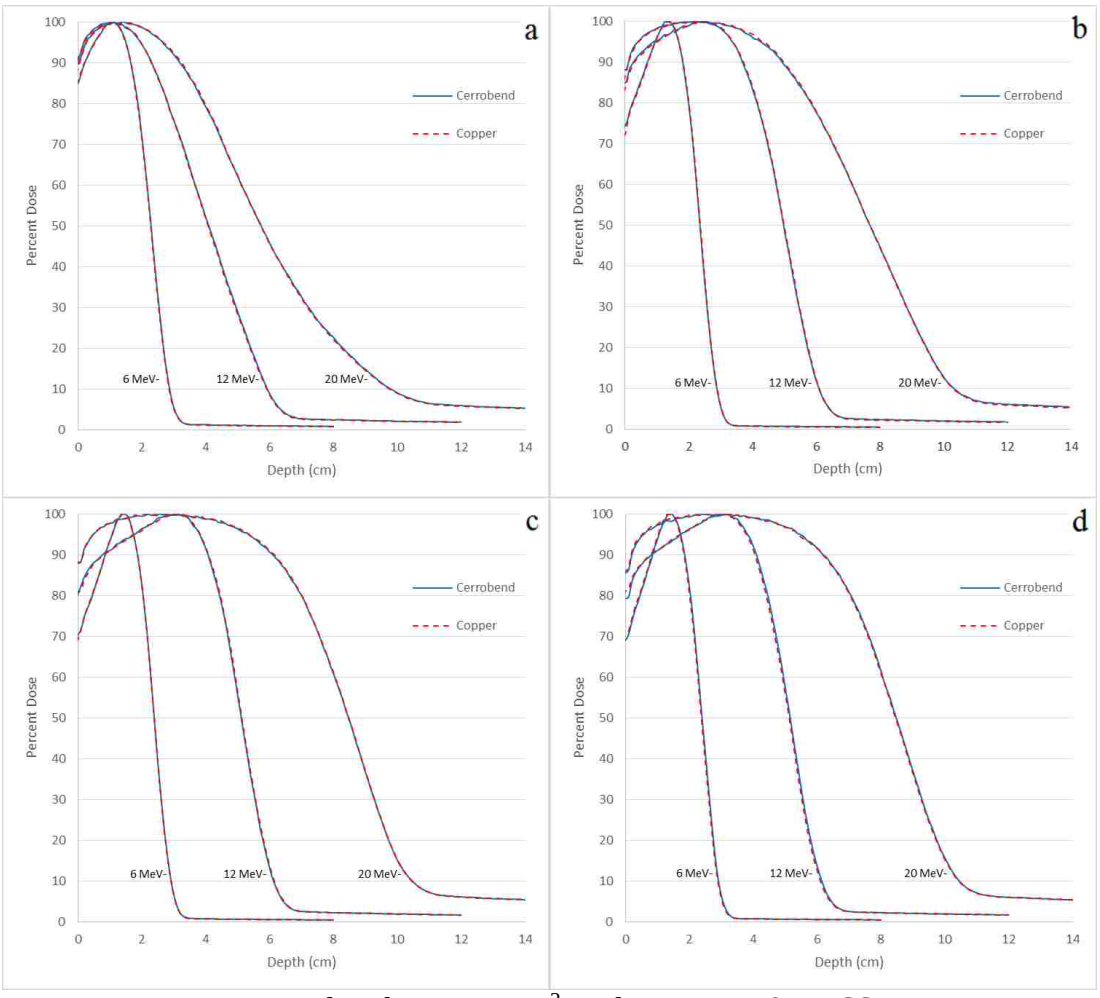

Figure B.2: PDDs measured in the 15x15 cm^2 applicator at 110 cm SSD using copper and Cerrobend inserts of field size: (a) 2x2 cm^2, (b) 4x4 cm^2, (c) 8x8 cm^2, and (d) 12x12 cm^2.

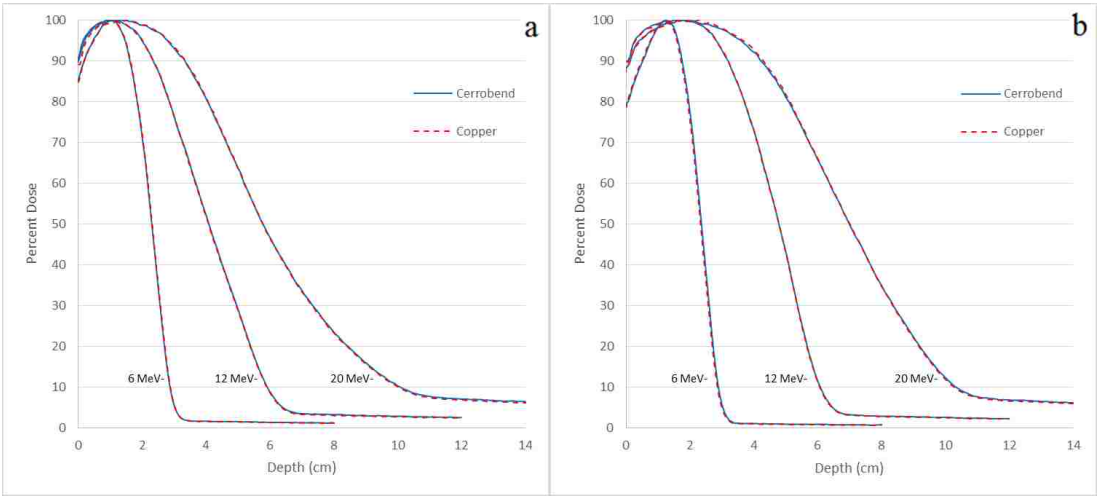

(Figure B.3 continued)

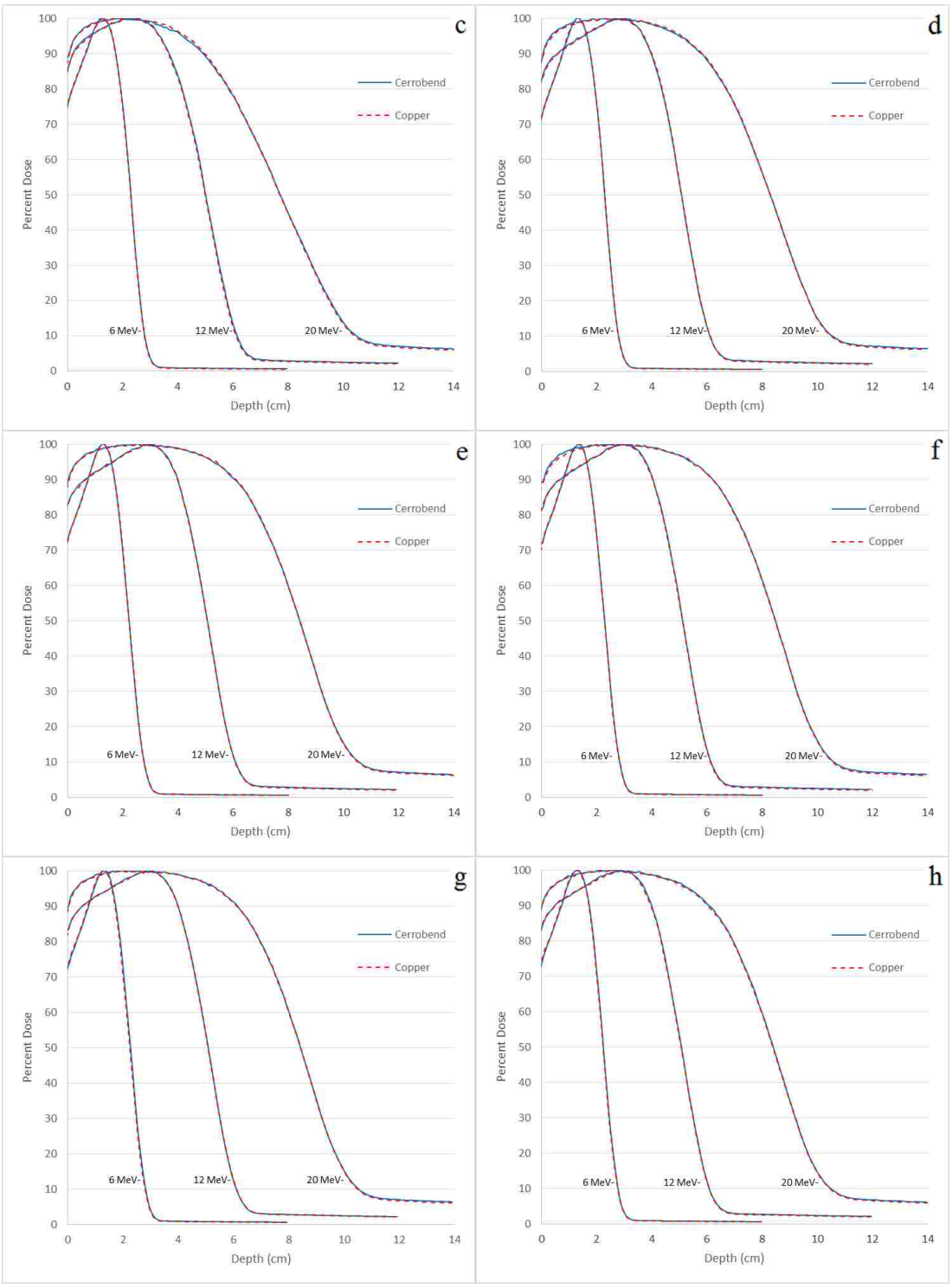

(Figure B.3 continued)

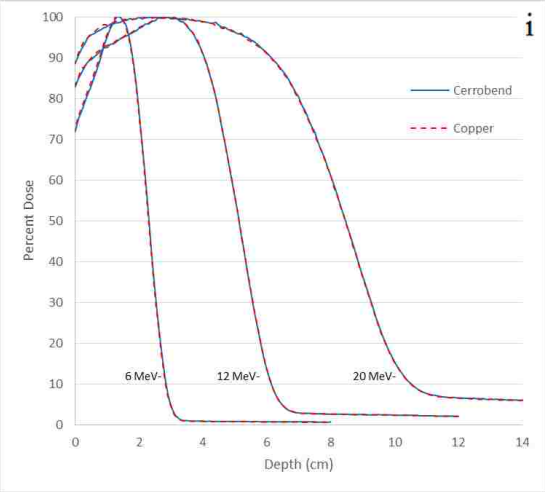

Figure B.3: PDDs measured in the 25x25 cm^2 applicator at 110 cm SSD using copper and Cerrobend inserts of field size: (a) 2x2 cm^2, (b) 3x3 cm^2, (c) 4x4 cm^2, (d) 6x6 cm^2, (e) 8x8 cm^2, (f) 10x10 cm^2, (g) 12x12 cm^2, (h) 15x15 cm^2, and (i) 20x20 cm^2.

Table B.1: Percent depth dose metrics at 110 cm SSD for a subset of field size, applicator size, and energy combinations.

Applicator Size (cm)	Field Size (cm)	Energy (MeV)	ΔR_{100} (cm)	R_{100} (cm)	ΔR_{90} (cm)	R_{90} (cm)	ΔR_{50} (cm)	R_{50} (cm)	$\Delta R_{80\text{-}20}$ (cm)	$R_{80\text{-}20}$ (cm)	$\Delta D_{1.0}$ (%D_{max})	$D_{1.0}$ (%D_{max})	ΔD_x (%D_{max})	D_x (%D_{max})
6x6	2x2	6	0.00	1.07	0.00	1.65	0.00	1.65	-0.01	0.81	0.30	100	0.00	0.8
6x6	2x2	9	-0.02	0.97	-0.01	2.3	0.00	2.3	-0.01	2.51	-0.20	99.8	-0.10	1.4
6x6	2x2	12	0.03	1.32	-0.03	3.2	0.00	3.2	0.00	4.24	0.30	99.7	0.00	4.5
6x6	2x2	16	0.00	1.21	0.00	1.72	0.00	1.72	0.00	0.76	0.00	98.6	0.00	0.5
6x6	2x2	20	-0.06	1.79	0.00	3.17	0.00	3.17	-0.02	1.91	0.30	98	0.00	1.4
6x6	3x3	6	-0.02	1.97	0.00	4.32	0.00	4.32	-0.01	3.93	-0.30	98.2	0.00	4.5
6x6	3x3	9	0.00	1.27	-0.01	1.72	0.00	1.72	0.00	0.71	-0.30	97.3	0.00	0.4
6x6	3x3	12	0.05	2.39	0.00	3.62	0.00	3.62	-0.01	1.59	0.20	95.7	0.10	1.4
6x6	3x3	16	-0.10	2.03	-0.01	4.88	0.00	4.88	0.01	3.53	-0.10	98.1	-0.10	4.5
6x6	3x3	20	0.02	1.09	-0.01	1.65	0.01	1.65	-0.01	0.81	-0.60	99.3	0.00	0.9
6x6	4x4	6	-0.10	1.01	0.02	2.32	0.00	2.32	0.02	2.6	0.40	100	0.10	1.9
6x6	4x4	9	-0.22	1.25	-0.09	3.18	0.00	3.18	0.09	4.37	-0.10	99.5	0.00	5.3
6x6	4x4	12	0.00	1.35	0.00	1.81	0.00	1.81	0.01	0.72	-0.20	96.1	0.00	0.5
6x6	4x4	16	-0.05	2.4	-0.02	3.69	0.00	3.69	0.00	1.59	0.10	95.2	0.10	1.8
6x6	4x4	20	-0.31	2.02	0.00	4.97	0.00	4.97	0.05	3.64	-0.30	97.9	0.10	5.4
15x15	2x2	6	0.00	1.43	0.00	1.86	0.00	1.86	0.00	0.7	0.10	93.4	0.00	0.5
15x15	2x2	9	0.04	3.13	-0.02	4.07	0.00	4.07	0.01	1.37	0.10	91.1	0.00	1.7
15x15	2x2	12	0.13	2.48	-0.02	6.11	0.00	6.11	-0.02	2.72	0.30	97.8	0.00	5.4
15x15	2x2	16	0.00	1.39	-0.01	1.85	0.00	1.85	0.00	0.73	-0.40	93.5	0.00	0.5
15x15	2x2	20	0.08	3.09	0.02	4.1	0.00	4.1	-0.01	1.35	-0.10	91	0.10	1.8
15x15	4x4	6	-0.28	2.45	0.01	6.19	0.00	6.19	0.00	2.7	-0.10	97.3	0.00	5.4
15x15	4x4	9	0.01	0.98	0.00	1.57	0.00	1.57	-0.01	0.85	0.00	100	0.00	1.1
15x15	4x4	12	0.03	0.98	-0.01	2.3	0.00	2.3	0.02	2.55	-0.10	99.9	0.20	2.5
15x15	4x4	16	0.19	1.41	0.00	3.3	0.00	3.3	0.05	4.39	0.80	99.8	0.30	6.1
15x15	4x4	20	0.01	1.23	0.02	1.73	0.00	1.73	-0.01	0.77	0.30	98.7	0.00	0.8
15x15	8x8	6	-0.06	1.83	0.00	3.2	0.00	3.2	0.02	1.97	0.20	98.2	0.10	2.3
15x15	8x8	9	-0.24	1.77	-0.07	4.22	0.00	4.22	0.06	4.11	0.20	99.1	0.20	6.2
15x15	8x8	12	-0.01	1.28	0.00	1.75	0.00	1.75	0.00	0.71	-0.20	97.1	0.10	0.7
15x15	8x8	16	0.03	2.38	0.00	3.66	0.00	3.66	0.01	1.63	0.10	96	0.20	2.3
15x15	8x8	20	-0.23	1.92	0.00	4.96	0.00	4.96	0.04	3.67	0.30	98.7	0.20	6.3
15x15	12x12	6	0.00	1.33	0.00	1.77	0.00	1.77	-0.01	0.69	-0.10	95.4	0.00	0.6
15x15	12x12	9	-0.03	2.87	0.00	3.98	0.00	3.98	0.00	1.4	0.50	92.8	0.10	2.2
15x15	12x12	12	-0.33	2.45	0.00	5.82	-0.01	5.82	0.03	3	0.50	98.4	0.40	6.5
15x15	12x12	16	0.00	1.29	0.00	1.7	0.00	1.7	0.01	0.73	0.10	96.4	0.00	0.6

(Table B.1 continued)

Applicator Size (cm)	Field Size (cm)	Energy (MeV)	ΔR_{100} (cm)	R_{100} (cm)	ΔR_{90} (cm)	R_{90} (cm)	ΔR_{50} (cm)	R_{50} (cm)	ΔR_{80-20} (cm)	R_{80-20} (cm)	$\Delta D_{1.0}$ (%D_{max})	$D_{1.0}$ (%D_{max})	ΔD_x (%D_{max})	D_x (%D_{max})
15x15	12x12	20	-0.02	2.97	0.00	4	0.00	4	0.00	1.4	0.30	92.1	0.20	2.2
25x25	2x2	6	-0.12	2.59	-0.01	6.09	0.00	6.09	0.03	2.78	-0.20	97.8	0.30	6.4
25x25	2x2	9	-0.01	1.34	0.00	1.76	0.00	1.76	0.00	0.73	0.00	95.2	0.00	0.6
25x25	2x2	12	0.03	2.98	0.00	4.04	0.00	4.04	0.00	1.4	0.30	91.9	0.20	2.3
25x25	2x2	16	-0.04	2.89	0.00	6.22	0.00	6.22	0.00	2.73	0.50	98.1	0.30	6.5
25x25	2x2	20	-0.01	1.3	0.00	1.72	0.00	1.72	0.01	0.74	0.10	96.4	0.00	0.6
25x25	3x3	6	-0.07	2.92	0.00	3.99	0.00	3.99	-0.01	1.41	-0.10	92.6	0.10	2.2
25x25	3x3	9	-0.37	1.96	0.02	6.13	0.00	6.13	0.00	2.73	0.60	98.8	0.20	6.3
25x25	3x3	12	0.01	1.3	0.00	1.72	0.00	1.72	0.01	0.71	-0.10	96.9	0.00	0.6
25x25	3x3	16	0.02	2.93	0.00	3.98	0.00	3.98	0.01	1.41	-0.50	92.6	0.10	2.2
25x25	3x3	20	-0.20	2.35	0.00	6.04	0.00	6.04	0.00	2.72	0.10	98.2	0.20	6.2
25x25	4x4	6	0.00	1.37	0.01	1.8	0.00	1.8	-0.01	0.71	-0.30	95.2	0.10	0.7
25x25	4x4	9	-0.04	2.87	0.01	4.04	0.00	4.04	0.00	1.4	-0.40	92.4	0.10	2.1
25x25	4x4	12	-0.25	2.56	0.02	6.14	0.00	6.14	-0.03	2.7	-0.40	97.6	0.10	6.1
25x25	4x4	16	0.00	1.07	0.00	1.65	0.00	1.65	-0.01	0.81	0.30	100	0.00	0.8
25x25	4x4	20	-0.02	0.97	-0.01	2.3	0.00	2.3	-0.01	2.51	-0.20	99.8	-0.10	1.4
25x25	6x6	6	0.03	1.32	-0.03	3.2	0.00	3.2	0.00	4.24	0.30	99.7	0.00	4.5
25x25	6x6	9	0.00	1.21	0.00	1.72	0.00	1.72	0.00	0.76	0.00	98.6	0.00	0.5
25x25	6x6	12	-0.06	1.79	0.00	3.17	0.00	3.17	-0.02	1.91	0.30	98	0.00	1.4
25x25	6x6	16	-0.02	1.97	0.00	4.32	0.00	4.32	-0.01	3.93	-0.30	98.2	0.00	4.5
25x25	6x6	20	0.00	1.27	-0.01	1.72	0.00	1.72	0.00	0.71	-0.30	97.3	0.00	0.4
25x25	8x8	6	0.05	2.39	0.00	3.62	0.00	3.62	-0.01	1.59	0.20	95.7	0.10	1.4
25x25	8x8	9	-0.10	2.03	-0.01	4.88	0.00	4.88	0.01	3.53	-0.10	98.1	-0.10	4.5
25x25	8x8	12	0.02	1.09	-0.01	1.65	0.01	1.65	-0.01	0.81	-0.60	99.3	0.00	0.9
25x25	8x8	16	-0.10	1.01	0.02	2.32	0.00	2.32	0.02	2.6	0.40	100	0.10	1.9
25x25	8x8	20	-0.22	1.25	-0.09	3.18	0.00	3.18	0.09	4.37	-0.10	99.5	0.00	5.3
25x25	10x10	6	0.00	1.35	0.00	1.81	0.00	1.81	0.01	0.72	-0.20	96.1	0.00	0.5
25x25	10x10	9	-0.05	2.4	-0.02	3.69	0.00	3.69	0.00	1.59	0.10	95.2	0.10	1.8
25x25	10x10	12	-0.31	2.02	0.00	4.97	0.00	4.97	0.05	3.64	-0.30	97.9	0.10	5.4
25x25	10x10	16	0.00	1.43	0.00	1.86	0.00	1.86	0.00	0.7	0.10	93.4	0.00	0.5
25x25	10x10	20	0.04	3.13	-0.02	4.07	0.00	4.07	0.01	1.37	0.10	91.1	0.00	1.7
25x25	12x12	6	0.13	2.48	-0.02	6.11	0.00	6.11	-0.02	2.72	0.30	97.8	0.00	5.4
25x25	12x12	9	0.00	1.39	-0.01	1.85	0.00	1.85	0.00	0.73	-0.40	93.5	0.00	0.5
25x25	12x12	12	0.08	3.09	0.02	4.1	0.00	4.1	-0.01	1.35	-0.10	91	0.10	1.8
25x25	12x12	16	-0.28	2.45	0.01	6.19	0.00	6.19	0.00	2.7	-0.10	97.3	0.00	5.4

(Table B.1 continued)

Applicator Size (cm)	Field Size (cm)	Energy (MeV)	ΔR_{100} (cm)	R_{100} (cm)	ΔR_{90} (cm)	R_{90} (cm)	ΔR_{50} (cm)	R_{50} (cm)	ΔR_{80-20} (cm)	R_{80-20} (cm)	$\Delta D_{1.0}$ (%D_{max})	$D_{1.0}$ (%D_{max})	ΔD_x (%D_{max})	D_x (%D_{max})
25x25	12x12	20	0.01	0.98	0.00	1.57	0.00	1.57	-0.01	0.85	0.00	100	0.00	1.1
25x25	15x15	6	0.03	0.98	-0.01	2.3	0.00	2.3	0.02	2.55	-0.10	99.9	0.20	2.5
25x25	15x15	9	0.19	1.41	0.00	3.3	0.00	3.3	0.05	4.39	0.80	99.8	0.30	6.1
25x25	15x15	12	0.01	1.23	0.02	1.73	0.00	1.73	-0.01	0.77	0.30	98.7	0.00	0.8
25x25	15x15	16	-0.06	1.83	0.00	3.2	0.00	3.2	0.02	1.97	0.20	98.2	0.10	2.3
25x25	15x15	20	-0.24	1.77	-0.07	4.22	0.00	4.22	0.06	4.11	0.20	99.1	0.20	6.2
25x25	20x20	6	-0.01	1.28	0.00	1.75	0.00	1.75	0.00	0.71	-0.20	97.1	0.10	0.7
25x25	20x20	9	0.03	2.38	0.00	3.66	0.00	3.66	0.01	1.63	0.10	96	0.20	2.3
25x25	20x20	12	-0.23	1.92	0.00	4.96	0.00	4.96	0.04	3.67	0.30	98.7	0.20	6.3
25x25	20x20	16	0.00	1.33	0.00	1.77	0.00	1.77	-0.01	0.69	-0.10	95.4	0.00	0.6
25x25	20x20	20	-0.03	2.87	0.00	3.98	0.00	3.98	0.00	1.4	0.50	92.8	0.10	2.2

Appendix C Output Correction Factors at 100 cm SSD

Table C.1 contains the output correction factors measured at 100 cm SSD for all possible field size, applicator size, and energy combinations. OCFs are a ratio of the output reading taken with a copper insert divided by the output taken with the matching Cerrobend insert (Equation 2.4).

Table C.1: Output correction factors measured at 100 cm SSD for all possible applicator size, field size, and energy combinations.

Applicator Size (cm)	Field Size (cm)	Energy (MeV)	OCF
6x6	2x2	6	1.000
6x6	2x2	9	1.004
6x6	2x2	12	1.005
6x6	2x2	16	1.003
6x6	2x2	20	1.003
6x6	3x3	6	1.007
6x6	3x3	9	1.006
6x6	3x3	12	1.005
6x6	3x3	16	1.005
6x6	3x3	20	1.007
6x6	4x4	6	1.004
6x6	4x4	9	1.004
6x6	4x4	12	1.004
6x6	4x4	16	1.004
6x6	4x4	20	1.007
10x10	2x2	6	0.997
10x10	2x2	9	1.004
10x10	2x2	12	1.004
10x10	2x2	16	1.000
10x10	2x2	20	0.997
10x10	3x3	6	1.005
10x10	3x3	9	1.006
10x10	3x3	12	1.005
10x10	3x3	16	1.003
10x10	3x3	20	1.004
10x10	4x4	6	1.004
10x10	4x4	9	1.004

(Table C.1 continued)

Applicator Size (cm)	Field Size (cm)	Energy (MeV)	OCF
10x10	4x4	12	1.004
10x10	4x4	16	1.003
10x10	4x4	20	1.007
10x10	6x6	6	1.003
10x10	6x6	9	1.003
10x10	6x6	12	1.003
10x10	6x6	16	1.004
10x10	6x6	20	1.009
10x10	8x8	6	0.999
10x10	8x8	9	0.999
10x10	8x8	12	1.000
10x10	8x8	16	1.001
10x10	8x8	20	1.006
15x15	2x2	6	0.993
15x15	2x2	9	0.997
15x15	2x2	12	0.998
15x15	2x2	16	0.994
15x15	2x2	20	0.991
15x15	3x3	6	1.002
15x15	3x3	9	1.002
15x15	3x3	12	1.000
15x15	3x3	16	0.998
15x15	3x3	20	0.995
15x15	4x4	6	1.008
15x15	4x4	9	1.006
15x15	4x4	12	1.003
15x15	4x4	16	1.001
15x15	4x4	20	0.997
15x15	6x6	6	1.002
15x15	6x6	9	1.002
15x15	6x6	12	1.001
15x15	6x6	16	1.001
15x15	6x6	20	1.003
15x15	8x8	6	0.999
15x15	8x8	9	1.000
15x15	8x8	12	1.000
15x15	8x8	16	1.001
15x15	8x8	20	1.003

(Table C.1 continued)

Applicator Size (cm)	Field Size (cm)	Energy (MeV)	OCF
15x15	10x10	6	0.998
15x15	10x10	9	0.998
15x15	10x10	12	0.999
15x15	10x10	16	0.999
15x15	10x10	20	1.001
15x15	12x12	6	0.996
15x15	12x12	9	0.996
15x15	12x12	12	0.996
15x15	12x12	16	0.997
15x15	12x12	20	1.000
20x20	2x2	6	0.993
20x20	2x2	9	1.001
20x20	2x2	12	0.999
20x20	2x2	16	0.995
20x20	2x2	20	0.988
20x20	3x3	6	1.002
20x20	3x3	9	1.003
20x20	3x3	12	1.001
20x20	3x3	16	0.998
20x20	3x3	20	0.994
20x20	4x4	6	1.002
20x20	4x4	9	1.002
20x20	4x4	12	1.001
20x20	4x4	16	1.000
20x20	4x4	20	0.998
20x20	6x6	6	0.998
20x20	6x6	9	0.998
20x20	6x6	12	0.997
20x20	6x6	16	0.997
20x20	6x6	20	0.995
20x20	8x8	6	0.997
20x20	8x8	9	0.996
20x20	8x8	12	0.997
20x20	8x8	16	0.998
20x20	8x8	20	1.000
20x20	10x10	6	0.996
20x20	10x10	9	0.996
20x20	10x10	12	0.996

(Table C.1 continued)

Applicator Size (cm)	Field Size (cm)	Energy (MeV)	OCF
20x20	10x10	16	0.997
20x20	10x10	20	1.000
20x20	12x12	6	0.997
20x20	12x12	9	0.996
20x20	12x12	12	0.996
20x20	12x12	16	0.997
20x20	12x12	20	0.998
20x20	15x15	6	0.997
20x20	15x15	9	0.997
20x20	15x15	12	0.996
20x20	15x15	16	0.995
20x20	15x15	20	0.996
25x25	2x2	6	0.992
25x25	2x2	9	0.999
25x25	2x2	12	1.000
25x25	2x2	16	0.996
25x25	2x2	20	0.991
25x25	3x3	6	0.995
25x25	3x3	9	0.992
25x25	3x3	12	0.988
25x25	3x3	16	0.983
25x25	3x3	20	0.986
25x25	4x4	6	0.999
25x25	4x4	9	0.996
25x25	4x4	12	0.994
25x25	4x4	16	0.990
25x25	4x4	20	0.988
25x25	6x6	6	0.997
25x25	6x6	9	0.996
25x25	6x6	12	0.995
25x25	6x6	16	0.993
25x25	6x6	20	0.994
25x25	8x8	6	0.997
25x25	8x8	9	0.996
25x25	8x8	12	0.995
25x25	8x8	16	0.995
25x25	8x8	20	0.994
25x25	10x10	6	0.998

(Table C.1 continued)

Applicator Size (cm)	Field Size (cm)	Energy (MeV)	OCF
25x25	10x10	9	0.997
25x25	10x10	12	0.995
25x25	10x10	16	0.996
25x25	10x10	20	0.996
25x25	12x12	6	0.997
25x25	12x12	9	0.996
25x25	12x12	12	0.995
25x25	12x12	16	0.996
25x25	12x12	20	0.997
25x25	15x15	6	0.995
25x25	15x15	9	0.994
25x25	15x15	12	0.994
25x25	15x15	16	0.993
25x25	15x15	20	0.995
25x25	20x20	6	0.996
25x25	20x20	9	0.997
25x25	20x20	12	0.995
25x25	20x20	16	0.995
25x25	20x20	20	0.995

Appendix D Output Correction Factors at 110 cm SSD

Table D.1 contains the output correction factors measured at 110 cm SSD for the subset of field size, applicator size, and energy combinations. OCFs are a ratio of the output reading taken with a copper insert divided by the output taken with the matching Cerrobend insert (Equation 2.4).

Table D.1: Output correction factors measured at 110 cm SSD for a subset of field size, applicator size, and energy combinations.

Applicator Size (cm)	Field Size (cm)	Energy (MeV)	OCF
6x6	2x2	6	1.005
6x6	2x2	12	0.994
6x6	2x2	20	1.002
6x6	3x3	6	0.997
6x6	3x3	12	1.000
6x6	3x3	20	1.003
6x6	4x4	6	1.004
6x6	4x4	12	1.004
6x6	4x4	20	1.001
15x15	2x2	6	0.993
15x15	2x2	12	0.996
15x15	2x2	20	0.997
15x15	4x4	6	1.006
15x15	4x4	12	1.005
15x15	4x4	20	1.000
15x15	8x8	6	1.006
15x15	8x8	12	1.005
15x15	8x8	20	1.002
15x15	12x12	6	1.000
15x15	12x12	12	0.999
15x15	12x12	20	1.000
25x25	2x2	6	0.990
25x25	2x2	12	0.997
25x25	2x2	20	0.993
25x25	3x3	6	1.003
25x25	3x3	12	0.999
25x25	3x3	20	0.990

(Table D.1 continued)

Applicator Size (cm)	Field Size (cm)	Energy (MeV)	OCF
25x25	4x4	6	1.003
25x25	4x4	12	1.002
25x25	4x4	20	0.990
25x25	6x6	6	1.001
25x25	6x6	12	0.998
25x25	6x6	20	0.992
25x25	8x8	6	1.004
25x25	8x8	12	1.002
25x25	8x8	20	0.995
25x25	10x10	6	1.004
25x25	10x10	12	1.002
25x25	10x10	20	0.997
25x25	12x12	6	1.002
25x25	12x12	12	1.000
25x25	12x12	20	0.997
25x25	15x15	6	1.000
25x25	15x15	12	0.999
25x25	15x15	20	0.999
25x25	20x20	6	1.000
25x25	20x20	12	1.000
25x25	20x20	20	1.000

Appendix E Isodose Comparison Plots at 100 cm SSD

Figure E.1 through Figure E.48 show the isodose comparison plots measured at 100 cm SSD for the subset of field size, applicator size, and energy combinations. Each plot includes labeled isodose lines corresponding to a specific dose value. Solid isodose lines correspond to the dose distribution with the Cerrobend insert, and the dashed isodose lines to the dose distribution with the copper inserts. Any points which did not meet the comparison criteria of 2% or 1 mm distance-to-agreement are indicated with red pixels.

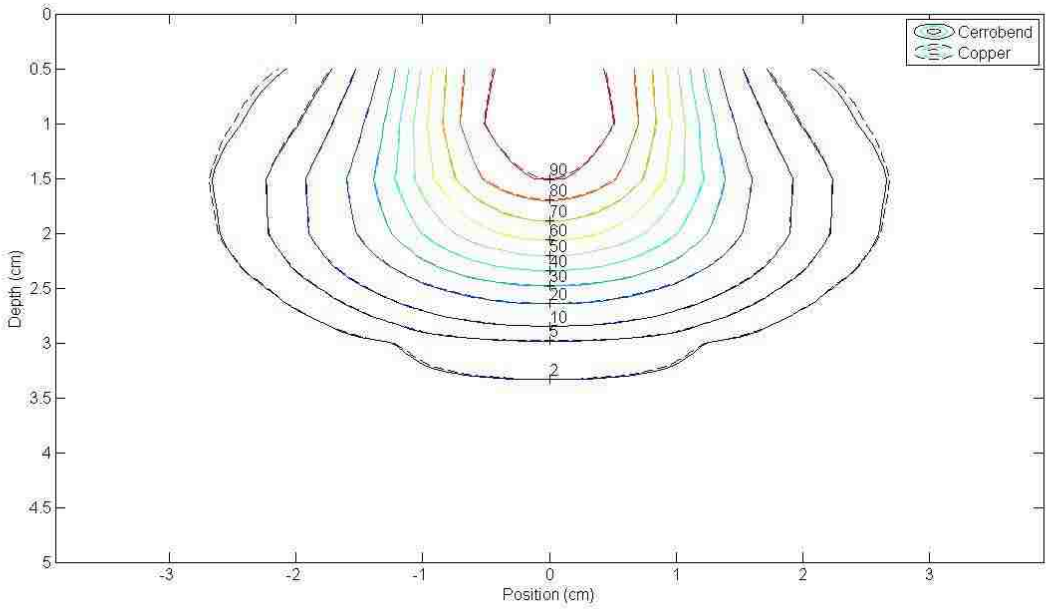

Figure E.1: 2x2 cm^2 field size in the 6x6 cm^2 applicator at 6 MeV.

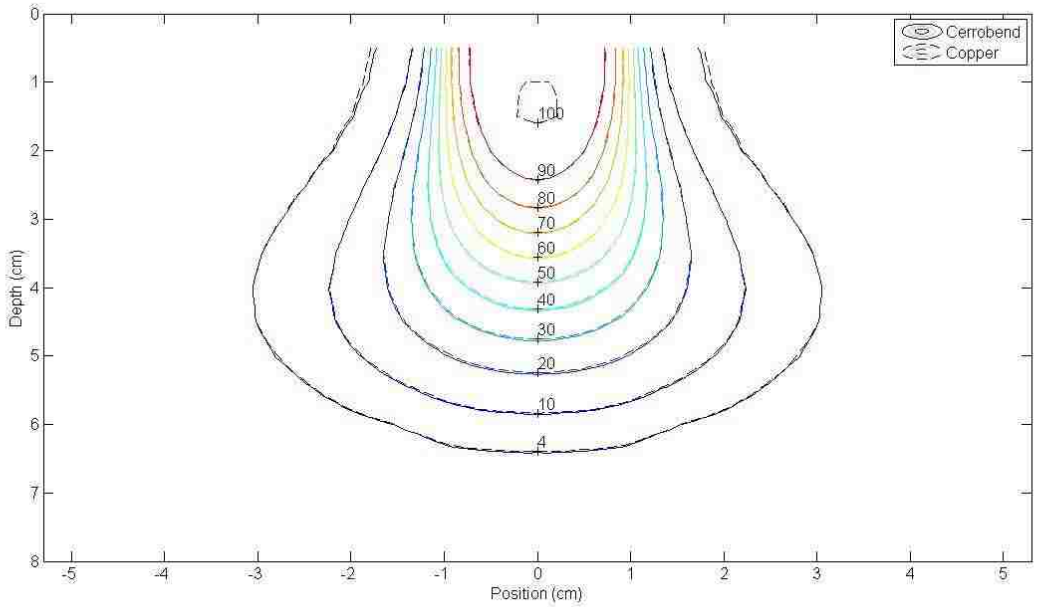

Figure E.2: 2x2 cm^2 field size in the 6x6 cm^2 applicator at 12 MeV.

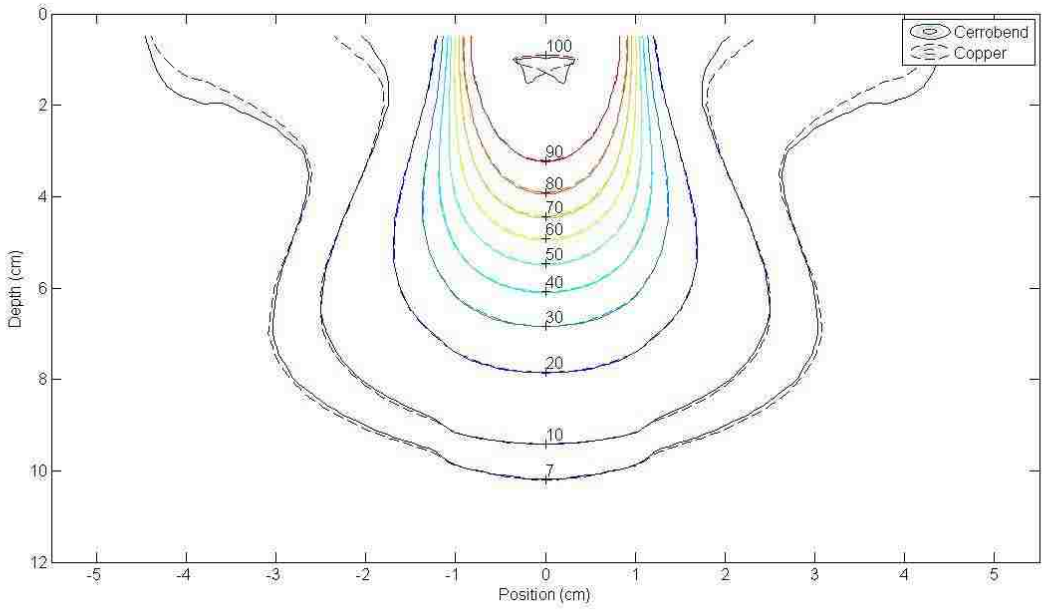

Figure E.3: 2x2 cm^2 field size in the 6x6 cm^2 applicator at 20 MeV.

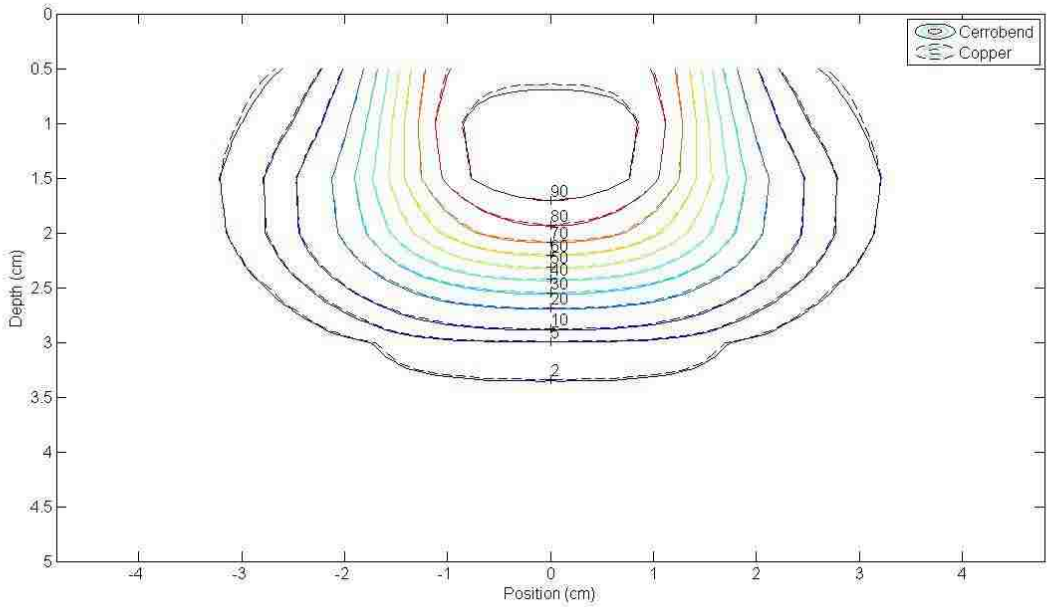

Figure E.4: 3x3 cm^2 field size in the 6x6 cm^2 applicator at 6 MeV.

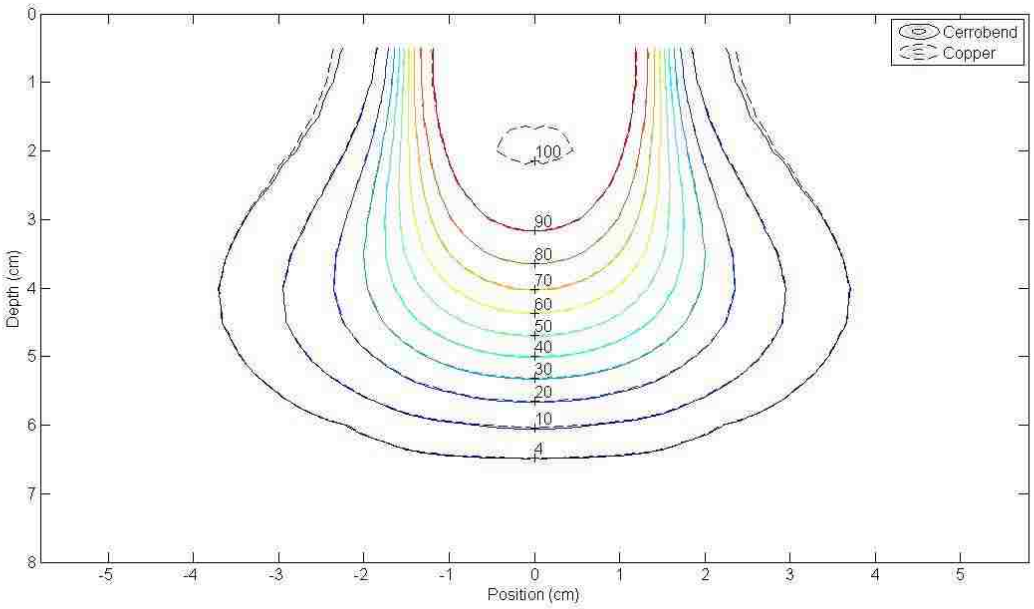

Figure E.5: 3x3 cm^2 field size in the 6x6 cm^2 applicator at 12 MeV.

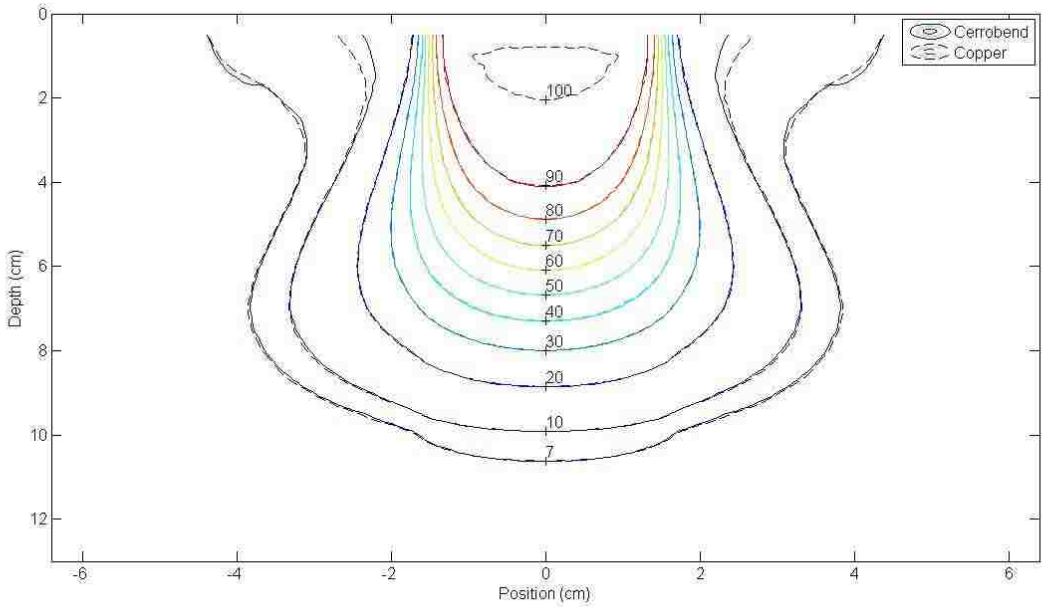

Figure E.6: 3x3 cm^2 field size in the 6x6 cm^2 applicator at 20 MeV.

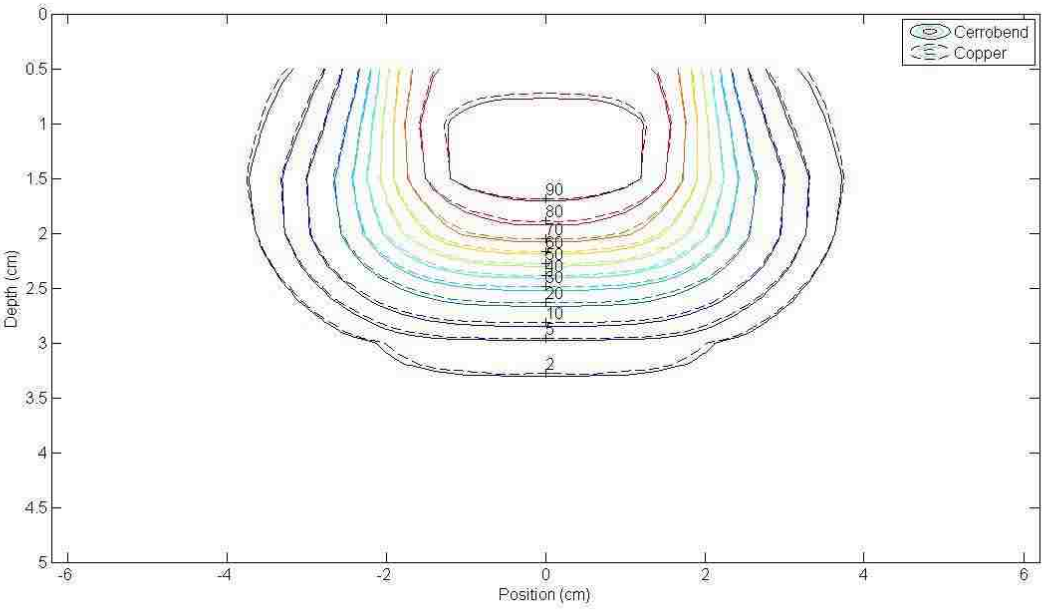

Figure E.7: 4x4 cm^2 field size in the 6x6 cm^2 applicator at 6 MeV.

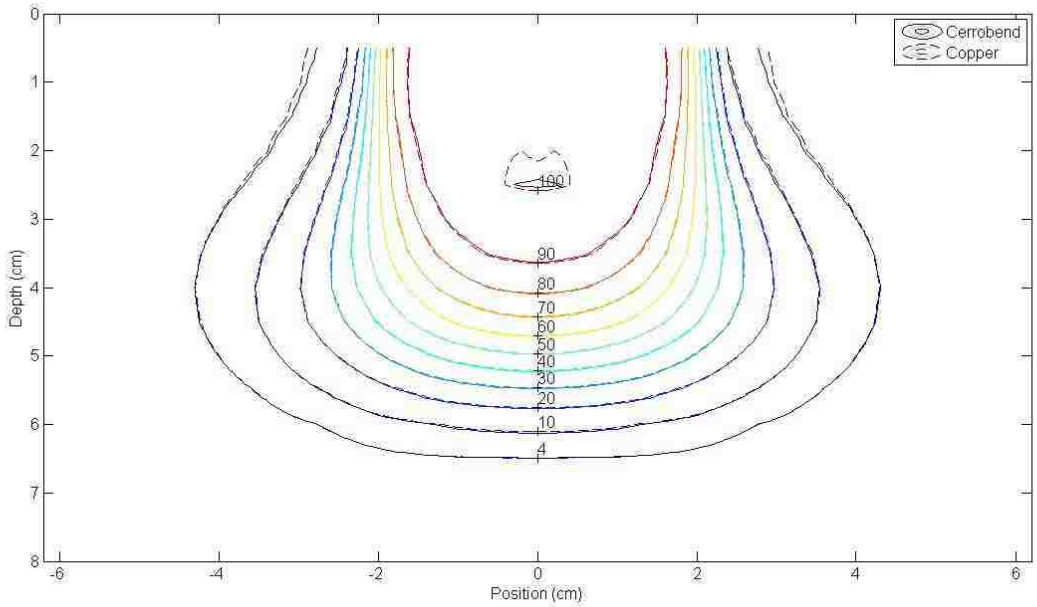

Figure E.8: 4x4 cm^2 field size in the 6x6 cm^2 applicator at 12 MeV.

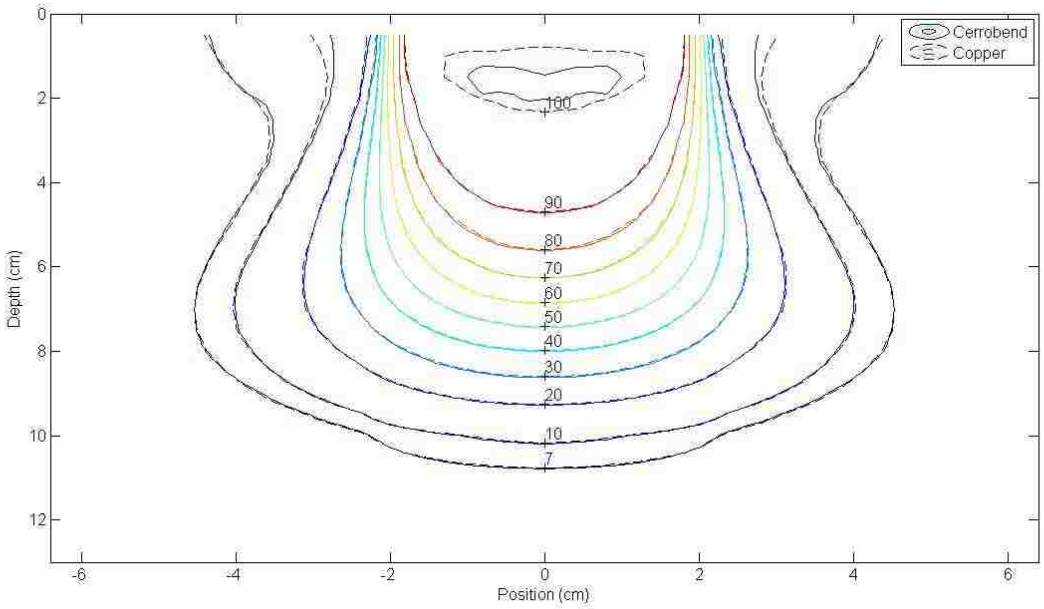

Figure E.9: 4x4 cm^2 field size in the 6x6 cm^2 applicator at 20 MeV.

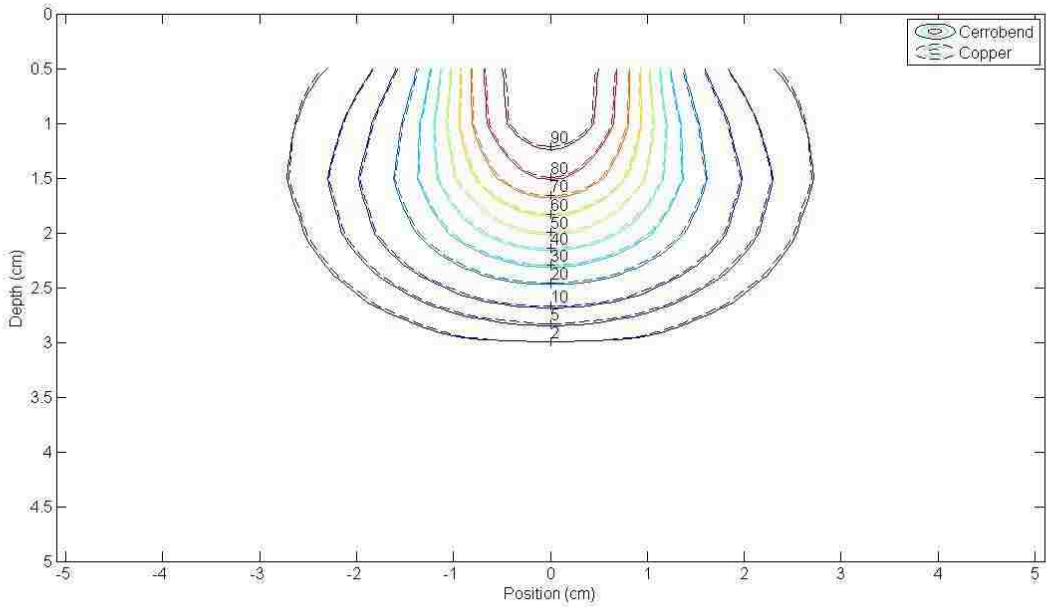

Figure E.10: 2x2 cm^2 field size in the 15x15 cm^2 applicator at 6 MeV.

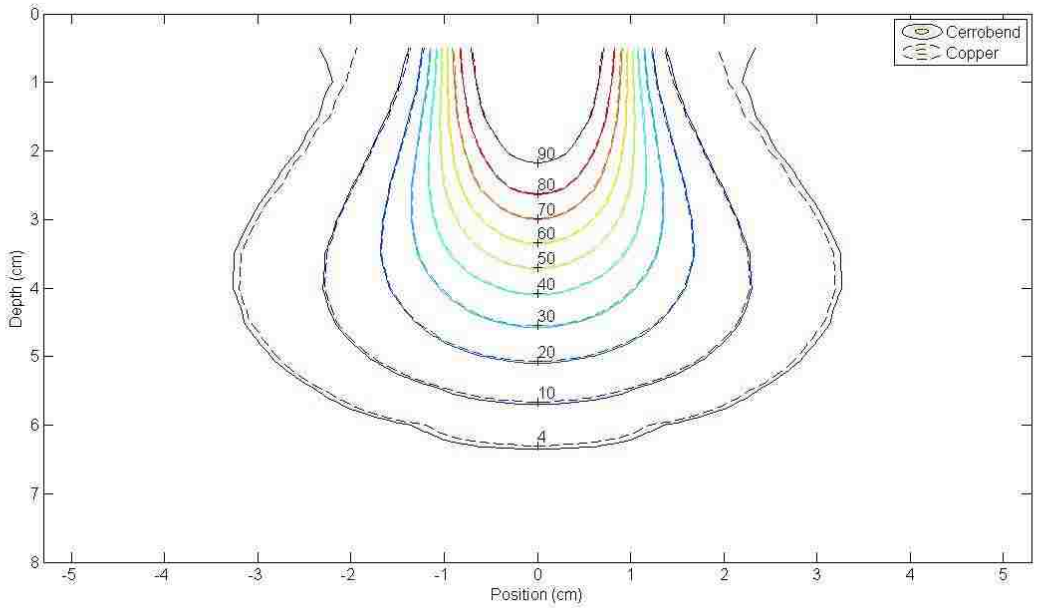

Figure E.11: 2x2 cm^2 field size in the 15x15 cm^2 applicator at 12 MeV.

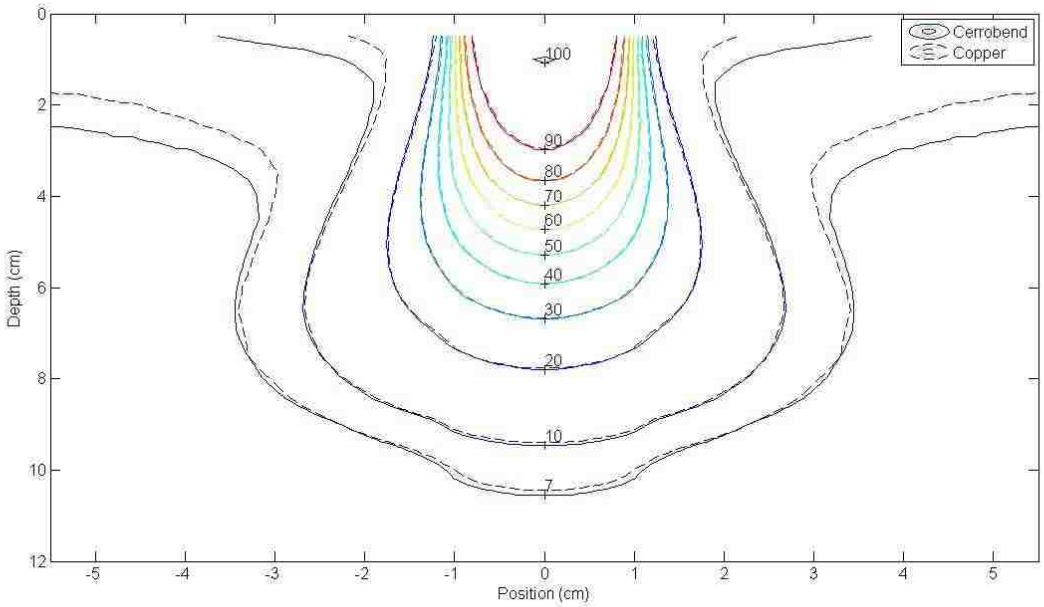

Figure E.12: 2x2 cm^2 field size in the 15x15 cm^2 applicator at 20 MeV.

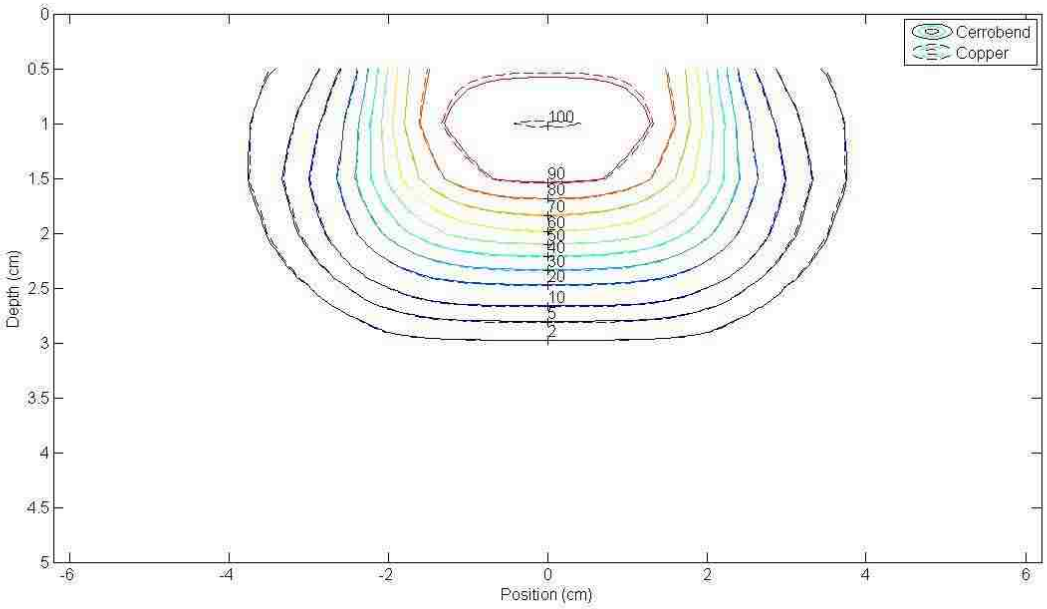

Figure E.13: 4x4 cm^2 field size in the 15x15 cm^2 applicator at 6 MeV.

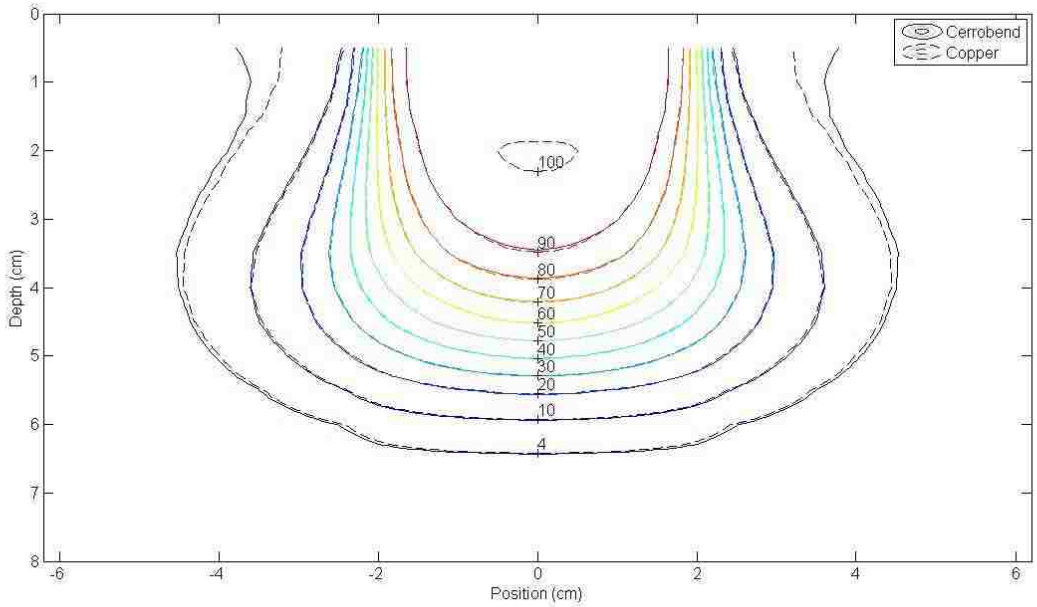

Figure E.14: 4x4 cm^2 field size in the 15x15 cm^2 applicator at 12 MeV.

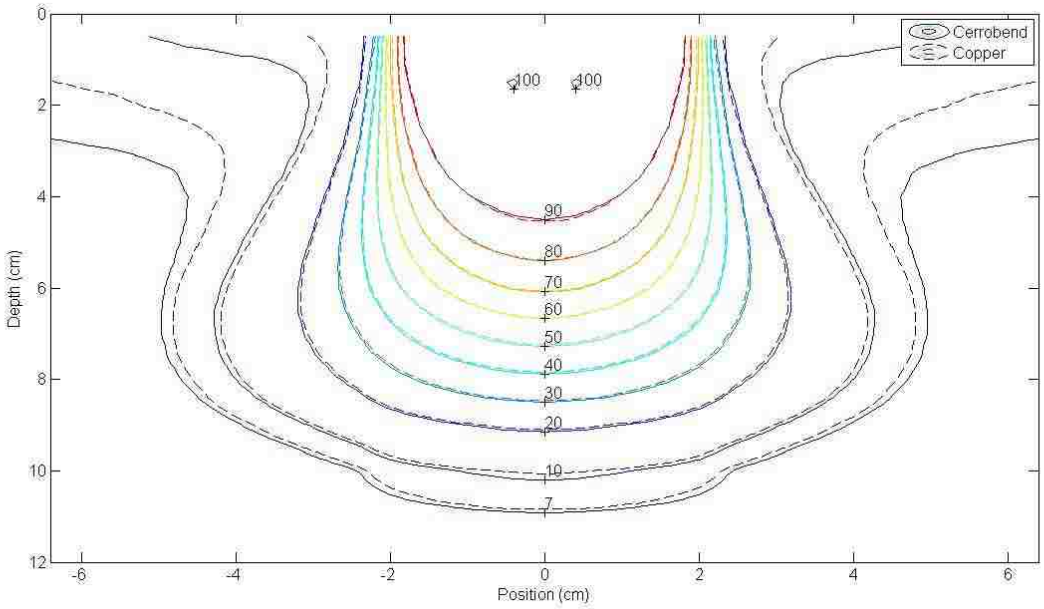

Figure E.15: 4x4 cm^2 field size in the 15x15 cm^2 applicator at 20 MeV.

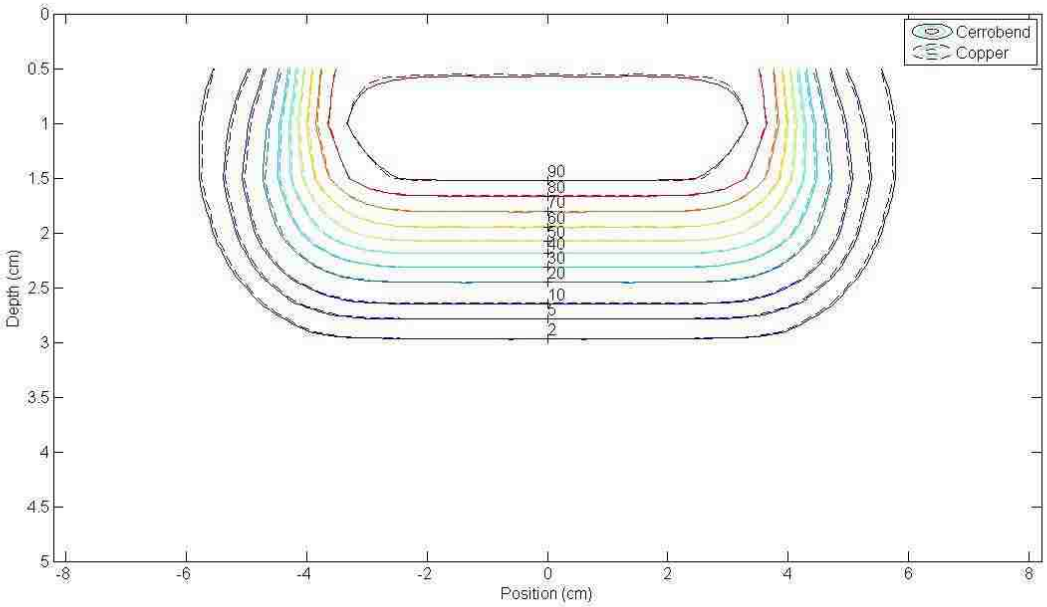

Figure E.16: 8x8 cm^2 field size in the 15x15 cm^2 applicator at 6 MeV.

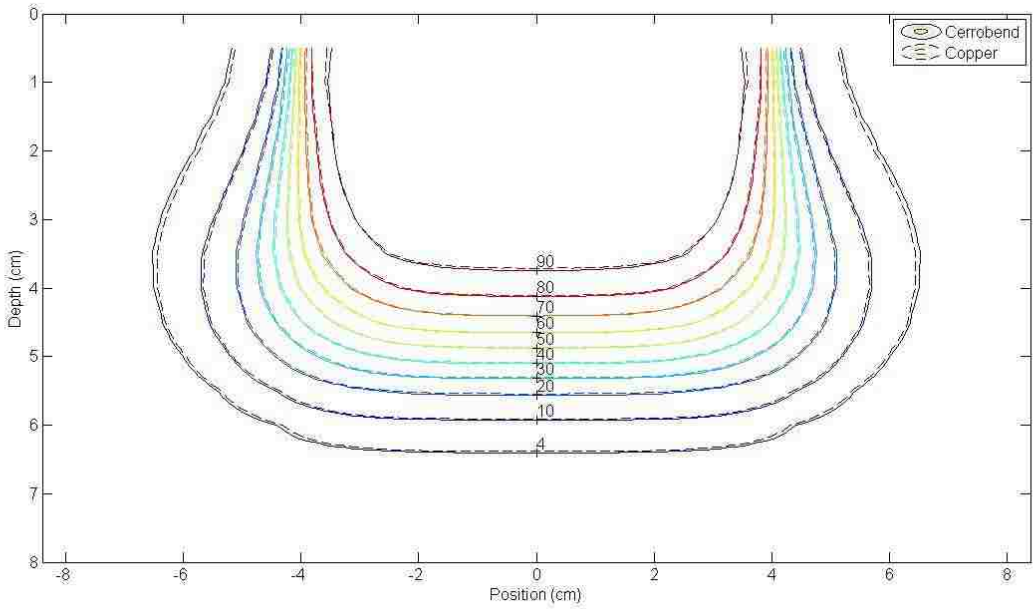

Figure E.17: 8x8 cm^2 field size in the 15x15 cm^2 applicator at 12 MeV.

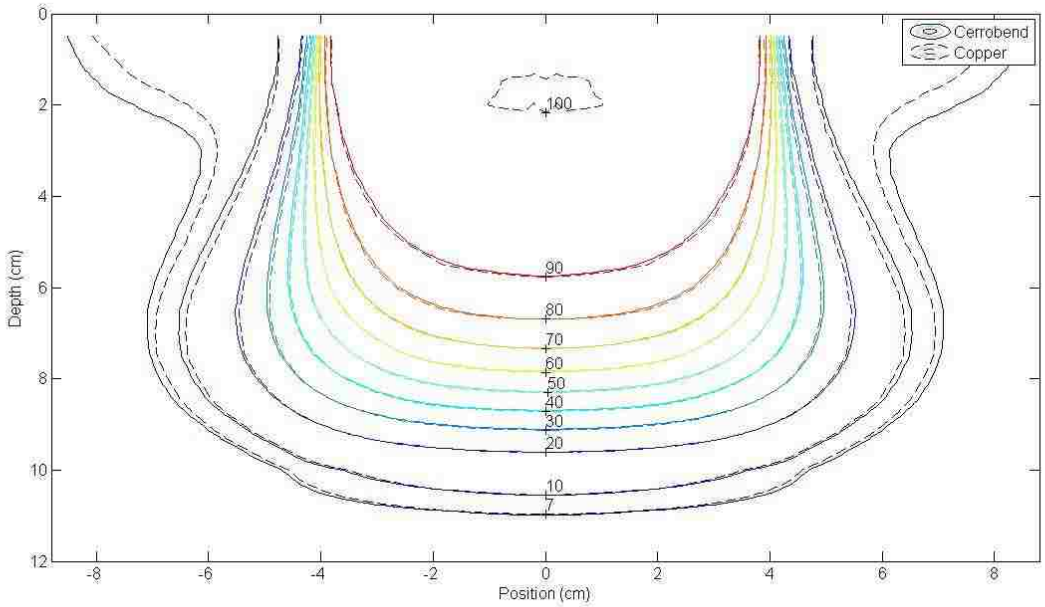

Figure E.18: 8x8 cm^2 field size in the 15x15 cm^2 applicator at 20 MeV.

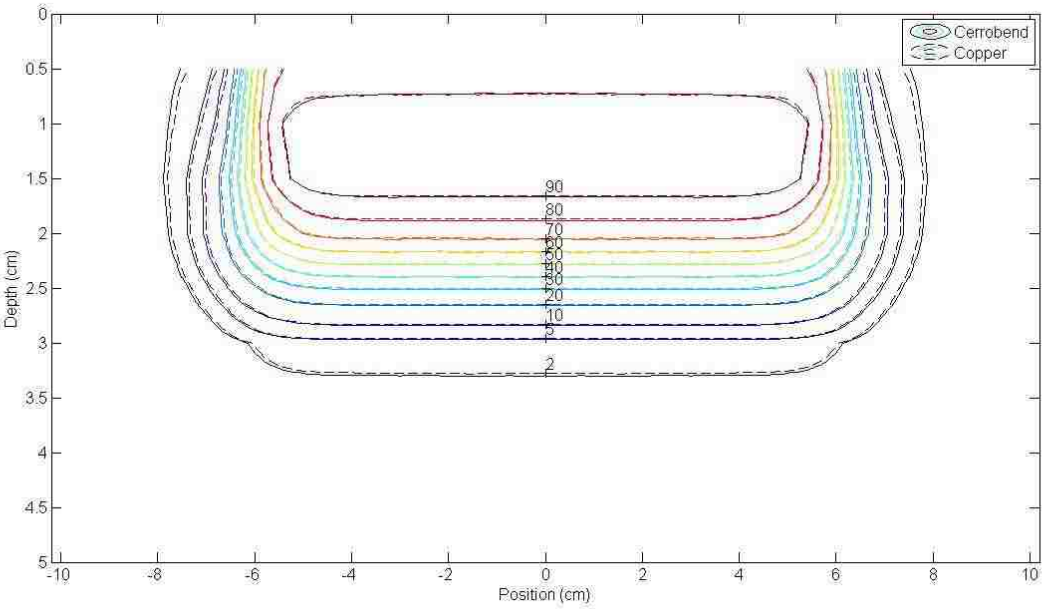

Figure E.19: 12x12 cm^2 field size in the 15x15 cm^2 applicator at 6 MeV.

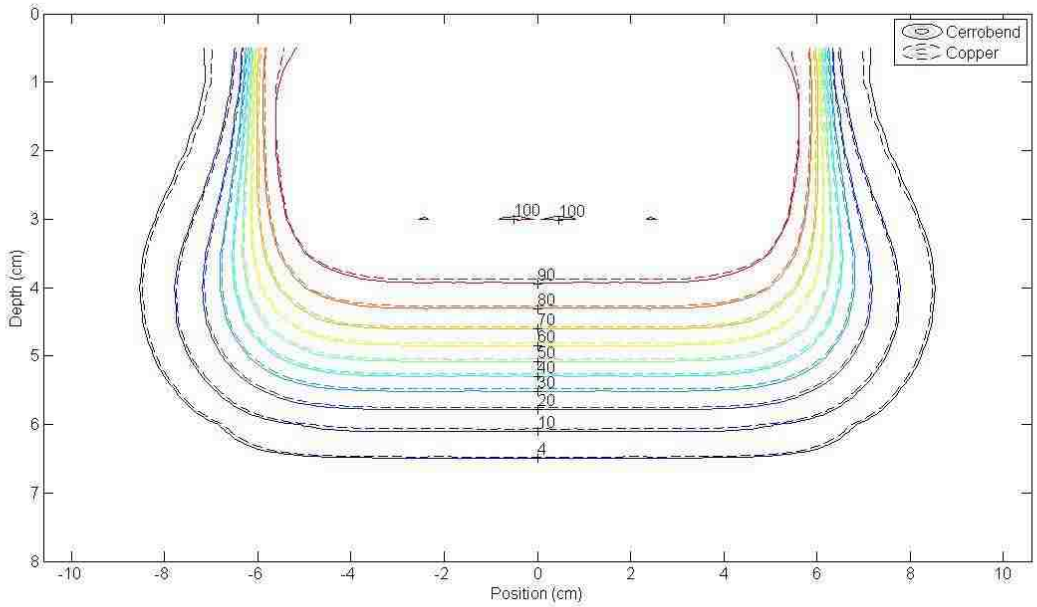

Figure E 20: 12x12 cm^2 field size in the 15x15 cm^2 applicator at 12 MeV.

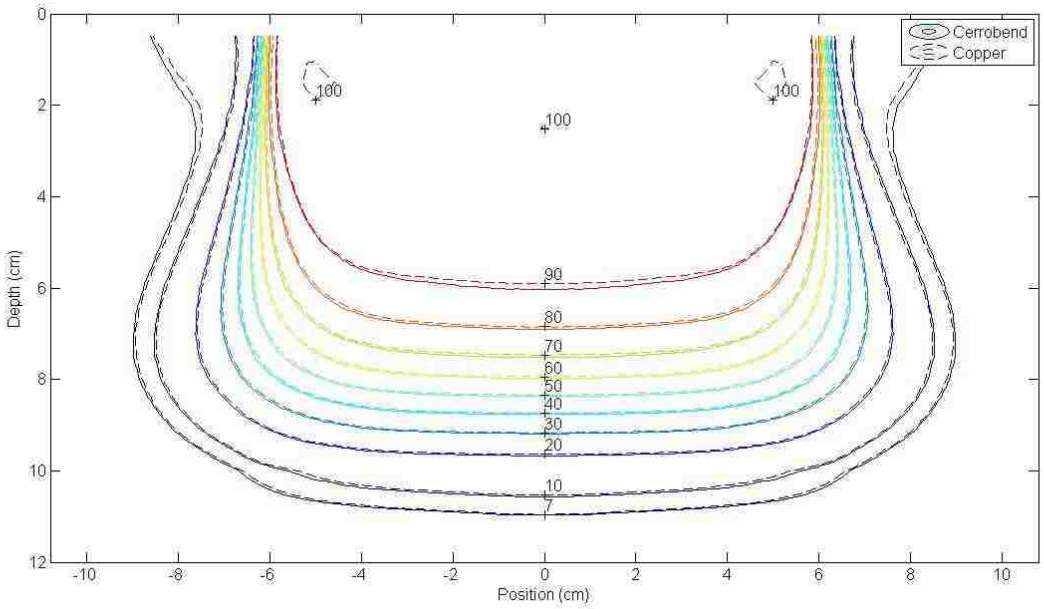

Figure E.21: 12x12 cm^2 field size in the 15x15 cm^2 applicator at 20 MeV.

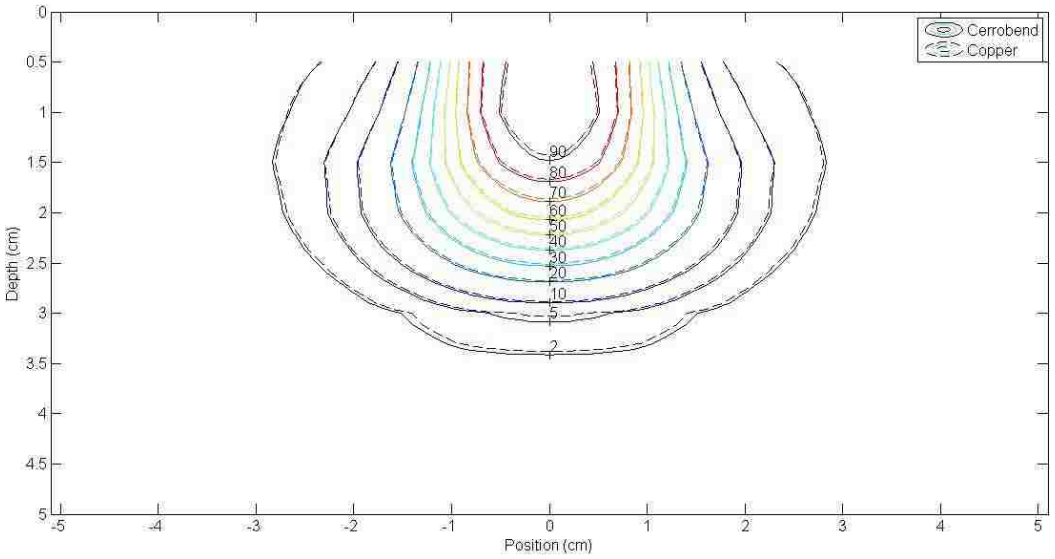

Figure E.22: 2x2 cm^2 field size in the 25x25 cm^2 applicator at 6 MeV.

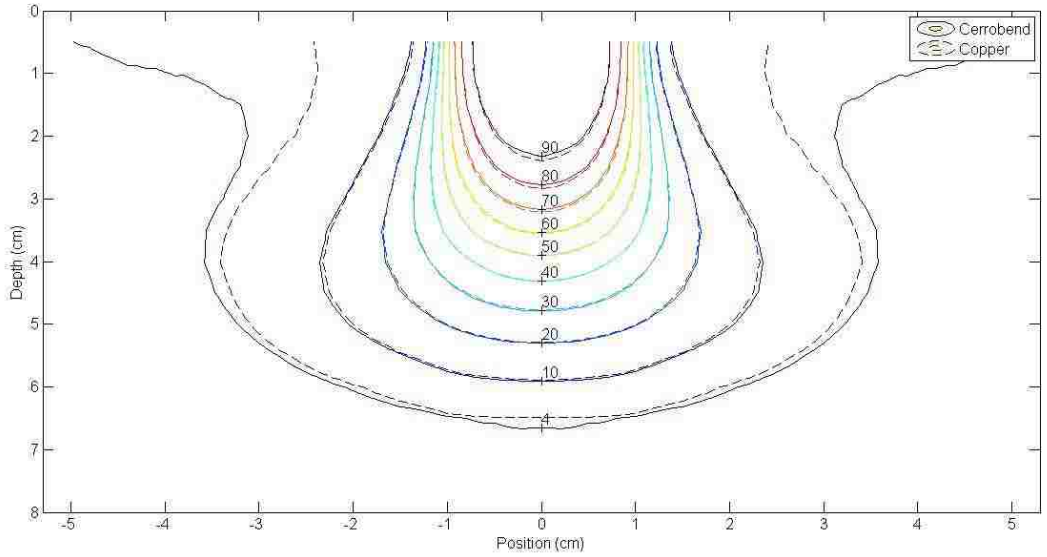

Figure E.23: 2x2 cm^2 field size in the 25x25 cm^2 applicator at 12 MeV.

\

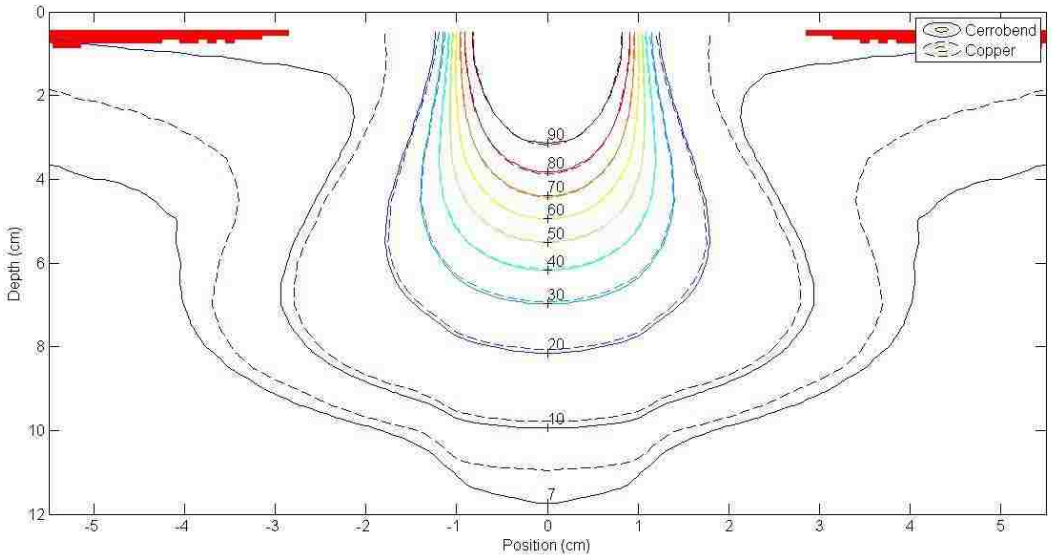

Figure E.24: 2x2 cm^2 field size in the 25x25 cm^2 applicator at 20 MeV.

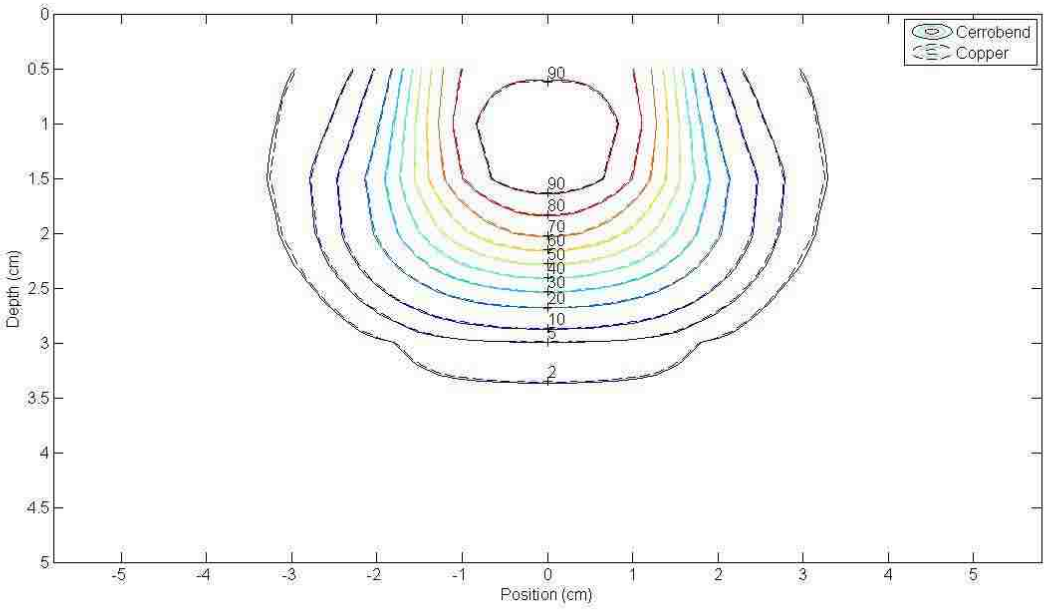

Figure E.25: 3x3 cm^2 field size in the 25x25 cm^2 applicator at 6 MeV.

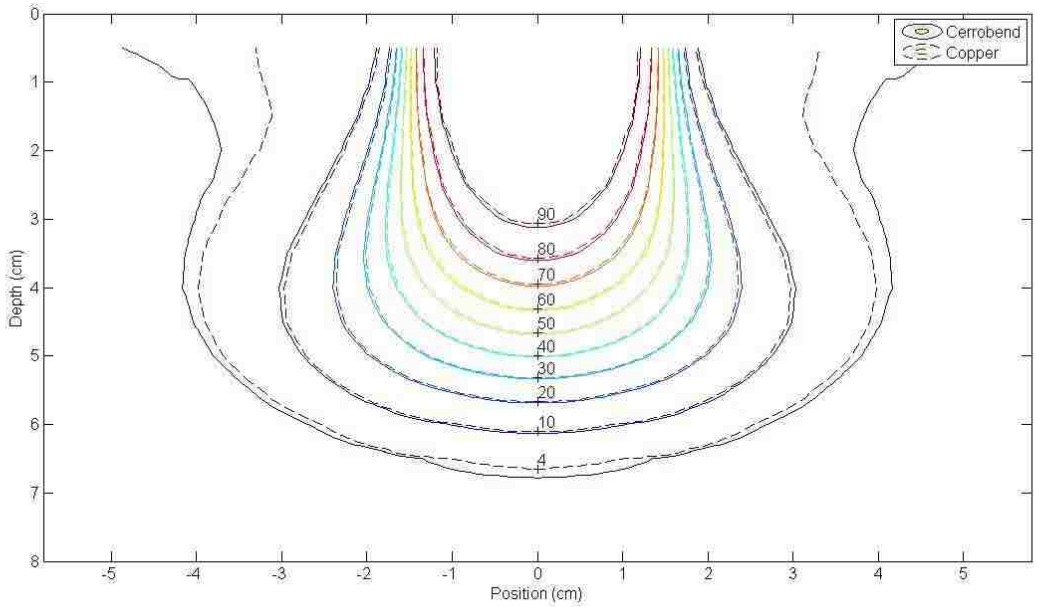

Figure E.26: 3x3 cm^2 field size in the 25x25 cm^2 applicator at 12 MeV.

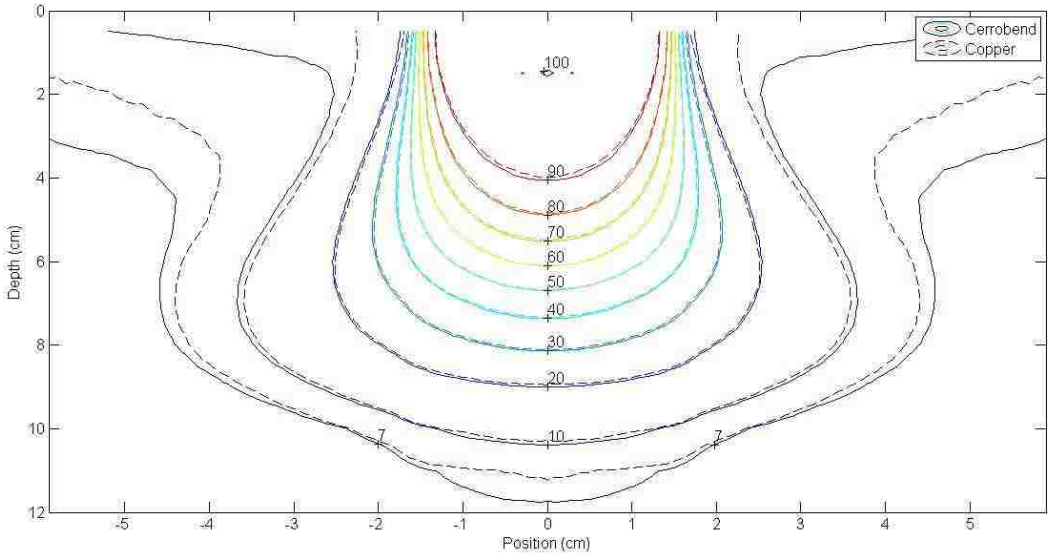

Figure E.27: 3x3 cm^2 field size in the 25x25 cm^2 applicator at 20 MeV.

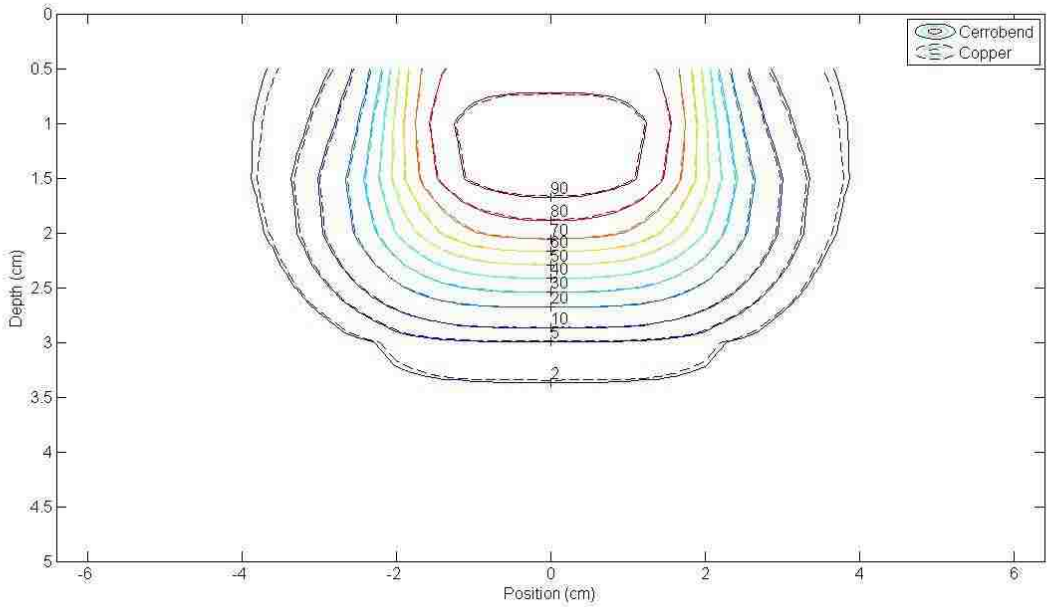

Figure E.28: 4x4 cm^2 field size in the 25x25 cm^2 applicator at 6 MeV.

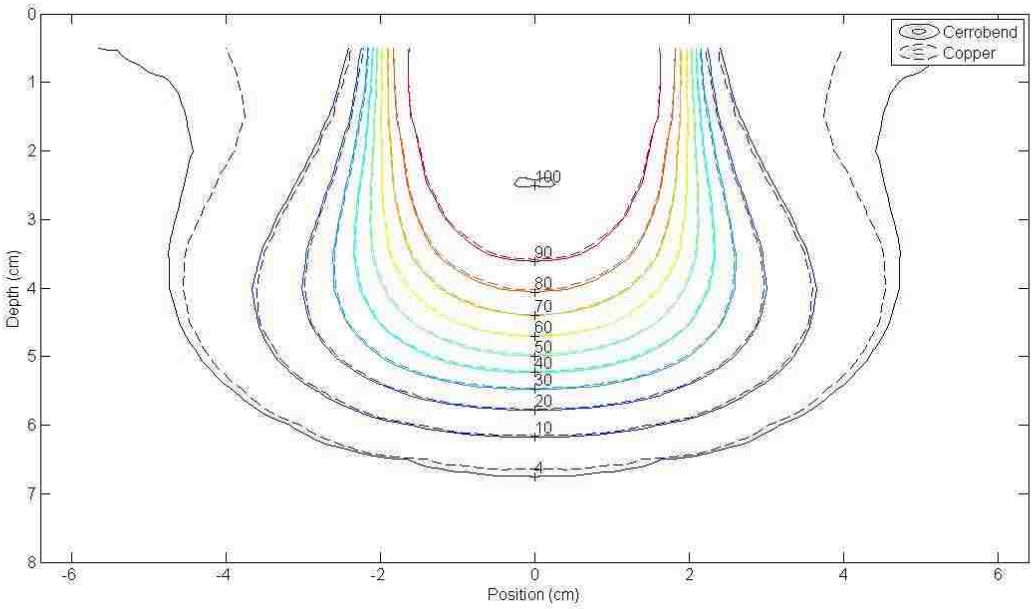

Figure E.29: 4x4 cm^2 field size in the 25x25 cm^2 applicator at 12 MeV.

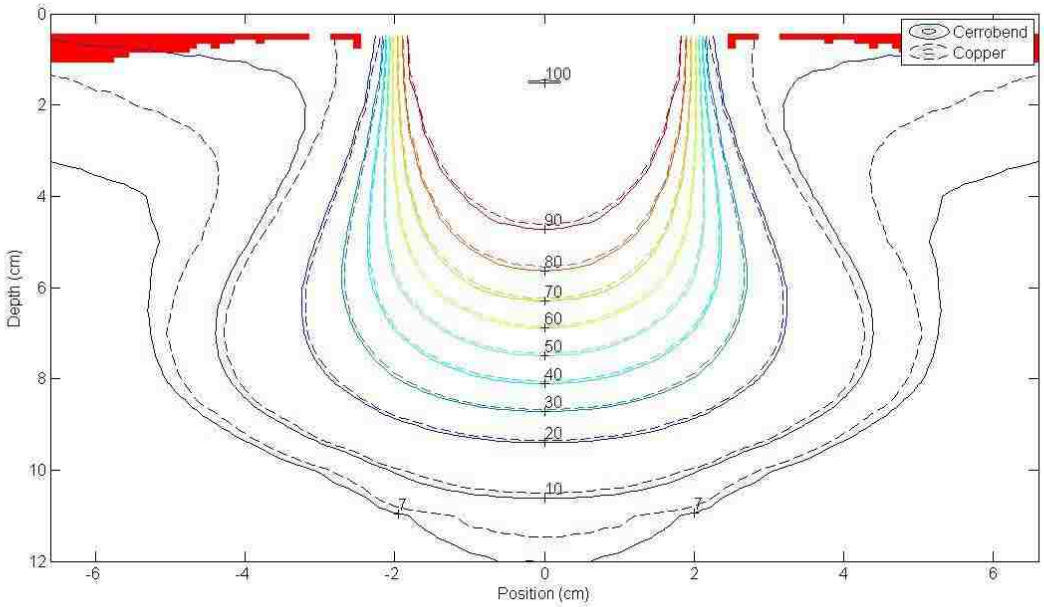

Figure E.30: 4x4 cm^2 field size in the 25x25 cm^2 applicator at 20 MeV.

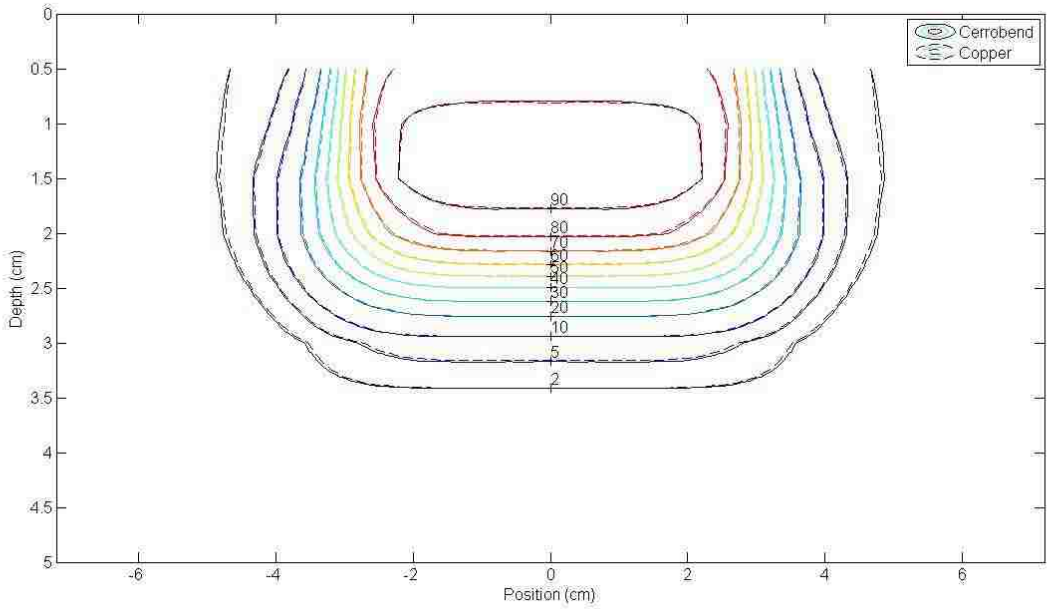

Figure E.31: 6x6 cm^2 field size in the 25x25 cm^2 applicator at 6 MeV.

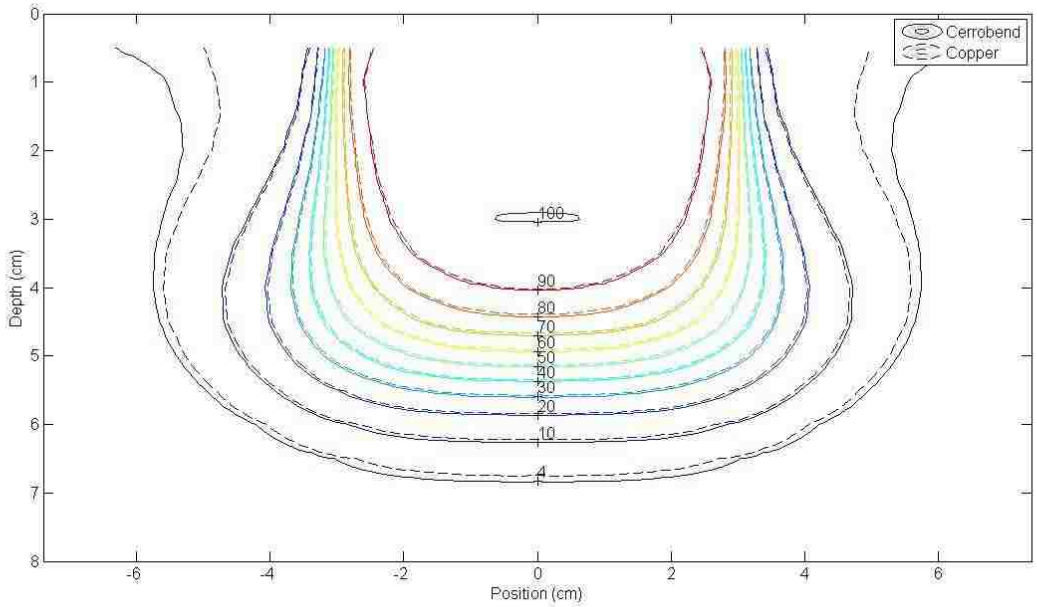

Figure E.32: 6x6 cm^2 field size in the 25x25 cm^2 applicator at 12 MeV.

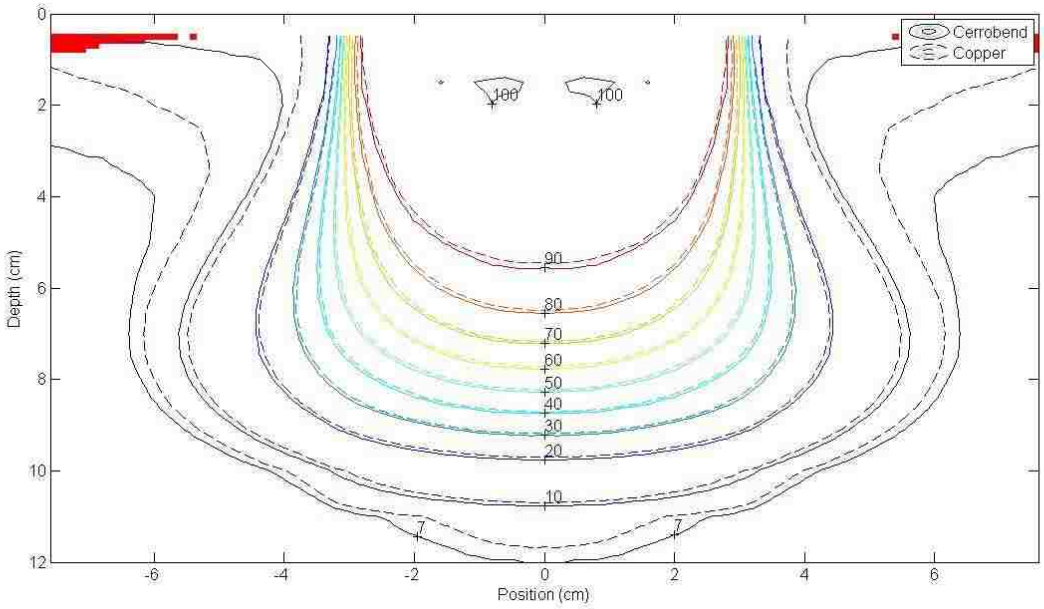

Figure E.33: 6x6 cm^2 field size in the 25x25 cm^2 applicator at 20 MeV.

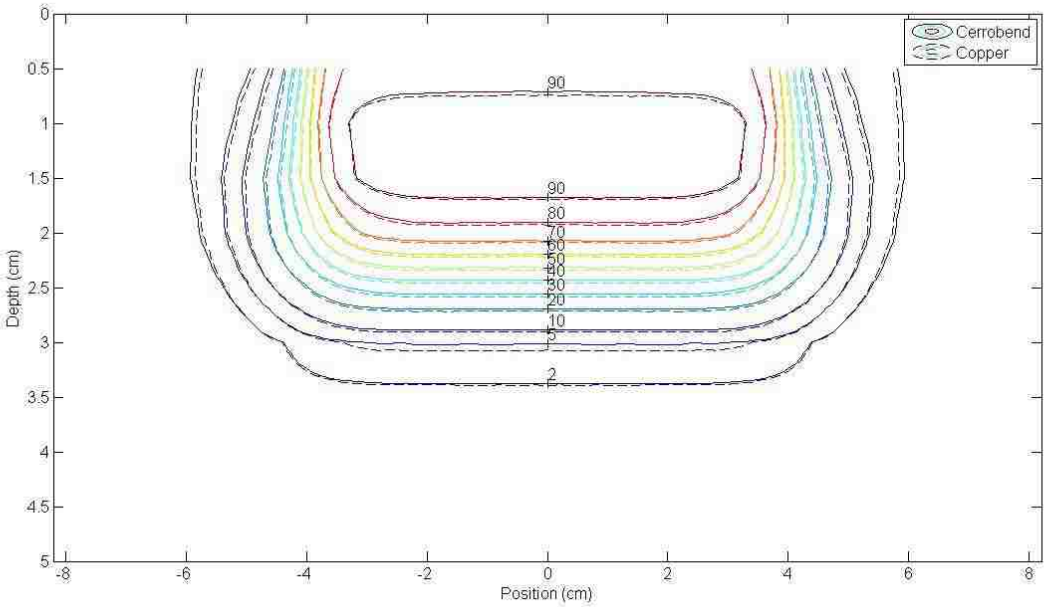

Figure E.34: 8x8 cm^2 field size in the 25x25 cm^2 applicator at 6 MeV.

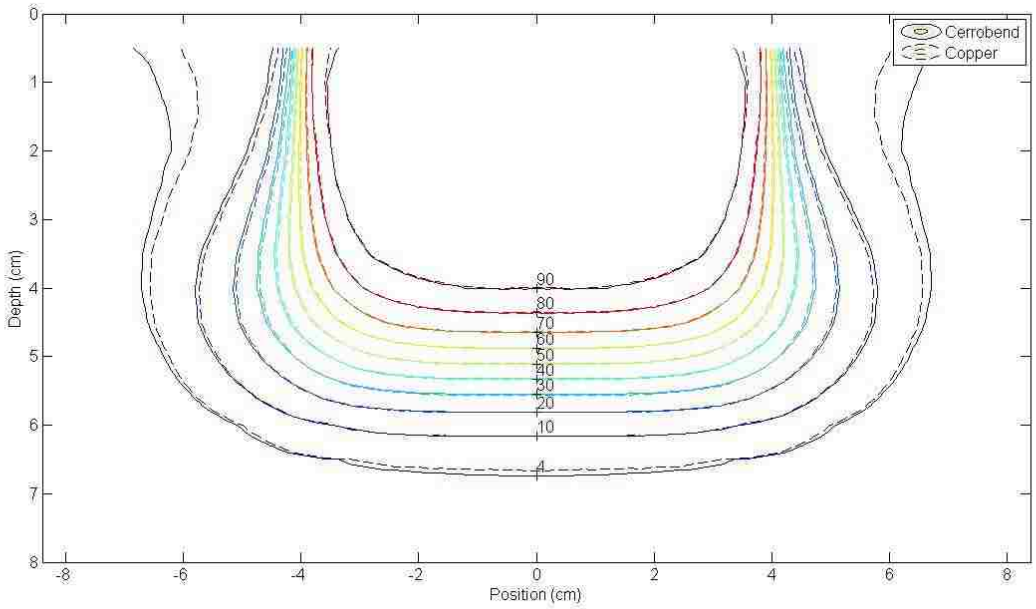

Figure E.35: 8x8 cm^2 field size in the 25x25 cm^2 applicator at 12 MeV.

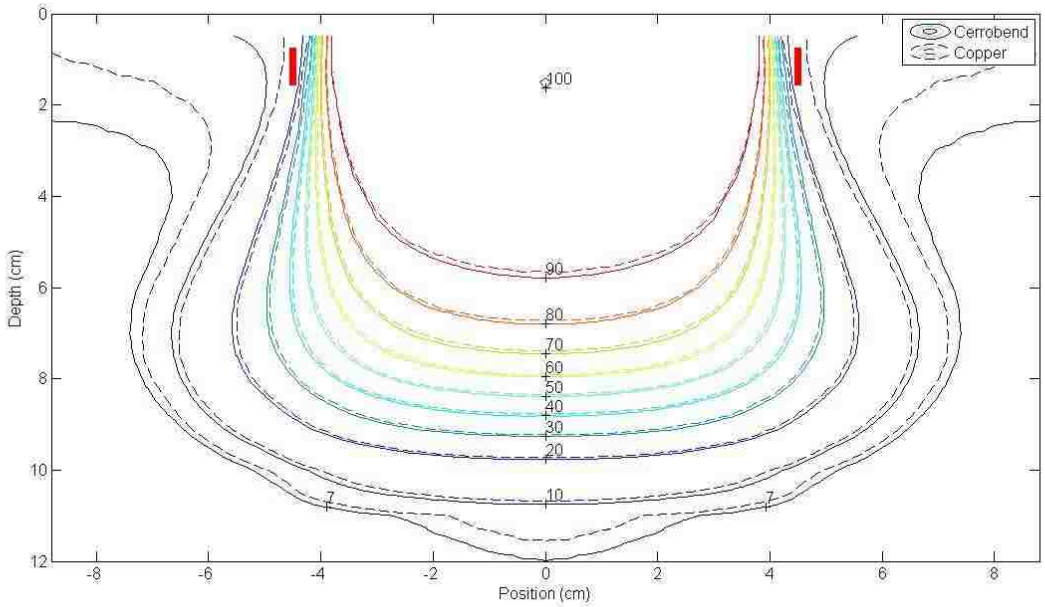

Figure E.36: 8x8 cm^2 field size in the 25x25 cm^2 applicator at 20 MeV.

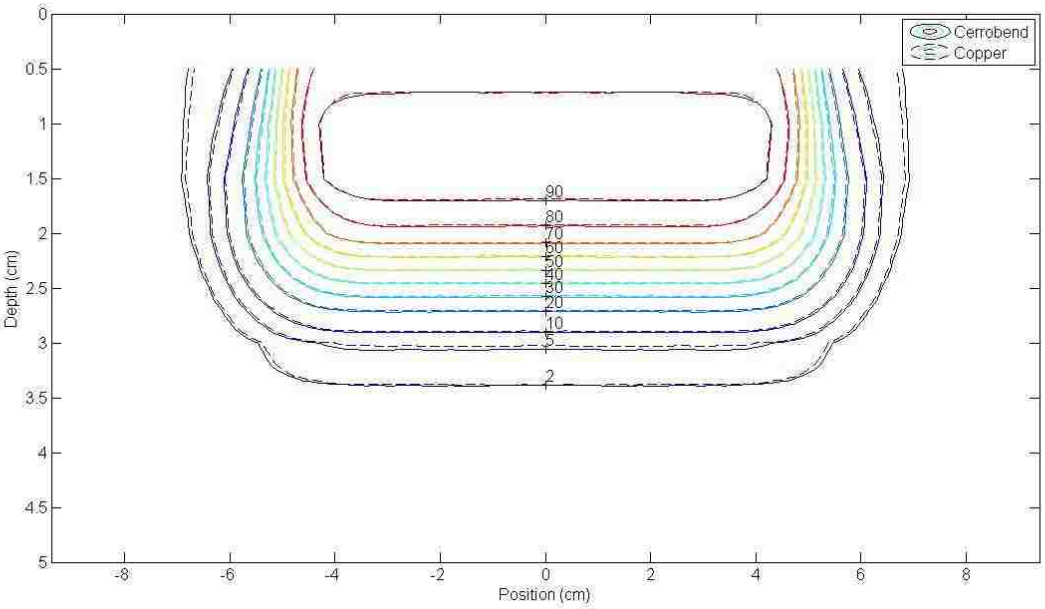

Figure E.37: 10x10 cm^2 field size in the 25x25 cm^2 applicator at 6 MeV.

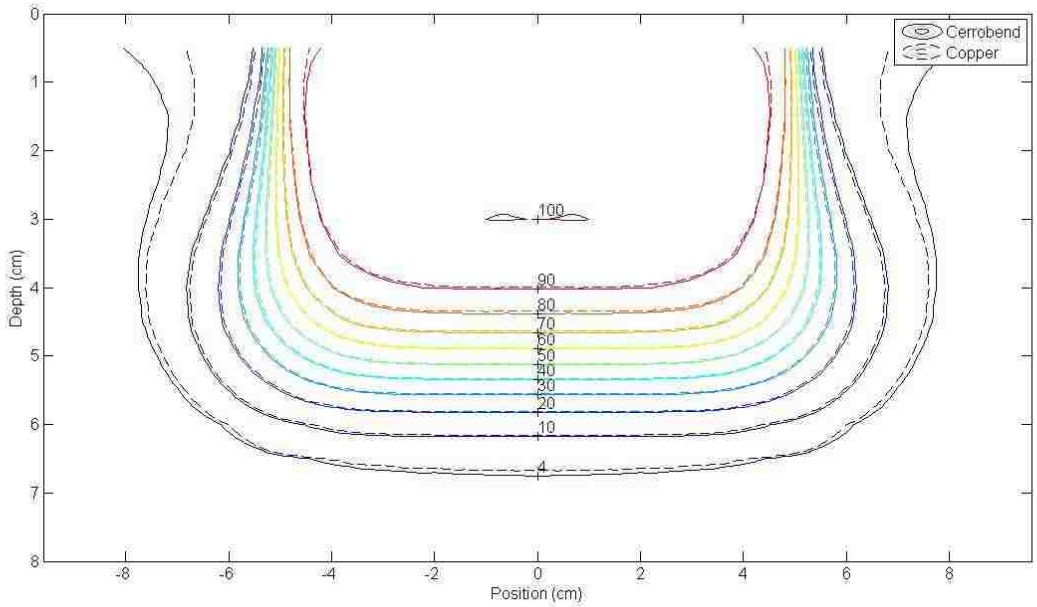

Figure E.38: 10x10 cm^2 field size in the 25x25 cm^2 applicator at 12 MeV.

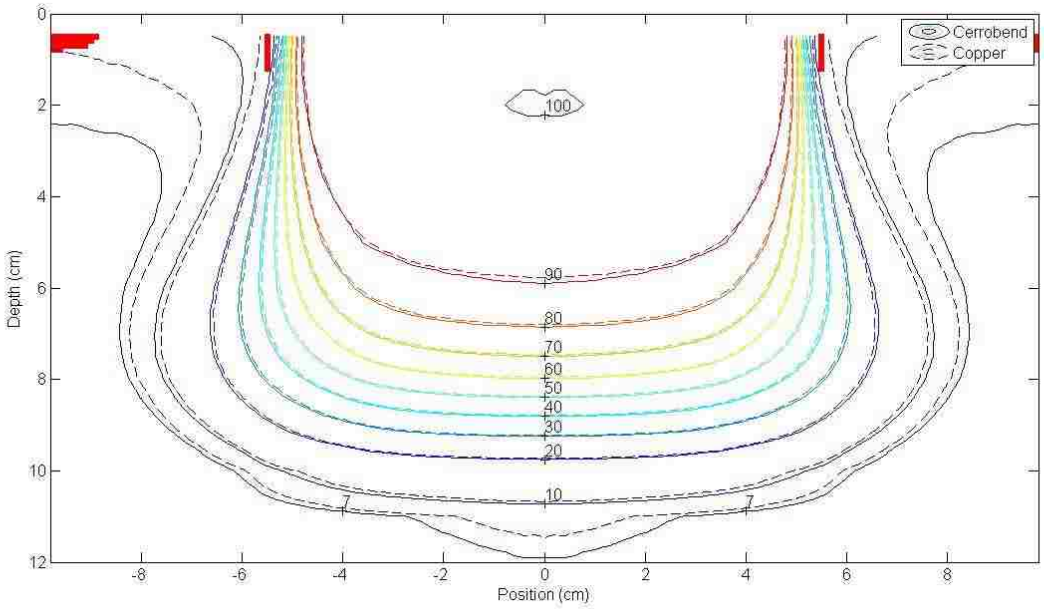

Figure E.39: 10x10 cm^2 field size in the 25x25 cm^2 applicator at 20 MeV.

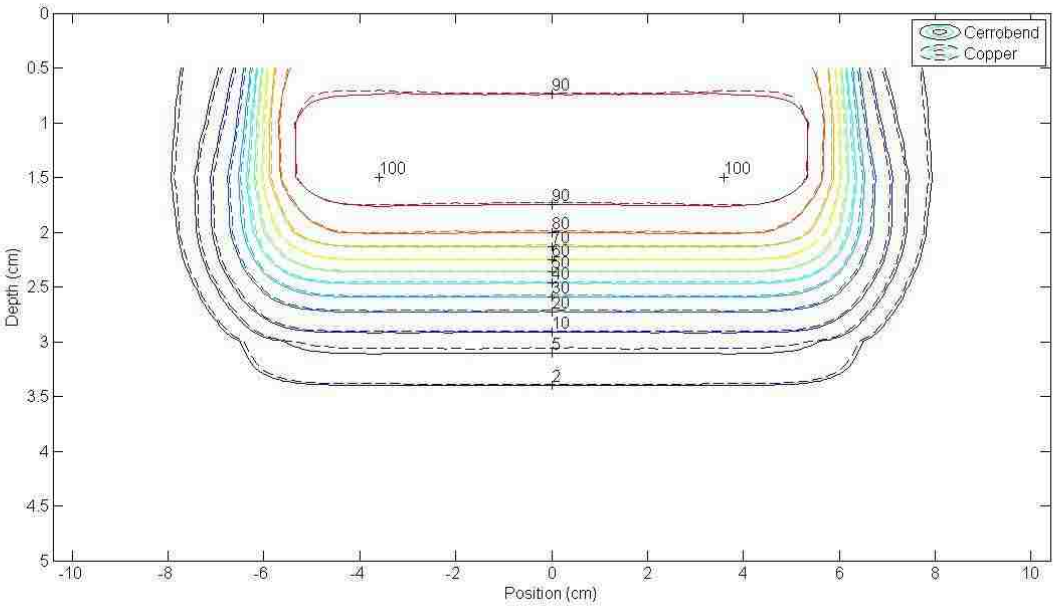

Figure E.40: 12x12 cm^2 field size in the 25x25 cm^2 applicator at 6 MeV.

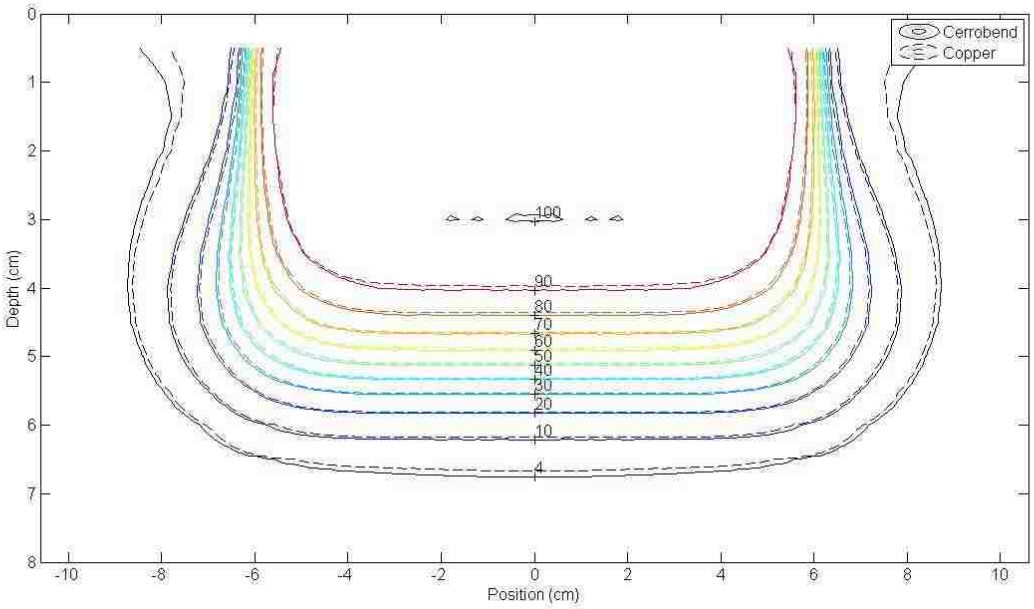

Figure E.41: 12x12 cm^2 field size in the 25x25 cm^2 applicator at 12 MeV.

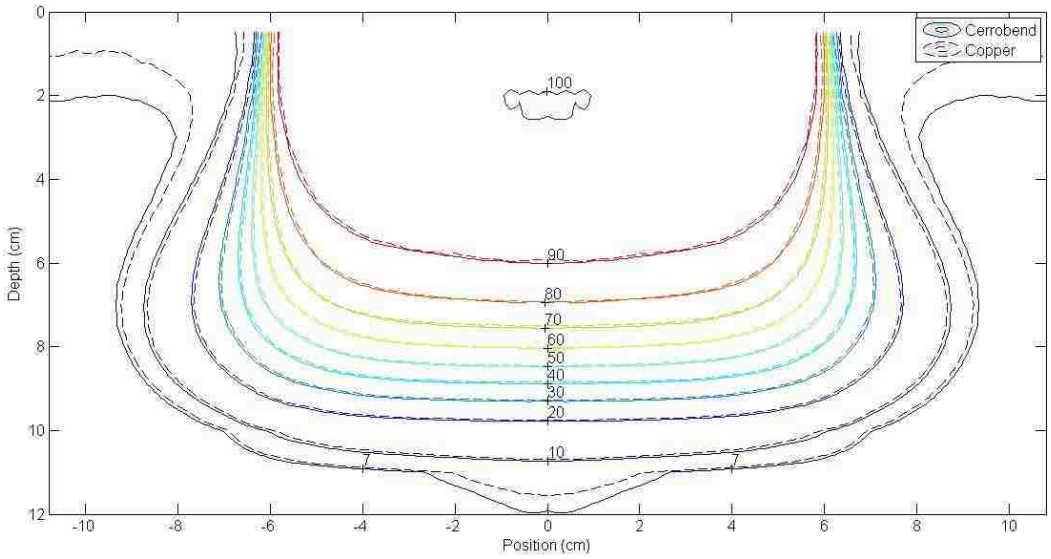

Figure E.42: 12x12 cm^2 field size in the 25x25 cm^2 applicator at 20 MeV.

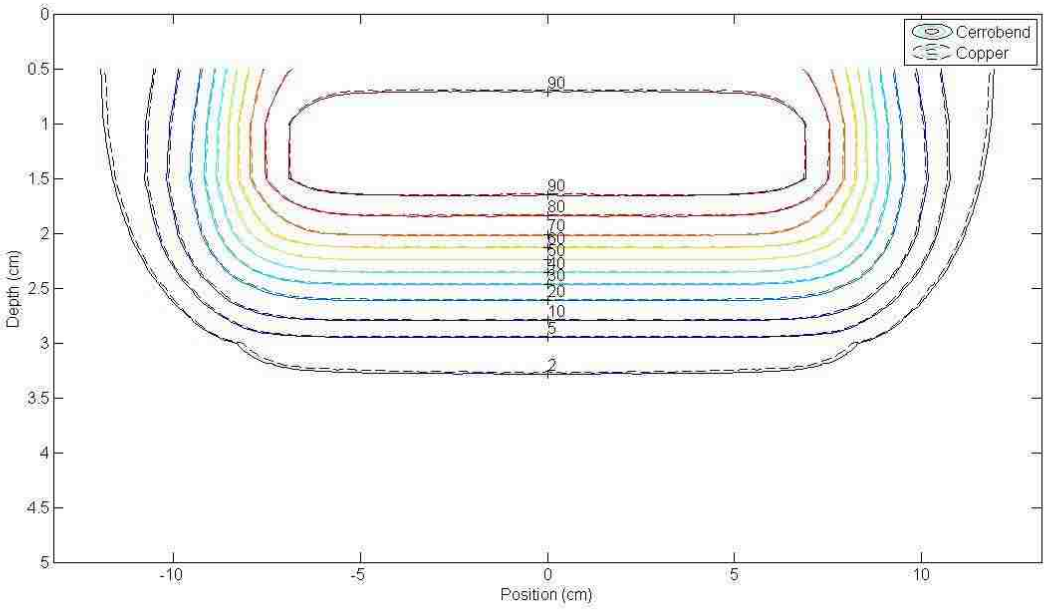

Figure E.43: 15x15 cm^2 field size in the 25x25 cm^2 applicator at 6 MeV.

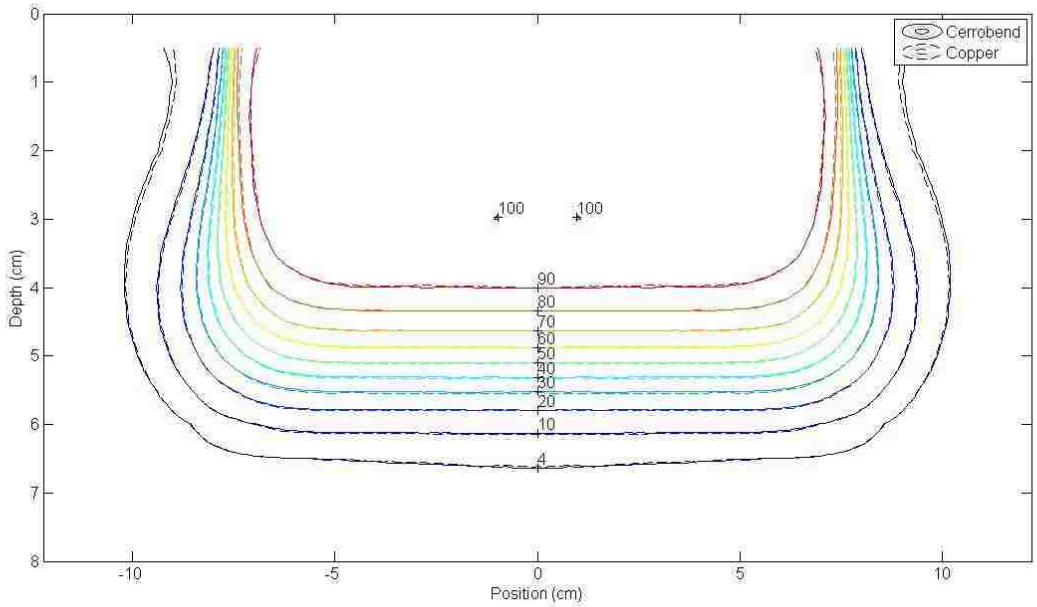

Figure E.44: 15x15 cm^2 field size in the 25x25 cm^2 applicator at 12 MeV.

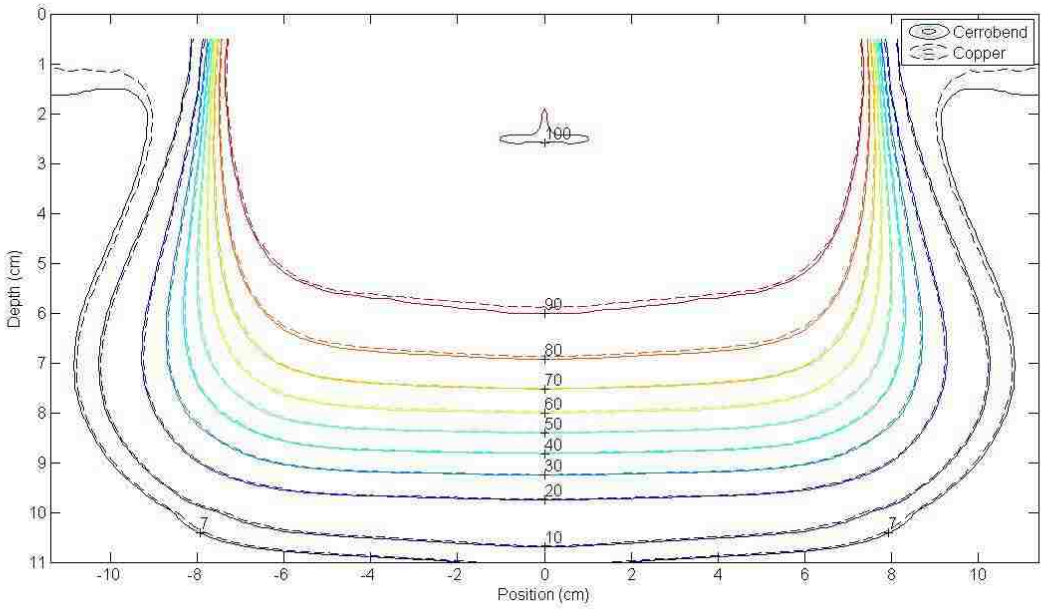

Figure E.45: 15x15 cm^2 field size in the 25x25 cm^2 applicator at 20 MeV.

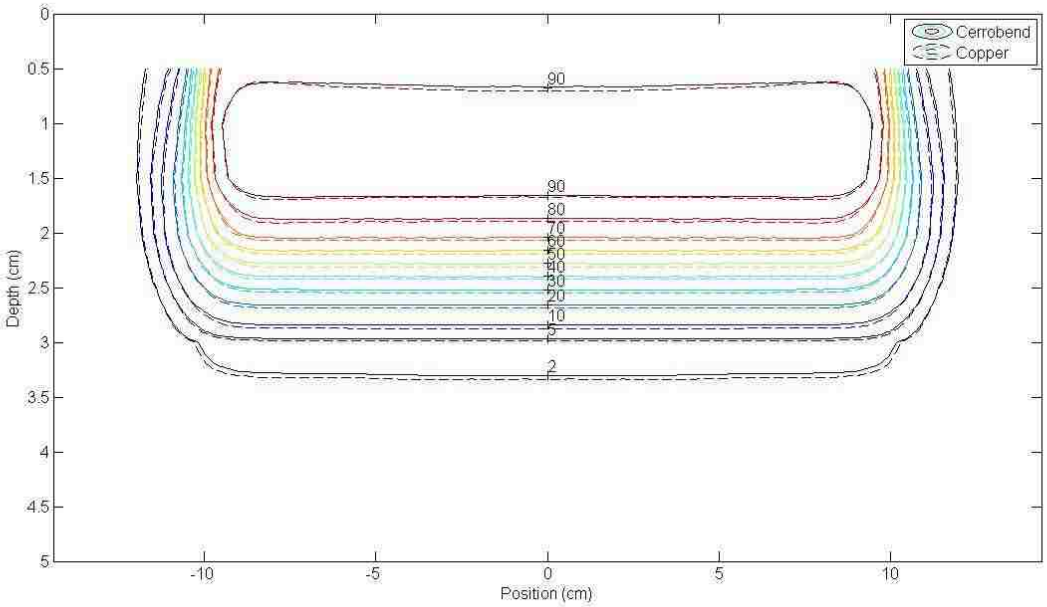

Figure E.46: 20x20 cm^2 field size in the 25x25 cm^2 applicator at 6 MeV.

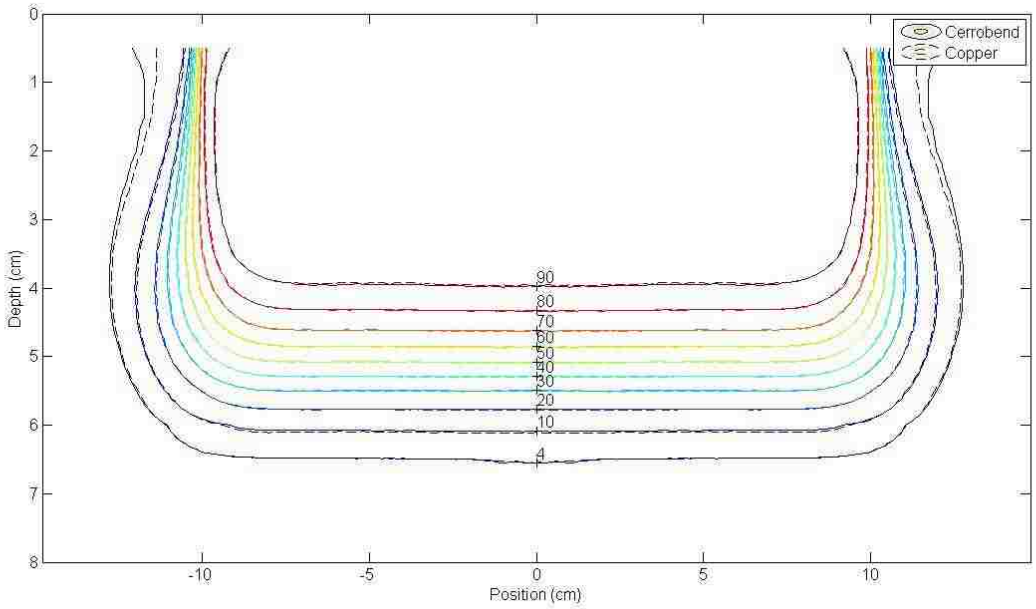

Figure E.47: 20x20 cm^2 field size in the 25x25 cm^2 applicator at 12 MeV.

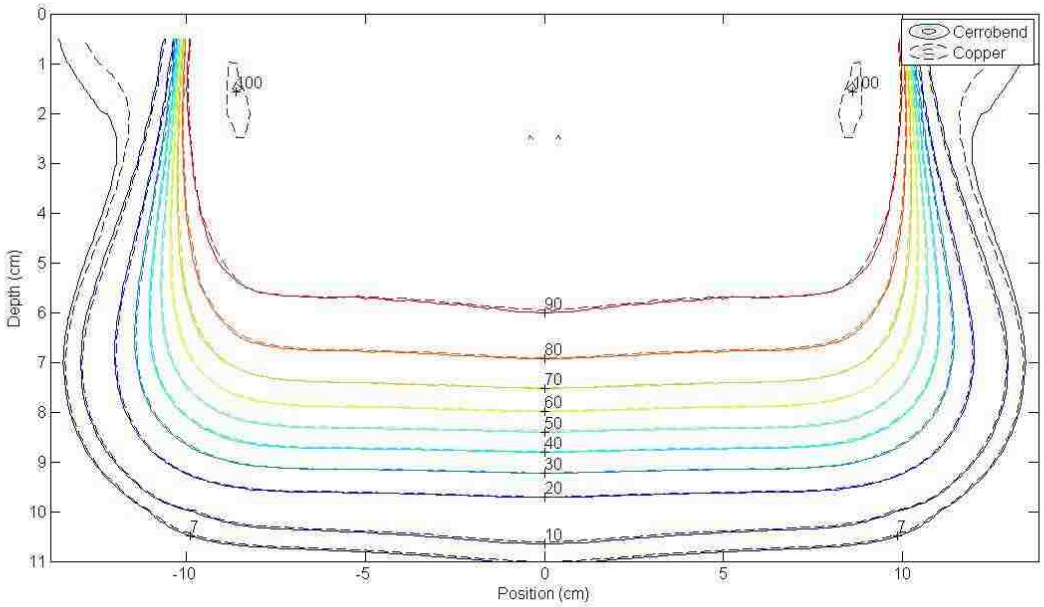

Figure E.48: 20x20 cm^2 field size in the 25x25 cm^2 applicator at 20 MeV.

Appendix F Isodose Comparison Plots at 110 cm SSD

Figure F.1 through Figure F.48 show the isodose comparison plots measured at 110 cm SSD for the subset of field size, applicator size, and energy combinations. Each plot includes labeled isodose lines corresponding to a specific dose value. Solid isodose lines correspond to the dose distribution with the Cerrobend insert, and the dashed isodose lines to the dose distribution with the copper inserts. Any points which did not meet the comparison criteria of 2% or 1 mm distance-to-agreement are indicated with red pixels.

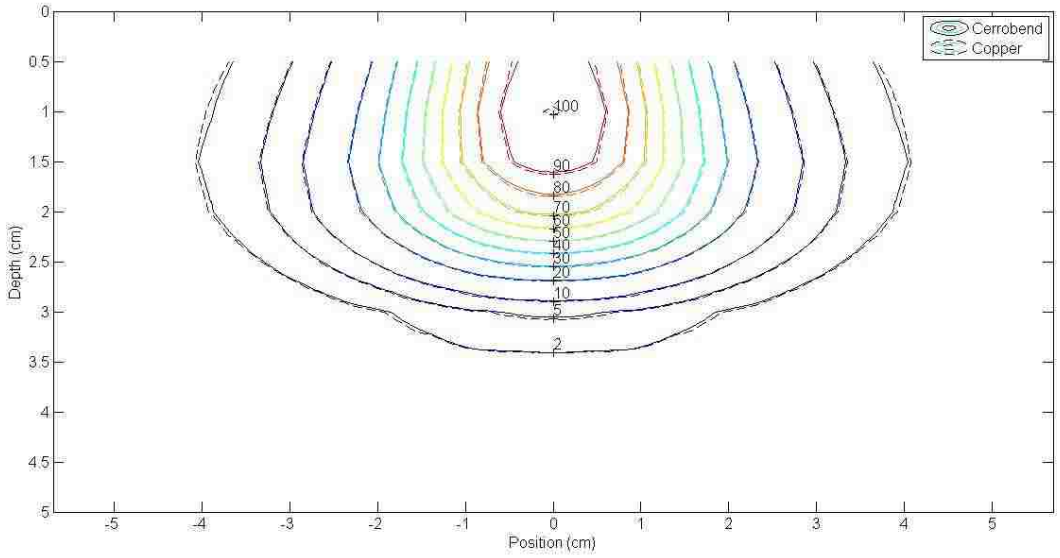

Figure F.1: 2x2 cm^2 field size in the 6x6 cm^2 applicator at 6 MeV.

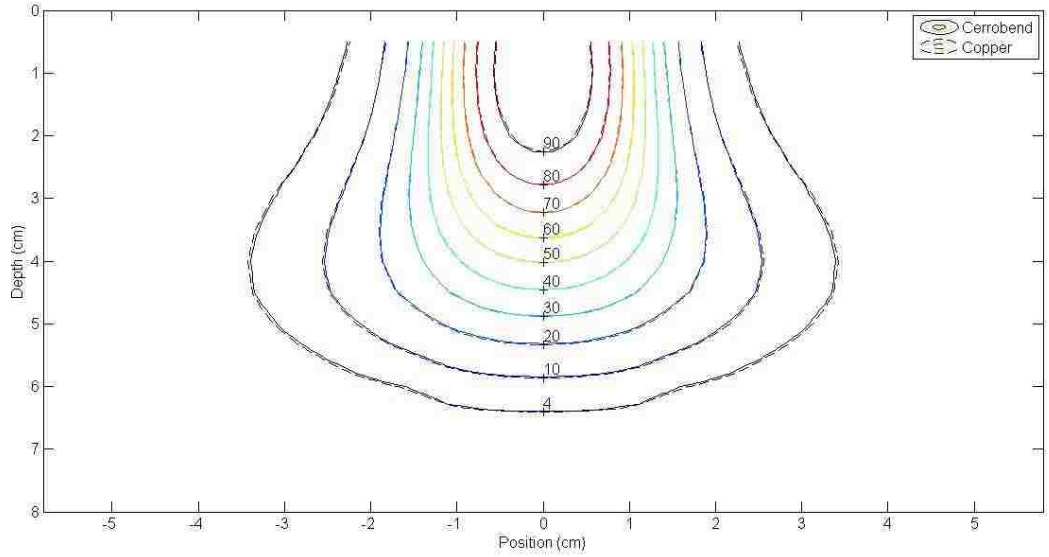

Figure F.2: 2x2 cm^2 field size in the 6x6 cm^2 applicator at 12 MeV.

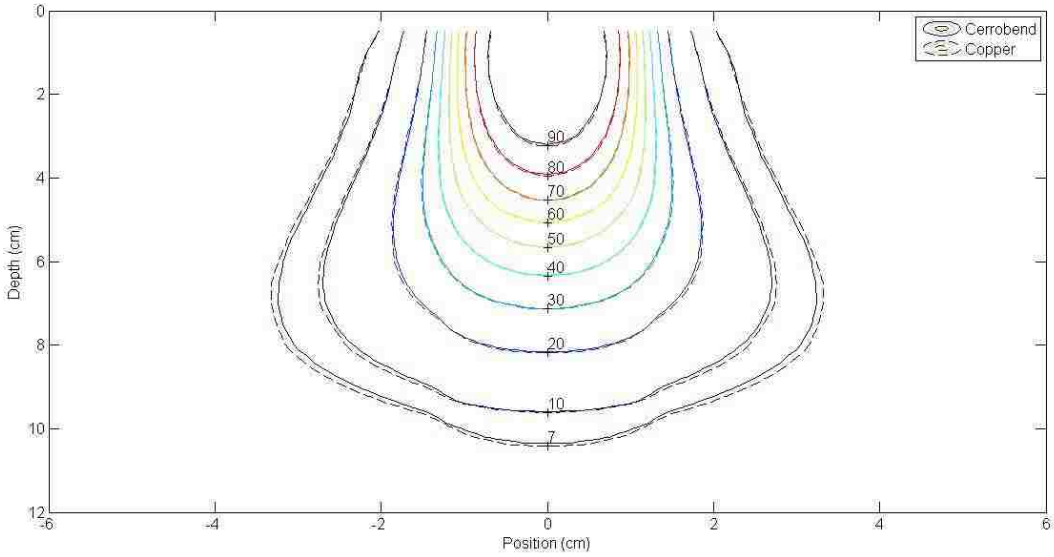

Figure F.3: 2x2 cm^2 field size in the 6x6 cm^2 applicator at 20 MeV.

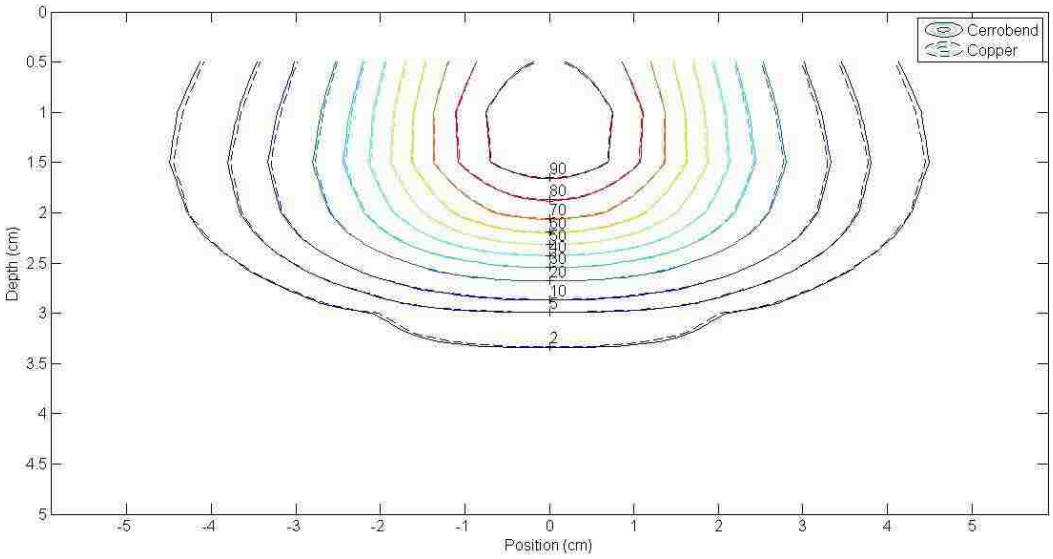

Figure F.4: 3x3 cm^2 field size in the 6x6 cm^2 applicator at 6 MeV.

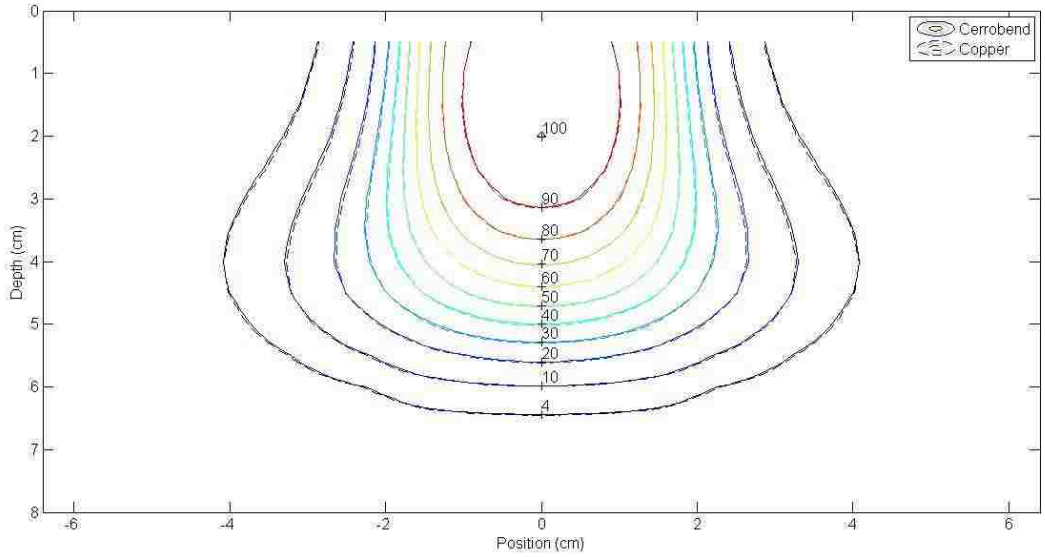

Figure F.5: 3x3 cm^2 field size in the 6x6 cm^2 applicator at 12 MeV.

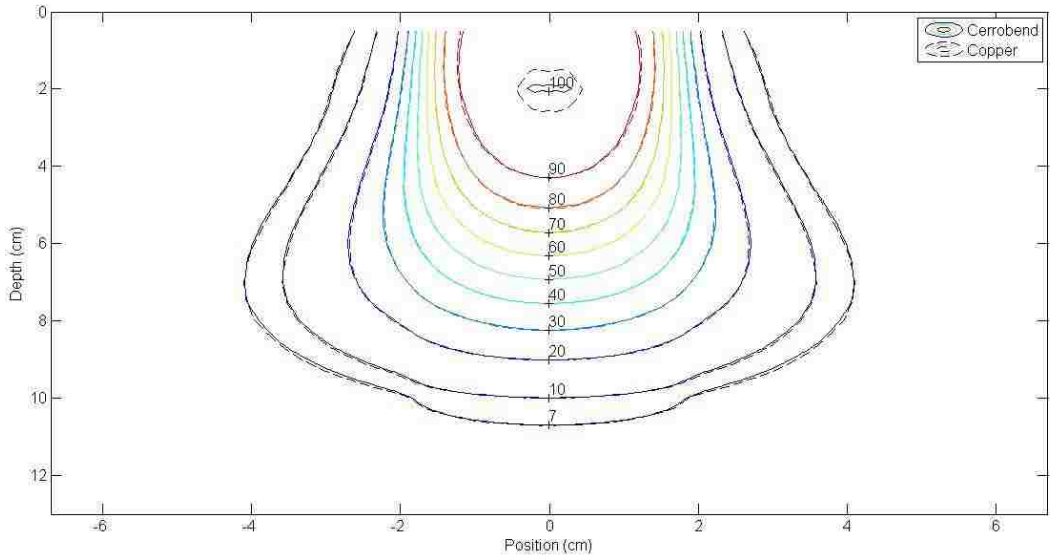

Figure F.6: 3x3 cm^2 field size in the 6x6 cm^2 applicator at 20 MeV.

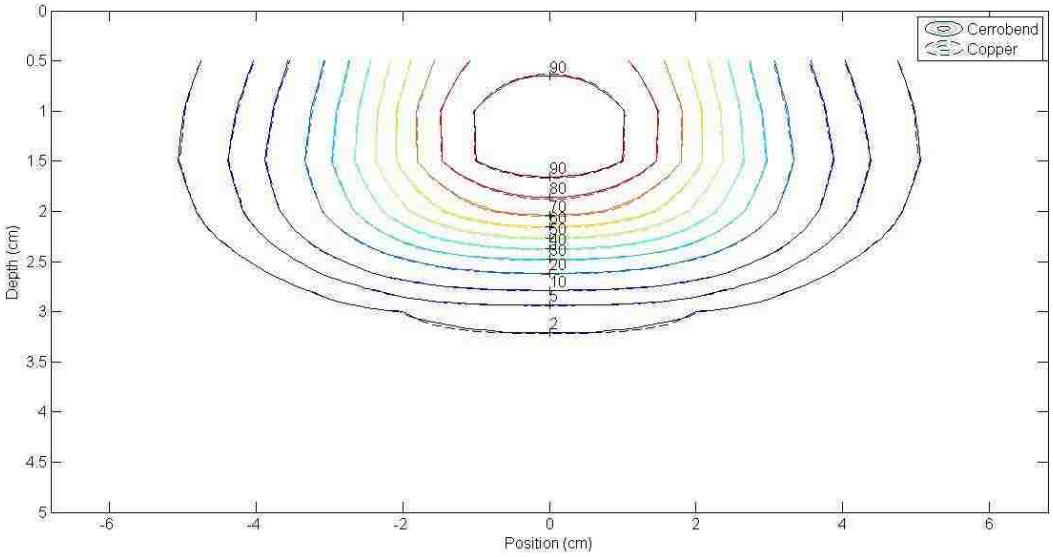

Figure F.7: 4x4 cm^2 field size in the 6x6 cm^2 applicator at 6 MeV.

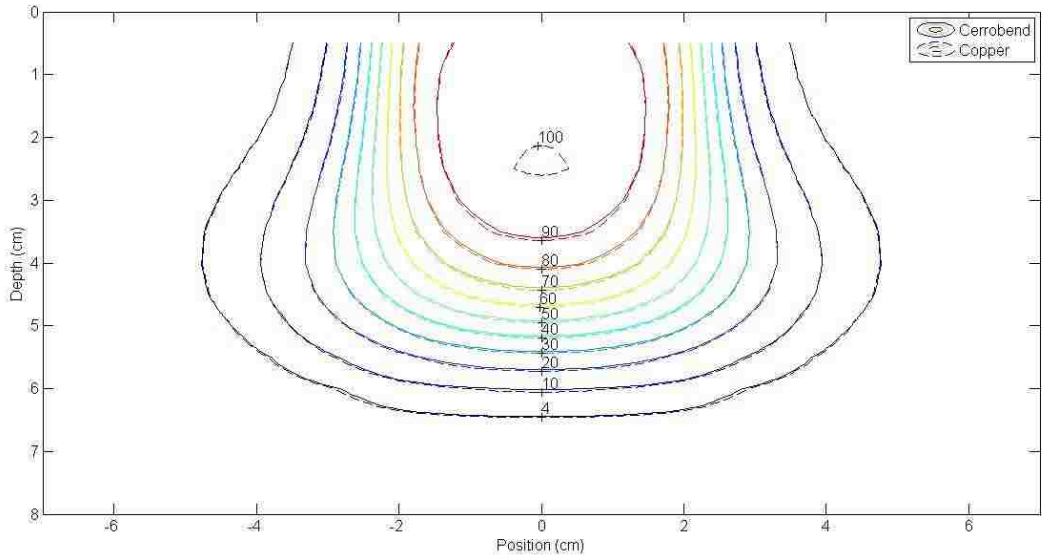

Figure F.8: 4x4 cm^2 field size in the 6x6 cm^2 applicator at 12 MeV.

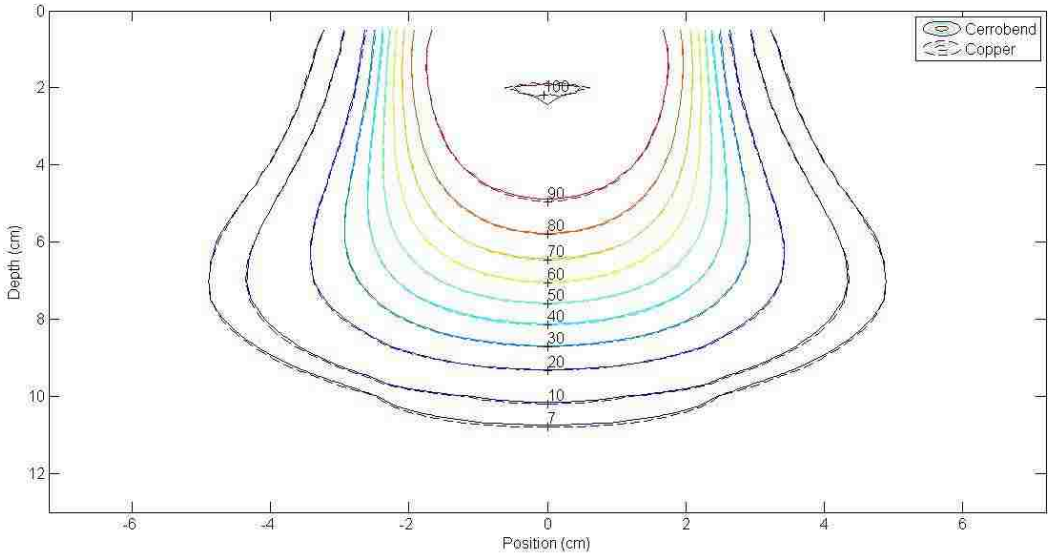

Figure F.9: 4x4 cm^2 field size in the 6x6 cm^2 applicator at 20 MeV.

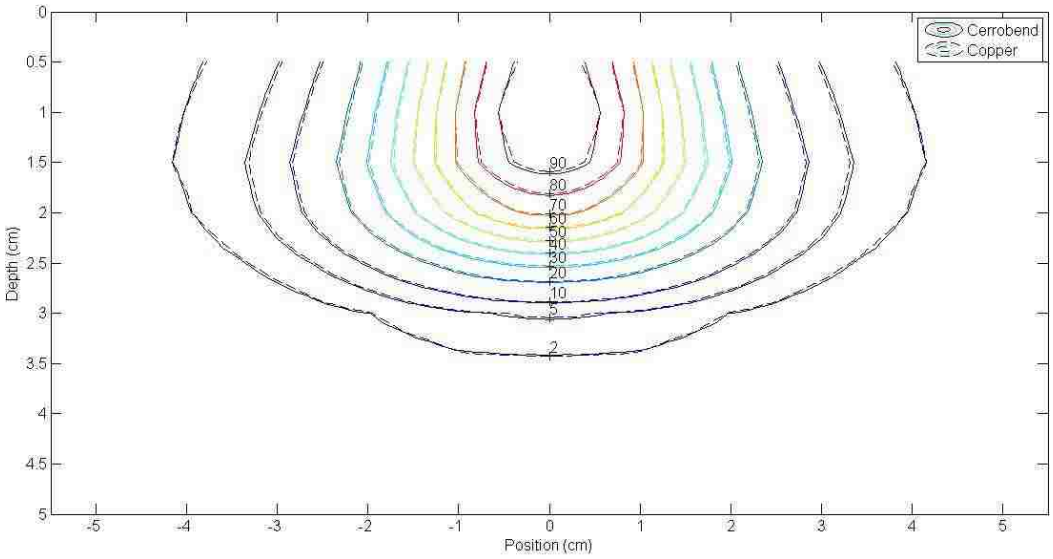

Figure F.10: 2x2 cm^2 field size in the 15x15 cm^2 applicator at 6 MeV.

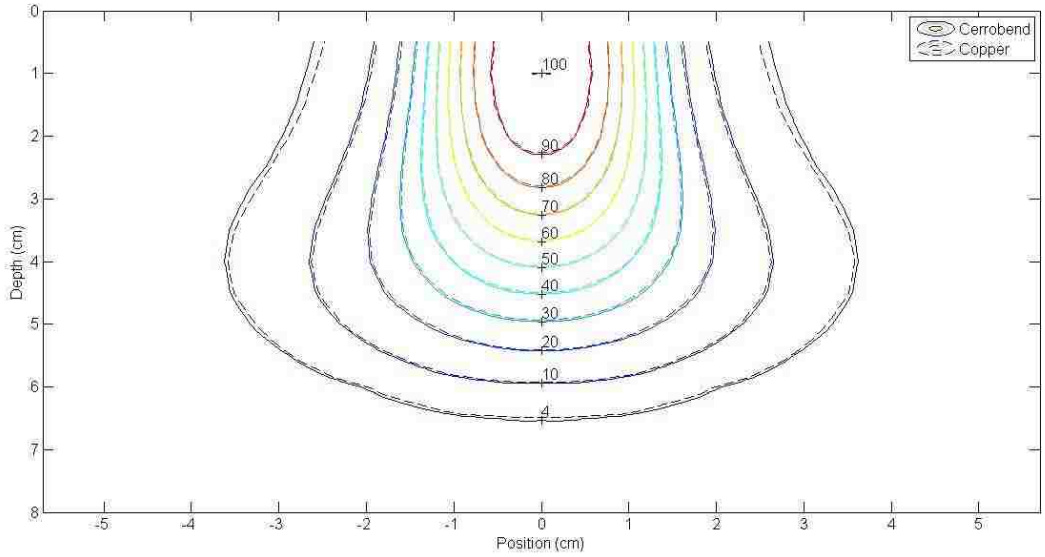

Figure F.11: 2x2 cm^2 field size in the 15x15 cm^2 applicator at 12 MeV.

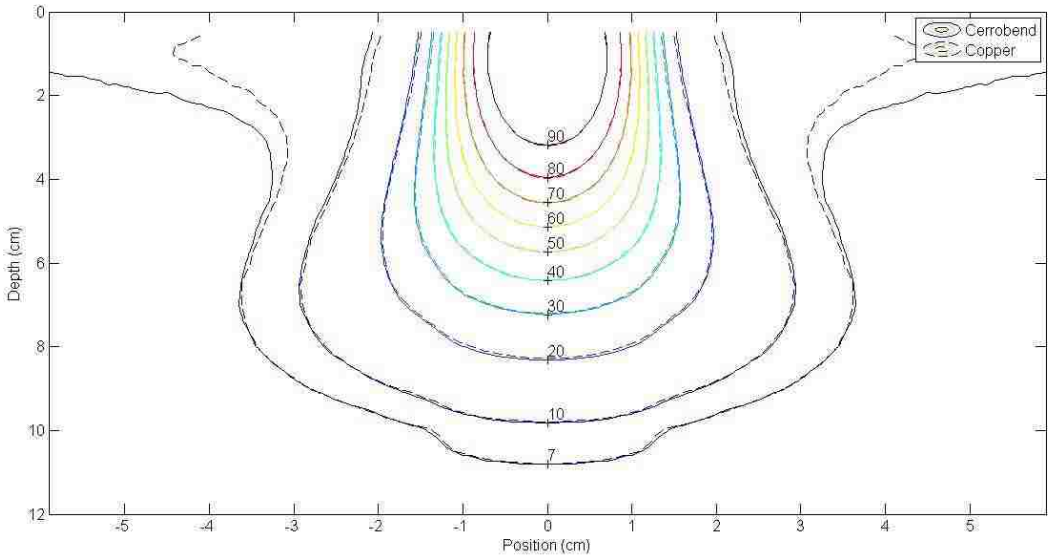

Figure F.12: 2x2 cm^2 field size in the 15x15 cm^2 applicator at 20 MeV.

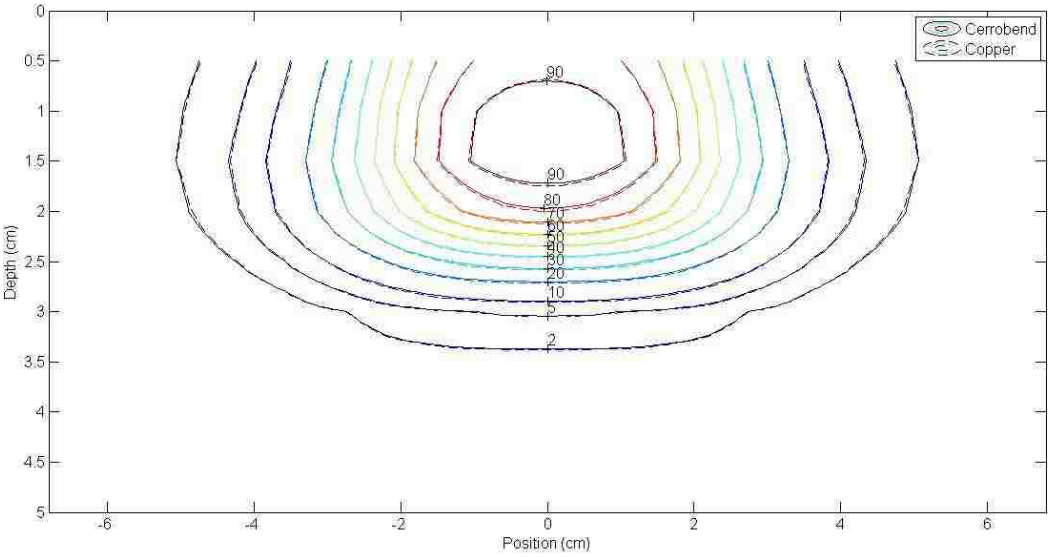

Figure F.13: 4x4 cm^2 field size in the 15x15 cm^2 applicator at 6 MeV.

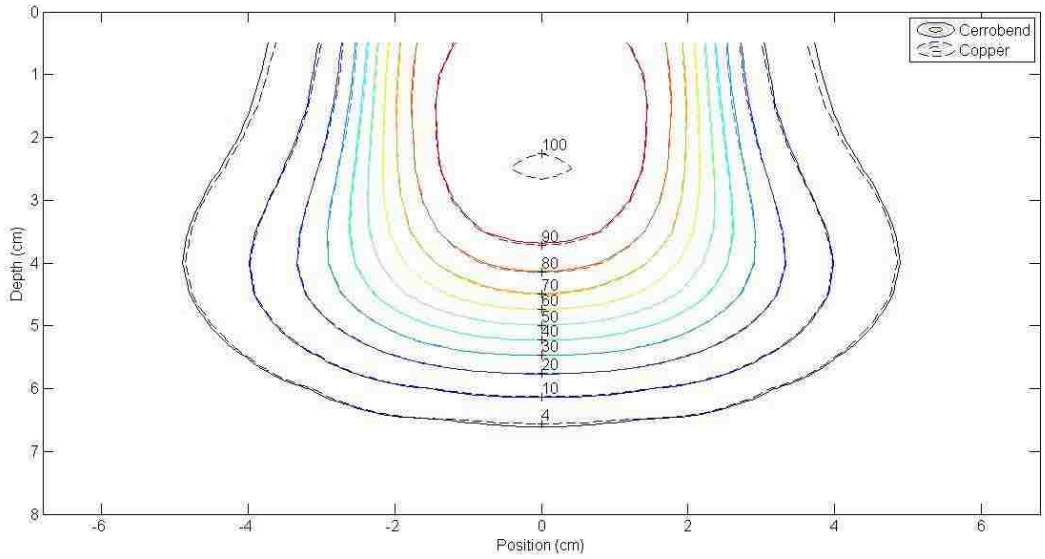

Figure F.14: 4x4 cm^2 field size in the 15x15 cm^2 applicator at 12 MeV.

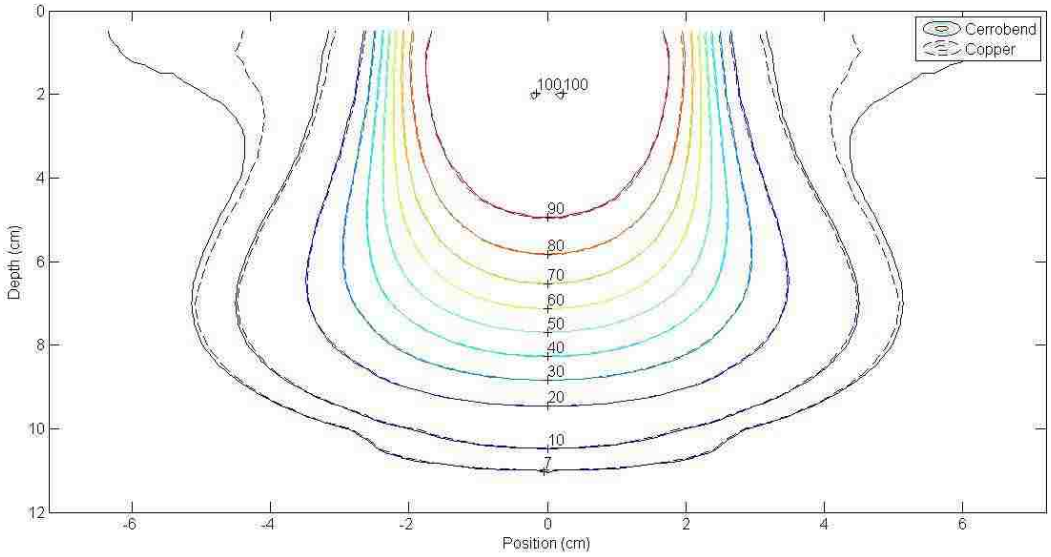

Figure F.15: 4x4 cm^2 field size in the 15x15 cm^2 applicator at 20 MeV.

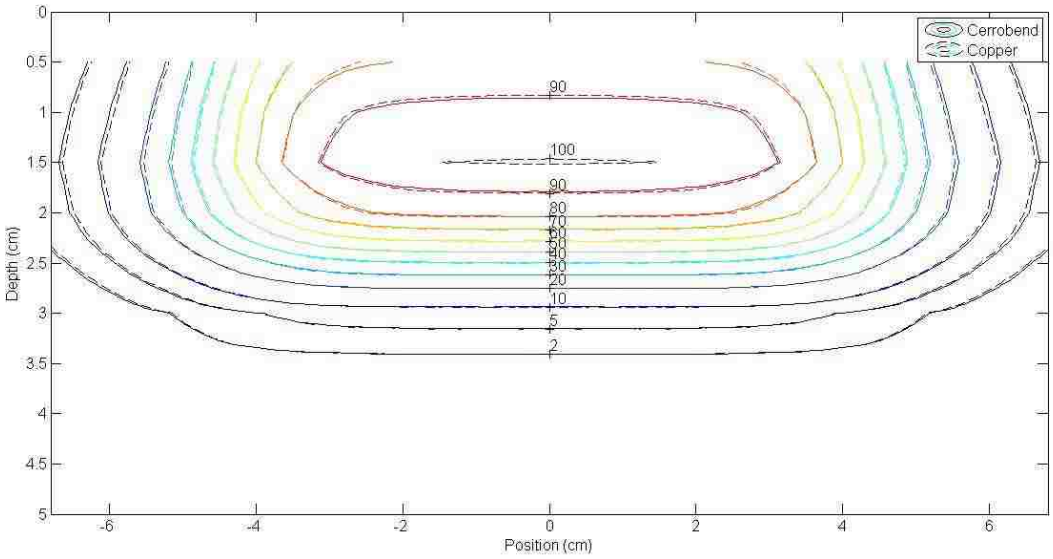

Figure F.16: 8x8 cm^2 field size in the 15x15 cm^2 applicator at 6 MeV.

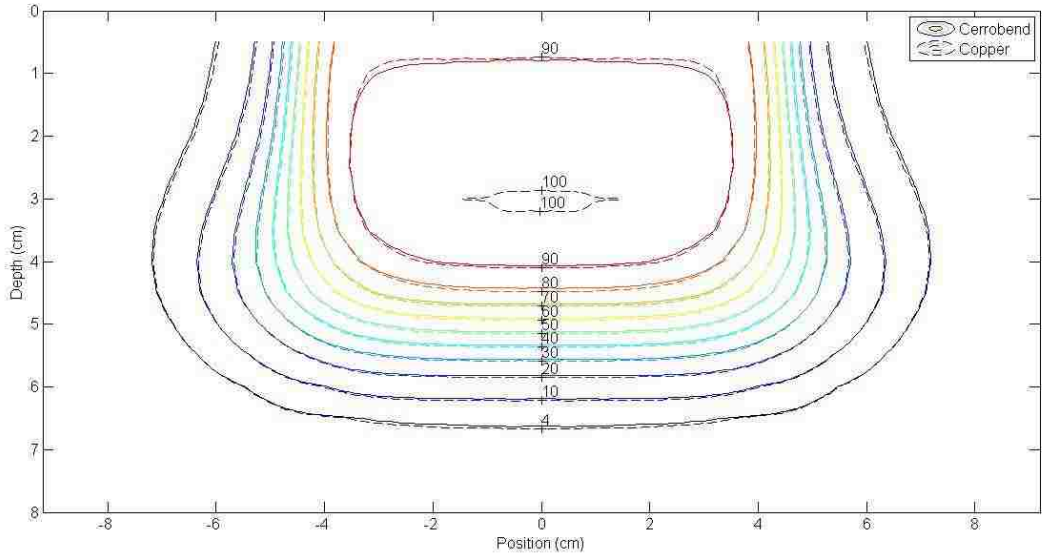

Figure F.17: 8x8 cm^2 field size in the 15x15 cm^2 applicator at 12 MeV.

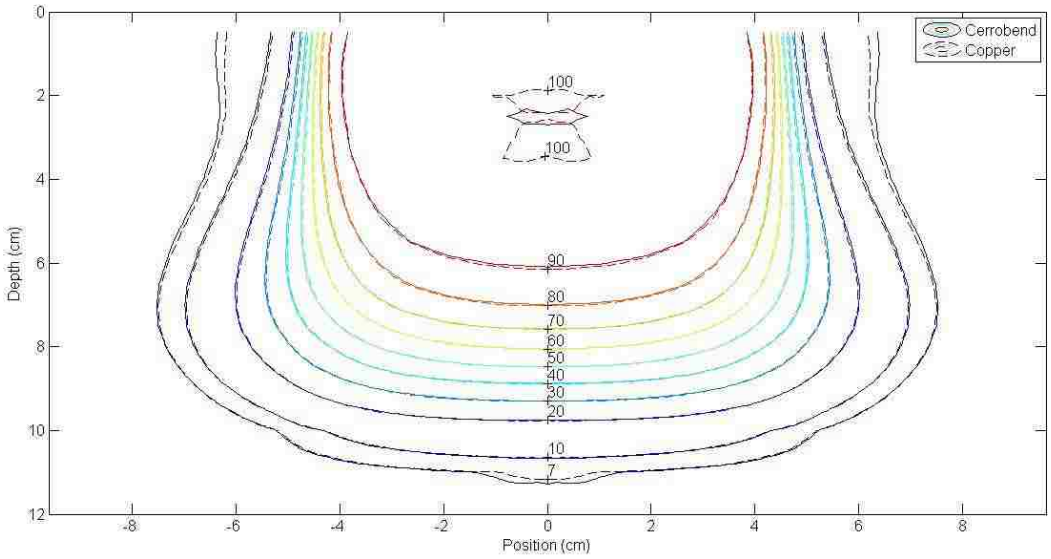

Figure F.18: 8x8 cm^2 field size in the 15x15 cm^2 applicator at 20 MeV.

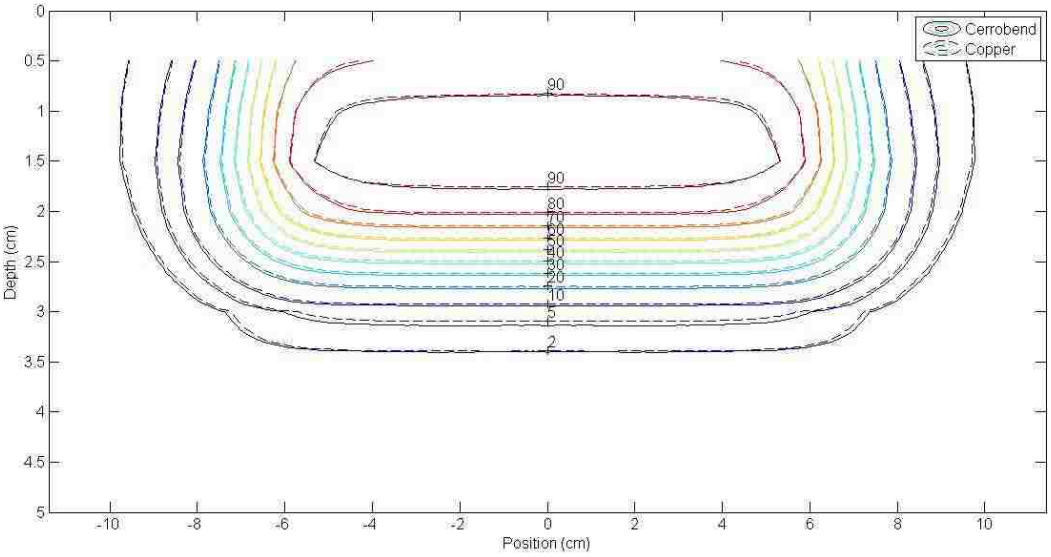

Figure F.19: 12x12 cm^2 field size in the 15x15 cm^2 applicator at 6 MeV.

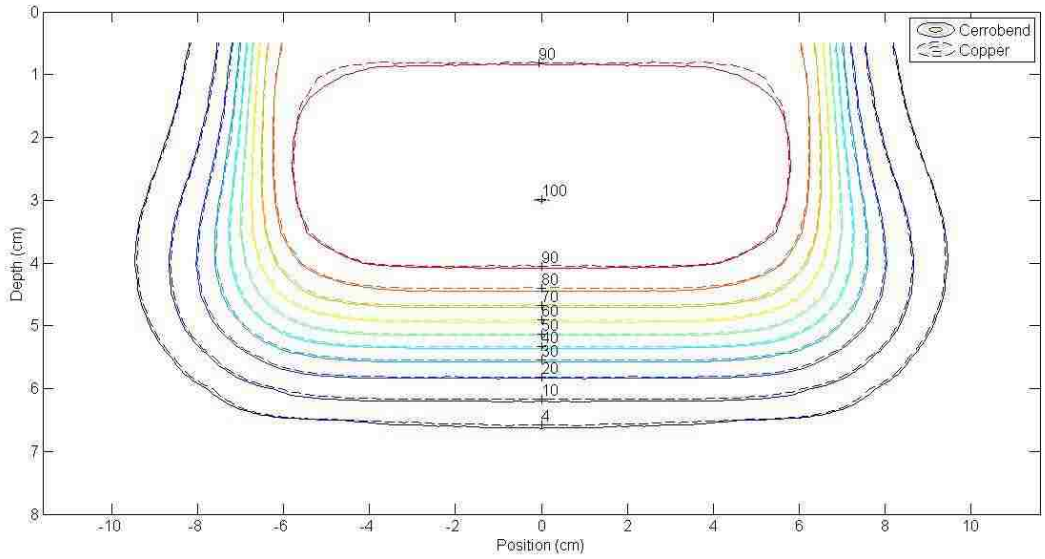

Figure F.20: 12x12 cm^2 field size in the 15x15 cm^2 applicator at 12 MeV.

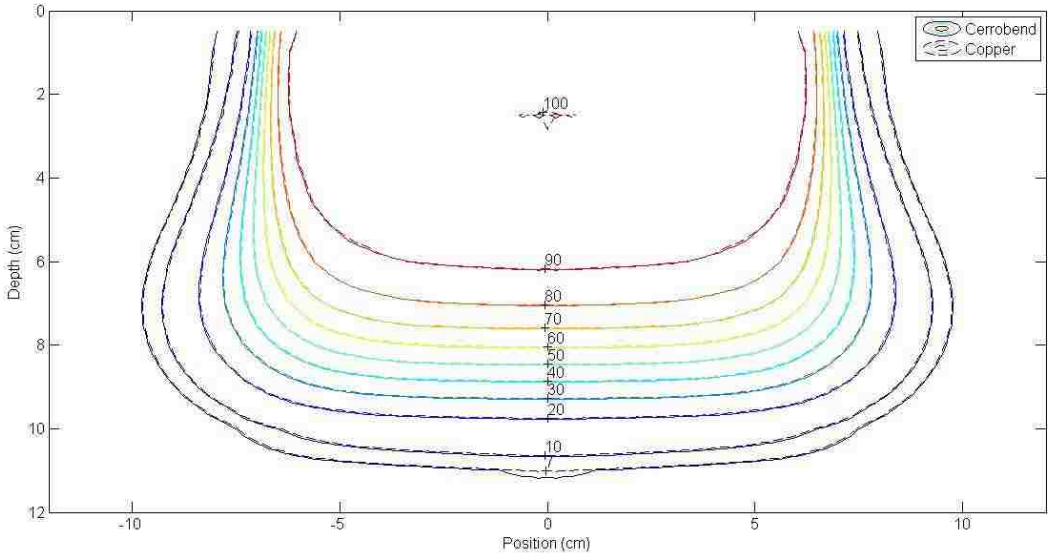

Figure F.21: 12x12 cm^2 field size in the 15x15 cm^2 applicator at 20 MeV.

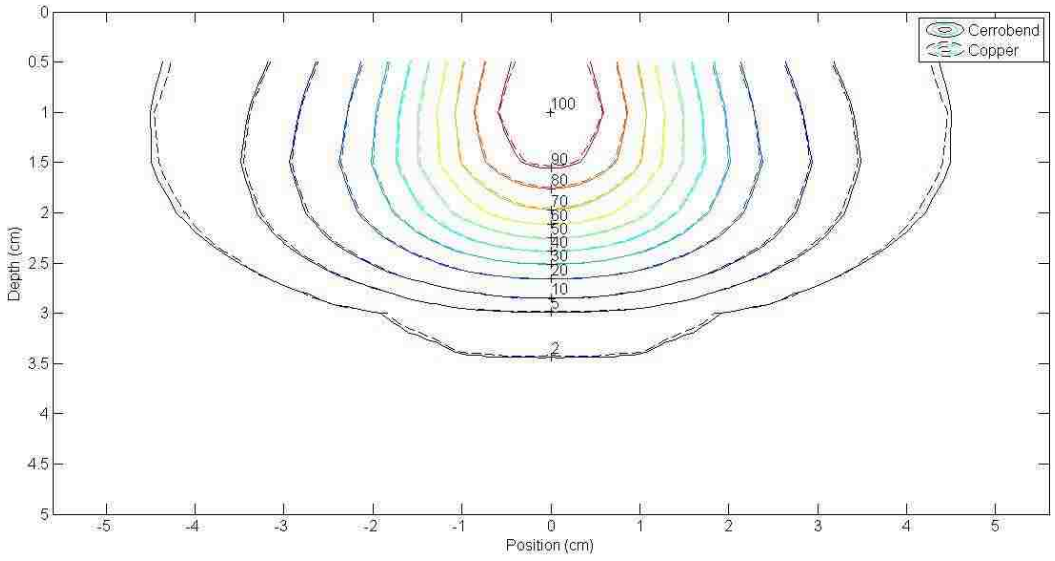

Figure F.22: 2x2 cm^2 field size in the 25x25 cm^2 applicator at 6 MeV.

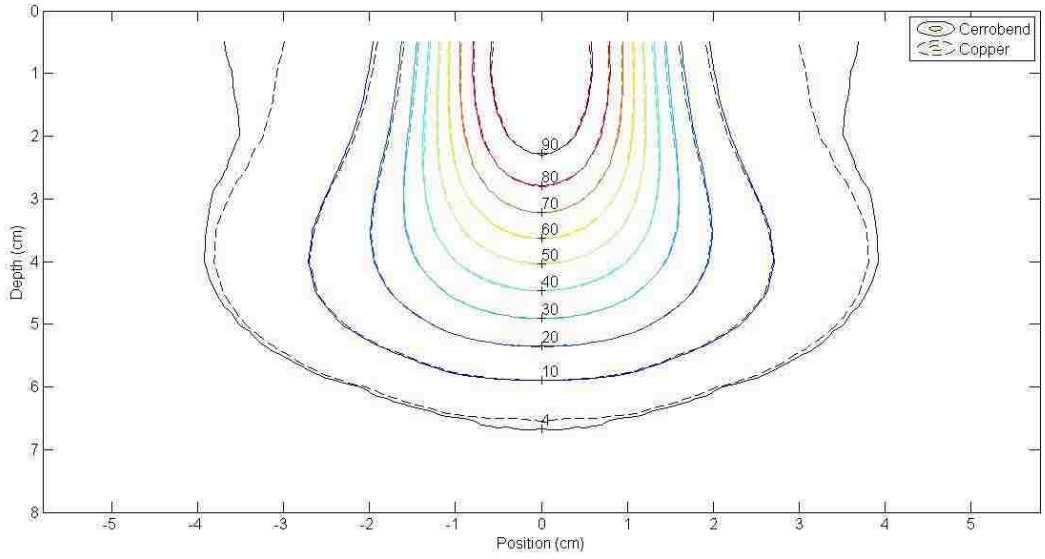

Figure F.23: 2x2 cm^2 field size in the 25x25 cm^2 applicator at 12 MeV.

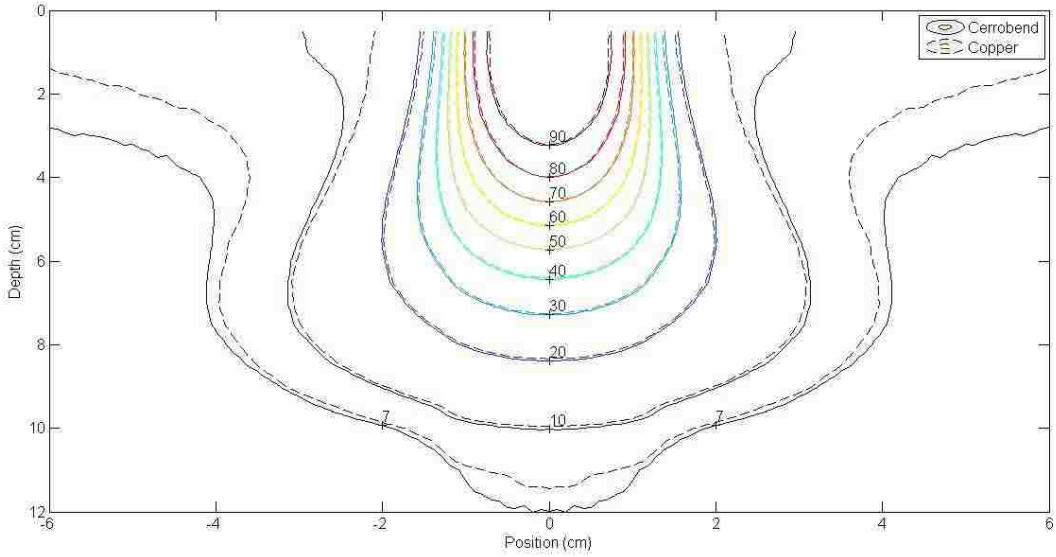

Figure F.24: 2x2 cm^2 field size in the 25x25 cm^2 applicator at 20 MeV.

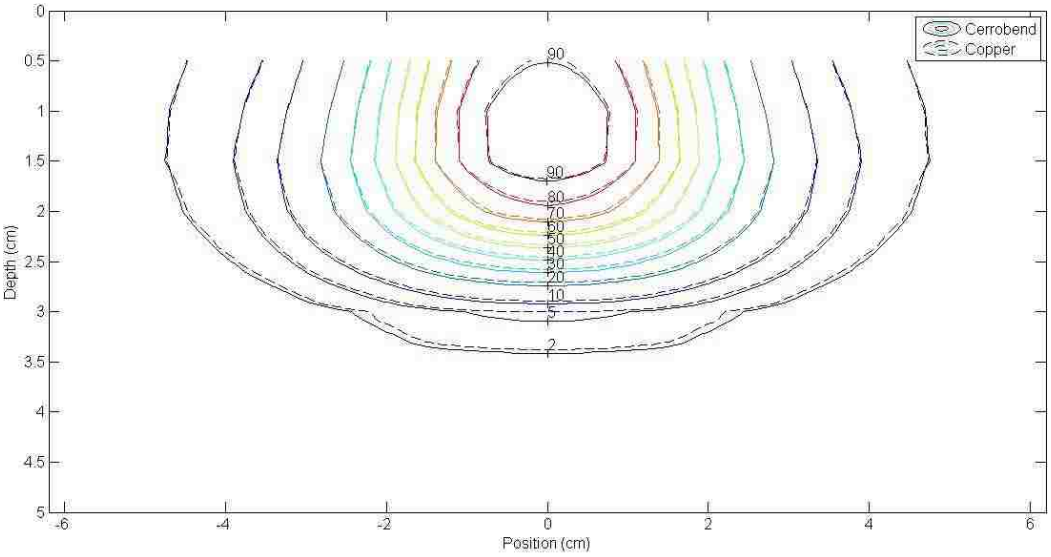

Figure F.25: 3x3 cm^2 field size in the 25x25 cm^2 applicator at 6 MeV.

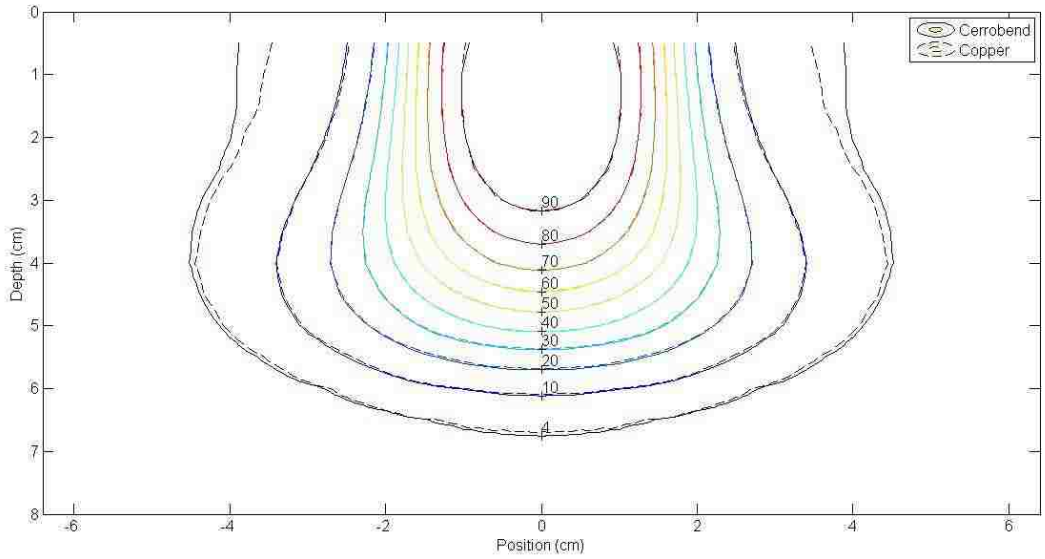

Figure F. 26: 3x3 cm^2 field size in the 25x25 cm^2 applicator at 12 MeV.

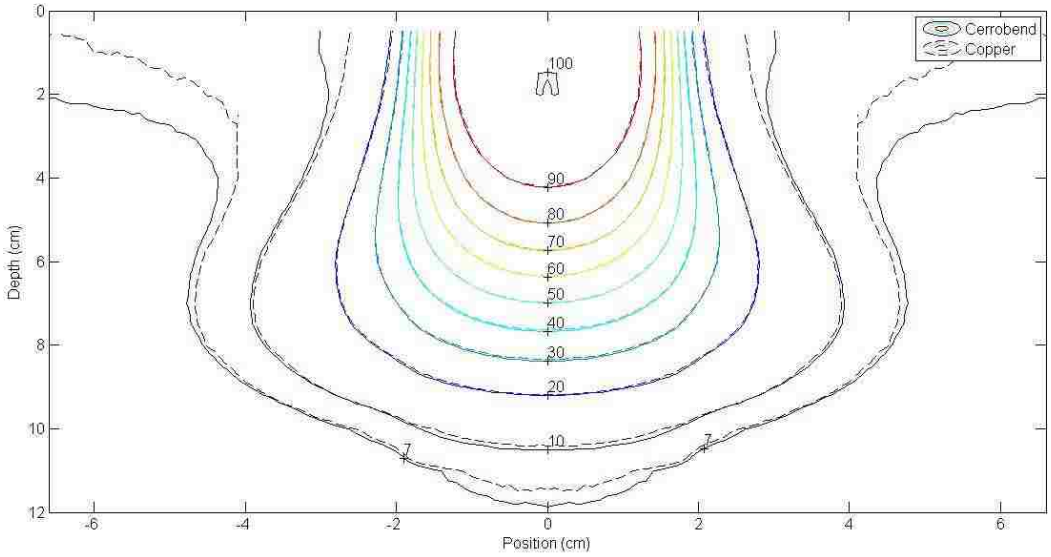

Figure F.27: 3x3 cm^2 field size in the 25x25 cm^2 applicator at 20 MeV.

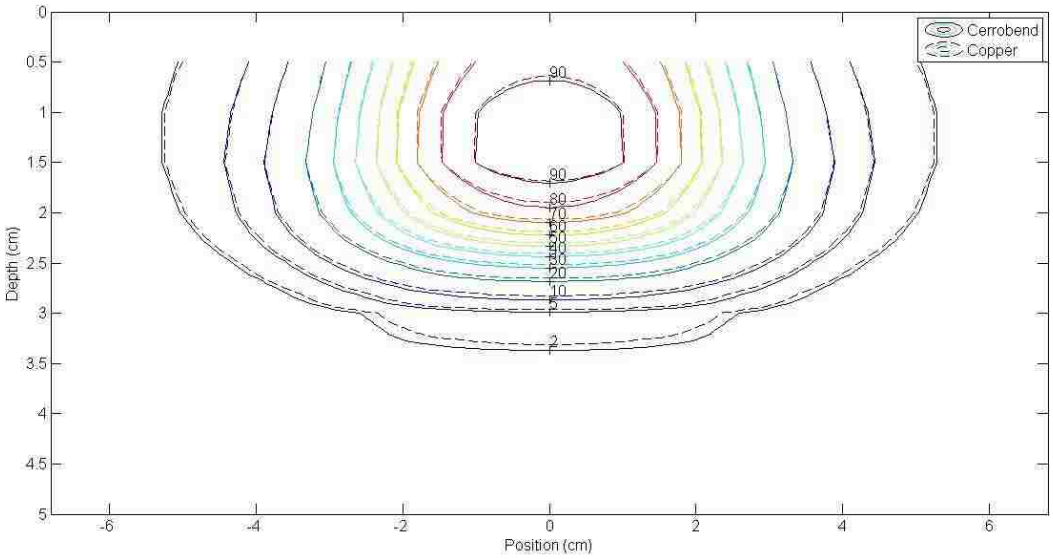

Figure F.28: 4x4 cm^2 field size in the 25x25 cm^2 applicator at 6 MeV.

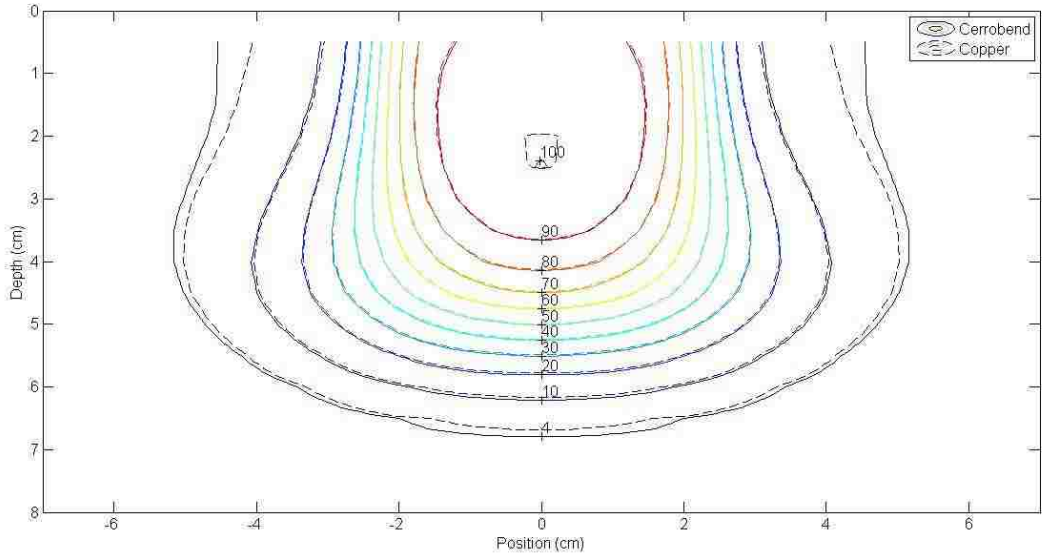

Figure F.29: 4x4 cm^2 field size in the 25x25 cm^2 applicator at 12 MeV.

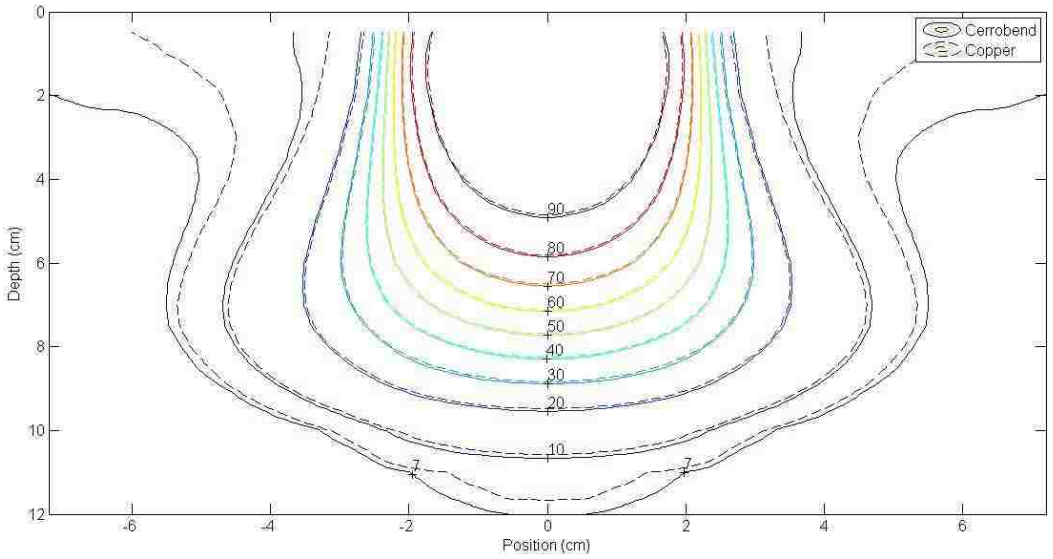

Figure F.30: 4x4 cm^2 field size in the 25x25 cm^2 applicator at 20 MeV.

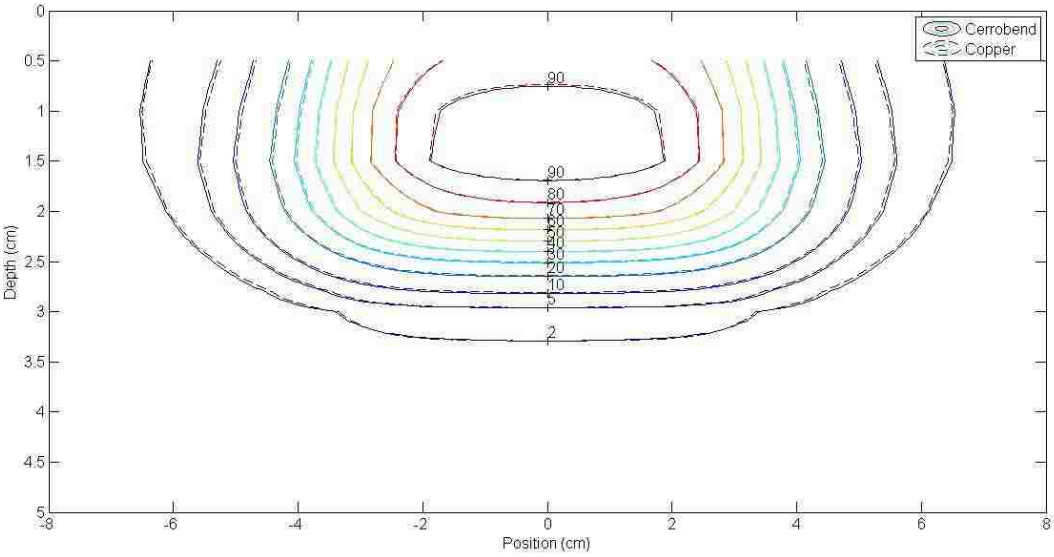

Figure F.31: 6x6 cm^2 field size in the 25x25 cm^2 applicator at 6 MeV.

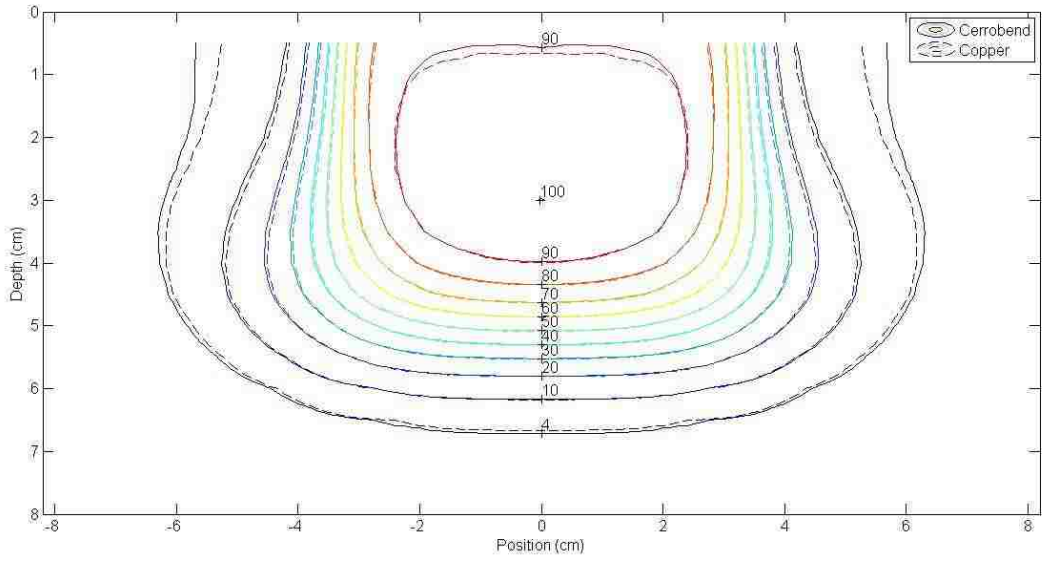

Figure F.32: 6x6 cm^2 field size in the 25x25 cm^2 applicator at 12 MeV.

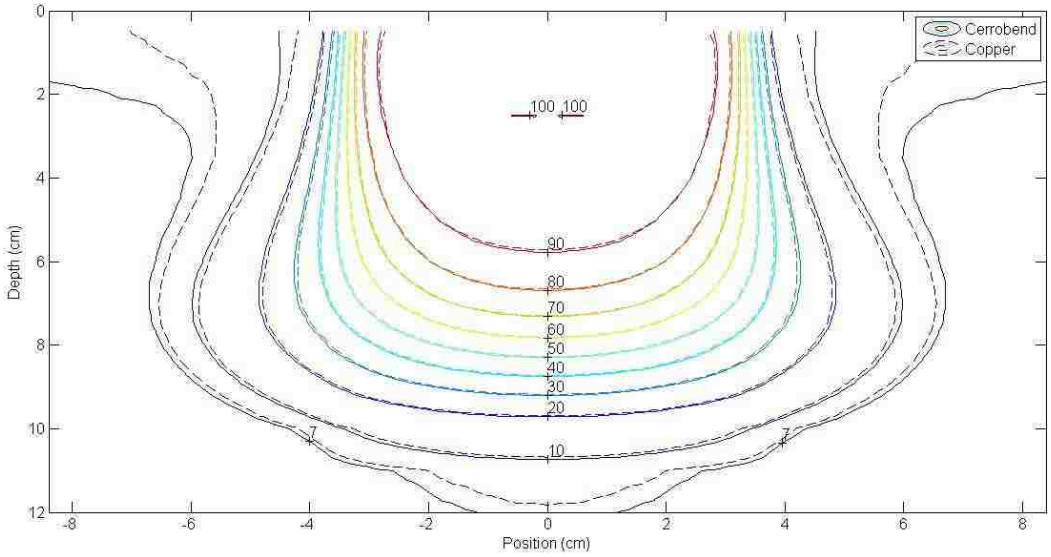

Figure F.33: 6x6 cm^2 field size in the 25x25 cm^2 applicator at 20 MeV.

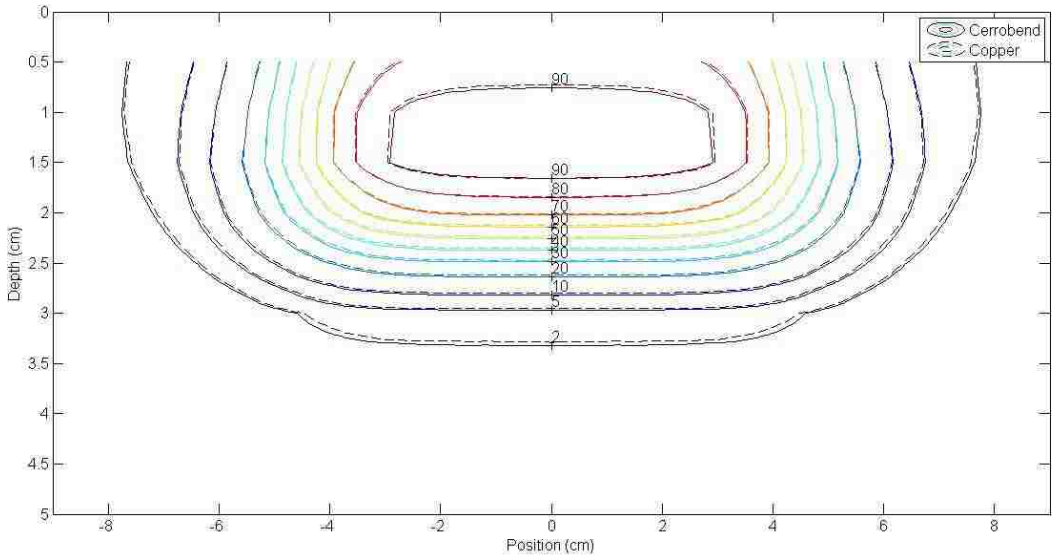

Figure F.34: 8x8 cm^2 field size in the 25x25 cm^2 applicator at 6 MeV.

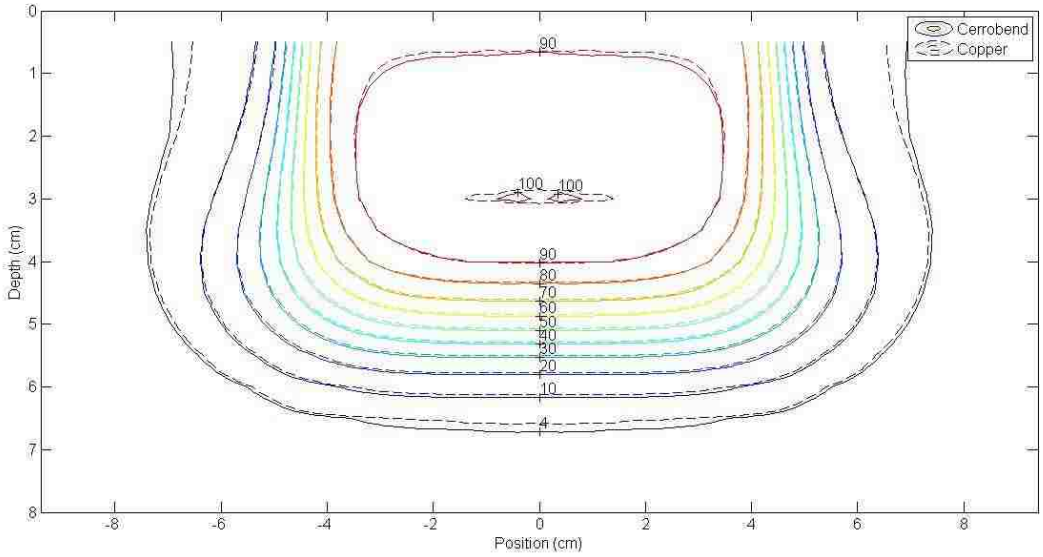

Figure F.35: 8x8 cm^2 field size in the 25x25 cm^2 applicator at 12 MeV.

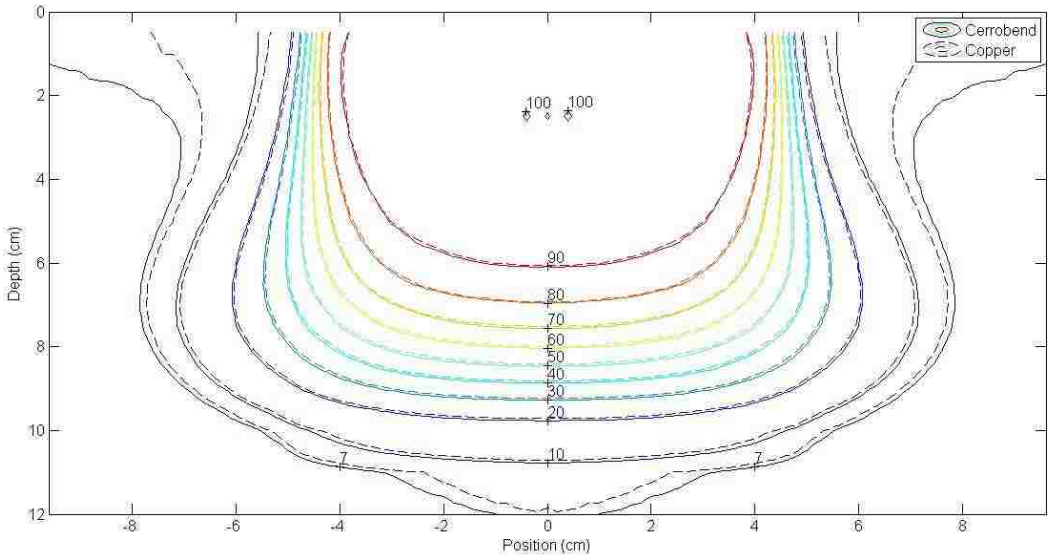

Figure F.36: 8x8 cm^2 field size in the 25x25 cm^2 applicator at 20 MeV.

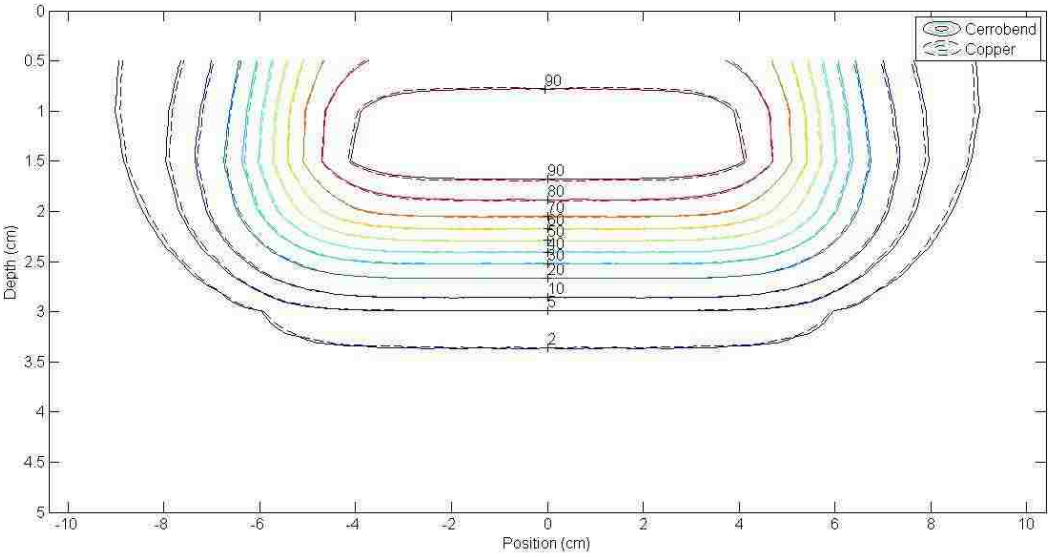

Figure F.37: 10x10 cm^2 field size in the 25x25 cm^2 applicator at 6 MeV.

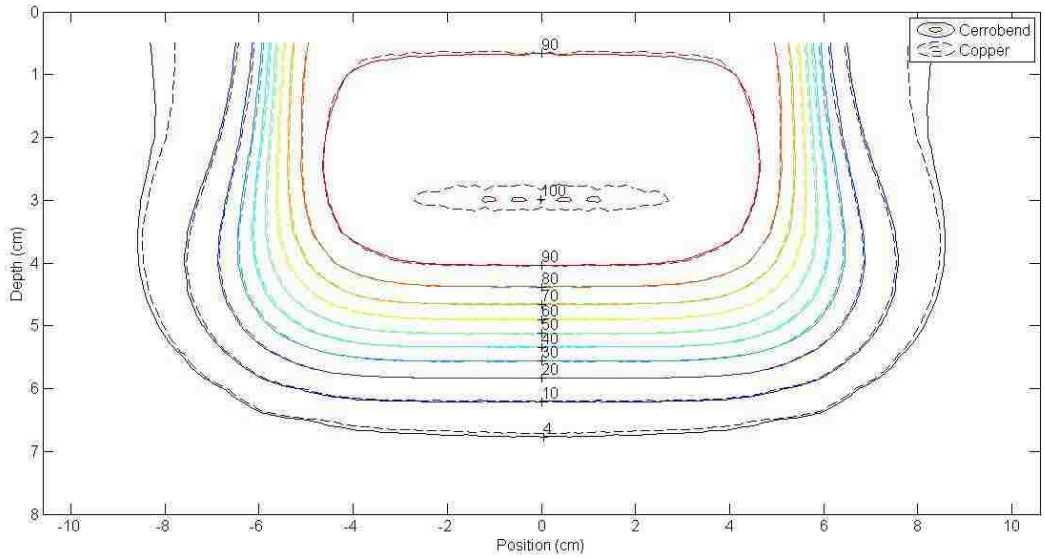

Figure F.38: 10x10 cm^2 field size in the 25x25 cm^2 applicator at 12 MeV.

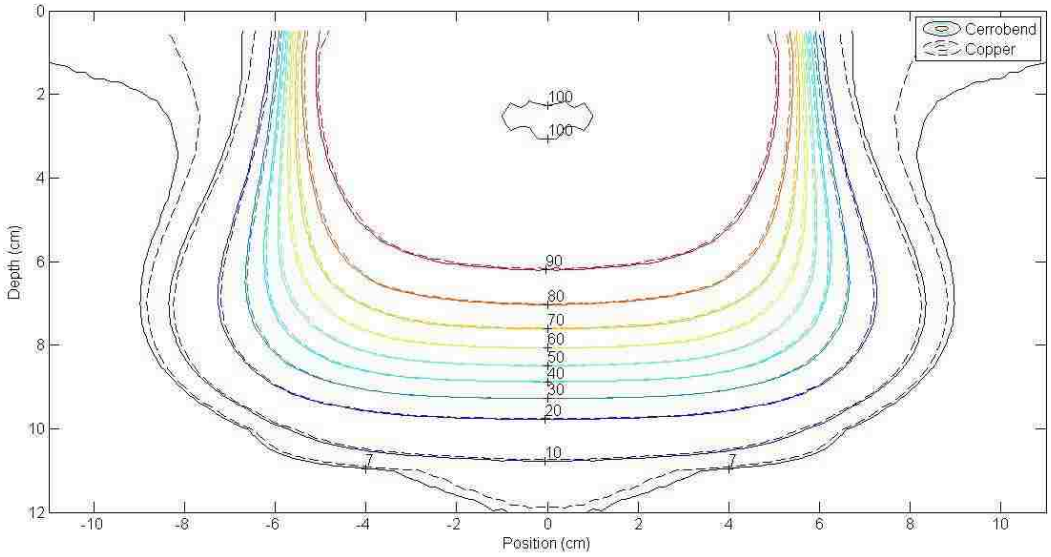

Figure F.39: 10x10 cm^2 field size in the 25x25 cm^2 applicator at 20 MeV.

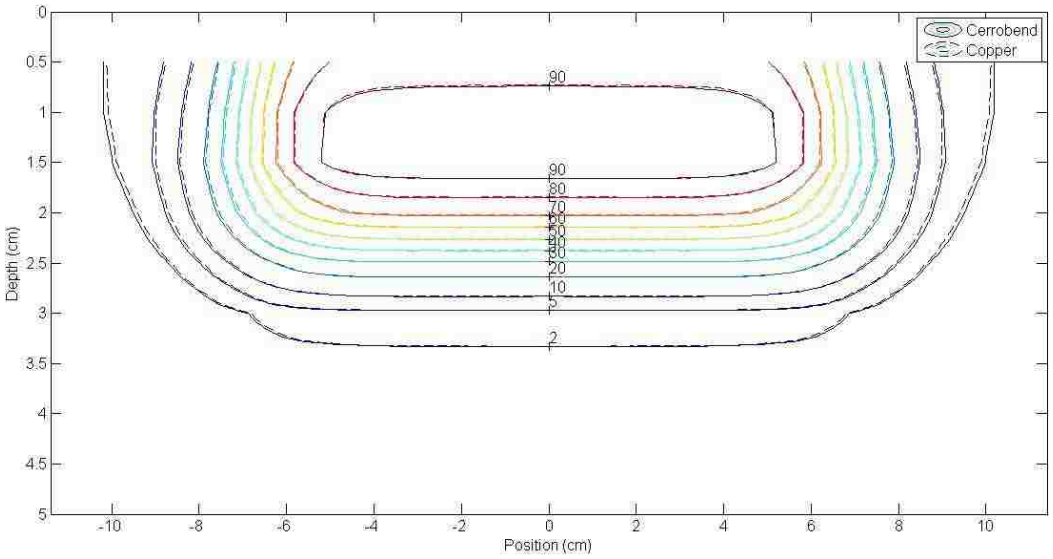

Figure F.40: 12x12 cm^2 field size in the 25x25 cm^2 applicator at 6 MeV.

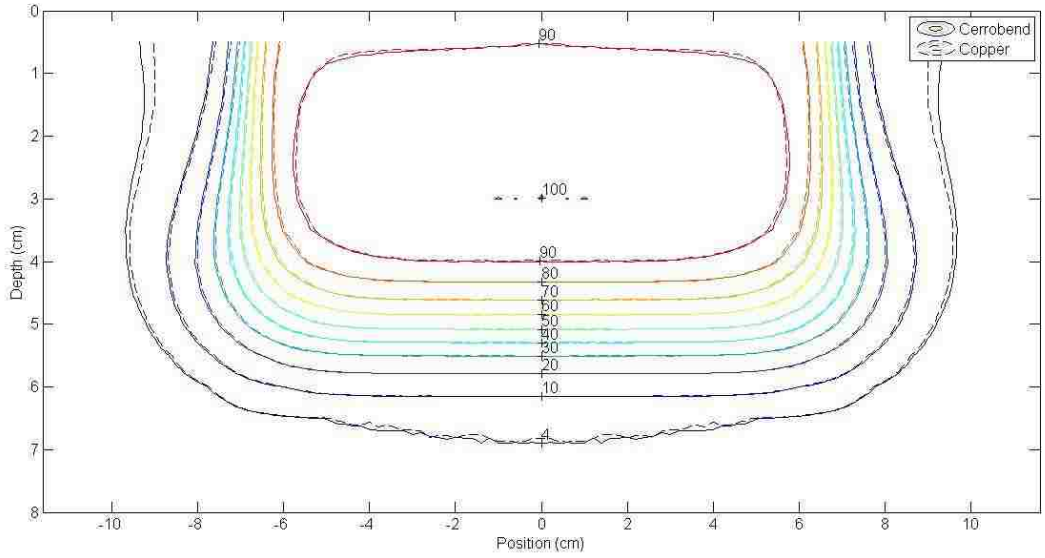

Figure F.41: 12x12 cm^2 field size in the 25x25 cm^2 applicator at 12 MeV.

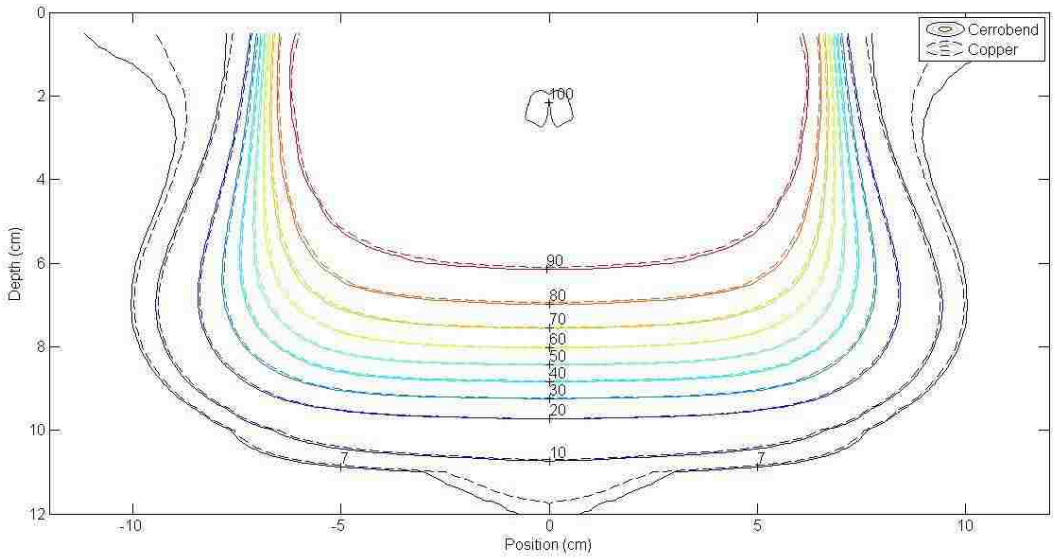

Figure F.42: 12x12 cm^2 field size in the 25x25 cm^2 applicator at 20 MeV.

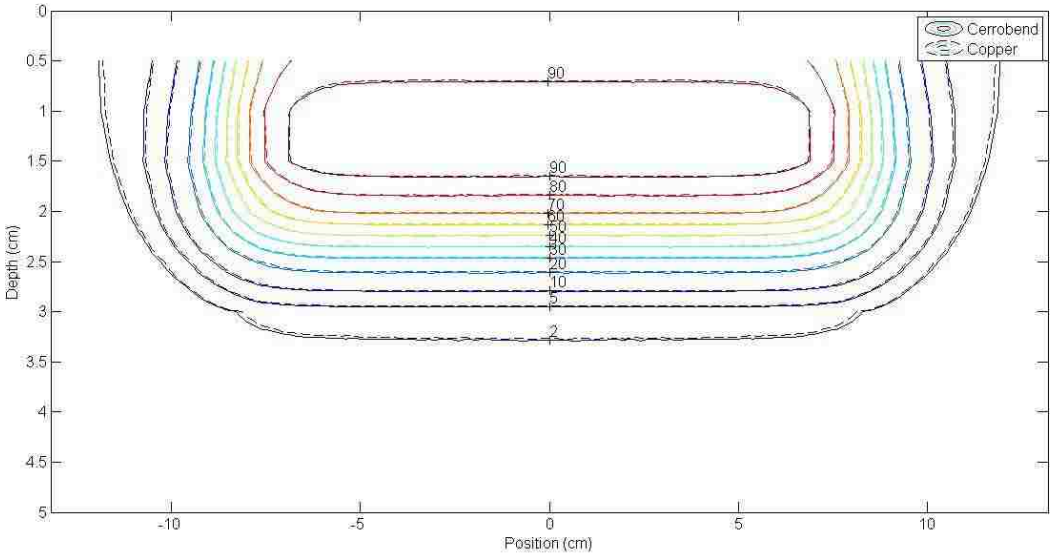

Figure F.43: 15x15 cm^2 field size in the 25x25 cm^2 applicator at 6 MeV.

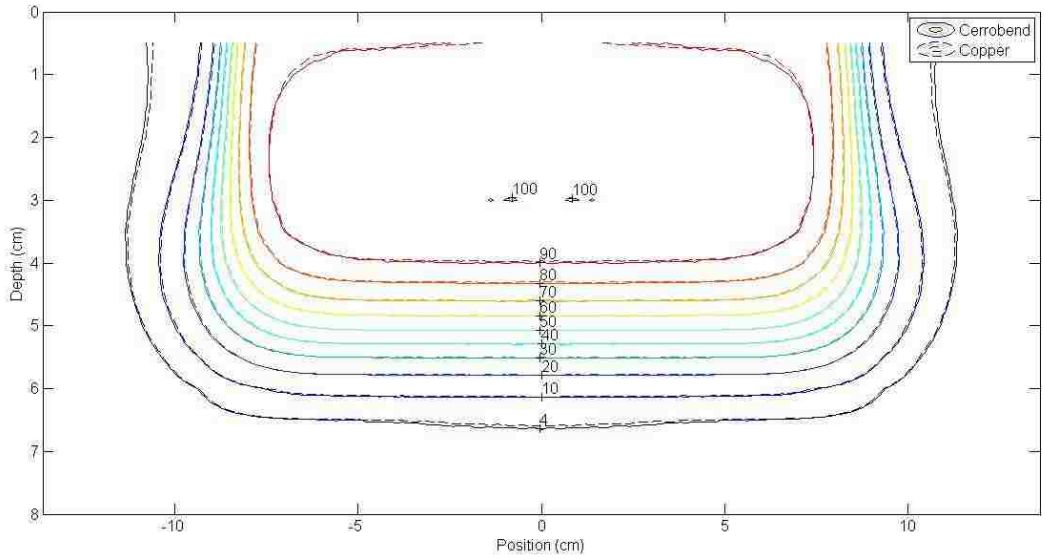

Figure F.44: 15x15 cm^2 field size in the 25x25 cm^2 applicator at 12 MeV.

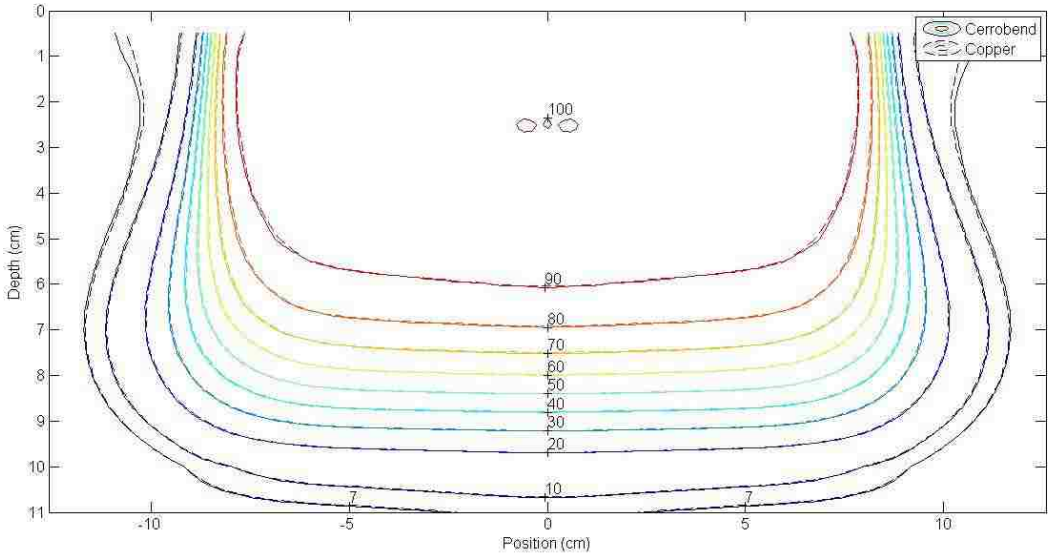

Figure F.45: 15x15 cm^2 field size in the 25x25 cm^2 applicator at 20 MeV.

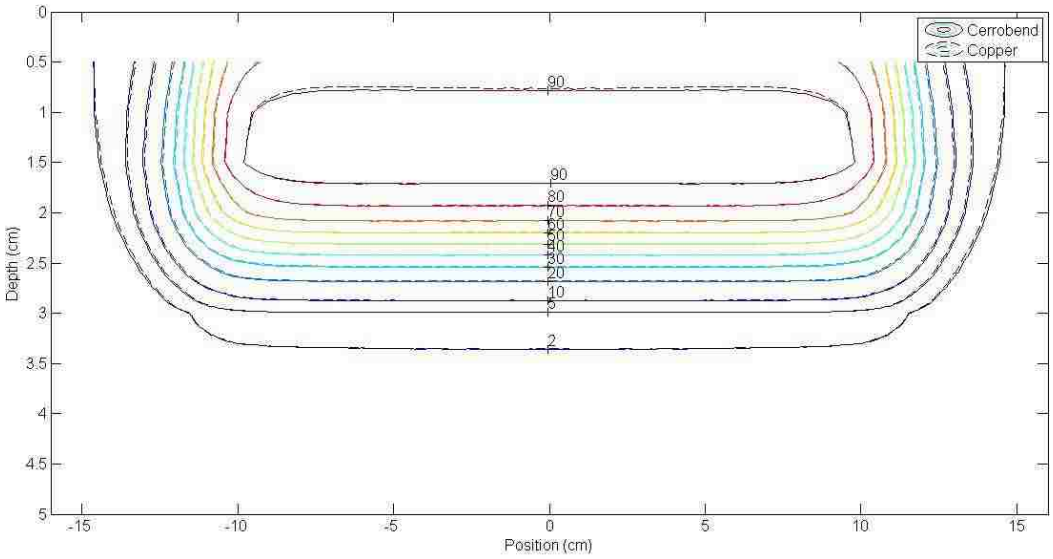

Figure F.46: 20x20 cm^2 field size in the 25x25 cm^2 applicator at 6 MeV.

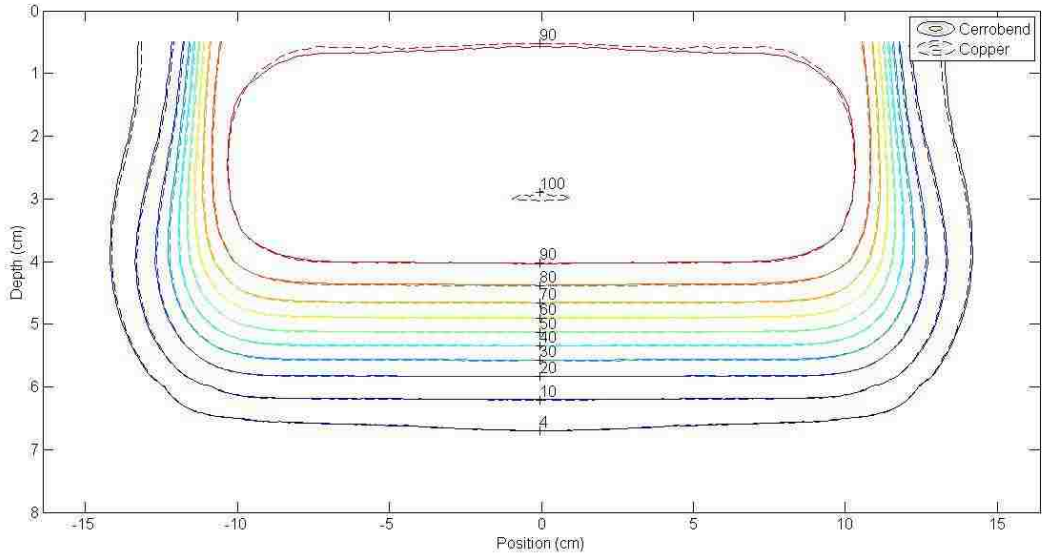

Figure F.47: 20x20 cm^2 field size in the 25x25 cm^2 applicator at 12 MeV.

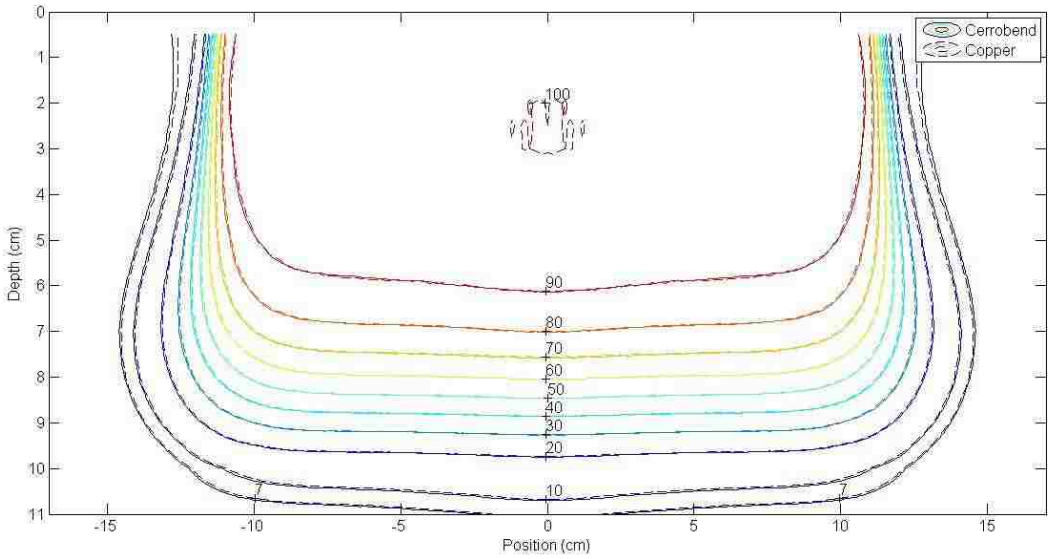

Figure F.48: 20x20 cm^2 field size in the 25x25 cm^2 applicator at 20 MeV.

Vita

Ben Rusk grew up in Dubuque, Iowa, a small town on the banks of the Mississippi River. After graduating high school, Ben attended Truman State University in Kirksville, Missouri where he lettered four years on the varsity tennis team and had the opportunity to live and study in Newcastle, Australia for six months. After graduating with a B.S. in Physics, Ben moved to Winter Park, Colorado to ski and work before beginning graduate school. He chose to attend Louisiana State University in Baton Rouge, Louisiana to pursue his Masters of Science in Medical Physics, a three-year program. He took classes the first year and, during the last two years, worked and did research at the program's clinical affiliate, Mary Bird Perkins Cancer Center. Ben will receive his master's degree in the summer of 2014 and plans to enter a clinical medical physics residency at Mary Bird Perkins Cancer Center.